# INFORMATION TO USERS

This manuscript has been reproduced from the microfilm master. UMI films the text directly from the original or copy submitted. Thus, some thesis and dissertation copies are in typewriter face, while others may be from any type of computer printer.

**The quality of this reproduction is dependent upon the quality of the copy submitted.** Broken or indistinct print, colored or poor quality illustrations and photographs, print bleedthrough, substandard margins, and improper alignment can adversely affect reproduction.

In the unlikely event that the author did not send UMI a complete manuscript and there are missing pages, these will be noted. Also, if unauthorized copyright material had to be removed, a note will indicate the deletion.

Oversize materials (e.g., maps, drawings, charts) are reproduced by sectioning the original, beginning at the upper left-hand corner and continuing from left to right in equal sections with small overlaps.

Photographs included in the original manuscript have been reproduced xerographically in this copy. Higher quality 6" x 9" black and white photographic prints are available for any photographs or illustrations appearing in this copy for an additional charge. Contact UMI directly to order.

Bell & Howell Information and Learning
300 North Zeeb Road, Ann Arbor, MI 48106-1346 USA

UMI®
800-521-0600

# SEISMIC TORSIONAL RESPONSE

# OF

# ASYMMETRICAL MULTI-STOREY FRAME BUILDINGS

By

ABDOREZA SARVGHAD-MOGHADAM, B.Sc., M.Sc.

A Thesis

Submitted to the School of Graduate Studies

in Partial Fulfilment of the Requirements

for the Degree

Doctor of Philosophy

McMaster University

# SEISMIC TORSIONAL RESPONSE

# OF

# ASYMMETRICAL MULTI-STOREY FRAME BUILDINGS

DOCTOR OF PHILOSOPHY (1998) McMaster University

(Civil Engineering) Hamilton, Ontario

TITLE: Seismic Torsional Response of Asymmetrical Multi-Storey Frame Buildings

AUTHOR: Abdoreza Sarvghad-Moghadam B.Sc. (Tehran University)
M.Sc. (Tehran University)

SUPERVISOR: Professor W.K. Tso

NUMBER OF PAGES: xv, 222

## ABSTRACT

Seismic torsional response has always been a principal cause of structural failure in every major earthquake. There are numerous observations of damages caused by excessive torsional response in buildings, bridges, and lifeline structures. The torsion-induced failures have been especially catastrophic for multi-storey buildings because torsional response changes the uniform translational seismic floor displacements and causes concentration of demand in elements at the perimeter of the building. This often leads to failure of the over-loaded elements, which in turn initiates progressive collapse of the building.

This study provides a conceptual explanation for the poor seismic performance of torsionally flexible asymmetric structures. These are buildings with a low level of torsional stiffness. Post-earthquake observations and also studies on single storey buildings have shown the vulnerability of these buildings to seismic damages. The study reported in this thesis extends the findings of previous research to multi-storey buildings and provides a theoretical foundation for understanding their seismic performance. Guidelines are developed and formulated to enable designers to identify torsionally flexible asymmetric buildings. This is of prime importance, as it is shown here that corrective measures taken by building codes in the form of statically applied torsional provisions are not effective for this type of structure.

The future generation of codes for designing new structures and retrofitting existing structures will be *performance based.* A structure designed with such an

approach has to meet a specific set of seismic performance criteria for a specific level of seismic hazard. Dynamic analyses of the building will be needed to assess the performance of the building at the many levels of seismic hazard. Preparation of input and interpretation of the large amount of output, resulting from an inelastic response analysis of multi-storey buildings is not practical, even for symmetric buildings. To overcome this, several simplified procedures based on inelastic static analyses are formulated in this thesis. Application of these procedures to some example multi-storey asymmetric buildings has shown that they are sufficiently simple and yet accurate for use in design offices. It is believed that a combination of these methods with sound engineering judgement will provide a practical and economical tool for the earthquake-resistant design profession to implement the performance-based design codes, currently being prepared by many countries, to protect life and property in urban centres in the event of an earthquake.

## ACKNOWLEDGEMENTS

The author is indebted to Professor W.K. Tso, who served as an inspiring advisor and contributed considerably to the research presented in this thesis. His valuable guidance and encouragement throughout the course of this research and his efforts in reviewing and improving the working drafts of this thesis are gratefully acknowledged.

Indebtedness is also owed to members of the supervisory committee, Professors R.M. Korol, D.S. Weaver and S.E. Semercigil for their constructive criticism and suggestions. Gratitude is furthermore owed to Dr. N. Naumoski, Dr. C.M. Wong and Mr. R.S. Smith who served patiently as discussion partners and shared from their experiences. Their friendship has been a great privilege for the author.

The author thanks Dr. K.N. Li who generously shared his computer code with him.

Gratefulness is also expressed to the Ministry of Culture and Higher Education of Iran and McMaster University for their generous support of the work presented in this thesis.

The author dedicates this thesis to his wife, son, and parents for their understanding, patience, and sacrifices.

# TABLE OF CONTENTS

LIST OF FIGURES

CHAPTER 4

# CHAPTER 1

# INTRODUCTION

## 1.1 Background and Literature Survey

It has been observed repeatedly in strong earthquakes that the presence of asymmetry in the plan of a structure makes it more vulnerable to seismic damages. There are reports of extensive damages to buildings that are attributed to excessive torsional responses caused by asymmetry in earthquakes such as the 1972 Managua earthquake (Pomares Calero 1995), the 1985 Michanocan earthquake (Esteva 1987) and the 1989 Loma Prieta earthquake (Mitchell et al. 1990). Figure 1.1 shows damages in a multi-storey building after the 1995 Hyogoken-Nanbu earthquake in Kobe, probably caused by excessive torsional responses because its core was eccentrically located in plan.

Asymmetry in plan causes torsion in a building because the centre of mass and the centre of rigidity[1] do not coincide. The distance between the two centres is termed structural eccentricity and the magnitude of this eccentricity can be estimated. Torsion can also arise in a building due to other sources for which estimating their magnitude is difficult. Some examples of these sources for the so-called *accidental torsion* are the rotational components in the ground motion, an unfavourable distribution of live load, and the difference between computed and actual stiffness/mass/yield strength of the elements. All these factors cause coupling between the lateral and torsional motions in a

1 *Centres of rigidity*: The set of points located at floor levels such that design lateral forces acting through them will produce no floor rotations about a vertical axis. (NBCC Commentaries 1995)

building that leads to non-uniform distribution of in-plan floor displacement. This results in uneven demands on the lateral resisting elements at different locations of the system.

Although torsion has long been recognised as a major reason for poor seismic performance of multi-storey buildings and many studies have been done on the seismic torsional responses of single storey buildings, the analytical and experimental studies on the inelastic seismic response of multi-storey buildings do not have a long history. The reason as explained by De la Llera & Chopra (1995c) is that "*most researchers have been discouraged to look into the multi-storey case in light of the already complex response of single storey asymmetric buildings*".

In most of the available studies on the seismic torsional response of multi-storey buildings, simple building models such as shear beam, are used and the conclusions of the studies are based on the responses of buildings subjected to a limited number of earthquake ground motions. Currently, there is no general agreement on how the torsional effect should be allowed for in seismic design. These observations provided the motivation for the present study in order to provide a better understanding of the problem of seismic damages caused by torsion in multi-storey reinforced concrete frame buildings.

A review of studies on inelastic torsional responses of multi-storey buildings is presented here. First, those investigations on torsional response that involve using the recorded data in buildings during earthquakes are explained. Then experimental research is reviewed, and finally, the analytical work on the subject is explored.

**Study on Responses of Buildings Recorded in Earthquakes**

Conducting experiments to study the inelastic response of a structure is not easy.

To obtain realistic estimations of the inelastic response, the test should be performed on a full-scale prototype building. This is not practical for most structures. However, the recorded motions of some instrumented buildings in earthquakes can provide valuable information about the seismic performance of such buildings. Safak and Celebi (1990) introduced a method to identify torsional vibration in an instrumented building. According to them, similar methods can be used to identify inelastic behaviour in vibrating structures. Lu and Hall (1992) studied the data from two low-rise, extensively instrumented buildings in the 1987 Whittier Narrows Earthquake. Their study involved the investigation of responses of buildings, responding in the elastic and marginally inelastic range, by comparing the behaviour of the buildings with computer simulations. Both buildings were modelled as frame structures using a shear beam idealisation. The recorded data at the basements were used as the ground motion input for the models. The results from unidirectional ground motion input were found to provide a reasonably close match of the actual responses during the earthquake. Using bi-directional ground motion inputs gave an even better match to the measurements.

Sedarat et al. (1994) studied the torsional response characteristics of three regular buildings in California, by analysing the strong motions recorded in these buildings during three recent earthquakes: the 1989 Loma Prieta earthquake, the 1986 Mt. Lewis earthquake, and the 1984 Morgan Hill earthquake. The responses of the buildings were compared with responses of models designed using the provisions of the 1988 Uniform Building Code. The results of their investigation indicated that the code provision was not adequate to account for the torsional responses of these buildings.

## Experimental Studies

Some experiments on scaled models are reported in the literature. Bourahla and Blakeborough (1994) examined the performance of knee braces in asymmetric frame buildings by designing and testing a one-twelfth-scale building model using a shaking table. The test structure was a four-storey frame, three bays deep and three bays wide. Several symmetric and asymmetric arrangements of the frame were tested. The changes in responses due to asymmetry and also due to the unbalanced strength were investigated. It was found that the effect of the unbalanced strength in a nominally symmetric frame buildings is less significant compared with other sources of asymmetry. The energy dissipation capacities of the frames were also studied. Based on the experimental results, it is concluded that the magnitude of the eccentricity in itself is meaningless, but it is the ability of the structure to resist torsion which is critical.

## Analytical Studies

### *Effects of torsion*

Analytical studies have been done to compare the effects of torsion on the elastic and inelastic behaviour of buildings. Study of a seven-storey frame-wall structure (Sedarat and Bertero 1990a, 1990b) demonstrated that linear dynamic analysis may significantly underestimate the effect of torsion on the inelastic dynamic response of the structure. On the other hand, the study of a thirteen storey regular space frame structure (Boroschek and Mahin 1992) showed that the effects of torsion were more severe if the building is modelled as an elastic structure instead of an inelastic one, and the results were found to be highly dependent on the characteristics of the earthquake motions.

Therefore, the issue of severity of torsional effect on the inelastic response of buildings has not been settled.

Teramoto et al. (1992) presented some results of dynamic analyses of an asymmetric 10-storey shear beam building. They used one earthquake record as the input motion. A conclusion of this study is that mass eccentric and stiffness eccentric systems behave differently. When mass eccentricity exists at upper floors only, the eccentricity will also have some effects on the lower floors. However, stiffness eccentricity only affects the floors where eccentricity exists.

Cruz and Cominetti (1992) used a five storey building model in their study and concluded that the overall ductility and the fundamental period of the building are the parameters that most strongly affect the responses of the building.

In a study by De la Llera and Chopra (1996) they concluded that increasing the torsional capacity of the building by introducing resisting planes in the orthogonal direction, and modifying the stiffness and strength distribution to localise yielding in selected resisting planes, are the two most important corrective measures for asymmetric buildings.

***Design Procedures***

Several issues related to the design of multi-storey buildings and evaluation of building codes have been studied in the literature. Bertero and Bertero (1992) developed formulae with the objective of considering the elastic and inelastic torsion in the preliminary design of tall buildings. Bertero (1995) used the classical theorems of plastic analysis to estimate the reduction in the strength of a special class of buildings. De la

Llera & Chopra (1995a) proposed a procedure for including the effects of accidental torsion in the seismic design of buildings.

Ozaki et al. (1988) proposed a seismic design method for multi-storey asymmetric buildings. Azuhata and Ozaki (1992) proposed a method for safety evaluation of shear-type asymmetric multi-storey buildings. In both of these studies, the damage potential due to torsion is evaluated based on the shear and torsional strength capacity and the design shear force and torsional moment for each storey of the building.

In a study by Duan and Chandler (1993) on an asymmetric multi-storey frame building model, they concluded that application of the static torsional provisions of some building codes may lead to non-conservative estimates of the peak ductility demand, particularly for structures with large stiffness eccentricity. In another study they (Chandler and Duan 1993) proposed a modified approach for improving the effectiveness of the static procedure for regular asymmetric multi-storey frame buildings.

**Shortcomings of the Previous Analytical Studies**

The number of parameters required to mathematically define the elastic and inelastic properties of a representative model of an asymmetric multi-storey building is enormous. Therefore, all studies that have been reported in the literature involved using simple models for the building and the conclusions are drawn based on a limited number of earthquake records as ground motions input.

In almost all these studies, the multi-storey frame buildings are modelled as shear buildings. The shear building model is not a good representative of the frame buildings in a seismic zone because a shear building model has strong beams, which causes the plastic

hinges to occur at the columns. This is in contradiction to the *strong column-weak beam philosophy* in earthquake design (Tso 1994). A study by Moghadam and Tso (1996b) has shown that shear-building modelling may lead to unreliable estimates of the important design parameters. Rutenberg and De Stefano (1997) have pointed out that some of the difference between the results of modelling a building as a shear building versus a ductile moment resisting frame building in the study by Moghadam and Tso (1996b) might be due to differences in the periods of the two compared models. Modelling of a building as a shear building involves changing the stiffness of beams to very high values. This in turn causes the period of the shear beam model to change. Therefore; modelling a ductile frame building as a shear building will cause changes in not only the mode of failure, but also the natural periods of the building. Thus, the relevance of observations of studies using shear beam modelling to actual ductile moment resisting frame structures in seismic active regions is questionable.

**Simplified Methods**

Some simplified approaches have been developed in the literature to estimate the inelastic seismic responses of multi-storey buildings. De la Llera and Chopra (1995c) developed a simple model for analysis and design of multi-storey buildings. Each storey of the building is represented by a single super-element in the simplified model. The use of storey shear and storey torque interaction surface (Kan and Chopra 1981, Palazzo and Fraternali 1988, De la Llera and Chopra 1995b) is an important component of this method. The storey shear and torque (SST) surface is basically the yield surface of the storey due to the interaction between storey shear and torque. Each point inside the

surface represents a combination of storey shear and torque that the storey remains elastic. On the other hand, each point on the surface represent a combination of shear and torque that leads to the yielding of the storey. It is shown that the SST surfaces can be used for single storey systems and multi-storey shear buildings. One major assumption embedded in the method is that the stories of a multi-storey building are considered as independent single storey systems. In other words, the floor diaphragms are assumed rigid, both in-plane and out-of-plane. This assumption of out-of-plane rigid diaphragms is equivalent to assuming rigid beams in the building. How realistic is such a model to represent the behaviour of ductile frame buildings in seismic regions is a subject that requires further investigation.

In the performance based design codes and in the guidelines for retrofitting of buildings, the use of different versions of a static inelastic response analysis procedure, commonly known as pushover analysis, has been suggested as a valid tool to evaluate the acceptability of any proposed design, or to assess the damage vulnerability of existing buildings. Moghadam and Tso (1996a) extended the application of the pushover analysis to asymmetrical buildings by using a 3-D inelastic program. Kilar and Fajfar (1997) developed a simple method to conduct pushover analysis for asymmetric buildings by modelling the building as a collection of planar macro-elements. Another method proposed by Tso and Moghadam (1997) incorporates the results of elastic dynamic analyses of the building in the pushover procedure. A further simplification is achieved by requiring only a two-dimensional inelastic analysis program to perform the pushover analysis on asymmetrical multi-storey buildings (Tso and Moghadam 1997, Moghadam

and Tso 1998). Rutenberg and De Stefano (1997) conducted pushover analyses on a 7-storey wall-frame building and found reasonable agreement between results of pushover and inelastic dynamic analyses.

## 1.2 Objectives and Scope

The present study intends, firstly, to investigate systematically the influence of torsion on the inelastic earthquake response of multi-storey ductile frame buildings designed not using torsional provisions. Then, the study evaluates the adequacy of the different forms of torsional provisions commonly used in design. Finally, it proposes some new simplified analysis procedures to facilitate the design of asymmetrical multi-storey ductile frame buildings in seismic regions.

## 1.3 Organization

Chapter 1 of this thesis is an introductory chapter that provides a review of the current literature on the inelastic seismic behaviour of multi-storey asymmetric buildings.

In Chapter 2, after introducing the building models, various parameters used to characterise the overall and local responses of the buildings are defined. Other parts of this chapter deal with issues such as the basic modelling assumptions, the types of analyses used in this study, and the ground motions used in the dynamic analyses.

Chapter 3 deals with the seismic behaviour of asymmetric buildings. The effects of torsion on the elements of the building and the influence of different factors such as torsional stiffness and eccentricity of the building are studied. In the final part of the chapter, a comparative study between the inelastic dynamic responses of two building models are presented to justify the use of the models which are chosen for this study.

The goal in Chapter 4 is to investigate application of different design methodologies to asymmetric multi-storey buildings to allow for torsional effects. The improvements in the behaviour of buildings are compared using three different approaches to distribute the lateral strengths among resisting elements. The approaches are: the static equilibrium method, the static torsional provisions based on the Uniform Building Code (UBC 1997), and the dynamic method based on response spectrum analysis. It is shown that static torsional provisions cannot allow for torsional effects in torsionally flexible buildings. In the final sections of this chapter, two procedures are developed to classify multi-storey buildings into torsionally stiff (TS) and torsionally flexible (TF) buildings. The first procedure uses the dynamic characteristics of buildings while the second procedure is based on the edge displacement ratios of the building under static elastic analyses.

Chapter 5 is devoted to development of simple methods for inelastic seismic response estimation of asymmetrical multi-storey buildings. A state-of-the-art review of the pushover methods is provided. The formulation of a 3-D pushover procedure and the issues related to its application to asymmetrical buildings are explained. Then the focus shifted toward developing a method based on 2-D pushover analysis for estimating the seismic response of asymmetrical buildings.

The final chapter of the thesis, Chapter 6, summarises the conclusions drawn in the previous chapters. It is concluded by a discussion on the future research needs in the area of seismic torsional responses of multi-storey buildings.

There are three appendices associated with this thesis; Appendix A describes the design procedure for the frames of the example buildings. The incorporation of code

torsional provisions in the design of the frames is explained in the Appendix B. In the Appendix C, the accuracy and reliability of the program CANNY (Li 1993), which will be used to perform the inelastic dynamic analyses of this study, are evaluated.

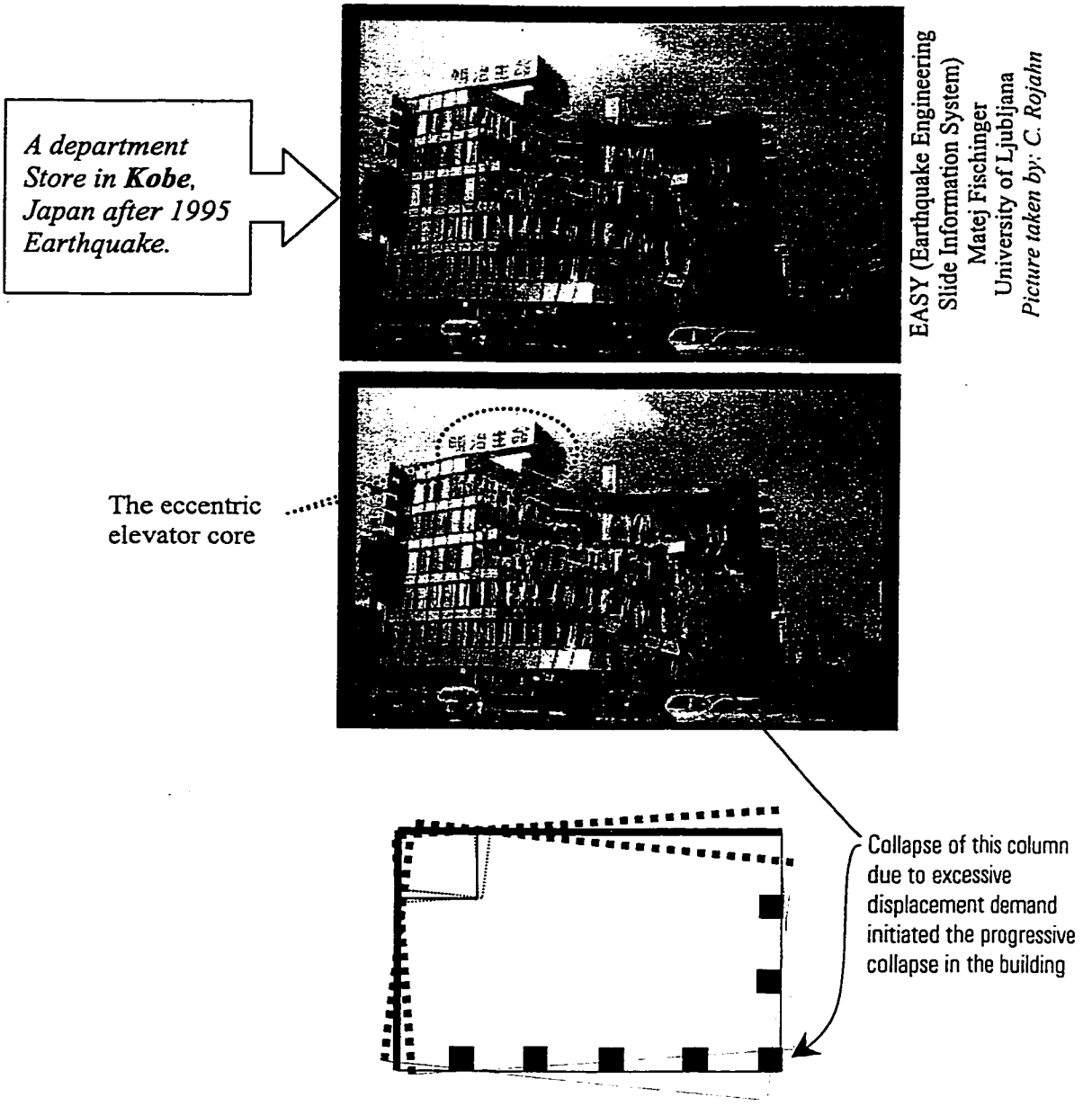


Figure 1.1. Example of structural collapse caused by torsion (Eccentric elevator core led to significant torsional deformation and the collapse of corner columns).

# CHAPTER 2

# STRUCTURAL MODELS, LOADING AND RESPONSE PARAMETERS OF INTEREST

## 2.1 Introduction

The research in this thesis is based on the analyses of a family of structural models representing multi-storey asymmetrical buildings. These models are subjected to both static and dynamic lateral loadings that resemble the loading on buildings during an earthquake. A set of response parameters is used to illustrate the effect of torsion in these buildings.

The purpose of this chapter is to present the basic assumptions and the tools utilised in this research. The different building configurations are introduced first. Then the methods and the loadings used in the analyses are discussed. Finally the chosen response parameters are outlined. The material presented in this chapter prepares the background information for the results to be presented in the subsequent chapters.

## 2.2 Building Configurations

The structural models used throughout this study are uniform seven-storey buildings. Seven-storey building are chosen because they can be considered sufficiently tall to demonstrate many of the features expected from multi-storey buildings subjected to seismic loading. The general plan of buildings is shown in Figure 2.1a. It has a rectangular floor plan of dimensions 17m by 24m, and a uniform floor height of 3m. The

plan considered is mono-symmetric. The asymmetry for the buildings is in the Y-direction and the axis in the X-direction is an axis of symmetry. For convenience, the Y-direction is referred to as the main direction and the X-direction is referred to as the transverse direction. To resist the lateral loads, there are three ductile moment resisting frames (DMRF) in the main direction. One frame is located at the geometric centre of the floor slab, while the other two frames are located at equal distance but at opposite side of the middle frame. It is assumed that the lateral load-resisting elements in the transverse direction are located along the X-axis and they do not contribute resistance to torsion caused by excitations coming from the main direction.

Four structural configurations are derived from general plan of Figure 2.1a. All four configurations have the same lateral stiffness but different torsional stiffness. This is achieved by varying the distance between the frames as shown in Figure 2.1b. Referring the individual frame as a type A frame, the configuration of a plan can be designated as AxAxA where A denotes the frame type and x shows the distance between frames in units of meters. When Frames 1 and 3 are located at the edge of the slab, the configuration becomes A12A12A. A configuration of A3A3A would represent a building that depends on a central core for seismic resistance. Configurations A3A3A and A6A6A represent buildings that are torsionally flexible (TF), while configurations A9A9A and A12A12A represent torsionally stiff (TS) buildings. The classification of these four buildings into TF and TS buildings will be justified later in chapters 3 and 4.

The asymmetry of the buildings is caused by the centre of mass (CM) of the floors being located between Frames 2 and 3. The distance of the CM from the geometric centre is the eccentricity of the building, e, and is measured as a fraction of b, the dimension of the

building normal to the direction of ground motion.

Each type A frame, which will be referred to as Frame A, consists of three bays with bay sizes having dimensions of 6m, 5m and 6m. The beam section is 300mm by 500mm deep and the column section is 500mm by 500mm. The floor and roof thicknesses are 125mm. The member sections and slab thickness remain unchanged along the height of the frame. It is designed to takes the gravity load from a tributary area of 3m by 17m. The remaining portion of the gravity load is assigned to gravity frames which do not contribute to the lateral resistance of the building, and are therefore omitted in the figure. In addition, each frame is designed to take one third of the seismic load calculated using the National Building Code of Canada (NBCC 1995). The lateral design strength is obtained using the base shear formula given in the code with the site factor v= 0.3 and the force modification factor R=4. The S factor in NBCC base shear formula has a spectral shape that is similar to the mean 5% damped Newmark-Hall spectrum (Newmark and Hall 1982). For ease of comparison later with the input ground motion spectra, the Newmark-Hall spectrum is used as the design spectrum. The design base shear for Frame A is 400 kN. No torsional provision is taken to arrive at the design base shear of the frame. The design of the beam and column reinforcements follows the Canadian concrete code (CSA Standard A23.3-94) for DMRF. The design loads and detail design procedure of Frame A are given in Appendix A.

### 2.3 Computer Code CANNY

The static and dynamic behaviour of the multi-storey asymmetric buildings in the inelastic range are the main focus of the study reported in this thesis. Therefore a

computer program with the ability of performing 3-D inelastic static and dynamic analysis was necessary. The program CANNY (Li 1993) has been chosen as the base computer code in performing the analyses. To ensure its reliability, a study has been carried out to evaluate this program by comparing its results with the responses derived from some other commonly used computer programs. The details of checking the reliability of CANNY can be found in Appendix C.

## 2.4 Basic Assumptions in Modelling

The following are the main modelling assumptions used in this study.

### *2.4.1 Modelling of the Building*

1- Rigid slab: It is assumed that all the frames in the buildings are connected by floor diaphragms that are rigid in their own plane. Therefore every floor has only two translational and one rotational degrees of freedom. The in-plane displacements of all the nodes on the floor are constrained by these degrees of freedom. However, the nodes can have independent vertical displacements.

2- Fixed base: The frames of buildings are assumed to be fixed at their base on an infinitely rigid foundation. No soil-structure interaction effect is considered in this study.

3- One directional earthquake input: Only one component of ground motion is applied at the base of the buildings. Due to the fixed base assumption, all supports are assumed to move in phase. No vertical ground motion components are applied to the buildings.

4- Lumped mass at floor level: The mass and the mass rotational moments of inertia of the buildings are assumed to be lumped at the floor levels.

5- Small deflections: The deflections of the frames are assumed to be small compared to their dimensions, and the static or dynamic equilibrium is established based on the initial configurations of the frames. In other words, the geometrical nonlinearity is ignored. However, the effect of gravity loads on storey shear and moment due to the lateral floor displacement (P-Δ effect) is taken into account.

6- Joints: It is assumed that the beam column joints are designed such that the joint deformation is negligible.

### *2.4.2 Modelling of the Frames*

There are different analytical models available to simulate structural frames. In this study a beam element and a column element are used to model the elements of the frames in the buildings.

The beam element is a one-component model. The inelastic flexural deformations are represented by the rotation of two inelastic bending springs at the ends of the element. The shear and the axial deformations of the beam are approximated by independent shear and axial springs placed at its mid-span. The model does not include the interactions among the bending, shear and axial deformations. Due to the rigid floor slab assumption, there is no axial deformation in the beams.

The column element used in this study is similar to the beam element. The main difference is that the stiffness of the column element against torsional deformation can be simulated by a torsional spring. A bilinear moment-rotation hysteretic model is considered for the inelastic springs at the ends of the beam and the column elements. The strain-hardening stiffness of the structural members is assumed to be 3% of their initial

elastic stiffness. It is assumed that sufficient transverse reinforcement has been provided for the structural members following the CSA (CSA Standard A23.3-94) design procedure such that the stiffness and strength deterioration due to shear and bond loss is not significant. Therefore, these effects are not modelled.

### *2.4.3 The P-Δ effect*

When a building deflects laterally, the gravity load of the floors causes extra (secondary) moments in the columns. This phenomenon is called the P-Δ effect and may increase the inelastic deformations. To allow for this effect the following linearised approximation of the geometric stiffness matrix has been used to modify the shear terms in the stiffness matrix of the elements:

$$[K_G]=\frac{P}{H}\begin{bmatrix}+1 & -1\\ -1 & +1\end{bmatrix} \tag{2.1}$$

where $[K_G]$ is the geometric stiffness matrix, $P$ the axial load in the column and $H$ the column height.

## 2.5 Loading to Obtain the Static Inelastic Responses

In this study, the static responses are obtained using pushover analyses. In a pushover analysis, a sequence of inelastic static analyses is performed on the building, when it is subjected to a set of monotonically increasing lateral loads. The load distribution along the height remains unchanged as the building deflects. In every load step, a linear force-displacement relationship is assumed and the structural stiffness matrix is kept constant. The incremental displacements corresponding to the degrees of freedom are calculated at the end of each load step. Based on the incremental

displacements, the incremental member deformations and forces are obtained. When an element reaches the inelastic range, the calculated increments of force and displacement will not satisfy the inelastic force-displacement relationship of that element. Then the stiffness matrix will be updated. To restore equilibrium, the unbalanced load is calculated and applied to the building in the beginning of the next load step.

The main result of a pushover analysis is the base shear versus top deflection curve. This curve is called the capacity curve or sometimes referred to as the performance curve of the structure. One application of the pushover analysis is to check the damage pattern of a structure. As an example, a pushover analysis is carried out to check if Frame A would behave with the characteristics of a frame that satisfies the strong column-weak beam design philosophy. The equivalent static lateral load distribution is taken to be triangular along the height of the frame. The capacity curve of the frame is shown in Figure 2.2a. It is linear initially. The hinge patterns at load stages 1,2 and 3 are shown in Figure 2.2b. Hinges start to form at the beams when the lateral load exceeds the design base shear value of 400kN as shown in load stage 1. At stage 2, column hinges have been formed at the base of the frame resulting in a significant stiffness deterioration of the structure. Further increase of the lateral load causes additional hinges to form at other locations in the beams and columns. It should be noted that there is no column with hinges at both the top and bottom during these stages of the pushover analysis. In other words, the side sway failure mechanism caused by top and bottom column hinging is unlikely to occur in this frame during an earthquake. This example shows that Frame A has the characteristics of a properly designed DMRF and also illustrates one typical application of pushover analysis.

It is interesting to note that a bilinear approximation of the capacity curve shows that the frame has an effective strength of 540 kN, which is 35% higher than the design strength of 400 kN. This overstrength is the result that Frame A is designed based on appropriate load combinations of the lateral and gravity loads, as specified in the Canadian design code (NBCC 1995).

### 2.6 Loading to Obtain the Seismic Responses

To obtain the responses under earthquake ground motion excitations, dynamic analyses are performed by solving the equations of motion for the building, using a step-by-step numerical integration procedure. Since, the masses of buildings are lumped at the CM of the floors, the mass matrix is a diagonal matrix given by:

$$[M]=\begin{bmatrix} m_1 & & & & & & \\ & m_1 & & & & & \\ & & I_{m1} & & & & \\ & & & \ddots & & & \\ & & & & m_n & & \\ & & & & & m_n & \\ & & & & & & I_{mn} \end{bmatrix} \qquad (2.2)$$

where $m_1$, ..., $m_n$ = lumped masses at floors levels, $I_{m1}$, ..., $I_{mn}$ = rotational mass moment of inertia of the floors at CM, and $n$ = total number of floors.

The damping in the building is assumed to be of the viscous type. In solving the equations of motion, it is further assumed that the damping matrix has the Rayleigh form. It means that the damping matrix can be written as a linear combination of the mass matrix and stiffness matrix:

$$[C]=\alpha\ [M]+\beta\ [K] \qquad (2.3)$$

where the two factors $\alpha$ and $\beta$ can be determined from the modal damping ratios of any two modes of the building:

$$\alpha = \frac{4\pi(T_m\xi_m - T_n\xi_n)}{T_m^2 - T_n^2} \tag{2.4a}$$

$$\beta = \frac{T_m T_n (T_m\xi_n - T_n\xi_m)}{\pi(T_m^2 - T_n^2)} \tag{2.4b}$$

where

$T_m$ and $T_n$ = undamped period of the $m^{th}$ and $n^{th}$ modes.

$\xi_m$ and $\xi_n$ = damping ratio of the $m^{th}$ and $n^{th}$ modes.

The first and second modes are used in this study to determine the $\alpha$ and $\beta$ factors. The damping ratios for these two modes are assumed to be 5% of critical damping. This value is considered appropriate for cracked reinforced concrete structures (Newmark and Hall 1982).

The stiffness matrix of a structure is assembled from the stiffness matrices of its elements. During each time increment, the stiffness matrix is assumed to remain constant. If the stiffness of one or more members has changed at the end of the current time step, the stiffness matrix will be updated based on the change of stiffness in those elements.

The Newmark-β method for numerical integration with $\beta = 0.25$ is employed to solve the equations of motion.

## 2.7 Earthquake Ground Motion Records

Inelastic dynamic analyses are carried out by subjecting the structural models to earthquake ground motion excitations at their bases. An ensemble of 10 horizontal ground motion records is used as input to reduce the dependency of the responses on the characteristics of a single earthquake excitation. The records are chosen based on the criterion that the shapes of their response spectrum are similar to the Newmark-Hall design spectrum in order to minimise the mismatch in frequency contents between the input ground motion and the design spectrum. Each record is scaled to a peak velocity of 0.3 m/s to match the design site factor value. The mean and mean plus one standard deviation of the 5% damped acceleration response spectra for the ensemble of records are shown in Figure 2.3. The appropriately scaled design spectra are also presented. Other information related to the records is listed in Table 2.1.

## 2.8 Response Parameters

The responses of a building during earthquake can be taken as a measure of damage potential to its structural and/or non-structural elements. To assess the performance of a building, different parameters are needed to express the level of responses produced in the building both locally and globally. The main response parameters considered in this study are: (i) the maximum interstorey drift, (ii) the maximum floor displacement, (iii) the maximum column ductility demand, and (iv) the maximum beam ductility demand in a storey. The first parameter is a good indicator of non-structural damage. The second parameter is important for evaluation of the pounding damage potential between buildings. These two parameters describe the global responses of

a building. The third and fourth parameters are traditionally used indicators of structural damage in DMRF. They represent the local (member) responses.

Since dynamic analyses are performed using an ensemble of ground motions as input, the mean values of the response parameters are focused in this study. When the dispersion of responses is also of interest, the range of response values will be presented by a bar graph as shown on the Figure 2.4.

In addition to the four designated response parameters, capacity curves (Figure 2.2a) can also be considered as a global response parameter. The capacity curve, produced by inelastic static (pushover) analysis, provides information about the overall stiffness and strength of the buildings.

## 2.9 Summary

The highlights of the tasks done in this chapter are:

- The building configurations considered in this study are introduced.
- The methods of analyses and modelling assumptions are explained.
- The ground motion excitations are summarised.
- The response parameters considered for comparing the performance of the buildings are explained.

Table 2.1. List of input ground motions

| Earthquake<br>*Site* | Date | Mag. | Soil | Source Dist. (km) | Y Comp. | X Comp. |
|---|---|---|---|---|---|---|
| Imperial Valley, California<br>*El Centro* | 05/18/40 | 6.6 | Stiff Soil | 8 | S00E | S90W |
| Kern County, California<br>*Taft Lincoln School Tunnel* | 07/21/52 | 7.6 | Rock | 56 | S69E | N21E |
| San Fernando, California<br>*Hollywood Storage P.E. Lot, LA* | 02/09/71 | 6.6 | Stiff Soil | 35 | N90E | S00W |
| San Fernando, California<br>*Griffith Park Observatory, LA* | 02/09/71 | 6.6 | Rock | 31 | S00W | S90W |
| San Fernando, California<br>*234 Figueroa St., LA* | 02/09/71 | 6.6 | Stiff Soil | 41 | N37E | S53E |
| Near S. Coast of Honshu, Japan<br>*Kushiro Central Wharf* | 08/02/71 | 7.0 | Stiff Soil | 196 | N90E | N00E |
| Near E. Coast of Honshu, Japan<br>*Kashima Harbor Works* | 11/16/74 | 6.1 | Stiff Soil | 38 | N00E | N90E |
| Monte Negro, Yugoslavia<br>*Albatros Hotel, Ulcinj* | 04/15/79 | 7.0 | Rock | 17 | N00E | N90W |
| Michanocan, Mexico<br>*El Suchil, Guerrero Array* | 09/19/85 | 8.1 | Rock | 230 | S00E | N90W |
| Michanocan, Mexico<br>*La Villita, Guerrero Array* | 09/19/85 | 8.1 | Rock | 44 | N90E | N00E |

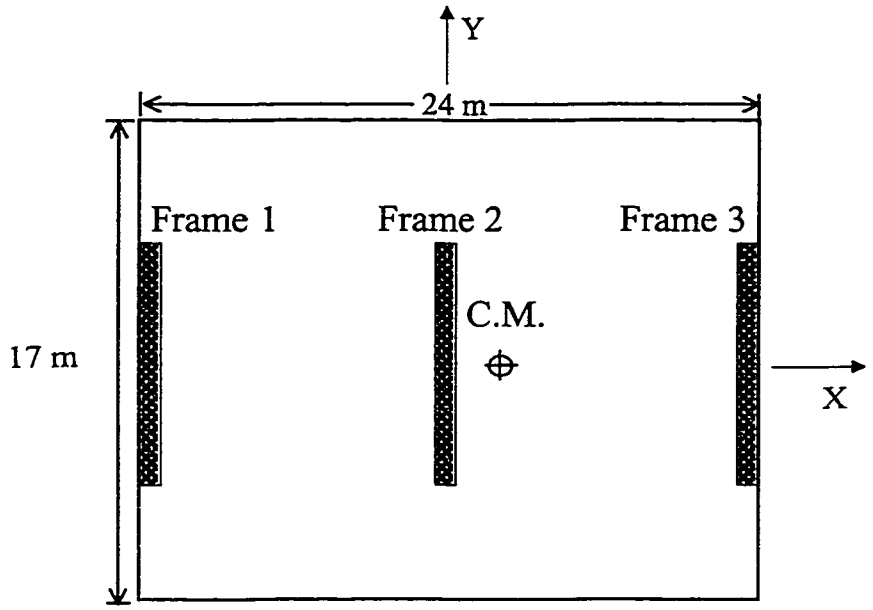


(a)

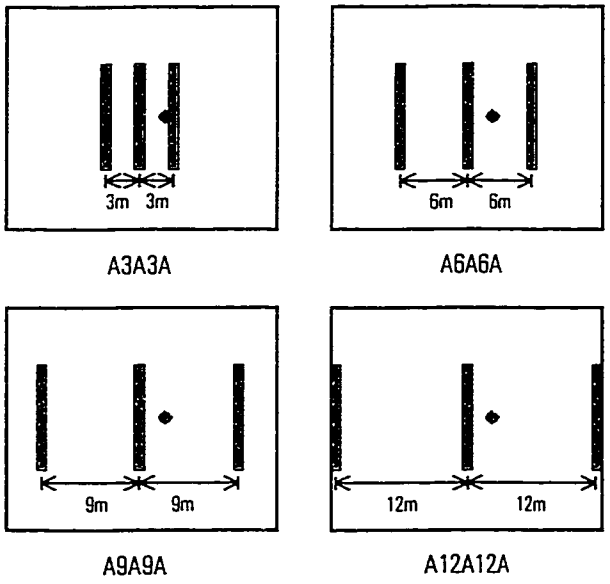


(b)

Figure 2.1. Plan configurations for the seven-storey buildings;
(a) General plan and dimensions
(b) Four different plan configurations

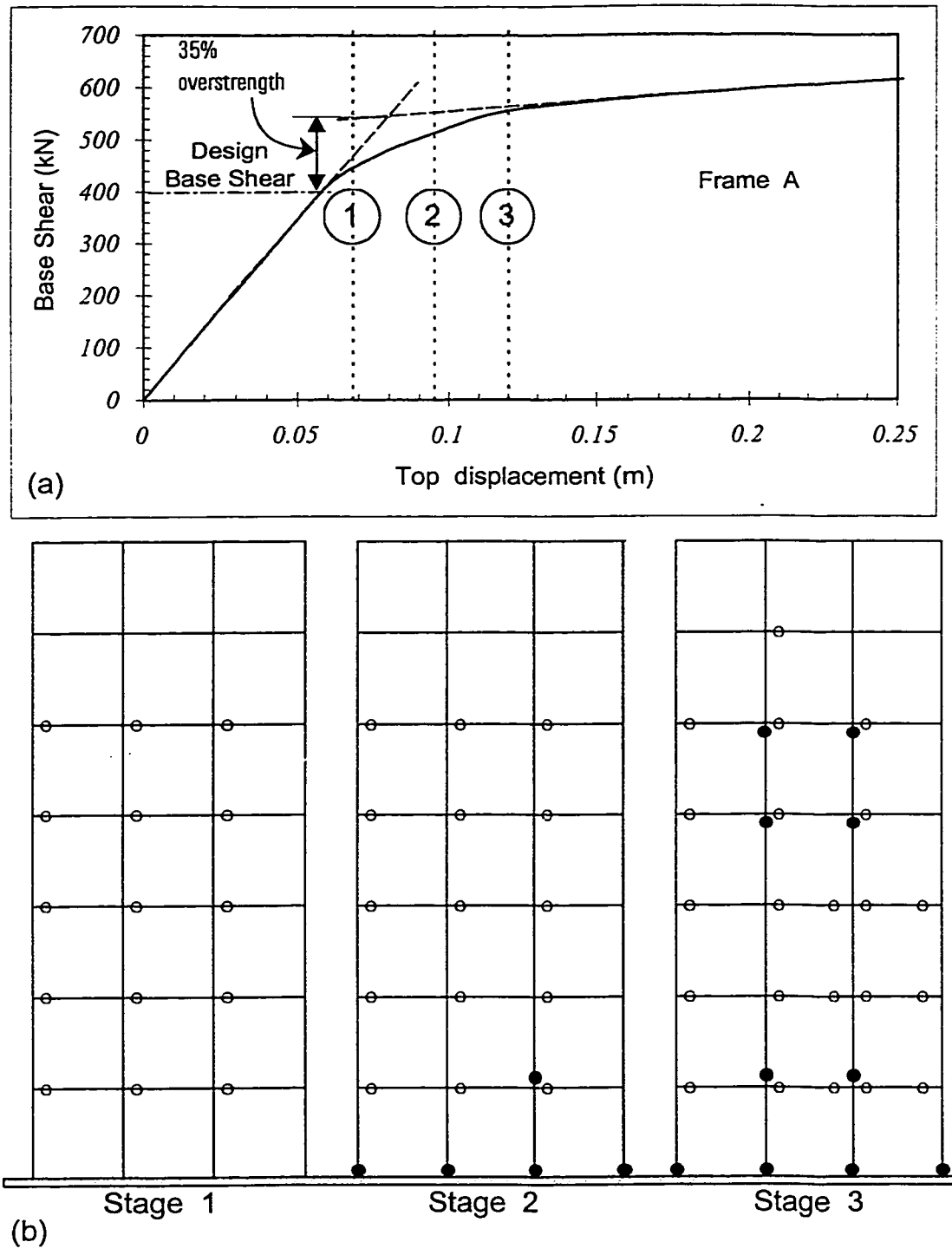


Figure 2.2. Hinging sequence in pushover analysis of Frame A
(a) Capacity curve (b) Hinge pattern of each stage

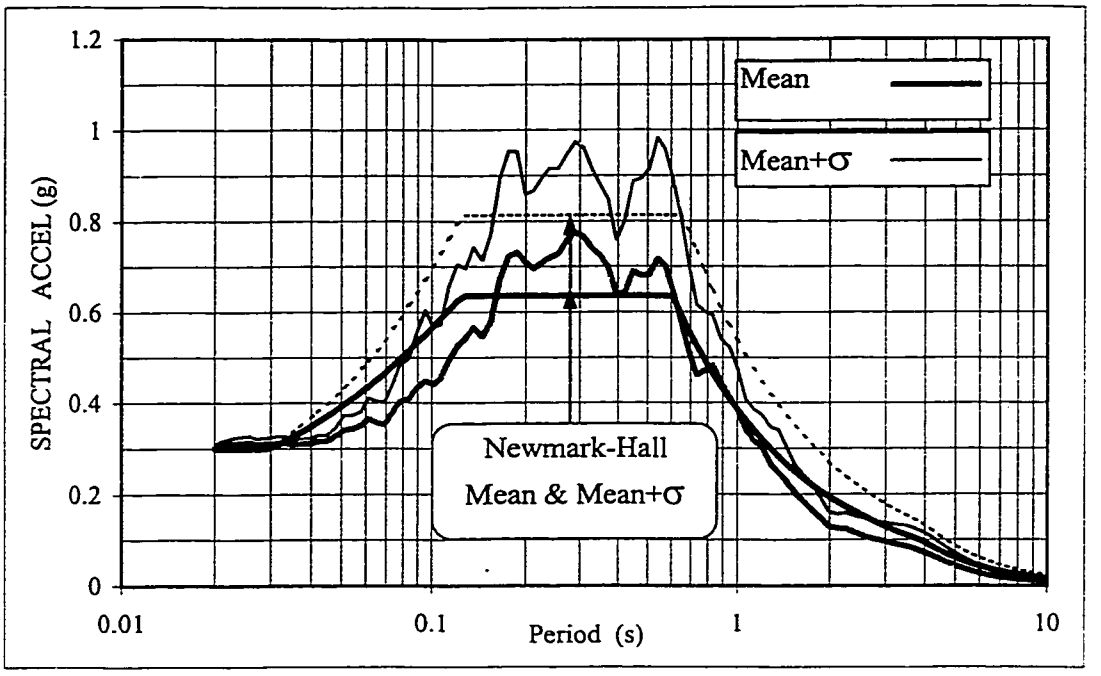


Figure 2.3. The response spectrum of ground motions

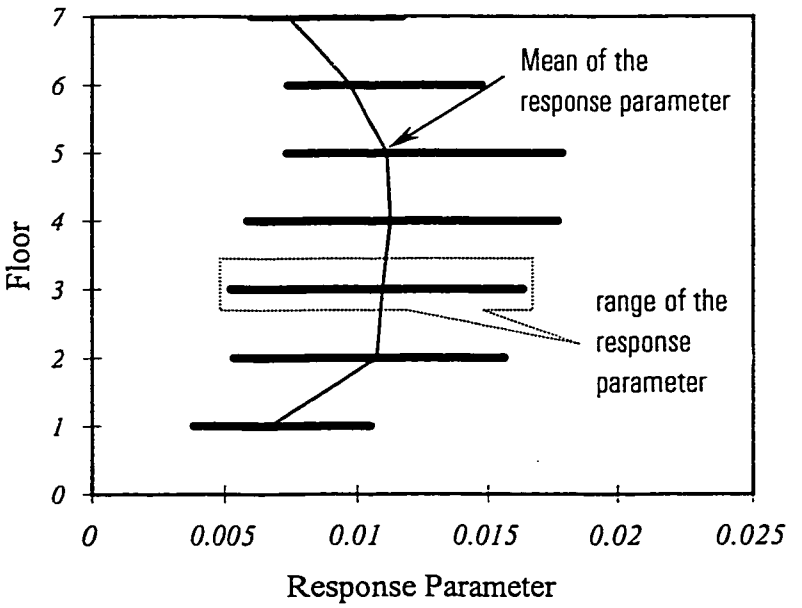


Figure 2.4. Mean and range of a typical response parameter

This page is intentionally left blank.

# CHAPTER 3

# SEISMIC BEHAVIOUR OF ASYMMETRICAL MULTI-STOREY FRAME BUILDINGS

## 3.1 Introduction

This chapter discusses the characteristics of asymmetric multi-storey buildings and the parameters that affect their seismic behaviour. The consequences of asymmetry on the different response parameters such as displacements, storey drifts, beam and column ductility are first discussed in section 3.2. Then the significance of torsional stiffness on the behaviour of asymmetric buildings are systematically studied and explained in section 3.3. The effects of eccentricity on different classes of multi-storey buildings are examined in section 3.4. Finally, a comparative study is conducted for a building with transverse frames subjected to bi-directional excitation, and a building without transverse frames but subjected to unidirectional excitation. The purpose of this comparative study is to show that the results from the present study can provide reliable trends applicable to actual asymmetric multi-storey frame buildings in the field.

## 3.2 Consequences of Asymmetry

Asymmetric and symmetric buildings behave differently in earthquakes. Unlike symmetrical buildings, the responses of asymmetrical buildings are affected by torsional responses. Torsion particularly influences the responses of the structural frames located near the perimeter.

To demonstrate the torsional effects, a study is carried out on two multi-storey buildings. The first building is a seven-storey symmetric building with three type A frames in the Y-direction (Figure 3.1a). The second building is also a seven-storey building but it is asymmetric due to the non-uniform mass distribution on its floors as shown in Figure 3.1b. In the asymmetric building, the CM of the floors are shifted 2.4m (10% of the width of the building) from the geometric centre towards Frame 3. For simplicity, these two buildings will be referred to as Building S (for symmetry) and Building A (for asymmetry) respectively.

Both buildings are subjected to unidirectional excitations along the main direction at their bases. The ensemble of 10 horizontal ground motion records described in chapter 2 is used as input. Each record is scaled to a peak velocity of 0.3 m/s to match the design site factor value for the buildings. The CANNY computer program is used to carry out the analyses.

Plots in Figure 3.2 show the mean of the parameters of interest at the edge frames (Frame 1 and Frame 3) of the two buildings. Since Building S has no torsional responses, the responses of Frames 1 and 3 are identical and hence there is only one curve shown for Building S. Figure 3.2a shows the mean of the maximum floor displacements; Figure 3.2b the mean of the maximum interstorey drift ratios. Figure 3.2c and Figure 3.2d show the mean of the maximum column and beam ductility demands respectively. A comparison of the response curves of Frames 1 and 3 of the asymmetric building to those of the symmetric building shows that torsion increases the responses of Frame 3 while decreases the responses of Frame 1 in Building A. The increase of response in Frame 3 is of the order of 30%. These results show that torsion caused noticeable changes in the

distribution of different response parameters at the edge frames of the asymmetrical building.

### 3.3 Effect of Torsional Stiffness

Four structural configurations are used to study the effect of torsional stiffness on the building responses. All four configurations have the same lateral stiffness but have different torsional stiffness. This is achieved by varying the distance between the frames. Figure 3.3 shows the four configurations. The A3A3A and A6A6A configurations represent buildings that are torsionally flexible (TF), when compared to configurations A9A9A and A12A12A which represent torsionally stiff (TS) buildings. All four buildings will have the same eccentricity of 0.1b, or 2.4m.

The overall static behaviour of these buildings under lateral loading can best be illustrated using their capacity curves as shown in Figure 3.4. They are obtained by carrying out pushover analyses on the buildings, using a triangular load distribution with the lateral loads applied at the CM of the floors. The capacity curve of a symmetrical building is also included for reference. This reference building has three type A frames symmetrically distributed but has no eccentricity, hence no torsional deformation under lateral loading. An alternative interpretation of this reference capacity curve is that it represents the capacity curve of a building having infinite torsional stiffness. A comparison of the five curves shows that a decrease in torsional stiffness of the building has the effect of lowering the effective stiffness of the building at CM, and also reducing the overall strength of the building. The curve for the reference building is an upper bound capacity curve for this set of buildings.

To study their seismic behaviour, the buildings are exposed to the chosen ensemble of earthquake records and their behaviours are discussed based on the mean of the maximum responses. For ease of reference, the two edges of buildings, parallel to the direction of loading, will be referred to as edge 1 or edge 3, as shown on Figure 3.3. Edge 1 is sometimes called the stiff edge while edge 3 is called the flexible edge in published literatures.

The means of the maximum interstorey drift ratios at the edge 1 of these buildings are shown in Figure 3.5. To highlight the contribution of torsion, the mean response of the reference model is also given. A comparison between the mean curves for the different configurations to that from the reference building shows that torsional response leads to additional interstorey drifts for the two TF buildings, but it decreases the interstorey drifts for the two TS buildings. The increase is substantial for the A3A3A configuration building, which is torsionally the most flexible of the four configurations.

The range of interstorey drifts experienced at different storeys is presented as horizontal bar lines. The range provides a measure of the dispersion of the responses. The results show that the dispersion is highest in the torsionally most flexible building and is lowest in the torsionally most stiff building. Therefore, TF buildings are not only susceptible to interstorey drift increase at the edge 1, but this increase is sensitive to the actual input ground motions. In the design context, this implies that more care is needed to establish the seismic interstorey drifts at this edge of TF buildings.

Another response parameter at this edge is the maximum floor displacements. The general trend shown by the interstorey drifts is repeated here, namely, there is substantial increase in floor displacements for the TF buildings and a marginally decrease in floor

displacements for the TS buildings as shown in Figure 3.6. The results on dispersion show that the floor displacement is also more sensitive to ground motion inputs in the TF buildings.

The information on the maximum interstorey drift ratios and maximum floor displacements at the other edge (edge 3) is presented in Figures 3.7 and 3.8. Unlike the responses at the edge 1, torsion always increases the interstorey drifts and floor displacements at the edge 3 of the buildings. The increase appears to be relatively insensitive to the torsional stiffness of the buildings as the interstorey drifts and also the floor displacements at this edge are similar in all four buildings.

The maximum column ductility demands in Frames 1 and 3 are shown in Figure 3.9. Only the results for the torsionally most flexible and the stiffest buildings are presented. Compared with the ductility demands of the reference building, the change in column ductility demands is minor in the TF building. For the TS building, the demands are reduced in Frame 1, but increased in Frame 3. The beam ductility demand results are presented in Figure 3.10. There is an increase of beam ductility demand in Frame 1, but a decrease of demand in Frame 3 in the TF building. The trend is reversed for the TS building.

While the trends shown in Figures 3.9 and 3.10 are correct, the actual magnitude of the change is distorted. Being more flexible, building A3A3A has a larger rotational response than the A12A12A building. However, the locations of Frames 1 and 3 in building A3A3A are closer to the centre of rotation than those in building A12A12A. In other words, the lever arms of the Frames 1 and 3 in building A3A3A are smaller. Due to this compensating factor, the magnitude of change in ductility demands turns out to be similar

for these two buildings.

Reviewing the results, it is evident that the torsional stiffness of a building has a strong influence on its seismic response, and will affect the design parameters at the edges of the building differently. The difference in behaviour of the TF and TS buildings can be explained in terms of the modal characteristics of coupled torsional-translational vibrations. In the first mode of vibration, the contributions from the translational and rotational floor motion to the lateral displacement at edge 1 is subtractive, while the contribution to the lateral displacement at edge 3 is additive as shown diagrammatically in Figure 3.11a. In the second mode of vibration, the translational and rotational floor motion contributions are additive at edge 1 and subtractive at edge 3 as shown in Figure 3.11b. Since the buildings are subjected to translational ground motions as input, the responses of the buildings come mainly from the lowest translational predominant mode. The TS buildings have their first mode as a translational predominant mode. As a result, torsion tends to decrease the responses at edge 1 while increase the responses at edge 3. The TF buildings have their second mode as the lowest translational predominant mode, with the consequence that there is a response increase at edge 1.

Since torsional stiffness has a large influence on the seismic response of asymmetrical buildings, there is a need to classify these buildings into TS (first mode is translational predominant) and TF (the second mode is translational predominant) buildings. A procedure to achieve such classification will be discussed in chapter 4.

### 3.4 Effect of Eccentricity

Eccentricity traditionally has been taken as the measure of asymmetry in a

building. It is defined as the distance between the centres of mass and rigidity. To study the effect of eccentricity on multi-storey asymmetric building responses, two structural configurations are considered. A building with configuration of A3A3A is used to represent TF buildings, while a building with configuration A12A12A is used to represent TS buildings. For each configuration, three values of eccentricity are considered, namely: 0.05b (1.2m), 0.1b (2.4m) and 0.15b (3.6m). Since the stiffness of each frame is the same, the centres of rigidity in both buildings are at the geometric centres. The different eccentricity used is due to different locations of the centres of mass from the geometric centres: A symmetric building is also included in this analysis to serve as the reference system. Inelastic dynamic analyses are performed on the buildings using the chosen ensemble of 10 ground motion records shown in Table 2.1.

Figure 3.12 shows the mean values for the maximum displacements and storey drift ratios for the symmetric building and the three frames in the TS building with different levels of eccentricity. There is a change of responses between the asymmetrical buildings and that of the reference building. Asymmetry causes a decrease of deformations at edge 1 but an increase in deformations at edge 3. However, the increase of the maximum deformations due to increase in the level of eccentricity is minimal. This implies that the responses of the TS building are relatively insensitive to further increases in eccentricity. Figure 3.13 shows the mean values of the maximum ductility demand on the beams and columns of the building. They follow the trend observed from the deformation curves.

Figure 3.14 shows the mean values for the maximum displacements and storey drift ratios for the symmetric building and the TF building with different eccentricities. A

small value of eccentricity (5%), leads to a considerable increase of deformations in edge 1 and a small increase in edge 3 of the TF building. However unlike the TS building, the rate of change in edge responses commensurates with change of eccentricity. It should be noted that the maximum deformations in the middle of the TF building remains close to deformation of symmetric building, while the edges experience much higher deformations. This demonstrates the importance of torsional response in the TF building.

Figure 3.15 shows the mean values of the maximum ductility demands on the beams and columns of the TF building. The maximum values of ductility demand for the beams and columns of the frames of the asymmetric building are similar to the symmetric building for small eccentricity. With the increase in eccentricity there is only a minor increase in the ductility demands of members in Frame 1 and a small decrease for those in Frame 3. Again, it should be realised that the lever arms from the centre of rotation to Frames 1 and 3 are small in this building. Therefore, the magnitude of change in ductility demands in A3A3A may not reflect the true change in response if the frames were located at the edges of the floor plan. The edge deformation responses discussed in Figure 3.14 are more representative of change in response of the TF building.

The study in this section shows another difference between TS and TF buildings. The TS building is not sensitive to increase in eccentricity, while the TF building is vulnerable to eccentricity increases.

## 3.5 Justification of Using Unidirectional Excitation on Models Used in this Study

Real buildings have lateral resisting elements in two orthogonal directions to

resist horizontal loading imposed by the ground motions and ensure building stability. Also, they will be subjected to horizontal ground motions from both orthogonal directions simultaneously (bi-directional excitation) during an earthquake. It is proposed in this study to represent buildings by structural models having lateral resisting elements in one direction only, and subject the models to ground motions coming from one direction. The purpose of this section is to justify the use of such simpler structural modelling and simpler mode of excitation by means of a comparative study.

The plans of the two buildings chosen for this study are shown in Figures 3.16a and 3.16b. The building shown in Figure 3.16a has three A frames spaced at 12m apart in the Y-direction, and has two type B frames spaced 18m apart in transverse direction. The stiffness and strength properties of beam and column elements in the type B frames are assigned 1.5 times of those in a type A frame. Thus the total lateral strength and stiffness of this building in the X and Y-directions are similar. The building shown in Figure 3.16b is a building designated as the A12A12A configuration used in this thesis. Both buildings are mass eccentric, with the centre of mass (CM) being shifted 2.4m from the geometric centre of the floors.

Both components of each earthquake ground motion record in the ensemble of records are applied to the building with transverse frames. The Y-direction component is scaled to level of design earthquake intensity (peak velocity = 0.3 m/s) and then the same scaling factor is applied to the other component along the X-direction. The A12A12A building is subjected to unidirectional excitation only.

A series of 3-D inelastic dynamic analyses of buildings subjected to ground motions are performed and the mean values for different response parameters are calculated. Figure

3.17 compares the Y-direction displacements and storey drift ratios while Figure 3.18 compares the beam and column ductility demands on the Y-direction frames of the two buildings. The solid lines show the maximum responses for the building with transverse frames subjected to bi-directional excitation and the dash lines show the responses for the A12A12A building. A comparison between solid and dash lines on these figures shows that the responses are similar in the two cases. The close agreement between the results justifies the structural modelling and unidirectional excitation used in this study. Similar observations have been made by Correnza et al. (1994) for single storey eccentric systems.

### 3.6 Summary

The highlights of material presented in this chapter are:

- The consequences of asymmetry on the different response parameters at the edges of asymmetrical buildings are discussed.
- The torsional stiffness of a building is an important parameter. One should classify asymmetric buildings into torsionally flexible (TF) and torsionally stiff (TS) buildings because the locations of the vulnerable frame in these two classes of buildings are different.
- The sensitivity of TS and TF buildings to increase of eccentricity is studied. It is concluded that the main change in behaviour of the TS building occurs when it changes from a symmetric building to an asymmetric building. Responses of building are not sensitive to further increase in eccentricity. However, vulnerability of the TF building depends on the value of eccentricity. Increase of eccentricity increases the

maximum responses in the edges of the building.

- The structural modelling and the unidirectional excitation that are used in this study are justified. It is believed that the trends found in this study should be applicable to actual asymmetrical multi-storey frame buildings.

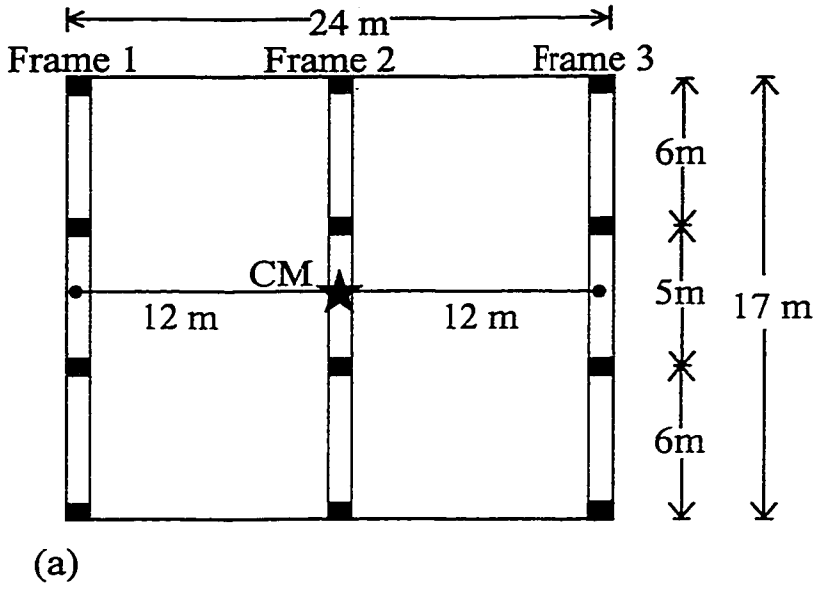


Figure 3.1. Plan configurations for the symmetric and asymmetric buildings;
(a) Building S
(b) Building A

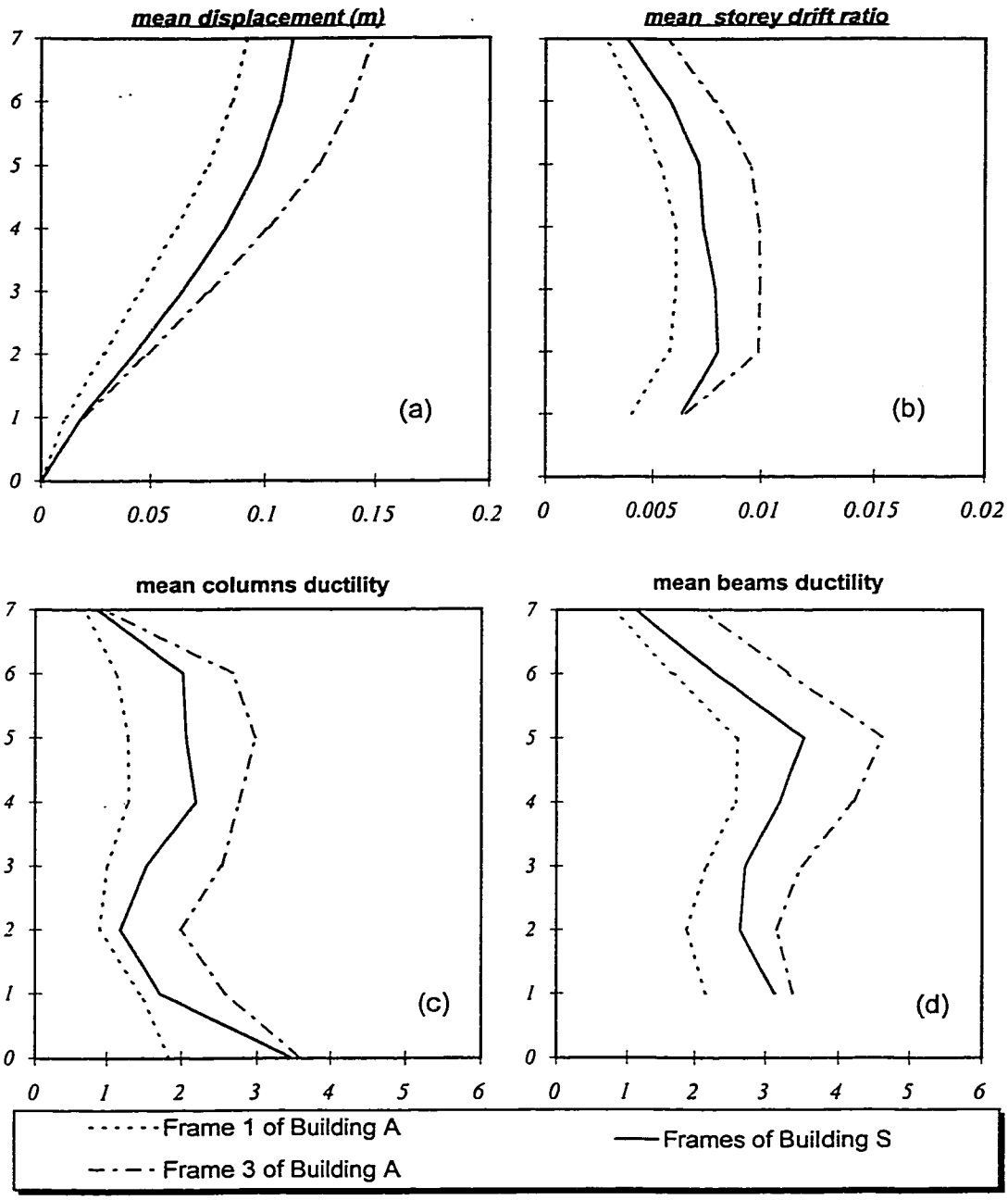


Figure 3.2. Consequence of asymmetry on frame responses; (a) Displacements, (b) Interstorey drifts, (c) Column ductility, (d) Beam ductility

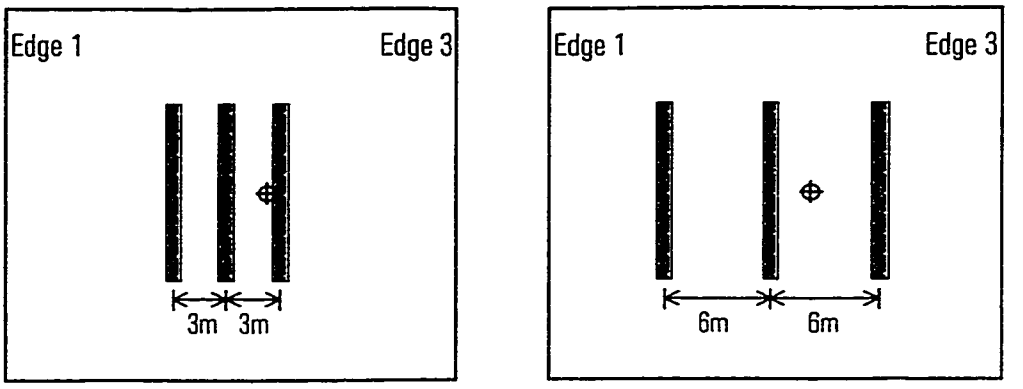


A3A3A.1 (a)

A6A6A.1 (b)

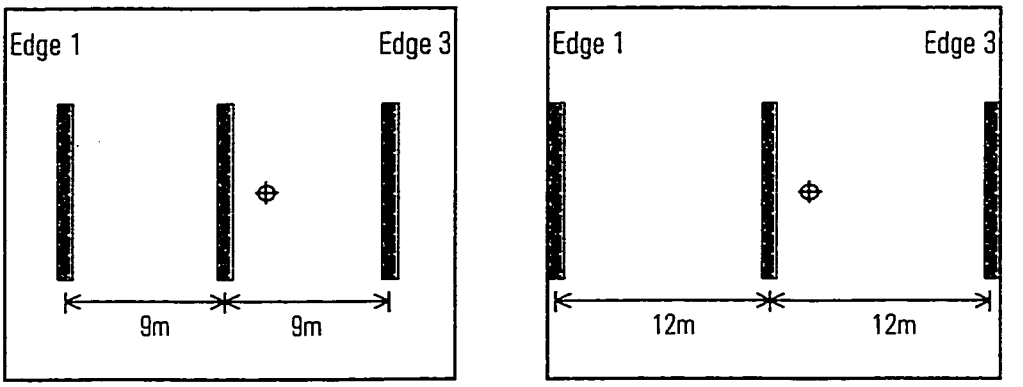


A9A9A.1 (c)

A12A12A.1 (d)

Figure 3.3. Four plan configurations for the seven-storey buildings;
(a) A3A3A with e/b =0.1,
(b) A6A6A with e/b =0.1,
(c) A9A9A with e/b =0.1,
(d) A12A12A with e/b =0.1

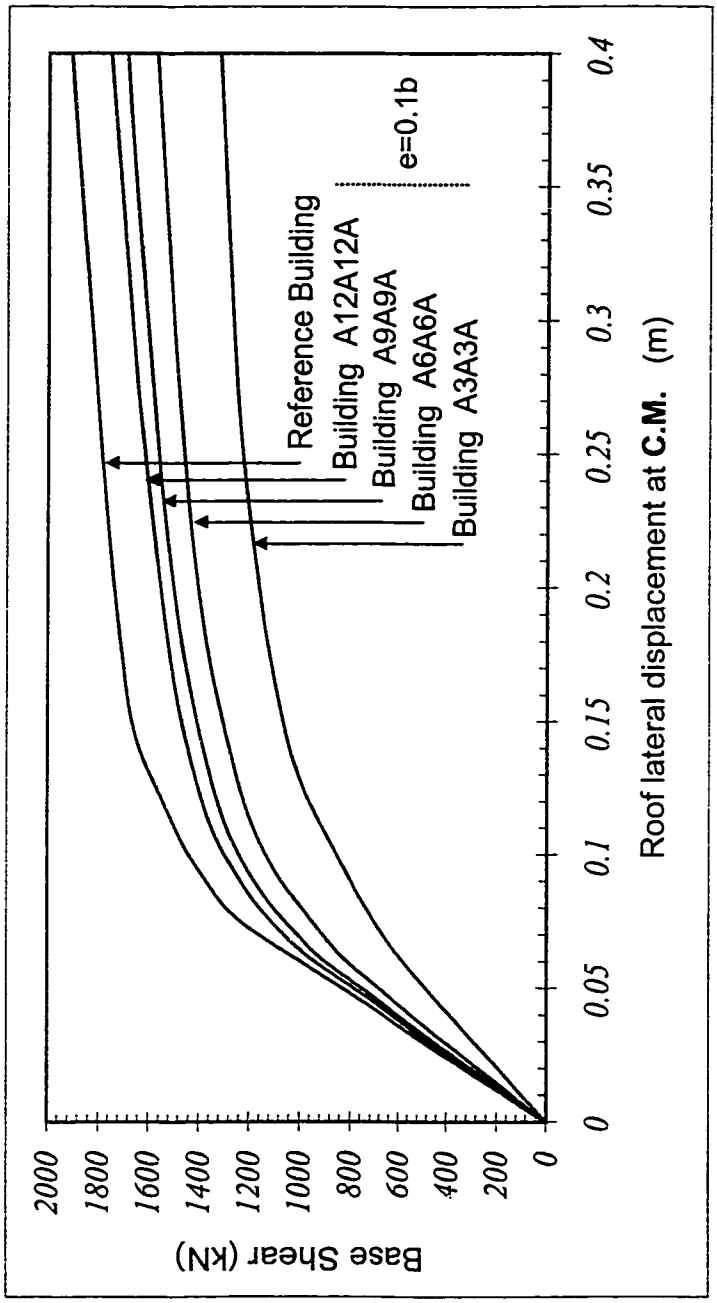


Figure 3.4. The capacity curves of the buildings

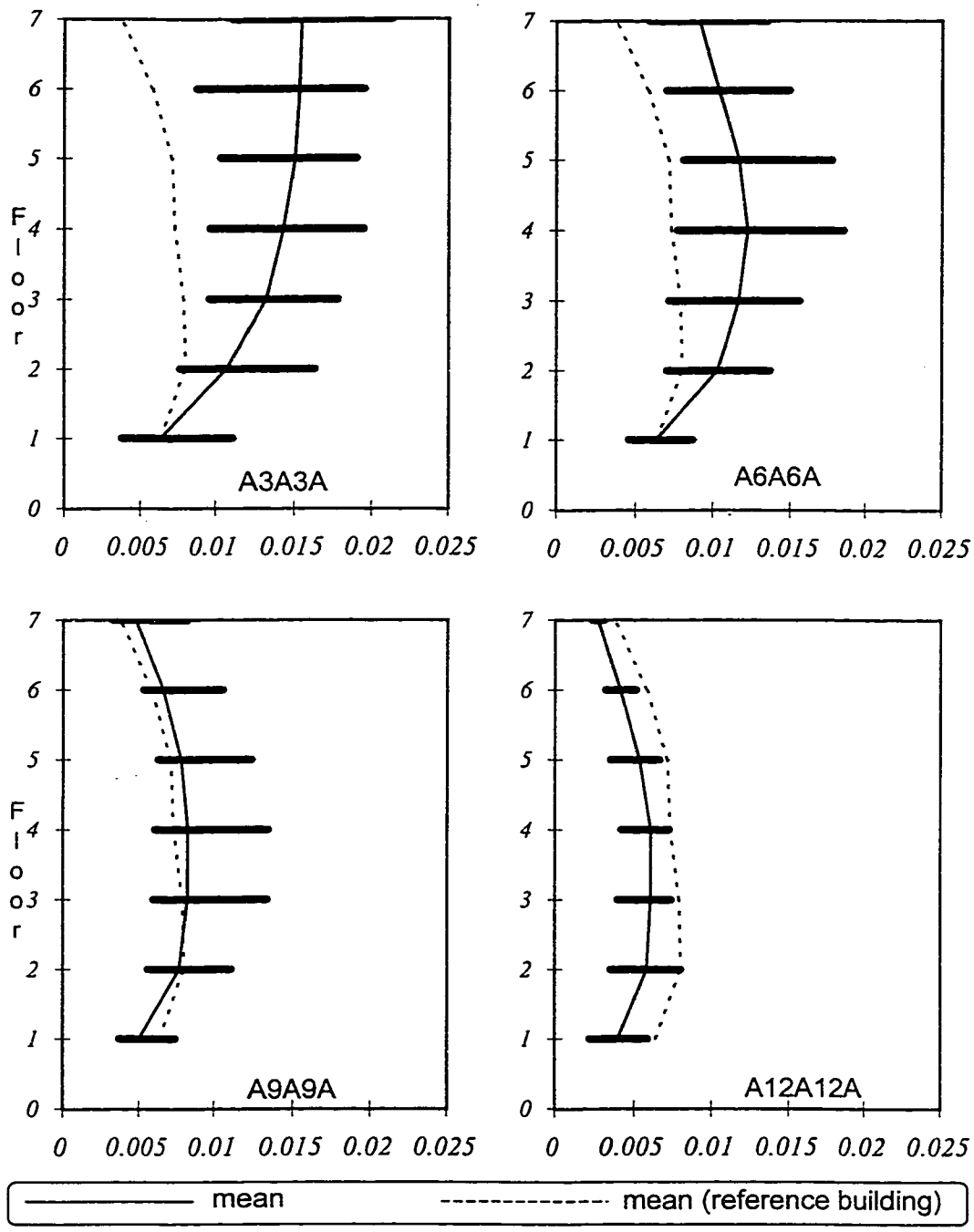


Figure 3.5. Edge 1: maximum interstorey drift ratio

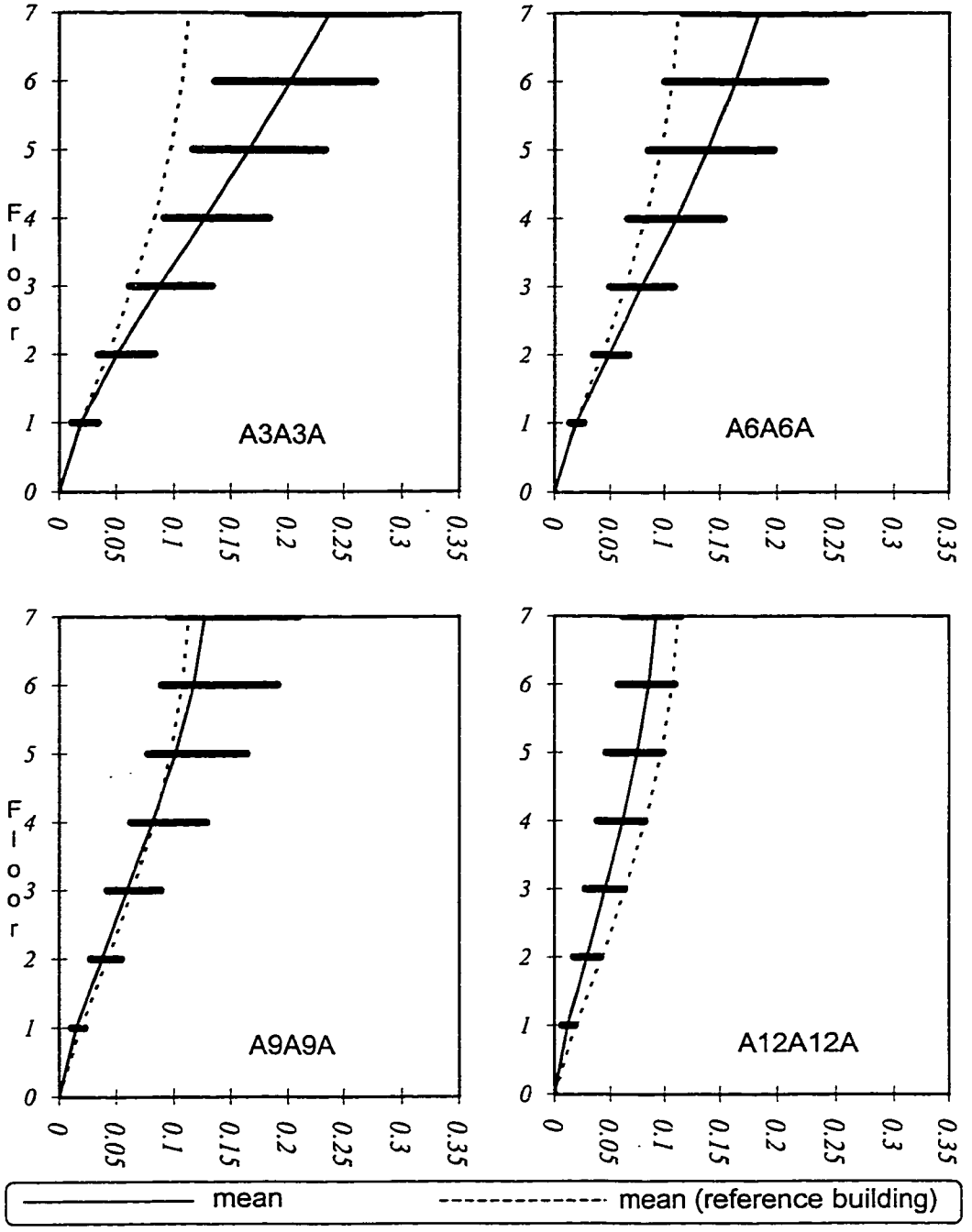


Figure 3.6. Edge 1: Maximum floor displacement (m)

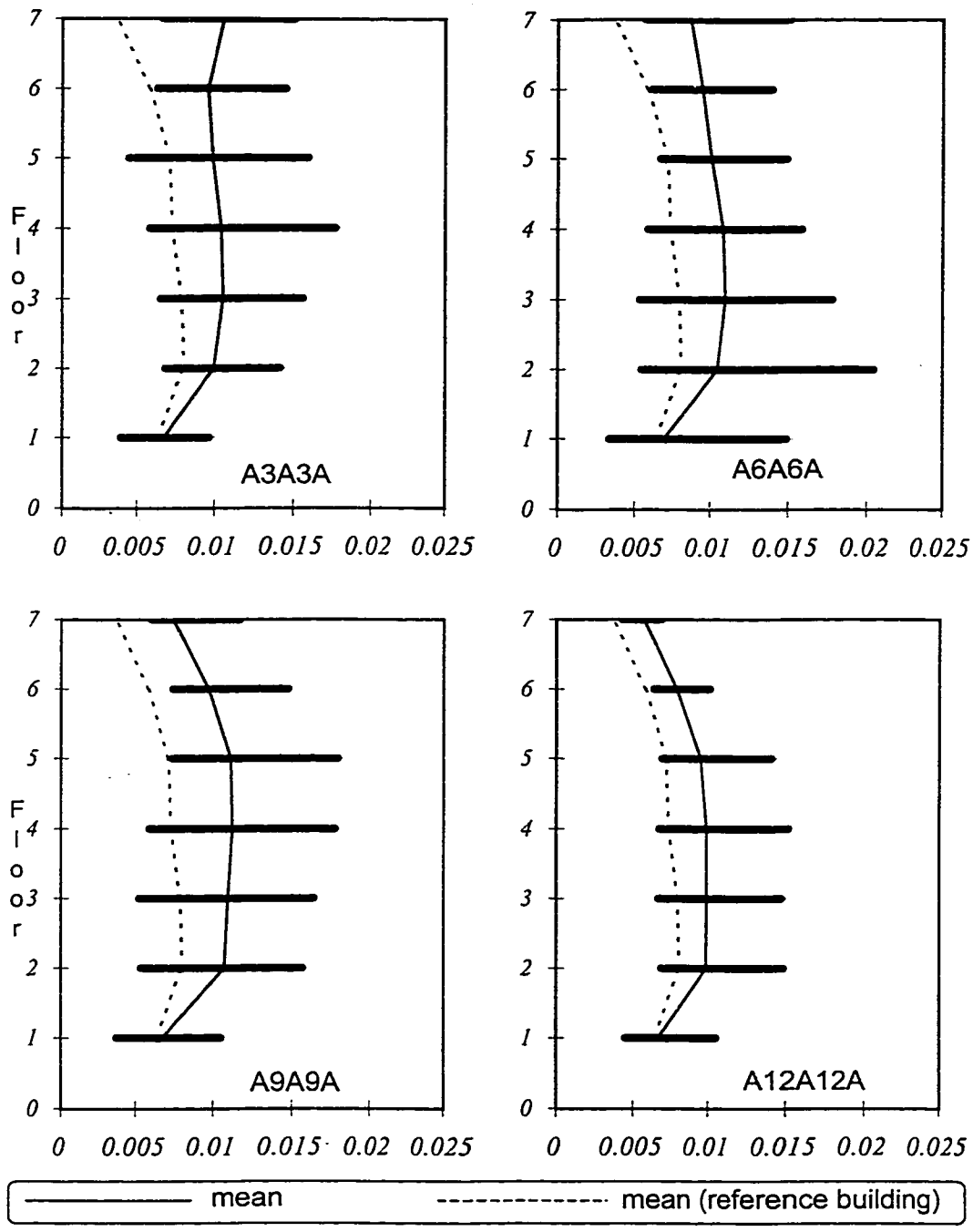


Figure 3.7. Edge 3: maximum interstorey drift ratio

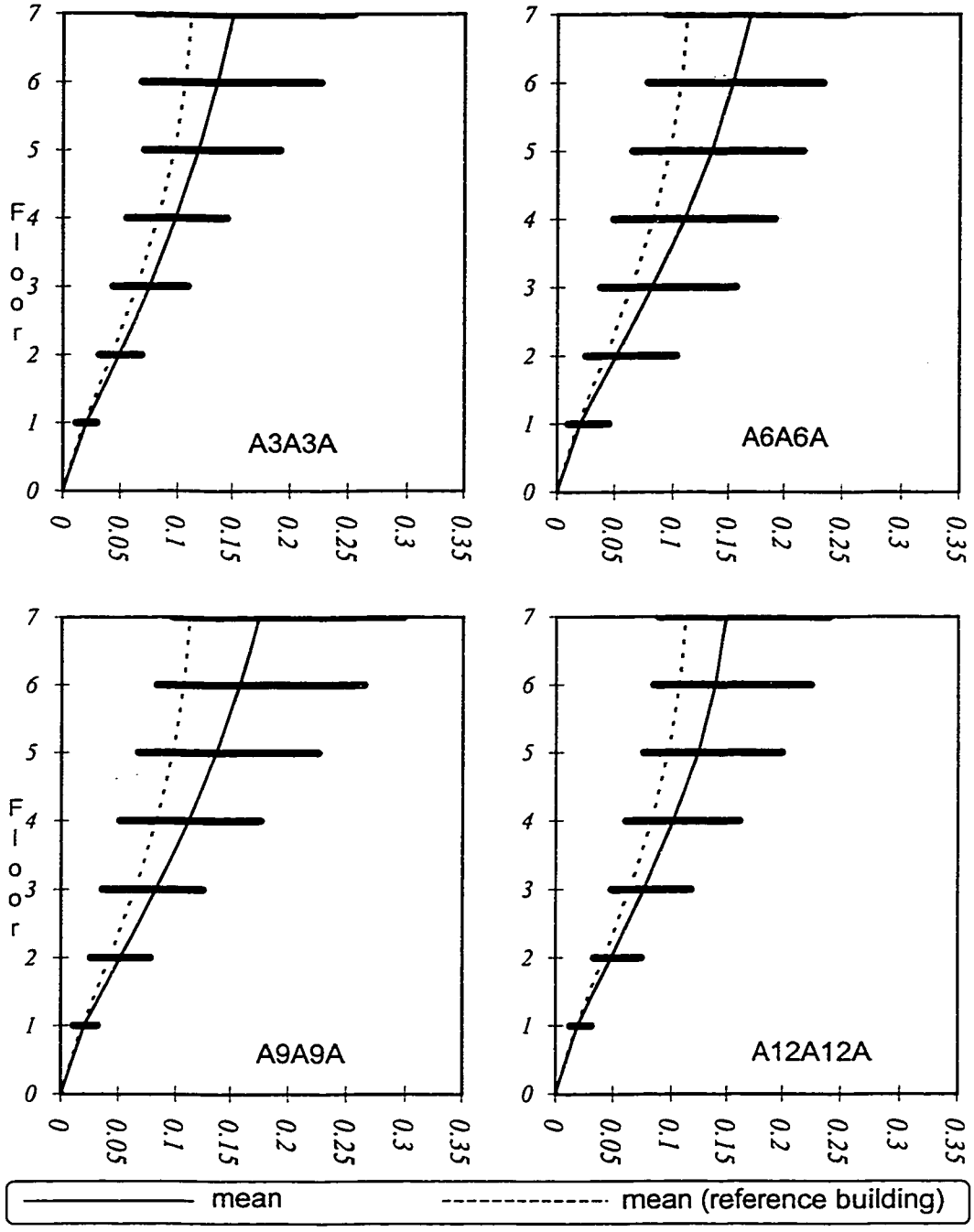


Figure 3.8. Edge 3: maximum floor displacement (m)

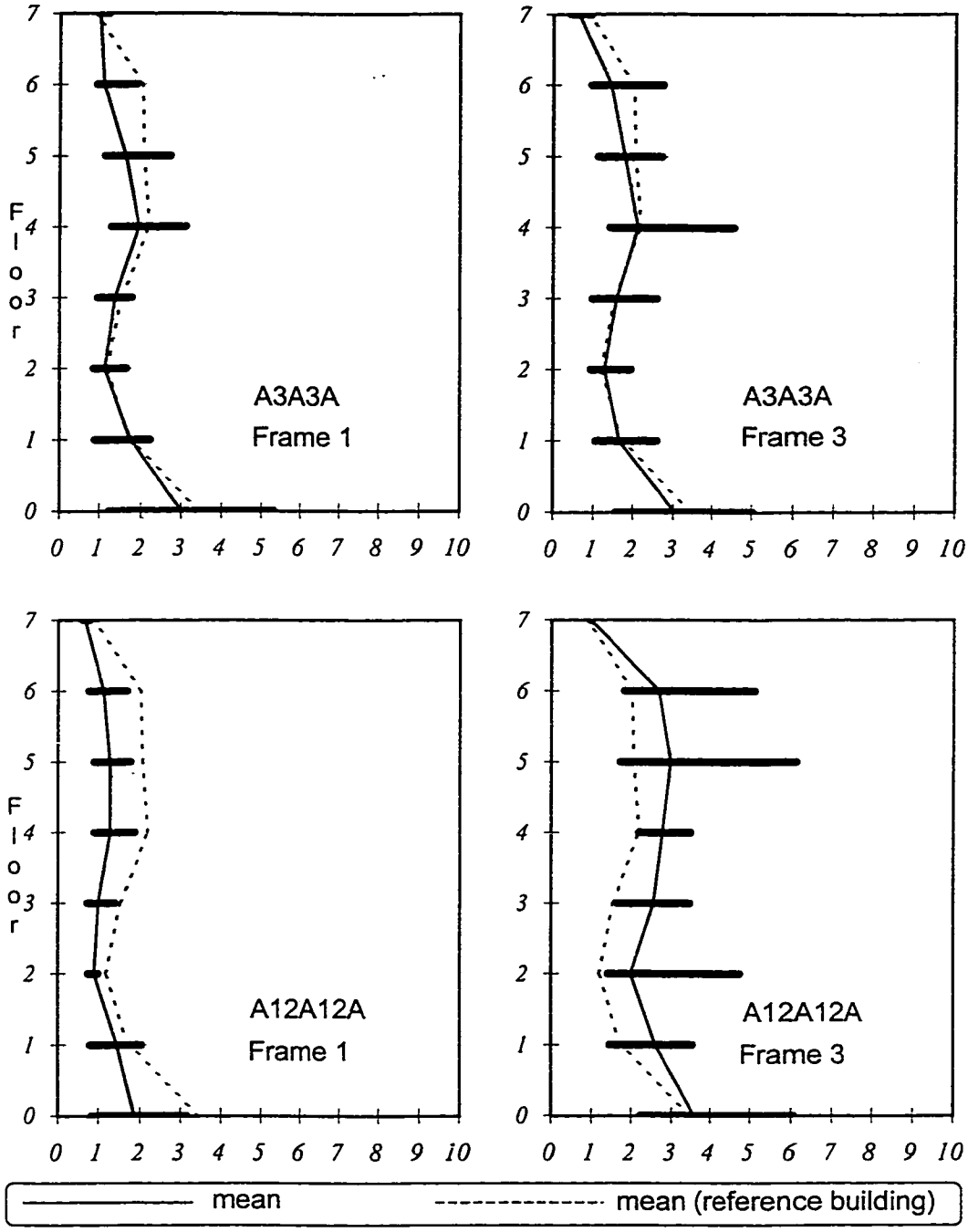


Figure 3.9. Maximum column ductility demands

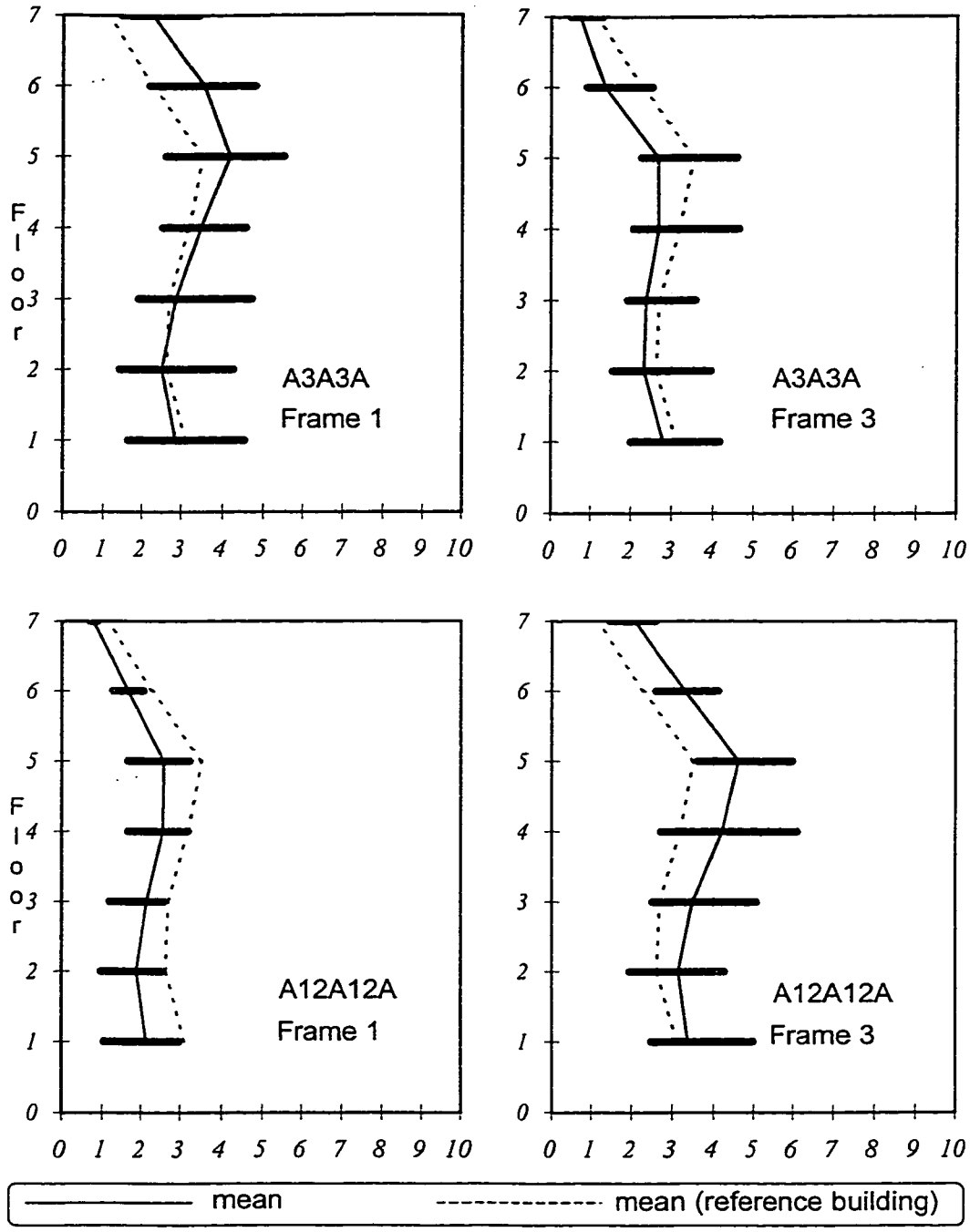


Figure 3.10. Maximum beam ductility demands

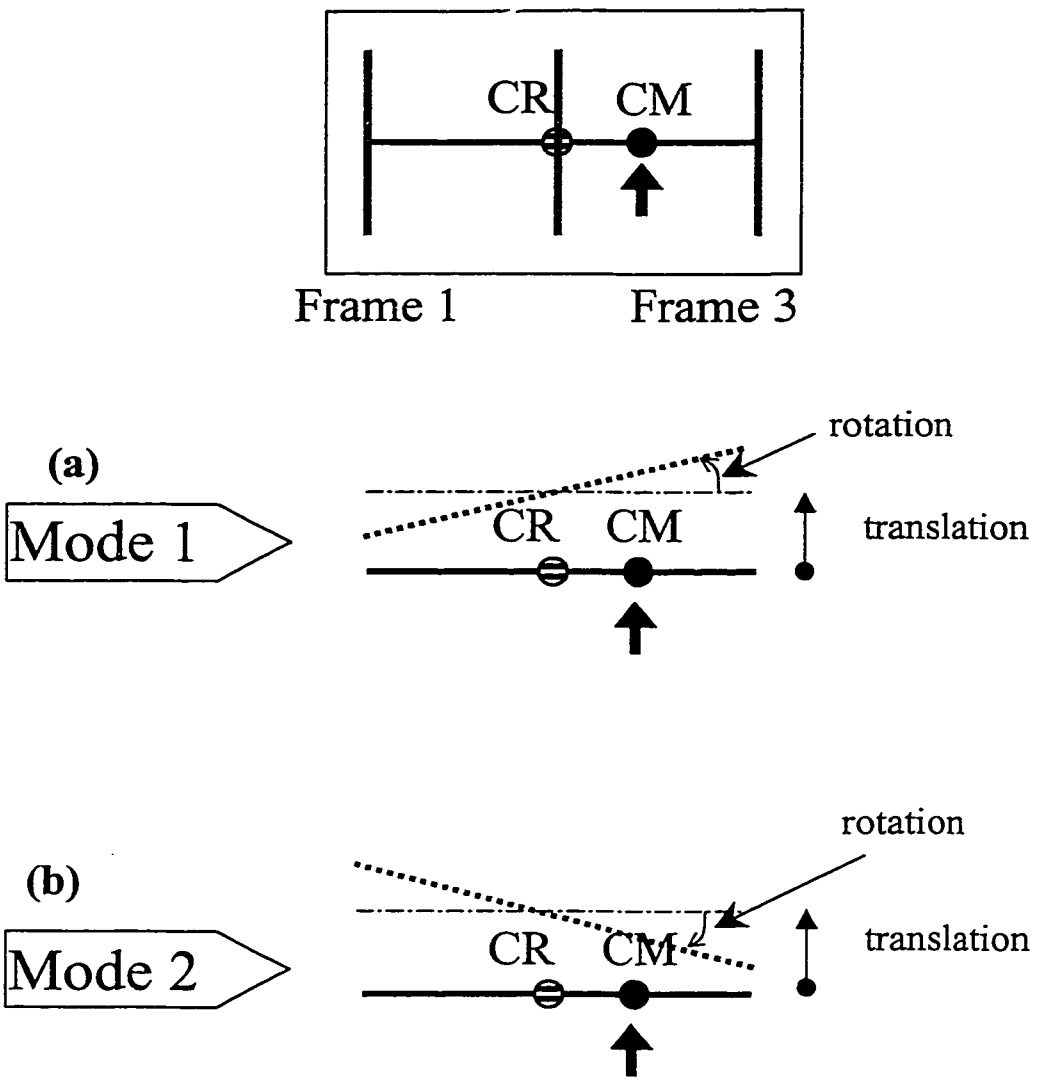


Figure 3.11. The first two mode shape (in plan) of a typical asymmetric Building:
(a) Mode 1
(b) Mode 2

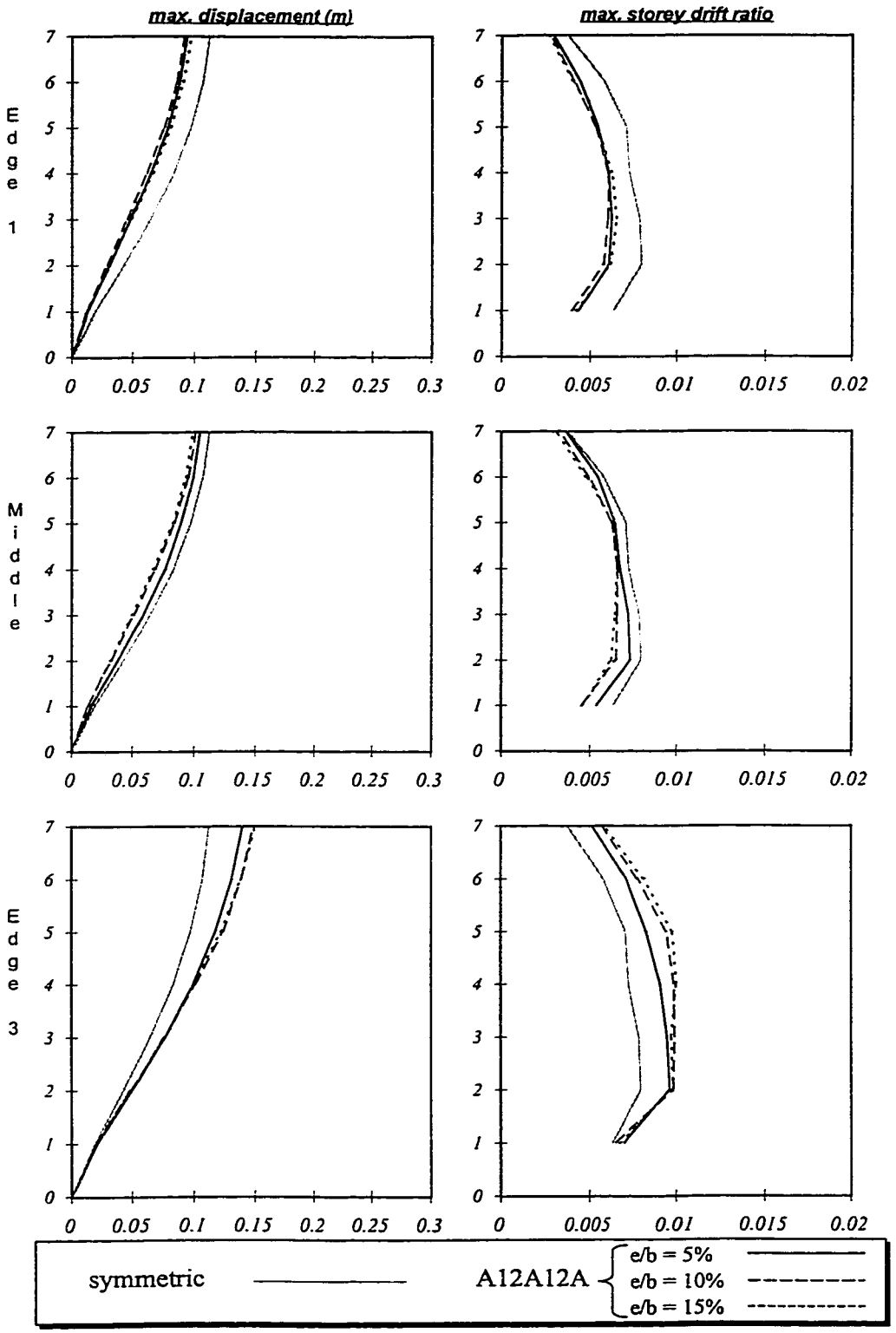


Figure 3.12. Effect of eccentricity on deformations of Building A12A12A

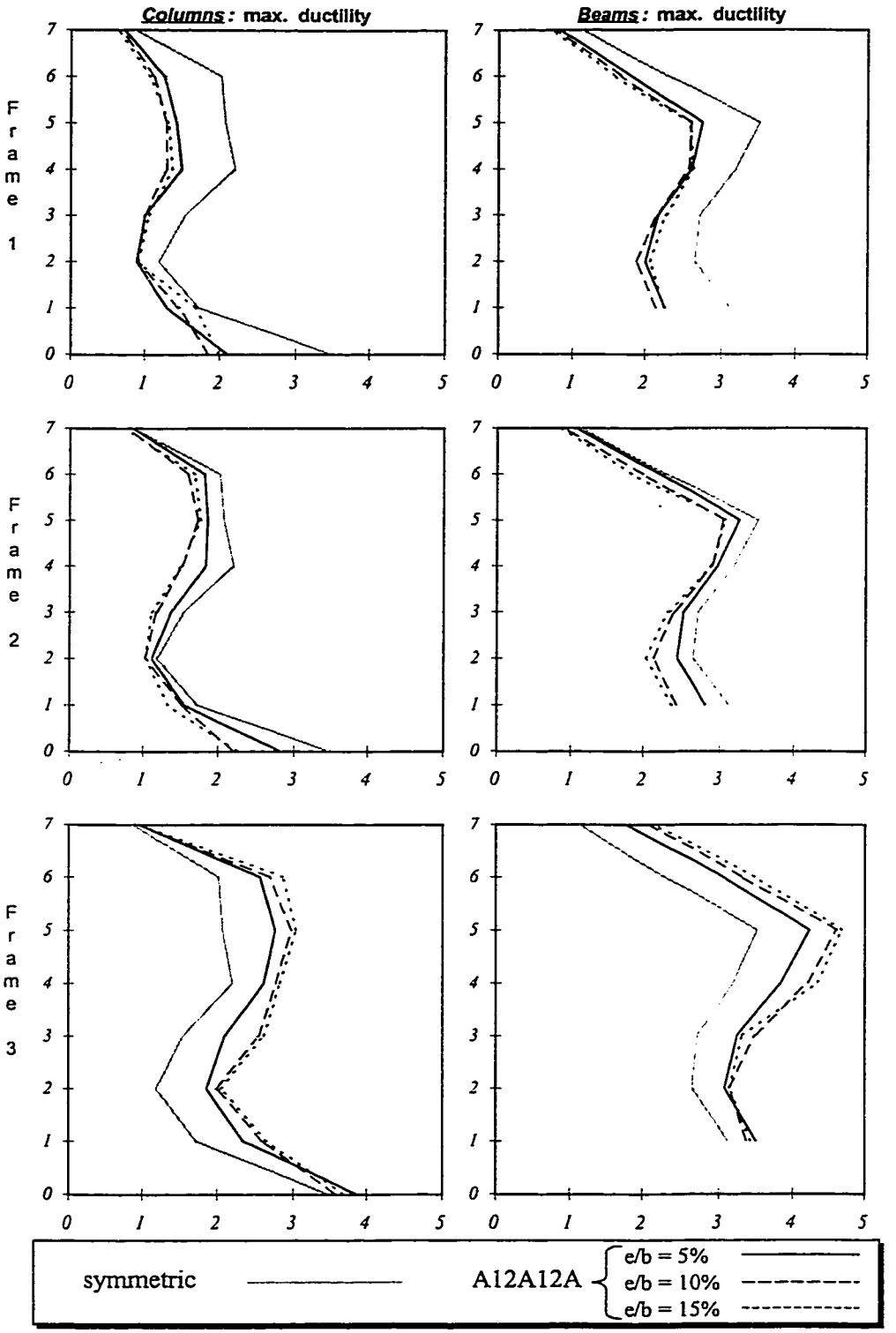


Figure 3.13. Effect of eccentricity on ductilities in Building A12A12A

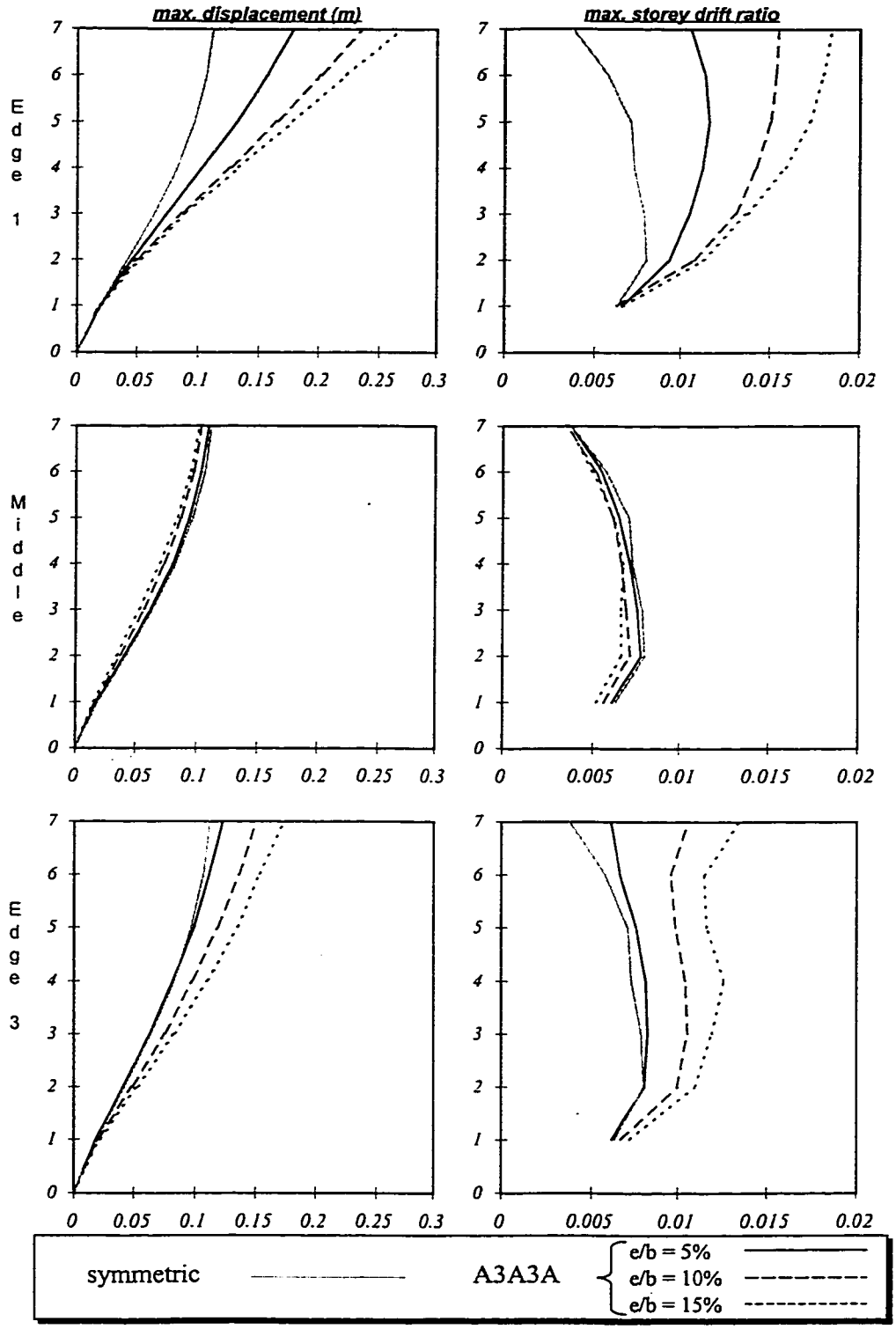


Figure 3.14. Effect of eccentricity on deformations of Building A3A3A

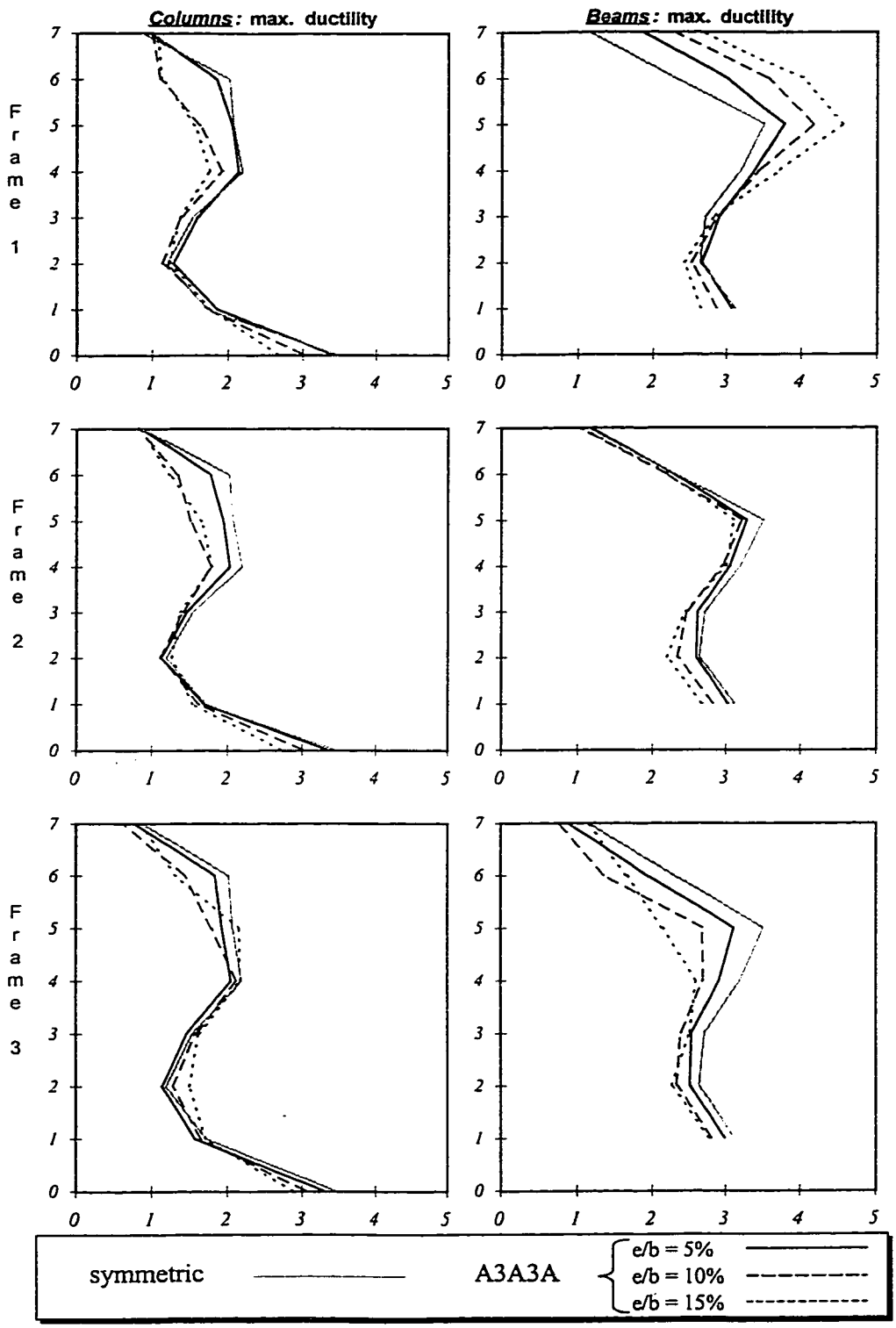


Figure 3.15. Effect of eccentricity on ductilites in Building A3A3A

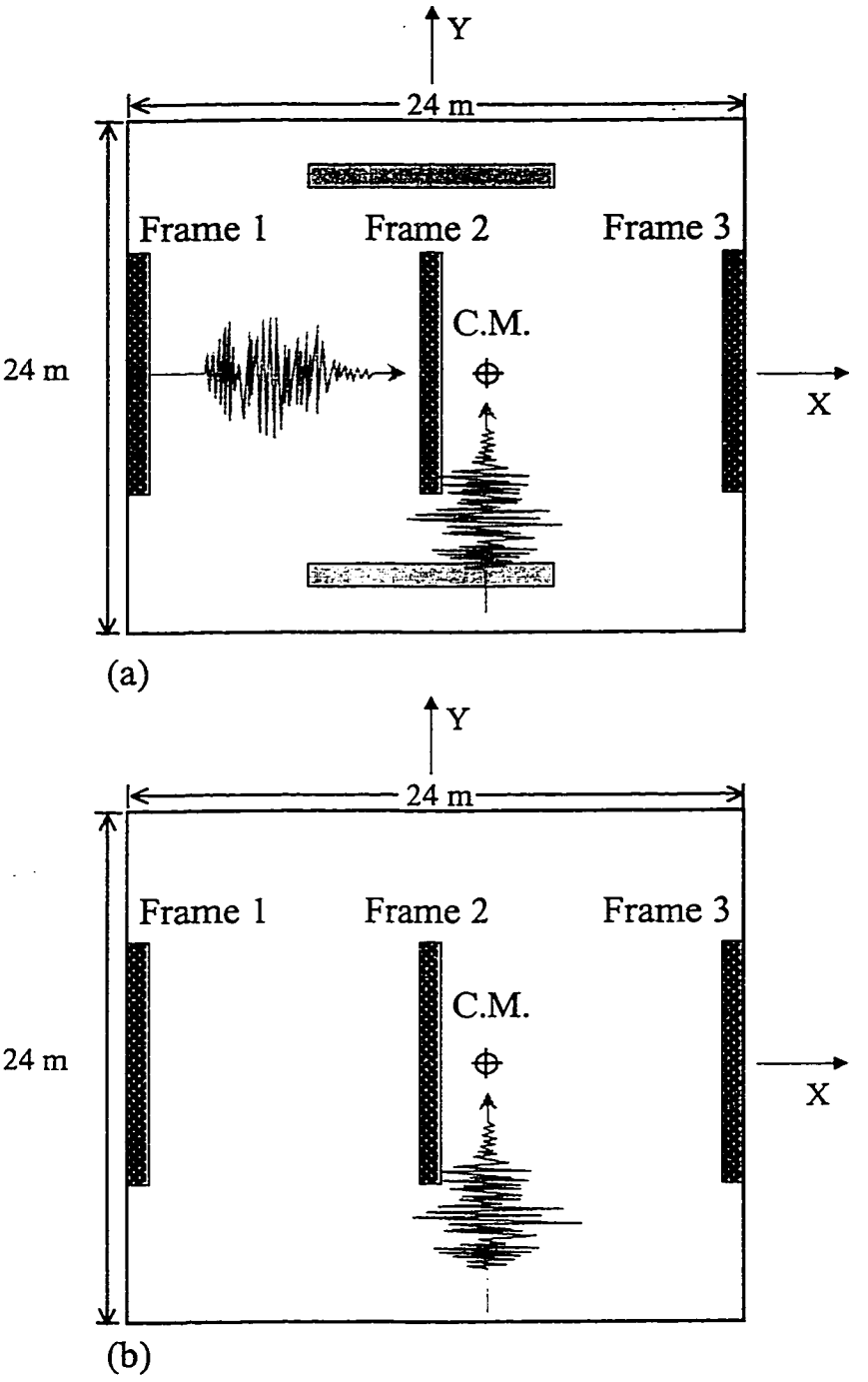


Figure 3.16. Two plan configurations for the seven-storey buildings;
(a) Building with transverse frames which contribute to the torsional stiffness
(b) Building A12A12A

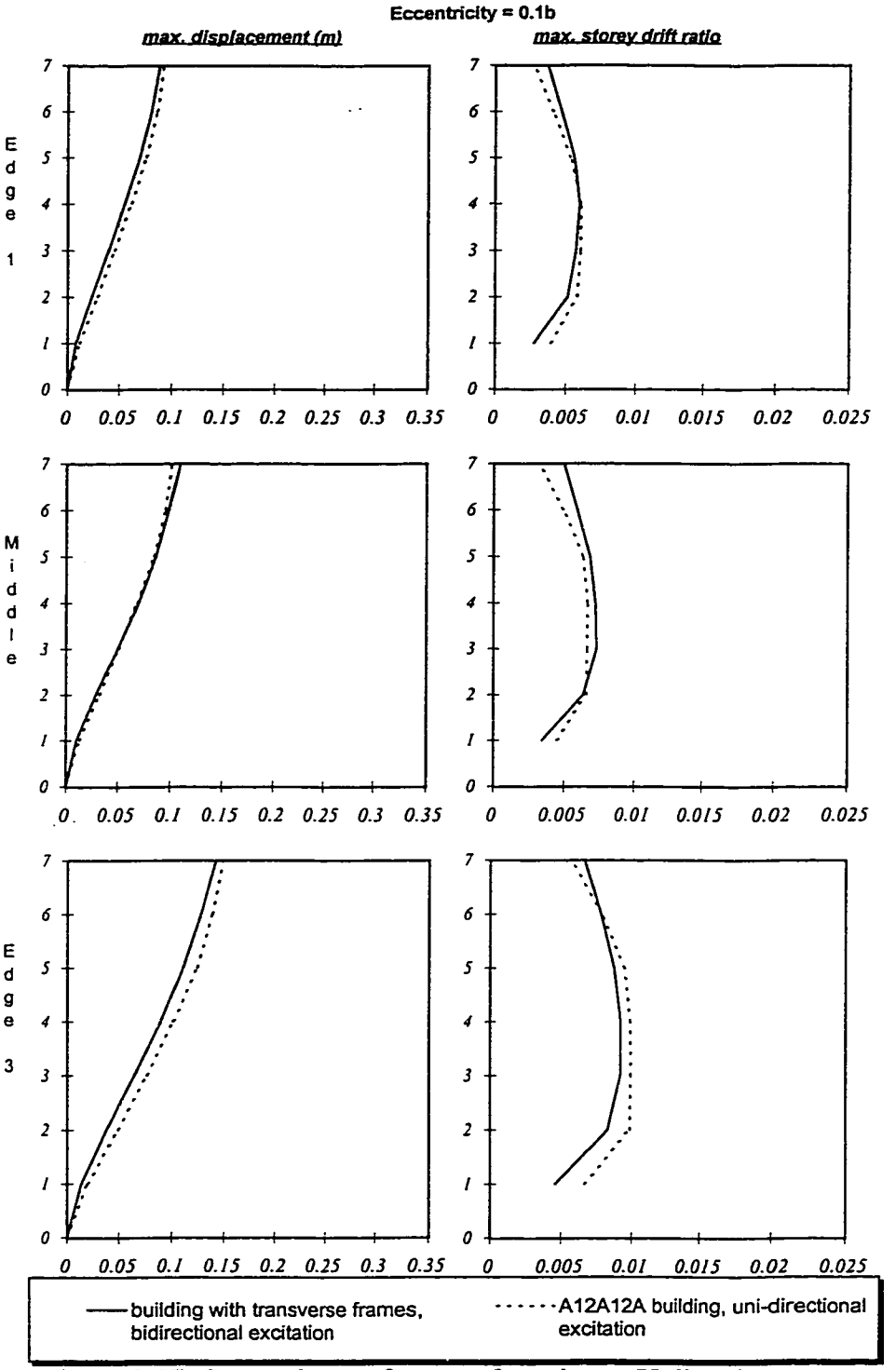


Figure 3.17. Comparisons of mean of maximum Y-direction displacements and storey drifts

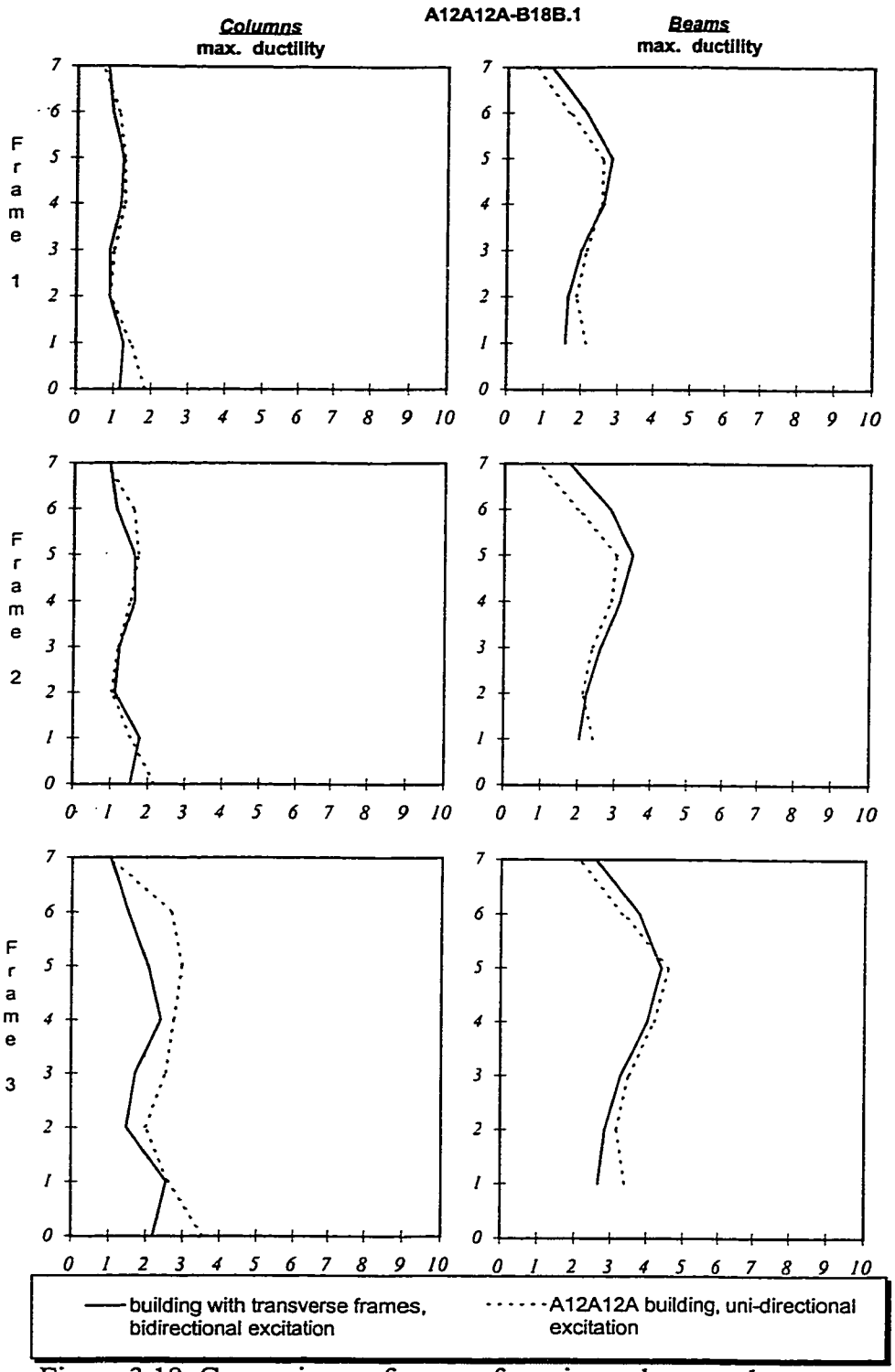


Figure 3.18. Comparisons of mean of maximum beam and column ductility on Y-direction frames

This page is intentionally left blank.

# CHAPTER 4

# ASYMMETRICAL MULTI-STOREY FRAME BUILDINGS DESIGNED INCORPORATING TORSIONAL PROVISIONS

## 4.1 Introduction

In a symmetric building, all the lateral load-resisting elements at different locations in plan experience the same lateral displacement when subjected to unidirectional ground motion excitation. As a result, the force induced in each element is proportional to its lateral stiffness. This observation leads to a guideline that calls for assigning the design strength of the lateral load-resisting elements according to their stiffness. In an asymmetric building, however, the location of a lateral load-resisting element affects the share of load that it should resist because the loadings on the rigid floors of these buildings are accompanied by torques caused by the structural eccentricity in the building. The force induced in each element from the floor torques is proportional to its contribution to the torsional stiffness of the building. The torque-induced force in an element is called the torsional shear. The location of an element not only determines the magnitude, but also the direction of the torsional shear. Depending on the direction of the torque, the torsional shear should be added to or subtracted from the forces induced in that element by the translational displacement of the floors.

To compensate the torsional effect on the performance of a building, different

approaches have been suggested to replace the rule of *distribution of strength among the elements proportional to their lateral stiffness*. These approaches can collectively be referred to as torsional provisions. The goal of this chapter is to evaluate the effectiveness of a few torsional provisions to improve the seismic performance of asymmetric multi-storey buildings.

The first approach that is studied here is distribution of the strength based on static equilibrium consideration. Then the static torsional provisions based on the Uniform Building Code (UBC) are studied. Finally, the application of response spectrum analysis to proportion the design strength of the elements is considered.

These studies lead to the observation that before using any static torsional design method, it is essential to make sure that the asymmetric multi-storey building under consideration is not a torsionally flexible (TF) building. Two procedures are developed to identify TF multi-storey buildings in the last part of this chapter. The first procedure uses the dynamic characteristics of the buildings while the second procedure is based on the static edge displacement ratios. Details of both procedures are explained and their effectiveness is demonstrated by means of examples.

## 4.2 Torsional provisions

Torsional provisions are incorporated in most building codes to redistribute the strength among elements to minimise the torsional effects. Codes usually divide the buildings into regular and irregular buildings and consider that static torsional provisions will be suitable for regular buildings. For irregular buildings, design based on dynamic analysis, such as the response spectrum method, is suggested.

## 4.3 Design according to static torsional provisions

The static torsional provisions require the application of static torsional moments to be included in the determination of the design forces. The product of the lateral force and the design eccentricity determines the value of the torsional moment. The design eccentricity can be different from the structural eccentricity in a building. To protect the elements on both side of the building, codes require two separate load cases to be considered involving two design eccentricities. The magnitudes of the two design eccentricities are usually derived from equations like:

$$(e_d)_1 = 1.5e + 0.1b \tag{4.1a}$$

$$(e_d)_2 = 0.5e - 0.1b \tag{4.1b}$$

where $(e_d)_1$ and $(e_d)_2$ are the two design eccentricities, $e$ is the structural eccentricity and $b$ is the width of the building. To design the elements, the forces required for resisting the torsional moments (torsional shears) should be combined with the shear from translational loading.

Figure 4.1 demonstrates how each design eccentricity affects the design strength of the elements on each side of a building. The torsional shear resulted from $(e_d)_1$ increases the design load on Frame 3, as shown in the Figure 4.1a. This torsional shear would add to the translational shear to form the design strength of Frame 3. The design eccentricity $(e_d)_2$, depends on its magnitude, may either cause an increase in design load of Frame 1 as shown in Figure 4.1c, or cause a lesser reduction in the design load of this frame than using $(e_d)_1$, as shown in Figure 4.1b. One would choose the worst case of

torsional shear to combine with the translational shear to design Frame 1.

### *4.3.1 Design for torsion based on static equilibrium criteria*

In this approach, the design forces in the elements are determined based on the static equilibrium of the building when subjected to lateral loads applied at the centre of mass of the floors. The design strengths for the elements are established in two steps. First, the static equilibrium of a single mass system is used to estimate the design force in each of the frames. Second, the strengths of the members of frame type A are adjusted to the ratios found in step one. Since Frame A is a frame designed for one third of the seismic load of the building, it represents a frame in a symmetric building designed without considering torsional provisions. To make a distinction, the notation $A^*$ is used to indicate any change in the strength of Frame A due to the use of torsional provisions. $A^*$ is a generic symbol and can represent different frames designed using different provisions. To pinpoint the actual frame design strength, the title of the appropriate torsional provision used will be mentioned along with the configuration of the building. Therefore a building that has a structural eccentricity equal to 0.1b and its frames have been designed based on the static equilibrium criteria will be referred to as *Building $A^*12A12A^*.1$ static equilibrium-designed.*

Using the static equilibrium criteria, Figure 4.2 shows the share of design load for each frame in the four different building configurations. Since the centres of rigidity in these configurations are at the middle of the floor plan, the design force of each frame can be found readily. The figure shows that if a design force equal to 3F is applied at the centre of mass, the middle frame always takes one third of the load while the shares of the

other two frames are different depending on their locations.

In the static equilibrium method, the torsional moment is obtained directly using the eccentricity of the building without modification. In other words, the design eccentricity $e_d$ is equal to the structural eccentricity e in this approach. Building A12A12A.1 taken as representative of a torsionally stiff (TS) building and Building A6A6A.1 taken as representative of a torsionally flexible (TF) building will be used to show the effectiveness of such a torsional provision. The strengths of members in the frames of these two buildings are assigned by adjusting the strength of Frame A with the factors shown in Figure 4.2.

**Static inelastic behaviour (pushover analysis)**

Pushover analyses are conducted on the frames in the two buildings to obtain the capacity curves of each frame as shown in Figure 4.3. The original capacity curve of Frame A is also shown as a reference. Since the strength of edge frames in both buildings are changed based on the static equilibrium criteria, the buildings will be denoted as A*12A12A*.1 and A*6A6A*.1 respectively. In Building A*12A12A*.1, the strength of Frame 1 is 0.9 times the strength of Frame A while the strength of Frame 3 is 1.1 times that of Frame A. In Building A*6A6A*.1, the strength of Frame 1 is 0.8 times and the strength of Frame 3 is 1.2 times that of Frame A. Frame 2 of both buildings has the same strength as Frame A.

There is no overstrength in a building as a whole, when the static equilibrium method is used. In other words, the total strength of the building remains unchanged. If there is an increase in the strength of Frame 3, there will be an equal decrease in the

strength of Frame 1.

Figure 4.4 compares the capacity curves of the individual frames of the asymmetric Buildings A*12A12A*.1 and A*6A6A*.1. Included in the comparison is the capacity curve of the frames of a symmetric reference building, which has three type A frames. The comparison shows that Frame 1 of the TF building has the lowest strength. This is expected since the strength of Frame 1 has been set to 0.8 times that of Frame A for the TF building compare to 0.9 times that of Frame A for the TS building. Frames 2 of all three buildings have the same strength. In the case of Frames 3, the strength of the frame in the TF building is higher than that in the TS building.

Figure 4.4 presents an overview of the relationship between the effect of torsional stiffness and the distribution of the design strength between the frames. As the level of torsional stiffness decreases, more strength is reduced from Frame 1 and added to Frame 3 of that building.

**Dynamic inelastic behaviour (seismic response analysis)**

To investigate the effect of using the static equilibrium criteria in designing the frame strength on the response of the buildings, the models are subjected to a series of 3-D inelastic dynamic analyses using the chosen ensemble of earthquake records as input.

Figure 4.5 compares the means of the maximum displacements and the storey drift ratios for the static equilibrium-designed asymmetric TS and TF buildings, with those of the reference building. The asymmetric TS building displays smaller deformations than the symmetric building at edge 1, but has greater deformations than its symmetric counterpart at edge 3. In the asymmetric TF building, both edges 1 and 3 show larger response when

compared to the symmetric building. The deformations of the middle frame are much smaller than the other two frames, an indication of the importance of contribution of torsion to the responses of the TF building.

The mean values of the maximum ductilities in the beams and columns of these buildings are shown in Figure 4.6. Frame 1 of the TS asymmetric building displays less ductility demand but Frame 3 has more demand than its symmetric counterpart. This conclusion is in agreement with what has been observed regarding the deformations of these frames. The TF building has a larger ductility demand in Frame 1 but a smaller ductility demand in Frame 3 than the corresponding frames in the reference building. According to Figure 4.5, both Frames 1 and 3 of the TF asymmetric building have an increase in deformations. However, as Frame 3 is designed with a higher strength, its ductility demand is reduced accordingly to a level below that of the reference building. This means that the static-equilibrium design is capable of protecting Frame 3 by reducing the ductility demand of this frame. However, it fails to control the excessive ductility demand in Frame 1 of this TF building.

A review of the study in this section leads to three conclusions about the use of the static equilibrium approach for distributing strength in the design of asymmetric buildings. First, it has little effect to reduce the deformations at the edge of both the TF and the TS buildings. Second, this design approach is effective in reducing the ductility demand in the TS building. Third, this approach is not effective in reducing the ductility demand of Frame 1, a frame at the stiff edge of the TF building.

### *4.3.2 Design based on the Uniform Building Code*

In this section, the ability of torsional provisions of a typical building code to improve the seismic responses of buildings is explored. The torsionally flexible building configuration A6A6A and the torsionally stiff building configuration of A12A12A are redesigned, using the static torsional provisions of the Uniform Building Code (UBC 1997). The design procedure using UBC static torsional provisions consists of three steps. The first step is a check for torsional irregularity. A building is considered torsionally irregular by UBC when the maximum edge storey drift, computed including accidental torsion, is more than 1.2 times the average of the storey drifts at the two edges of the structure. This check in UBC is not meant to be used as a measure to exclude a building from using the static torsional provisions. The purpose of the check is to increase the accidental eccentricity of any building found to be torsionally irregular. The second step is the calculation of a factor ($A_X$) needed to amplify the accidental eccentricity if the building has been determined to be torsionally irregular. The third step in the procedure is the calculation of horizontal torsional moments using the following design eccentricity $e_d$ expressions:

$$e_d = e + A_x(0.05b) \qquad (4.2a)$$

$$e_d = e - A_x(0.05b) \qquad (4.2b)$$

where e represents the structural eccentricity and b is the plan dimension of the building perpendicular to the direction of the lateral forces. Appendix B gives the details of design calculations using the UBC torsional provisions.

The results of calculations for the UBC amplification factors ($A_X$) for the two asymmetric buildings are listed in Tables 4.1 and 4.2, respectively. According to these tables, both these buildings are considered torsionally irregular by UBC. For the TS building, the average value of $A_X$ is 1.41. The calculated average value of $A_X$ for the asymmetric TF building is 4.35. However, the upper limit of 3.00, as suggested by UBC, is actually used in the design.

Having calculated the value of $A_X$ for each building, the design eccentricities, and the torsional moments, can be obtained. The effect of including these torsional moments in the design process would lead to some increases in strength of the frames. For a TS building with no structural eccentricity, the accidental eccentricity provision will lead to approximately 5% strength increase of the edge Frames 1 and 3. For the same building but with a structural eccentricity equal to 10% of width of the building, the strength in Frame 1 is unchanged, as UBC does not allow negative torsional shears to be taken into account for design. However, additional strength is required for Frame 3 located at the flexible edge. The required strength increase of this frame is approximately 17%.

Figure 4.7 compares the strength of the frames for the two buildings using the static equilibrium criteria and the UBC static torsional provisions. The required strengths in the frames of the TS building are similar for the two approaches. However, UBC requires larger increase in the strength of edge frames in the TF building.

There are many options open to a designer to implement the required increase in strength of a frame as specified by the code. Consider the TS building where the required strength increase in Frame 3 is 17%. As noted in Figure 2.2a, Frame A has an effective strength 35% greater than its design base shear value. Therefore one can interpret that

Frame A already has the strength required by the torsional provisions and no redesign is necessary. If this option is taken, Frame A will serve as the frame at the edge 3 of the building. Alternatively, one may choose to increase the beam and column capacities of Frame A by 17%, resulting a modified Frame A* to be used as Frame 3 in the buildings. The lateral strength of Frame A* would then match the increase that is required by the torsional provisions. A third option is to redesign Frame A, requiring the new frame to satisfy an increase of design base shear values, as specified by the torsional provisions. This option does not automatically guarantee that the lateral strength of the redesigned frame will be 17% higher than Frame A because the design of member reinforcements are based on the critical load combinations of both the gravity and seismic load effects. This last interpretation is used in adjusting the frames of the two buildings in this study.

**Static inelastic behaviour (pushover analysis)**

Figure 4.8 shows the capacity curves of the individual frames of the two buildings. The capacity curve of Frame A is also included as a reference. Figure 4.8a shows that the capacity curves for Frames 1 and 2 and the type A frame in Building A12A12A*.1 are the same. There is no extra design force on the Frame 2 since it is centrally located. The design force of Frame 1 could be reduced by the design calculation. But the UBC code does not allow negative shear to be included in the design. Therefore a type A frame will serve as Frame 1 in this building. Since the UBC torsional provisions requires an increase in the strength of Frame 3 without reducing the strength of Frame 1, following this torsional provisions will lead to some overstrength of the building.

Figure 4.8b shows the capacity curves of the frames in the A*6A6A*.1 building.

There is an increase in the strength of both Frames 1 and 3 of this building. Using a value of 3 for $A_X$ in Equation 4.2b causes a change in the sign of the design eccentricity. Applying the design torques corresponding to this negative design eccentricity leads to an increase of the design load on Frame 1. Frame 3 of this building has a large increase in strength as demanded by the code. The strength of this frame has increased to a value more than twice that of Frame A. The increase in the design strength of Frames 1 and 3 causes a substantial overstrength in the asymmetric Building A*6A6A*.1. The capacity curves of the frames of Buildings A12A12A*.1 and A*6A6A*.1 are compared on a per frame basis in Figure 4.9. One can see the large increase in strength of Frame 3 in the torsionally flexible building.

**Dynamic inelastic behaviour (seismic response analysis)**

To investigate the influence of the UBC torsional provisions on the response of the buildings, a series of 3-D inelastic dynamic analyses are carried out, with the models being subjected to the chosen ensemble of earthquake records.

The seismic displacements and the interstorey drift ratios of the two UBC-designed asymmetric buildings are presented in Figure 4.10. Only the means of the responses are presented. The responses of the TS and TF buildings are shown in solid and dashed lines respectively, while the responses of reference building are shown in grey lines. A comparison of the results shows that the additional responses caused by torsion can be significant, even in the case of buildings with only moderate level of eccentricity. Comparisons of the responses between the asymmetric and the reference buildings show an expected trend for the TS building, namely, the asymmetric building has less deformation

on the edge 1 but more deformation on edge 3. In case of TF building A*6A6A*.1, both edges of the building display much higher deformation than the reference building.

The member ductility demands at the various frames of these buildings are presented in Figure 4.11. Using the member ductility demand on the reference building as reference, the figure gives the impression that the member ductility demands of both buildings are well controlled by the code provisions. However, a comparison between the ductilities of Frame 1 and Frame 3 of the TF building shows that this asymmetric building has much higher ductility demand on Frame 1. This result again highlights the fact that static torsional provisions are under-designing the Frame 1 in torsionally flexible buildings. Due to the high design strength, the ductility demands of Frame 3 are much smaller than Frame 1 in the TF building. In fact the design strength assigned to the Frame 3 by UBC is so high that the ductility demand of this frame is even lower than the reference building. As Figure 4.11 displays, the beams and columns in most of the floors of Frame 3 of this building remain elastic.

There are three main conclusions about the use of the UBC approach for distributing strength in asymmetric buildings. First, the use of this method has negligible effect to change the deformations of the TS building. Its influence on the deformations of the TF building is also minor. Second, this design approach correctly recognises Frame 3 of the TS building as the vulnerable frame and by assigning more strength to it reduces the ductility demand of this frame. Third, this approach does not recognise the vulnerability of the Frame 1 in the TF building. It over-protects elements at the flexible side of the TF building but does not assign enough strength for elements near the stiff edge.

## 4.4 Design based on dynamic torsional provisions

It is shown in the previous sections that for the TS building, the static torsional provisions generally work well to protect the lateral load-resisting edge elements of the structure. However, it is shown that static torsional provisions become deficient when applied to the TF building. Low torsional stiffness in an asymmetric building causes the rotational modes to have a more important role in the deformations of the elements. The subsequent change in dynamics of the TF buildings is such that the pattern of seismic demand in the elements is not in agreement with the arrangement of strength distribution suggested by the static torsional provisions.

In this section, the method of design by dynamic analysis is applied to the two example asymmetric buildings. The method consists of three steps. Step 1 involves a response spectrum analysis of the building, using the 5% damped acceleration design spectrum of NBCC 1995. Then in step 2, the base shear resulting from the response spectrum analysis is scaled to the value of the static design base shear. Step 3 is the incorporation of the effects of accidental torsion in the design. Accidental torsion is incorporated by applying static torsional moments on the building and combining the effects of this loading with the results obtained from response spectrum analysis, as suggested in NBCC 1995.

### Static inelastic behaviour (pushover analysis)

Figure 4.12a shows the capacity curves of the frames in the TS building designed using the response spectrum approach. The strength of Frame 2 is unchanged. However, Frame 1 has a slightly less strength and Frame 3 has a considerable larger strength than

Frame A. As the strength of both edge frames has changed in this building, it is named *A*12A12A*.1 spectrum designed.*

The capacity curves of the frames in the TF building (A6A6A.1) are shown in Figure 4.12b. Use of the response spectrum design approach resulted in an increase in strength for all three frames of the building. There is a small increase in the strength for the middle frame but there are large increases in the strengths of both edge frames. Contrary to static torsional provisions, Frame 1 is assigned the highest strength in the TF building, when using the spectrum-design approach.

Figure 4.13 compares the capacity curves of the frames in the reference building with the frames of the two spectrum-designed buildings. Negative torsional shear obtained in the spectrum approach is allowed, which leads to a small reduction in the strength of Frame 1 of the TS building, compare to Frame A. Frame 3 of spectrum-designed TS asymmetric building has a large increase of strength. In the asymmetric TF Building, there is a large increase in the strength of Frame 1. It is almost twice that of Frame A. It is of interest to note the similarity of strengths in Frame 3 of the two buildings.

**Dynamic inelastic behaviour (seismic response analysis)**

The response parameters of these buildings are computed, when they are subjected to the chosen ensemble of ground motions as base input.

The mean seismic displacements and the interstorey drift ratios of the buildings are presented in Figure 4.14. The responses of the asymmetric TS and TF buildings are shown in solid and dashed lines respectively, while the responses of the reference building in grey

lines. Comparison of the responses between the asymmetric TS building and the reference building shows that the TS building has smaller deformations on the edge 1 but larger deformations on edge 3. Both edges of the TF building, especially edge 1, display higher deformation than the reference building.

The member ductility demands at the various frames of these buildings are presented in Figure 4.15. Comparing to the results of the reference building, the figure shows that the member ductility demands of the asymmetric TS building are in general well controlled by using the spectrum design approach. Comparisons between the frames of the TF building and the reference building also show good performance for the frames. All three frames of the spectrum-designed TF building have smaller ductility demands than the frames of the reference building. Unlike designs based on static torsional provisions, the spectrum design approach has been able to appropriately protect elements at both edges of the TF building.

## 4.5 Comparing the performance of torsional provisions

Three different methodologies for the distributing lateral strength to resisting elements in asymmetric buildings have been investigated. These are the static equilibrium design, the design based on UBC-97 static torsional provisions and finally the response spectrum method. The results of each approach, as applied to a TS and a TF building with moderate eccentricity, are presented in the previous sections of this chapter. In the present section, those results are regrouped in order to give an overview of the effects of each of the design approaches in improving the seismic performance of the asymmetric buildings.

Incorporating torsional provisions has only minor effects on the maximum

displacements and the maximum storey drifts at the edges of the asymmetric buildings studied in this chapter. Therefore this discussion will focus on the effect of torsional provisions to control the ductility demands in the edge elements.

Figure 4.16 shows the mean of the maximum ductility demands for beams and columns of the TS asymmetric buildings designed with different approaches. The ductility demands of elements in an asymmetric building designed without considering any torsional provision also included as a reference. This building is referred to as A12A12A.1. It has the same nominal eccentricity as the TS buildings but it has three type A frames as resisting elements. The graphs of ductility demand for Frame 1 show that similar results are obtained in all design approaches. For Frame 3, all of the design approaches have reduced the ductility demands as compared to the building designed without torsional considerations. The spectrum and UBC approaches are especially successful in this regard. A similarity between ductility demands of the two edge frames of the building can be viewed as representative of uniform damage distribution across the building and can be considered as a measure of improvement to overcome the torsional effect. It is seen that none of the design methods are completely successful in this regard. However, the distributions of the ductility demand in the two edge frames of the spectrum-designed building are the most similar, and in this respect, the response spectrum approach is the best approach to distribute the lateral strength of elements for the TS buildings.

Figure 4.17 compares the mean maximum ductility demands of beams and columns of the TF asymmetric buildings. The ductility demands of the elements in a similarly asymmetrical building, designed without any torsional provision are also

included as reference. This building is designated as A6A6A.1. Unlike the case of the TS building, the ductility demands of Frame 1 are quite sensitive to the design method used. Frame 1 of a building designed based on the static equilibrium method leads to a performance even worse than the building designed without torsional provisions. The lowest level of ductility demand is in Frame 1 of the building designed by the spectrum approach.

Frame 3 in the building designed by the static equilibrium method shows less ductility demand than Frame 3 in the building designed without torsional provisions. However, Frame 3 in buildings designed by UBC or spectrum approaches performed much better as shown by their smaller ductility demands.

Taking the similarity between distribution of ductility demand on the edge frames as a measure of improvement for a design approach, it is seen that the spectrum approach is also the best method in this regard. The distribution of ductility demand in the two edge frames of the spectrum-designed building are similar in shape and values.

### 4.6 Classification of asymmetric buildings into TS and TF buildings

Results reported in the previous sections of this chapter have shown that static torsional provisions are effective in limiting additional seismic demands on the edge elements of TS eccentric buildings. However, these provisions are not effective when applied to TF structures. The reason is that static torsional provisions primarily provide corrective measures to systems that experience larger seismic demands at the edge 3 and smaller seismic response at the edge 1 of the structure. The dynamic behaviour of TS buildings follows such a trend. However, it is not uncommon that torsion induces

additional responses at the edge 1 of TF buildings. The application of static torsional provisions will not compensate for the additional seismic responses at the edge 1 of such buildings. Therefore, there is a need of simple procedures to identify these TF buildings.

Procedures are presented in this section to divide the eccentric buildings into two broad classes; Torsionally Stiff (TS) and Torsionally Flexible (TF) buildings. The condition under which additional response will occur at the edge 1 or edge 3 of an asymmetrical structure depends on the nature of the first mode of vibration of the structure. Vibrational modes of an eccentric system are coupled modes, with the mode shapes consist of a combination of translational and rotational motions of the floors. A mode in which translational motion of the floors is predominant is termed a translation predominant mode. If the rotational motions are predominant, the mode is termed a torsion predominant mode. When the building is subjected to horizontal ground motions, the major contribution to most parameters of design interest is from contribution of the lowest translation predominant mode. The location of additional edge responses, whether at the edge 3 or the edge 1, depends on whether the lowest translation predominant mode is the first mode, or the second mode of the building. For eccentric buildings that are regular in elevation, the first coupled mode shape is such that the translational and rotational motions are in phase. As a result, the contributions from the translation and rotation to the displacement at the edge 3 of the building are additive. This would lead to additional response at the edge 3 of the structure. In the second mode, the translational and rotational motions are out of phase, and their effect to displacement is subtractive at the edge 3, but additive at the edge 1. For TS buildings, the first mode is translation predominant and therefore, additional responses occur at the edge 3 of the structure. For

TF buildings, the first mode is torsion predominant. The second mode is translation predominant. The end result is that the additional response can occur at the edge 1 of the building. Based on the above discussion, one can classify eccentric buildings into TS and TF buildings by examining the nature of the first coupled mode in these buildings.

In this section, two methods are introduced for such classification. One method is to carry out a free vibration analysis of the structure to identify the coupled modes of vibration. The second method is based on elastic static analyses of the structure.

### *4.6.1 Classification of asymmetric buildings using free vibration analysis*

One procedure to classify a building is to carry out a free vibration analysis. The nature of a mode can be identified using the modal mass information derived from the free vibration analysis.

Free vibration analyses are performed on the four buildings A3A3A.1, A6A6A.1, A9A9A.1 and A12A12A.1 to illustrate the procedure. Shown on the Figures 4.18 to 4.21 are the dynamic properties of these buildings. The first two mode shapes of the buildings and also the effective modal masses of the first 6 modes of the buildings are presented. The mode shapes of the buildings are given in two formats. In one format, the displacements and rotations at CM of the floors are given for each mode. In the second format, the lateral displacements of the three frames are shown for each mode.

Based on structural dynamics, it can be shown that translation predominant modes in general have larger modal masses than torsional predominant modes. In the figures, the effective modal masses are plotted against the natural periods of the four buildings. It can

be seen that for the A3A3A and the A6A6A building, the first modal mass is significantly less than the second modal mass, indicating that the first mode is torsional predominant. The first translation predominant mode is the second mode as can be seen by the large modal masses associated with the second mode for these two buildings. A review of the mode shapes of these two buildings also leads to the same conclusion. On the other hand, a comparison of the modal masses of the first two modes for the A9A9A.1 and the A12A12A.1 buildings shows that the first mode of these buildings has a larger modal mass and therefore, is translation predominant.

A parameter defined here as *effective modal moment of inertia* provides a quantitative way of identifying the contribution of different modes to the displacements of edge 1 and edge 3 of a building. Depending on the sign of this parameter one can show whether the effects of the rotational and translational components of a coupled mode are additive or subtractive on each edge of the building. The *effective modal moment of inertia for the nth mode* is defined as $I^*_{On}$ (Chopra 1995, where this parameter is called *modal static response for base torque*):

$$I^*_{On} = \sum_{j=1}^{N} r^2 \Gamma_n m_j \phi_{j\theta n} \qquad (4.3)$$

This equation is developed for an asymmetric building with eccentricity in one direction only, such that floor rotations are coupled with floor displacements in the *Y*-direction. In the equation, $N$= total number of floors, $n$= the mode number, $r$= mass radius of gyration, $m$= mass of floor, $\phi_{j\theta n}$= the rotational element on the $j$th floor in the $n$th vibration mode shape.

$\Gamma_n$ is defined as:

$$\Gamma_n = \frac{\sum_{j=1}^{N} m_j \phi_{jyn}}{\sum_{j=1}^{N} m_j \phi_{jyn}^2 + r^2 \sum_{j=1}^{N} m_j \phi_{j\theta n}^2} \qquad (4.4)$$

where $\phi_{jyn}$ is the translational element on the $j$th floor in the $n$th vibration mode.

The *effective modal moment of inertia* idea is based on the concept of modal expansion (Chopra, 1995) that uses the effective modal mass and the effective modal moment of inertia to expand the effective force vector of a structure. It is best explained graphically by Figure 4.22. The figure shows the plan of an asymmetric single mass system, with the effective earthquake force assumed to be proportional to the mass of system and is schematically shown as a vector m. The modal expansion of the effective earthquake force distribution for the two modes of the system are also shown on the figure. These are, in fact, the effective modal masses and effective modal moments of inertia for the two modes. The effective moment of inertia for mode 1 has the same sign as the effective modal mass. The directions of the loadings show that the deformations resulting from rotational and translational components of the first mode are additive on edge 3 and subtractive on edge 1. In the second mode the effects are reversed. Calculation shows that the effective moment of inertia has an opposite sign to the effective mass in this mode.

The fundamental periods for Buildings A3A3A.1, A6A6A.1, A9A9A.1 and A12A12A.1 are 3.54, 1.95, 1.52 and 1.41 second, respectively. The effective modal mass and effective moment of inertia are computed for these four buildings and are given in the

graphs at the bottom of the Figures 4.18 to 4.21. The small square symbols on the graph show the effective modal masses and the small triangle symbols show the effective modal moments of inertia. The sign of the effective modal moment of inertia indicates whether the effects of rotational and translational components of different modes are additive or subtractive for the displacements of edge 1 and edge 3 of a building. A positive sign for the *effective modal moment of inertia* indicates that the translational and rotational motions are in phase and a negative sign implies that the two components are out of phase.

By observing the magnitudes of the modal masses, and the sign of the effective moment of inertia of the first two modes of each building, one can arrive at the conclusion that buildings A3A3A.1 and A6A6A.1 are TF buildings, while buildings A9A9A.1 and A12A12A.1 are TS buildings.

### *4.6.2 Classification of asymmetric buildings using static analyses*

The method discussed in section 4.6.1 requires a free vibrational analysis to be carried out to classify eccentric buildings into TS and TF buildings. In order to give such information at an early stage of design to alert the designers not to use the static torsional provisions for the planned TF building, a practical procedure based on static analyses is present in this section.

The proposed procedure is based on the theory that the nature of the first coupled mode of vibration of an eccentric system can be determined using the frequency ratio ($\Omega$) of the system. The frequency ratio is defined as the ratio of the first uncoupled torsional frequency to the first uncoupled translational frequency of the eccentric system. In single

mass eccentric systems, it has been shown (Tso and Dempsey 1980) that if the frequency ratio is less than unity, the first coupled mode of the eccentric system would be torsion predominant. If the frequency ratio is larger than unity, the first coupled mode will be translation predominant. Therefore, the frequency ratio $\Omega$ is a convenient index to classify TS and TF buildings. The uncoupled torsional frequency of the system depends on the torsional stiffness ($K_\theta$) and the mass moment of inertia ($I_m$) while the uncoupled translational frequency depends on the lateral stiffness (K) and the mass (M) of the system. Therefore, the frequency ratio ($\Omega$) can be expressed as

$$\Omega = \sqrt{\frac{K_\theta}{K} \times \frac{M}{I_m}} \tag{4.5}$$

Defining $\rho_k$ as the normalised radius of gyration for stiffness and $\rho_m$ as the normalised radius of gyration for mass, both quantities being normalised to the plan dimension b orthogonal to the direction of excitation,

$$\rho_k = \frac{1}{b}\sqrt{\frac{K_\theta}{K}} \tag{4.6a}$$

$$\rho_m = \frac{1}{b}\sqrt{\frac{I_m}{M}} \tag{4.6b}$$

the frequency ratio can be written as

$$\Omega = \frac{\rho_k}{\rho_m} \tag{4.7}$$

For a single mass system, both $\rho_m$ and $\rho_k$ can be determined readily because the stiffness and mass parameters are scalar quantities. If one restricts consideration to multi-storey

buildings that are regular in elevation, there would only be minor variations of the floor plan dimensions or shape along the height of the buildings. In this case, $\rho_m$ can be determined based on the mass distribution in a typical floor of the building. If the mass distribution across the plan is uniform, $\rho_m$ can be related to the overall plan dimension d. Typically, $\rho_m$ is of the order of 0.3 d for many building plans of compact shape (Dempsey and Tso 1982).

The determination of $\rho_k$ is more problematic in multi-storey buildings because the torsional and translational stiffnesses of these buildings are normally expressed in terms of matrices. Consequently, $\rho_k$ cannot be determined directly using Equation 4.6a. In anticipation of this difficulty, an alternative way to obtain $\rho_k$ is taken here. This alternative is based on the use of a torsional index $\Delta$. The torsional index $\Delta$ is defined as the ratio of the elastic displacements at edge 1 and edge 3, when the building is subjected to the static equivalent loading applied through the centre of mass. This index is related to $\rho_k$ by the following formula (Tso and Wong 1995):

$$\Delta = \frac{\delta_{\min}}{\delta_{\max}} = 1 - \left(\frac{e}{\rho_k^2}\right)\left[1 + \left(\frac{e}{\rho_k^2}\right)(0.5 + \eta)\right]^{-1} \qquad (4.8)$$

where

$\Delta$ = displacement ratio with the load at CM,

$\delta_{min}$ = minimum edge displacement with the load at CM,

$\delta_{max}$ = maximum edge displacement with the load at CM,

e = distance between centre of mass and centre of rigidity of the floor, normalised

to width of the floor,

$\eta$ = distance between geometric centre and centre of rigidity of the floor, normalised to width of the floor.

The usefulness of this index is that $\Delta$ can be computed based on quantities such as $\delta_{min}$ and $\delta_{max}$ which are readily available to designers. On the other hand, quantities such as $\rho_k$, eccentricity e and location of centre of rotation $\eta$ are quantities not readily available.

The development of the procedure is first presented in terms of a single mass eccentric system. It involves two loading cases. First, the structure is subjected to the equivalent static lateral load applied at the centre of mass (CM) of the system. The second set of loading involved applying the same static lateral load at a convenient distance from CM. A location at CM+$\beta$b is chosen for the current development where $\beta$ is the accidental torsion coefficient usually specified in design codes. In each of these loadings, the elastic edge displacements in the direction of loading and their ratios are calculated. In addition, the floor rotation $\theta$ for each loading is determined.

$$\begin{cases} \theta = \dfrac{\delta_{\max} - \delta_{\min}}{b} = \dfrac{P.b.e}{K_\theta} & (4.9a) \\ \theta^+ = \dfrac{\delta^+_{\max} - \delta^+_{\min}}{b} = \dfrac{P.b.(e+\beta)}{K_\theta} & (4.9b) \end{cases}$$

A superscript + is used in the equations to denote the corresponding quantities associated with the load applied at the CM+$\beta$b location.

Eliminating $K_\theta$ from Equation 4.9,

$$e = \frac{\beta \times \theta}{\theta^{+} - \theta} \tag{4.10}$$

Based on geometry as shown in Figure 4.23, one can relate the position of the centre of rotation $\eta$ by

$$\eta = 0.5 + e - \alpha \tag{4.11}$$

where $\alpha$ is the distance between CM and edge 1.

The edge displacements can be expressed in terms of the displacement at CR, $\delta_{CR}$, by the following expressions:

$$\begin{cases} \delta_{\min} = \delta_{CR} - \theta \times (\frac{b}{2} - \eta b) & (4.12a) \\ \delta_{\max} = \delta_{CR} + \theta \times (\frac{b}{2} + \eta b) & (4.12b) \end{cases}$$

Expressing the displacement at the rigidity centre (CR) and the floor rotation in terms of the translational and torsional stiffnesses of the system, the displacement ratio "$\Delta$" can be written as:

$$\Delta = \frac{\rho_k^2 - e(0.5 - \eta)}{\rho_k^2 + e(0.5 + \eta)} \tag{4.13}$$

Rewriting Equation 4.13, we get

$$\rho_k^2 = \left[\frac{0.5(1+\Delta)}{1-\Delta} - \eta\right] e \tag{4.14}$$

Once the edge displacements $\delta_{max}$, $\delta_{min}$, $\delta^{+}_{max}$ and $\delta^{+}_{min}$ are found from the static

analyses of the structure, e and $\eta$ can be computed from Equations 4.10 and 4.11, and $\rho_k$ from Equation 4.14. Once both $\rho_k$ and $\rho_m$ are known, the frequency ratio $\Omega$ can be found using Equation 4.7.

While the derivation is based on a single mass system, examples will illustrate that the procedure is also applicable to eccentric multi-storey buildings that are regular in elevation. The four asymmetric multi-storey buildings having the same translational stiffness but different torsional stiffnesses will be used to illustrate the proposed procedure.

To classify these buildings using the static procedure, sets of static lateral loads having a triangular distribution along the height of the buildings are applied at the CM and then at location CM+0.05b in each of the four buildings. The maximum edge displacements and the displacement ratios at each floor are presented in Tables 4.3 to 4.6 from the two static loading cases. Also included are the computed quantities e, $\rho_k$ and finally the frequency ratio $\Omega$. The normalised radius of gyration of mass ($\rho_m$) used in the calculation for $\Omega$ equals 0.28.

Two approaches are used to obtain e, $\rho_k$ and $\Omega$. First, they are calculated on a per floor basis. Alternatively, the average values of the maximum edge displacements are used. An examination of the last three columns in the tables will show that for all three quantities, the variation on a per floor basis is small and both approaches give similar results. All four buildings have an eccentricity e equal to 0.1. The calculated eccentricities based on the edge displacement results are within 15% of the true eccentricity. While there is a larger variation regarding the frequency ratio $\Omega$ from floor to floor, they provide

the same information on the nature of the first mode of the buildings. The frequency ratios for the A3A3A and A6A6A buildings are less than unity, while those for the A9A9A and A12A12A buildings are larger than unity. Therefore, the A3A3A and A6A6A buildings would have their first mode being torsion predominant while the A9A9A and A12A12A buildings have their first mode translation predominant. Therefore, buildings A3A3A and A6A6A should behave like TF buildings and buildings A9A9A and A12A12A behave like TS buildings. The validity of these conclusions has already demonstrated in chapter 3.

## 4.7 Summary

Followings are the highlights of the tasks presented in this chapter:

- Using different design methods to allow for the torsional effect, the improvement to reduce the seismic displacements and storey drifts responses at the edges are minimal.
- The design based on static equilibrium reduces the ductility demand in the TS buildings but is not able to reduce the ductility demand in the torsionally flexible (TF) buildings.
- In TS buildings, the incorporation of the static torsional provisions of UBC can reduce the additional ductility demands in the beams and columns for frames at the edge 3 of the building. However, the additional interstorey drifts and floor displacements caused by torsion are minimally affected by the incorporation of the provisions. This implies that while the structural damage will be reduced, the torsional provisions may not be effective in reducing the non-structural damage at the edge 3 of the building.

- The design based on UBC static torsional provisions is not efficient in the design of TF building as it over-protects the elements located at the flexible side (edge 3) of the building but does not assign enough strength on the elements on the stiff side (edge 1) of the building.
- The use of a design based on response spectrum analysis has a negligible effect to change the deformations of TS buildings and has only a small effect on the deformations of TF buildings. However, this design approach is effective in reducing the ductility demands in both the TS and TF buildings studied here.
- Since the static application of lateral loads at the CM of the floors will lead to a decrease in response at the edge 1 and an increase of response at the edge 3, it cannot correctly predict the distribution of additional responses caused by torsion in TF buildings. Therefore, the static torsional provisions should not be applied to TF buildings, even though the buildings themselves are regular in elevation.
- It is noted that unlike single mass models, there can be many possible ways to implement the strength increase requirements obtained from the torsional provisions. Clear guideline should be given to designers so that the intent of the torsional provisions will be reflected in the actual design.
- A procedure is developed based on the natural vibration properties of the building to classify buildings as torsionally stiff or torsionally flexible. The modal masses of the system are key parameters in this method. A comparison of modal masses is a reliable method to determine the nature of the modes of vibration.
- A second procedure to identify torsionally flexible systems is developed based on

static analyses. The advantage of this second procedure is that only elastic static analyses are involved and is based on information already available to designers early in the design process.

Table 4.1. UBC amplification factor for A12A12A.1

| (1) | (2) | (3) | (4) | (5) | (6) |
|---|---|---|---|---|---|
| | $\frac{max.\ storey\ drift}{avg.\ storey\ drift}$ | | $A_x = \left[\frac{\delta_{max}}{1.2\delta_{avg}}\right]^2$ | | |
| **Floor** | **Load at** (CM+0.05b) | **Load at** (CM-0.05b) | **Load at** (CM+0.05b) | **Load at** (CM-0.05b) | **$A_x$** |
| 7 | 1.48 | 1.16 | 1.43 | 0.92 | **1.43** |
| 6 | 1.45 | 1.15 | 1.43 | 0.92 | **1.43** |
| 5 | 1.45 | 1.15 | 1.42 | 0.91 | **1.42** |
| 4 | 1.44 | 1.15 | 1.42 | 0.91 | **1.42** |
| 3 | 1.44 | 1.15 | 1.40 | 0.91 | **1.40** |
| 2 | 1.42 | 1.14 | 1.39 | 0.9 | **1.39** |
| 1 | 1.40 | 1.14 | 1.35 | 0.89 | **1.35** |

Table 4.2. UBC amplification factor for A6A6A.1

| (1) | (2) | (3) | (4) | (5) | (6) |
|---|---|---|---|---|---|
| | $\frac{max.\ storey\ drift}{avg.\ storey\ drift}$ | | $A_x = \left[\frac{\delta_{max}}{1.2\delta_{avg}}\right]^2$ | | |
| **Floor** | **Load at** (CM+0.05b) | **Load at** (CM-0.05b) | **Load at** (CM+0.05b) | **Load at** (CM-0.05b) | **$A_x$** |
| 7 | 3.23 | 1.75 | 4.89 | 1.7 | **3.00** |
| 6 | 2.87 | 1.64 | 4.74 | 1.67 | **3.00** |
| 5 | 2.77 | 1.60 | 4.62 | 1.65 | **3.00** |
| 4 | 2.71 | 1.58 | 4.48 | 1.62 | **3.00** |
| 3 | 2.62 | 1.56 | 4.27 | 1.58 | **3.00** |
| 2 | 2.47 | 1.51 | 3.96 | 1.51 | **3.00** |
| 1 | 2.24 | 1.43 | 3.49 | 1.41 | **3.00** |

Table 4.3. Building A3A3A.1

| Floor | δmax | δmin | Δ | θ | δmax+ | δmin+ | Δ+ | θ+ | e | ρk | Ω |
|---|---|---|---|---|---|---|---|---|---|---|---|
| 7 | 1.068 | -0.635 | -0.59 | 0.0710 | 1.488 | -1.052 | -0.71 | 0.1058 | 0.102 | 0.114 | 0.41 |
| 6 | 0.947 | -0.542 | -0.57 | 0.0620 | 1.315 | -0.908 | -0.69 | 0.0926 | 0.101 | 0.117 | 0.42 |
| 5 | 0.800 | -0.441 | -0.55 | 0.0517 | 1.106 | -0.745 | -0.67 | 0.0771 | 0.102 | 0.121 | 0.43 |
| 4 | 0.625 | -0.330 | -0.53 | 0.0398 | 0.860 | -0.563 | -0.65 | 0.0593 | 0.102 | 0.126 | 0.45 |
| 3 | 0.431 | -0.213 | -0.49 | 0.0268 | 0.590 | -0.371 | -0.63 | 0.0400 | 0.102 | 0.131 | 0.47 |
| 2 | 0.238 | -0.106 | -0.44 | 0.0143 | 0.322 | -0.189 | -0.59 | 0.0213 | 0.102 | 0.140 | 0.50 |
| 1 | 0.075 | -0.027 | -0.36 | 0.0043 | 0.101 | -0.053 | -0.52 | 0.0064 | 0.102 | 0.154 | 0.55 |
| mean | 0.598 | -0.328 | -0.51 | 0.0390 | 0.826 | -0.554 | -0.64 | 0.0580 | 0.102 | 0.129 | 0.46 |

Table 4.4. Building A6A6A.1

| Floor | δmax | δmin | Δ | θ | δmax+ | δmin+ | Δ+ | θ+ | e | ρk | Ω |
|---|---|---|---|---|---|---|---|---|---|---|---|
| 7 | 0.453 | -0.024 | -0.05 | 0.0199 | 0.571 | -0.141 | -0.25 | 0.0297 | 0.102 | 0.214 | 0.76 |
| 6 | 0.418 | -0.017 | -0.04 | 0.0181 | 0.525 | -0.123 | -0.23 | 0.0270 | 0.102 | 0.217 | 0.78 |
| 5 | 0.366 | -0.011 | -0.03 | 0.0157 | 0.460 | -0.103 | -0.22 | 0.0235 | 0.101 | 0.218 | 0.78 |
| 4 | 0.298 | -0.005 | -0.02 | 0.0126 | 0.372 | -0.079 | -0.21 | 0.0188 | 0.102 | 0.222 | 0.79 |
| 3 | 0.216 | 0.000 | 0.00 | 0.0090 | 0.269 | -0.052 | -0.19 | 0.0134 | 0.102 | 0.226 | 0.81 |
| 2 | 0.127 | 0.004 | 0.03 | 0.0051 | 0.157 | -0.026 | -0.16 | 0.0076 | 0.102 | 0.234 | 0.84 |
| 1 | 0.044 | 0.004 | 0.09 | 0.0017 | 0.054 | -0.006 | -0.11 | 0.0025 | 0.106 | 0.252 | 0.90 |
| mean | 0.275 | -0.007 | -0.00 | 0.0120 | 0.344 | -0.076 | -0.20 | 0.0180 | 0.102 | 0.225 | 0.80 |

Table 4.5. Building A9A9A.1

| Floor | δmax | δmin | Δ | θ | δmax+ | δmin+ | Δ+ | θ+ | e | ρk | Ω |
|---|---|---|---|---|---|---|---|---|---|---|---|
| 7 | 0.324 | 0.104 | 0.32 | 0.0092 | 0.378 | 0.051 | 0.13 | 0.0136 | 0.105 | 0.320 | 1.14 |
| 6 | 0.302 | 0.099 | 0.33 | 0.0085 | 0.352 | 0.049 | 0.14 | 0.0126 | 0.104 | 0.321 | 1.15 |
| 5 | 0.266 | 0.088 | 0.33 | 0.0074 | 0.310 | 0.045 | 0.14 | 0.0110 | 0.103 | 0.320 | 1.14 |
| 4 | 0.218 | 0.074 | 0.34 | 0.0060 | 0.254 | 0.038 | 0.15 | 0.0090 | 0.100 | 0.318 | 1.14 |
| 3 | 0.160 | 0.055 | 0.35 | 0.0044 | 0.186 | 0.030 | 0.16 | 0.0065 | 0.105 | 0.329 | 1.18 |
| 2 | 0.096 | 0.035 | 0.36 | 0.0025 | 0.111 | 0.020 | 0.18 | 0.0038 | 0.096 | 0.320 | 1.14 |
| 1 | 0.034 | 0.013 | 0.39 | 0.0009 | 0.039 | 0.008 | 0.21 | 0.0013 | 0.113 | 0.359 | 1.28 |
| mean | 0.200 | 0.067 | 0.35 | 0.0060 | 0.233 | 0.034 | 0.16 | 0.0080 | 0.104 | 0.327 | 1.17 |

Table 4.6. Building A12A12A.1

| Floor | δmax | δmin | Δ | θ | δmax+ | δmin+ | Δ+ | θ+ | e | ρk | Ω |
|---|---|---|---|---|---|---|---|---|---|---|---|
| 7 | 0.277 | 0.152 | 0.55 | 0.0052 | 0.308 | 0.121 | 0.39 | 0.0078 | 0.100 | 0.413 | 1.48 |
| 6 | 0.258 | 0.142 | 0.55 | 0.0048 | 0.287 | 0.113 | 0.40 | 0.0073 | 0.096 | 0.406 | 1.45 |
| 5 | 0.229 | 0.126 | 0.55 | 0.0043 | 0.254 | 0.101 | 0.40 | 0.0064 | 0.102 | 0.420 | 1.50 |
| 4 | 0.188 | 0.104 | 0.55 | 0.0035 | 0.208 | 0.083 | 0.40 | 0.0052 | 0.103 | 0.424 | 1.51 |
| 3 | 0.138 | 0.077 | 0.56 | 0.0025 | 0.153 | 0.062 | 0.41 | 0.0038 | 0.096 | 0.412 | 1.47 |
| 2 | 0.083 | 0.047 | 0.57 | 0.0015 | 0.092 | 0.038 | 0.42 | 0.0023 | 0.094 | 0.412 | 1.47 |
| 1 | 0.030 | 0.017 | 0.58 | 0.0005 | 0.033 | 0.014 | 0.43 | 0.0008 | 0.083 | 0.396 | 1.41 |
| mean | 0.172 | 0.095 | 0.56 | 0.0030 | 0.191 | 0.076 | 0.41 | 0.0050 | 0.096 | 0.411 | 1.47 |

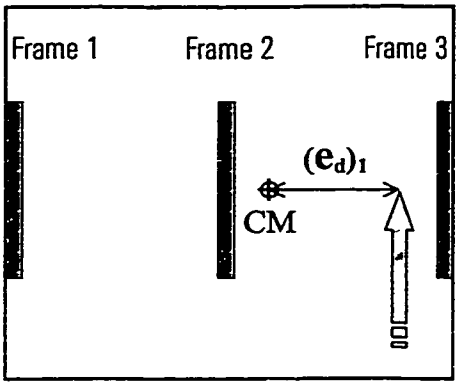


(a)

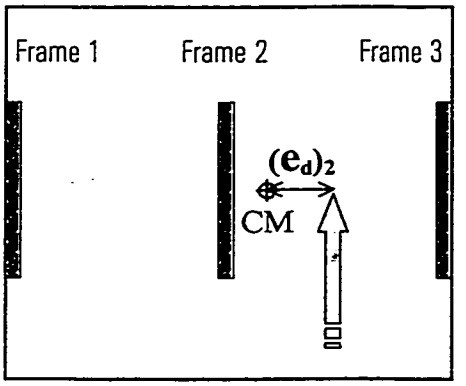


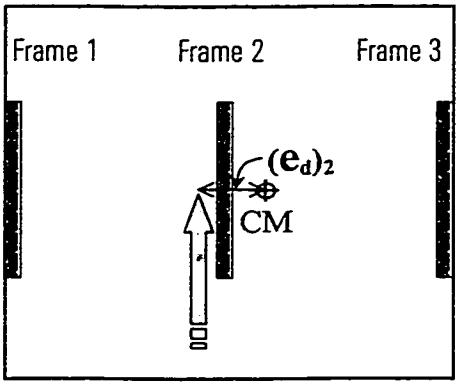


(b) (c)

Figure 4.1. Effect of the two design eccentricities in strength distribution:
(a) Design of Frame 3 is governed by the first eccentricity
(b&c) Two different possibilities for the second eccentricity to affect the design strength of Frame 1

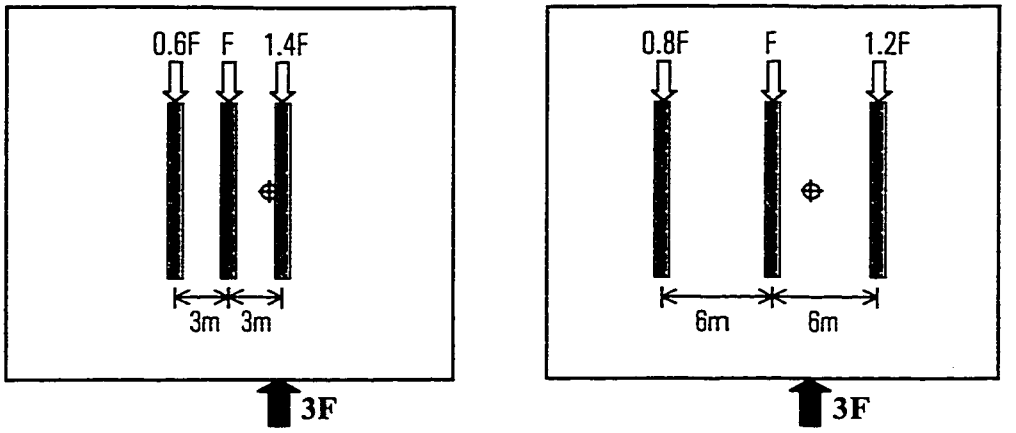


(a) A3A3A.1 (b) A6A6A.1

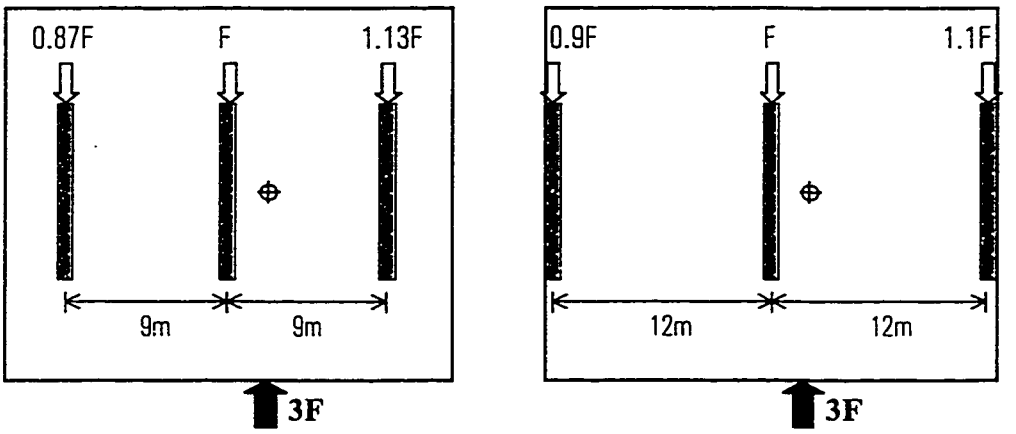


(c) A9A9A.1 (d) A12A12A.1

Figure 4.2. Distribution of strengths in frames of the seven-storey buildings based on static equilibrium.
(a) A3A3A with e/b =0.1
(b) A6A6A with e/b =0.1
(c) A9A9A with e/b =0.1
(d) A12A12A with e/b =0.1

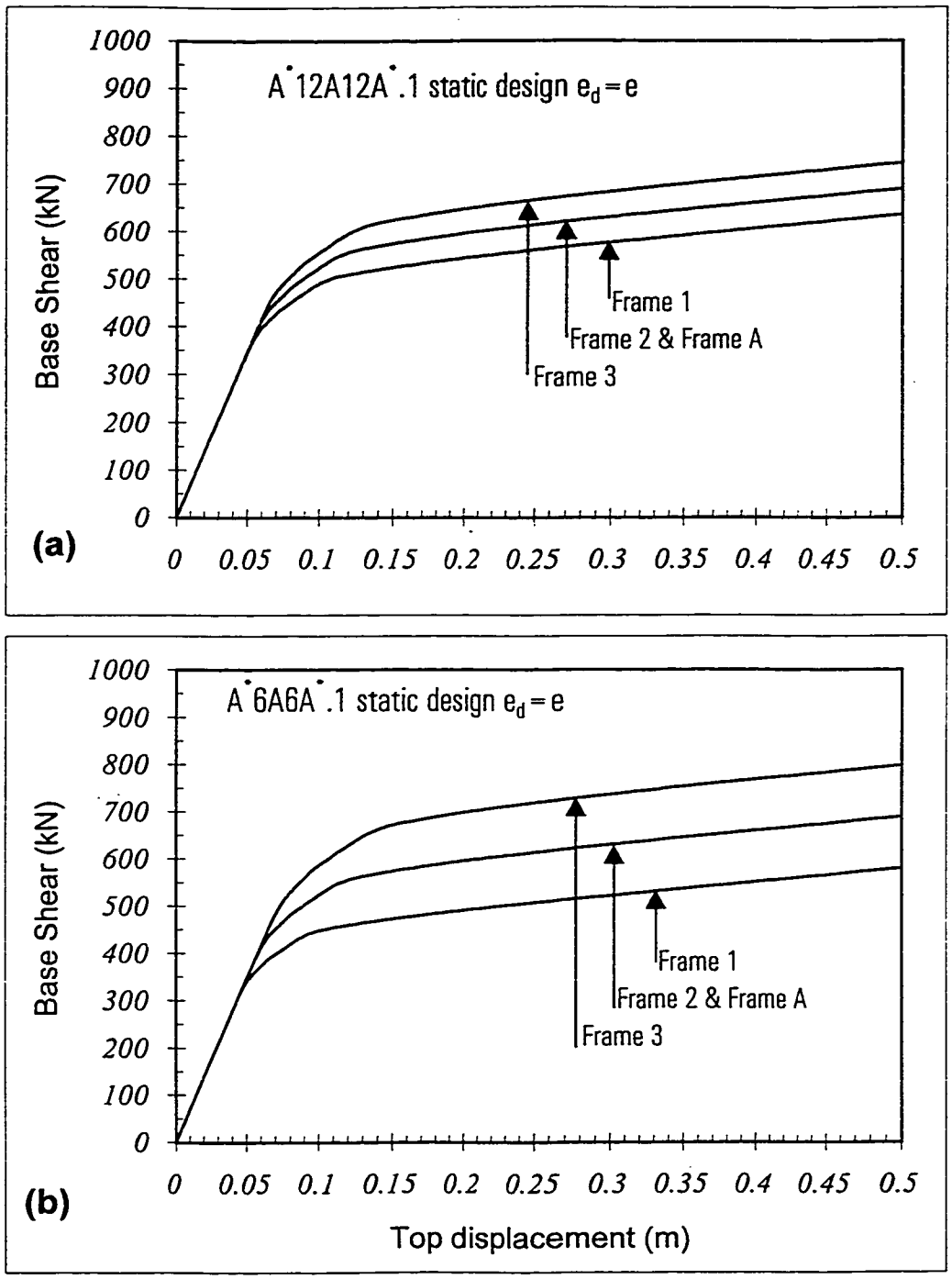


Figure 4.3. 2-D pushover of the frames in buildings designed for torsion based on static equilibrium method:
(a) Building A*12A12A*.1,
(b) Building A*6A6A*.1

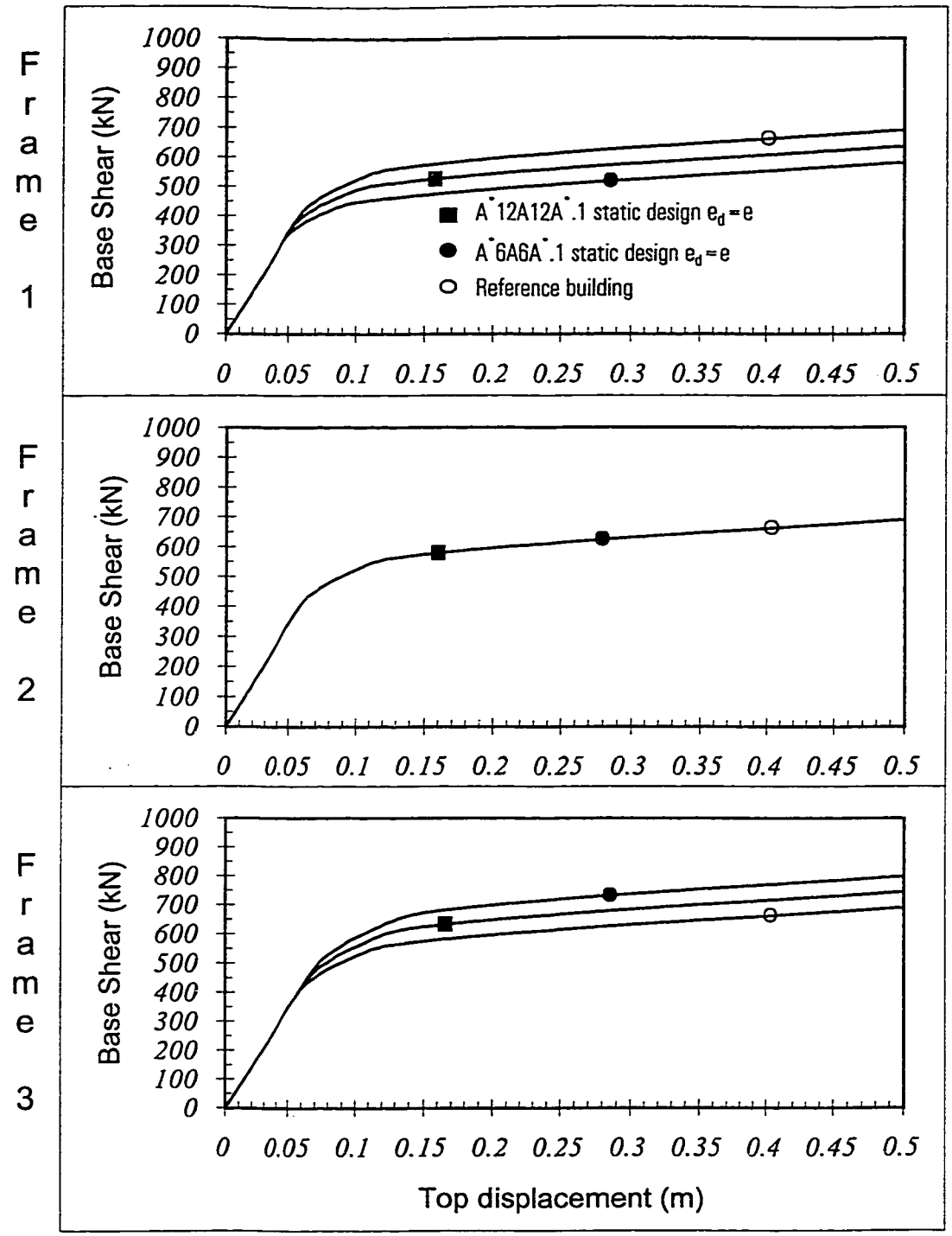


Figure 4.4. 2-D pushover of the frames in buildings designed for torsion based on static equilibrium method and also frames of the reference building

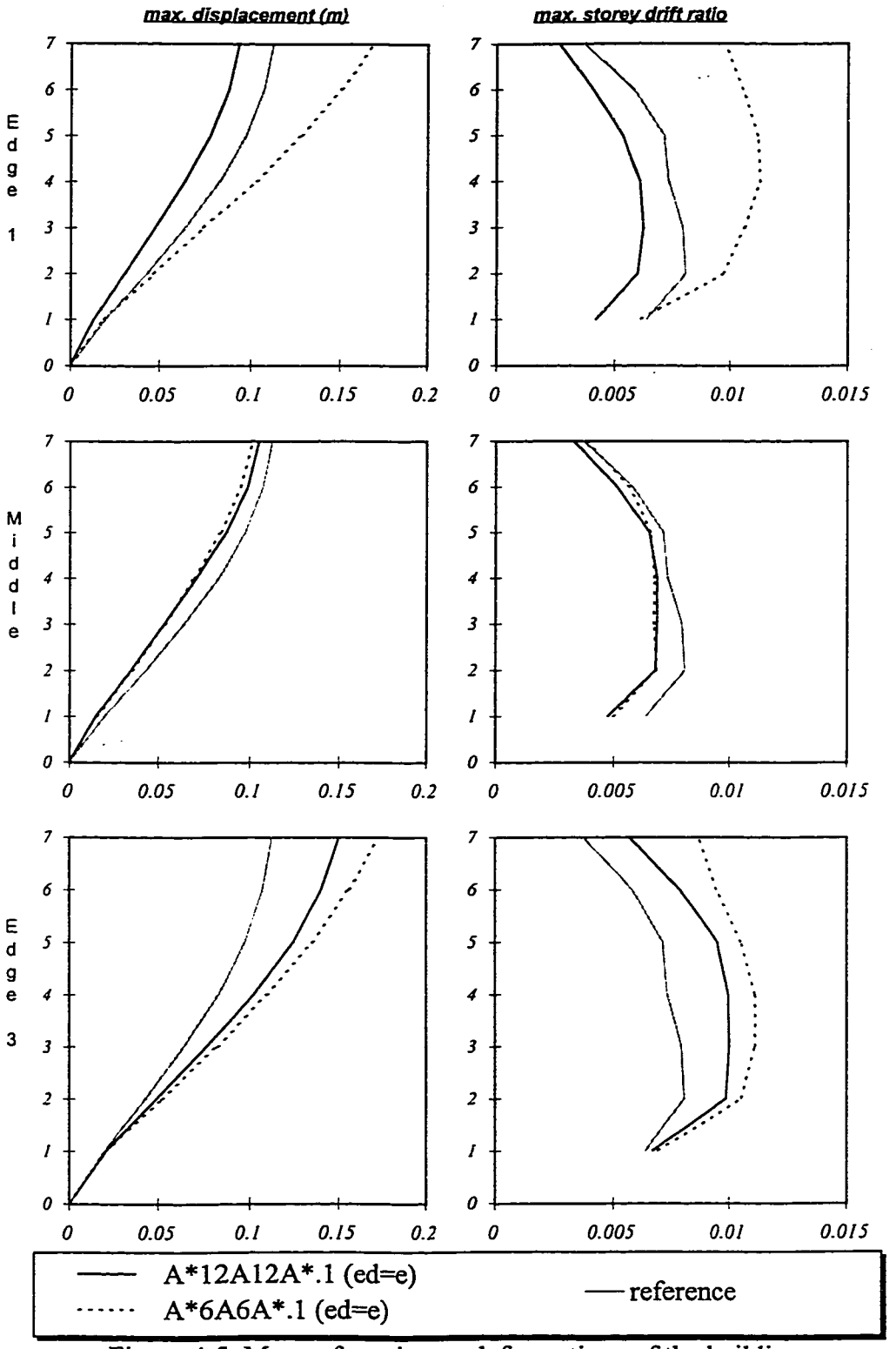


Figure 4.5. Mean of maximum deformations of the buildings

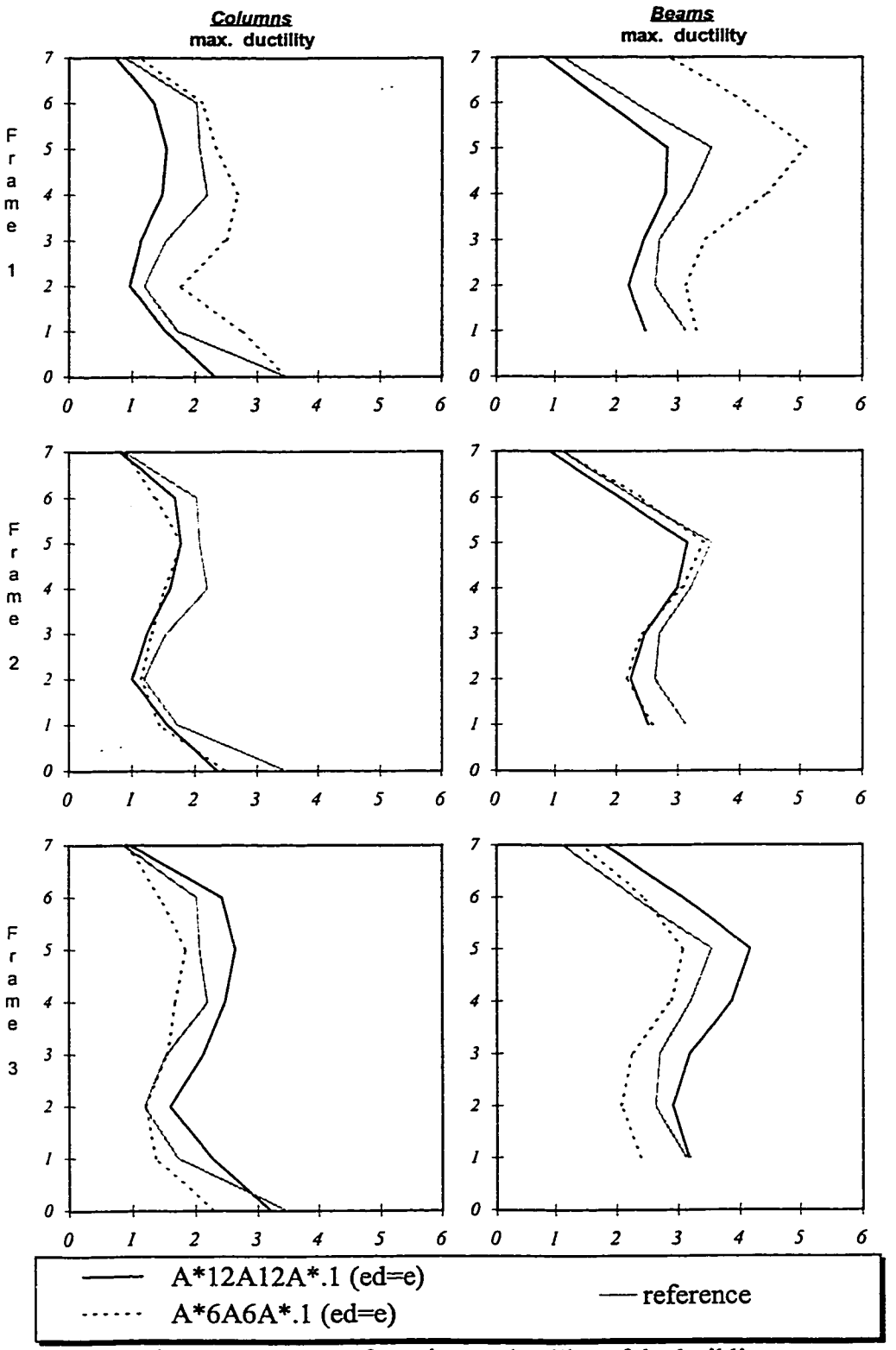


Figure 4.6. Mean of maximum ductility of the buildings

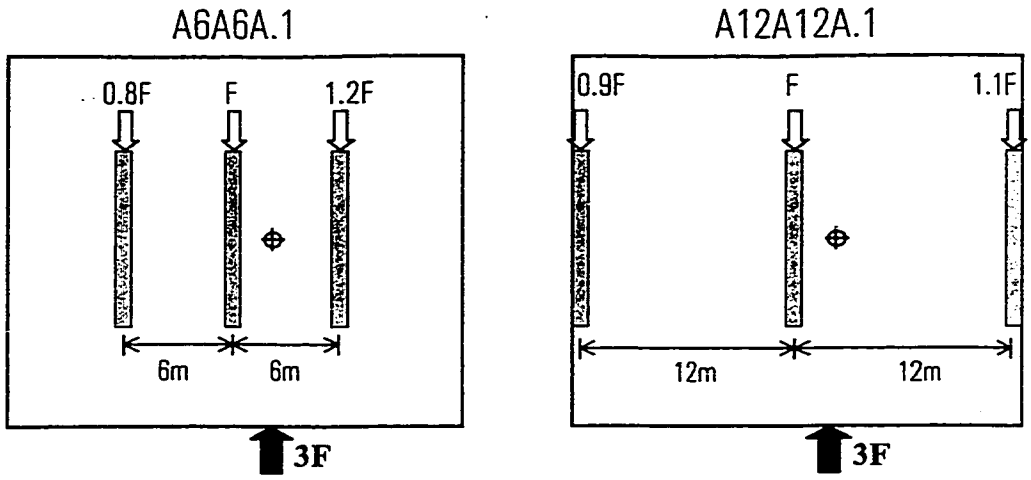


*(a) Static equilibrium*

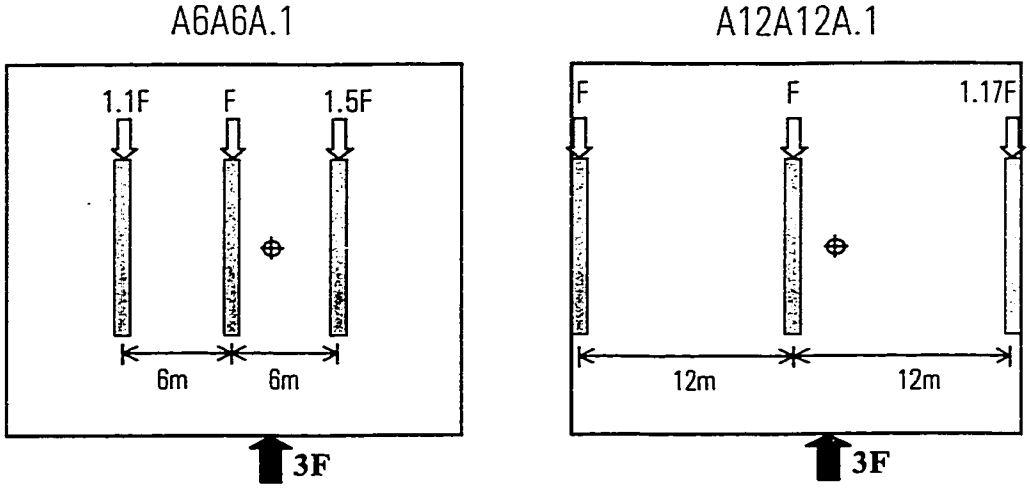


*(b) UBC*

Figure 4.7. Comparison of design strength distribution in the frames of the buildings:
(a) Based on static equilibrium
(b) Based on UBC torsional provisions

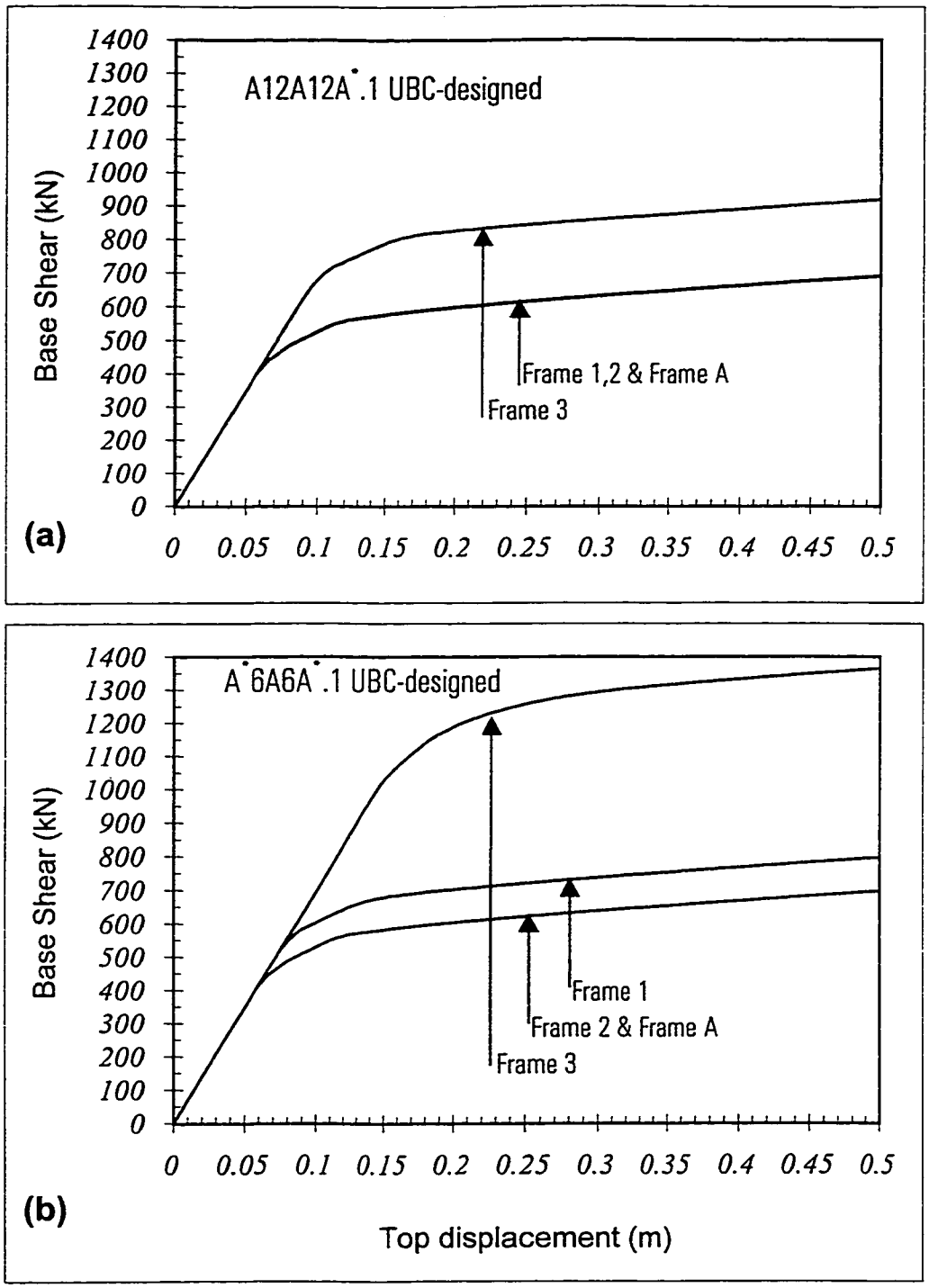


Figure 4.8. 2-D pushover of the frames in buildings designed for torsion based on UBC code:
(a) Building A12A12A*.1, (b) Building A*6A6A*.1

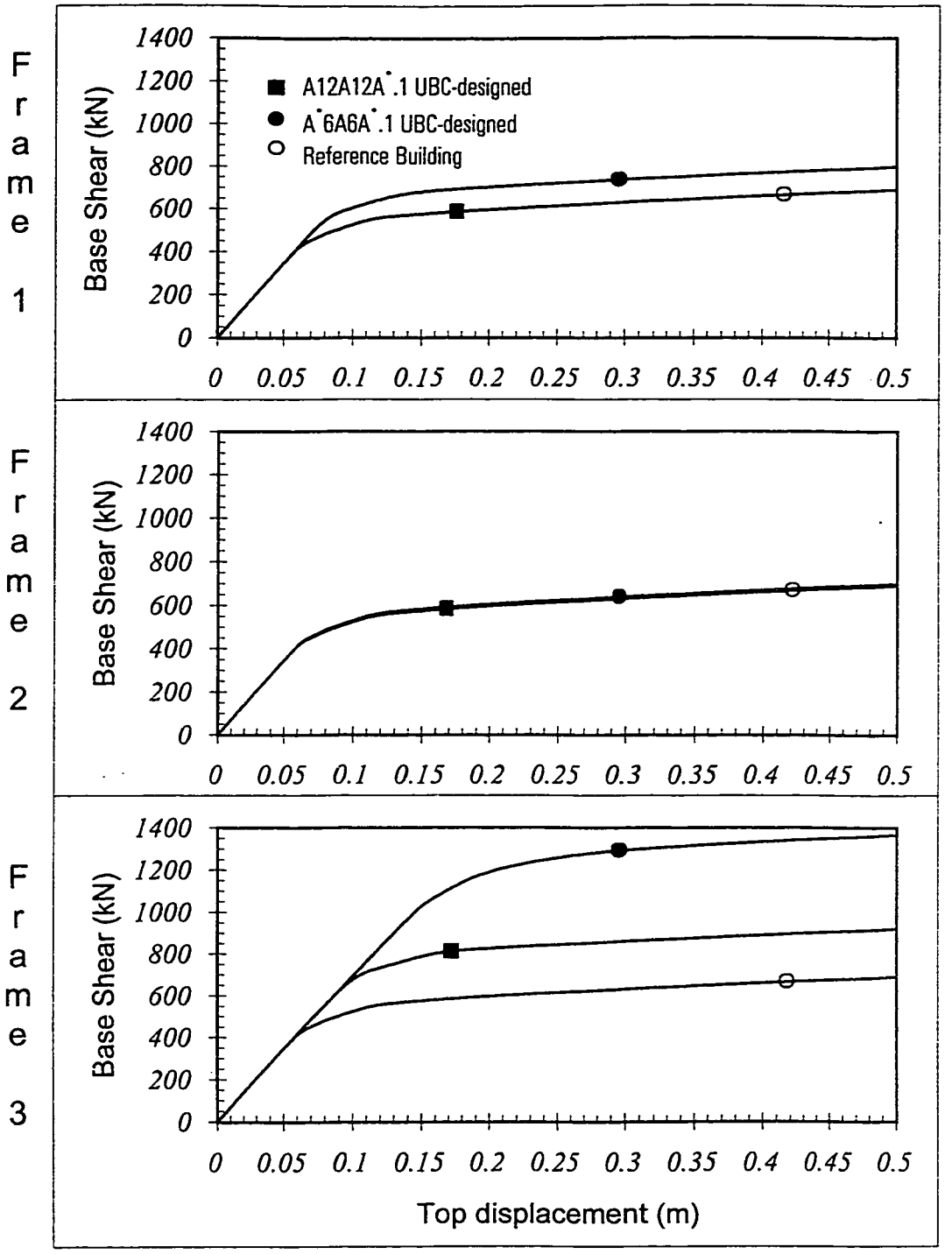


Figure 4.9. 2-D pushover of the frames in buildings designed for torsion based on UBC and also frames of the reference building

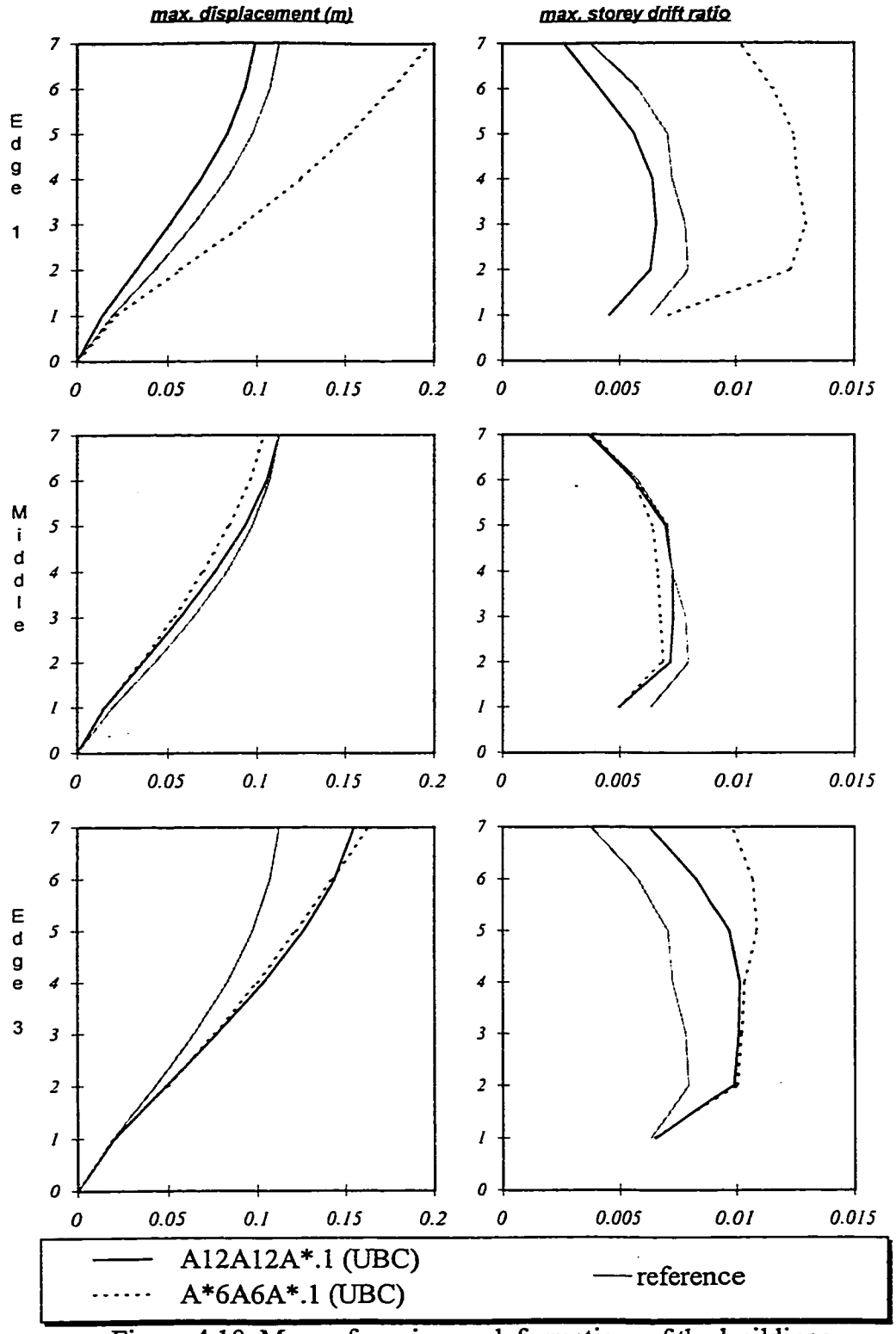


Figure 4.10. Mean of maximum deformations of the buildings

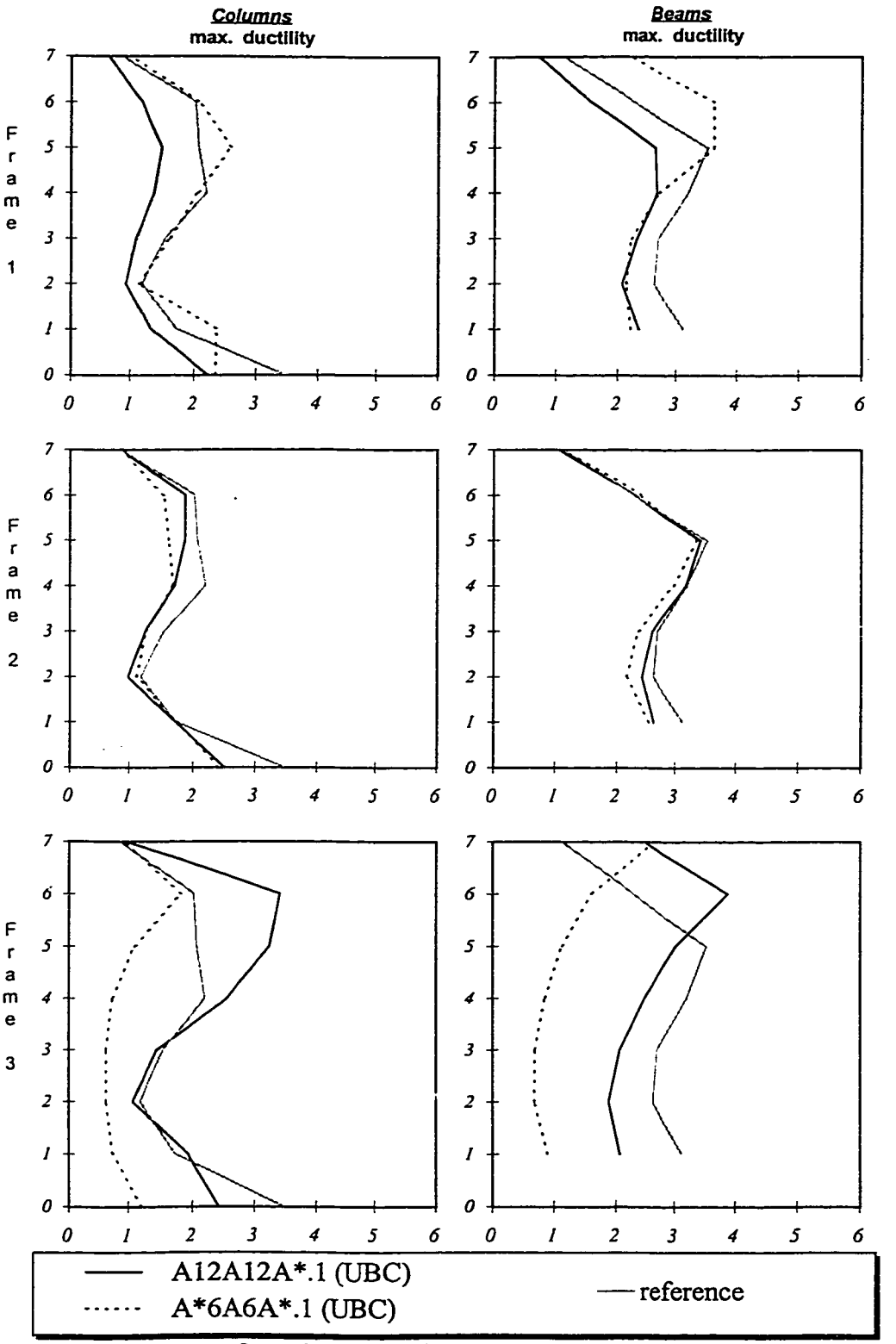


Figure 4.11. Mean of maximum ductility demand of the buildings

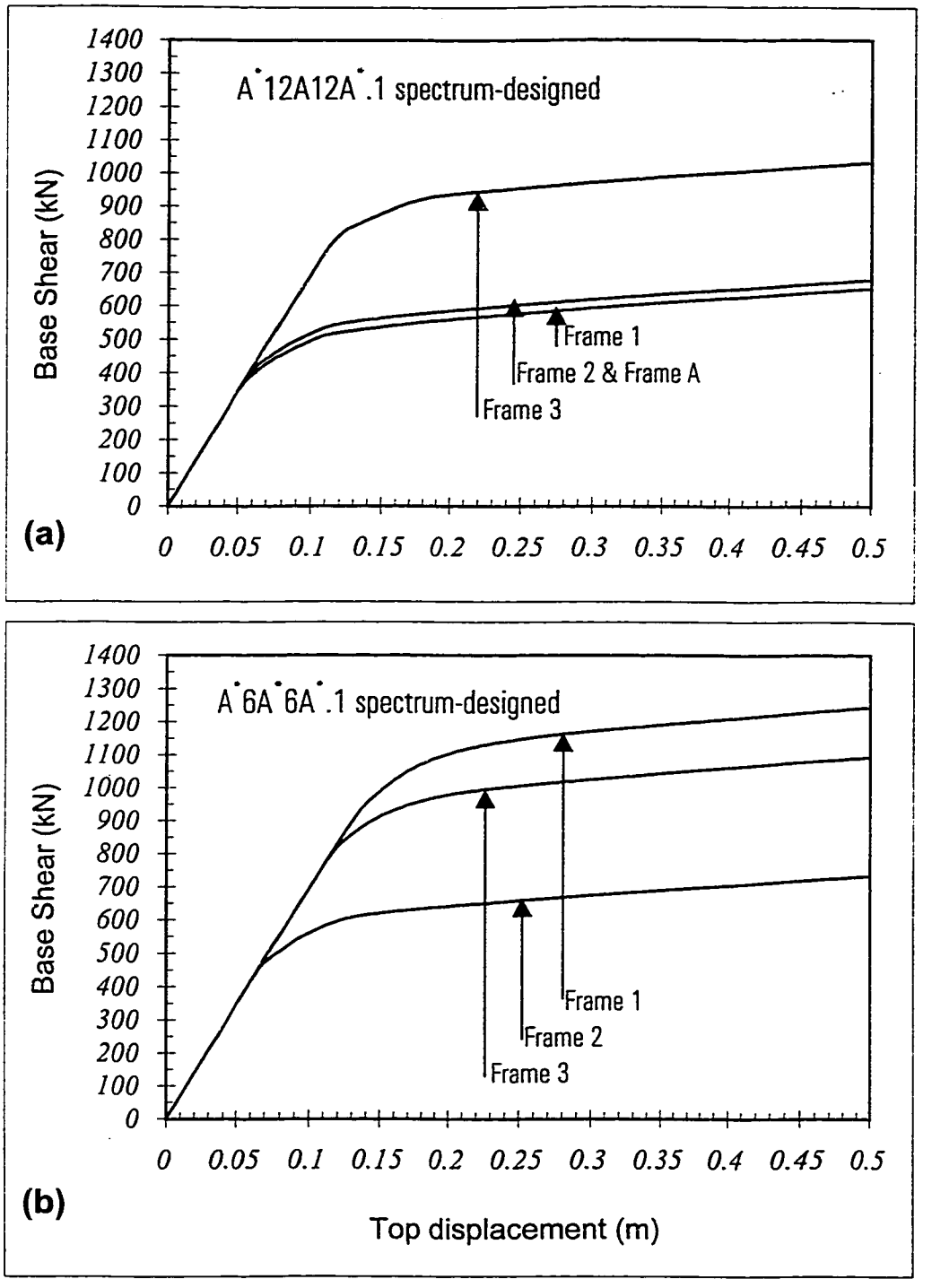


Figure 4.12. 2-D pushover of the frames in buildings designed for torsion based on spectrum analysis:
(a) Building A*12A12A*.1, (b) Building A*6A*6A*.1

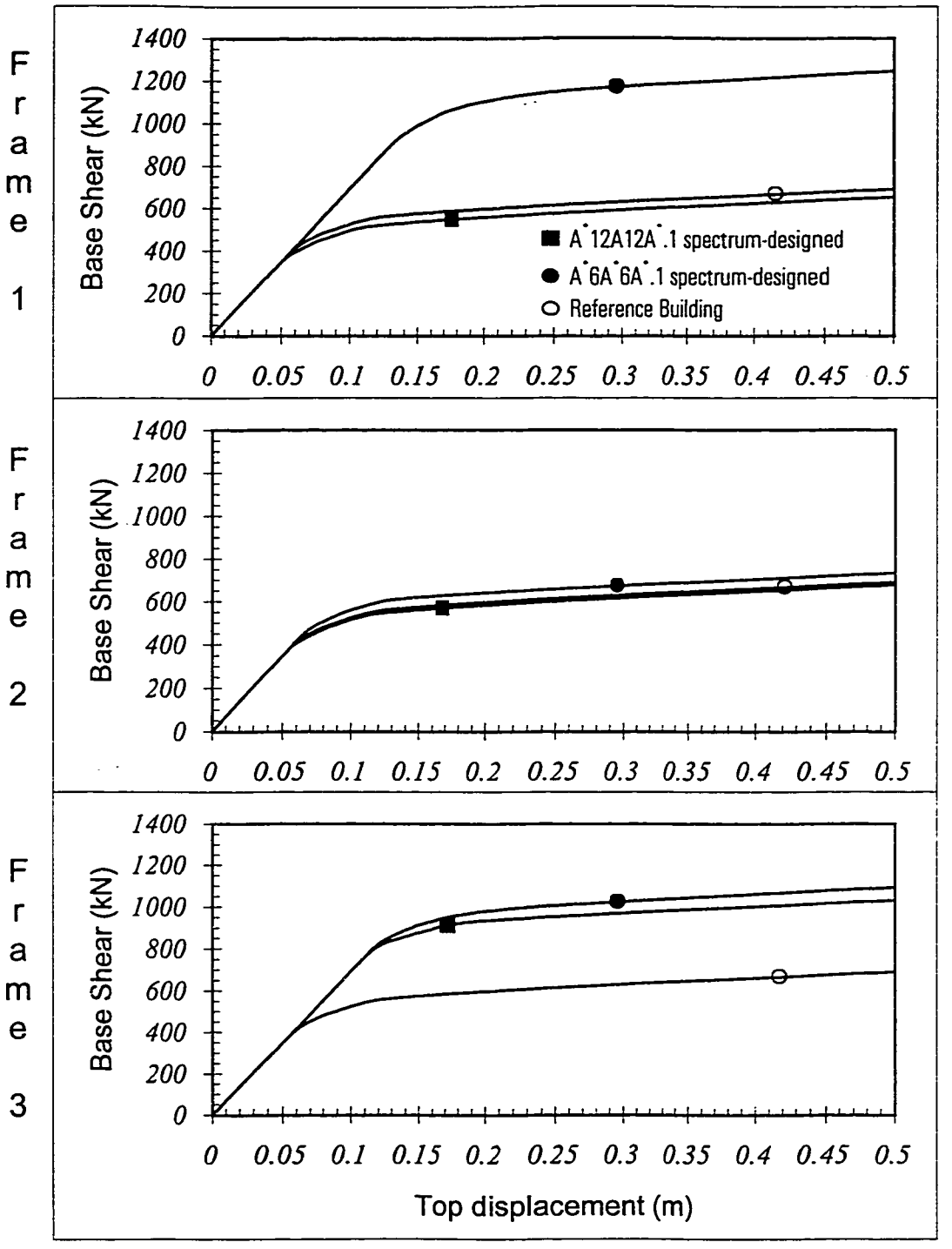


Figure 4.13. 2-D pushover of the frames in the buildings designed for torsion based on spectrum and also frames of the reference building

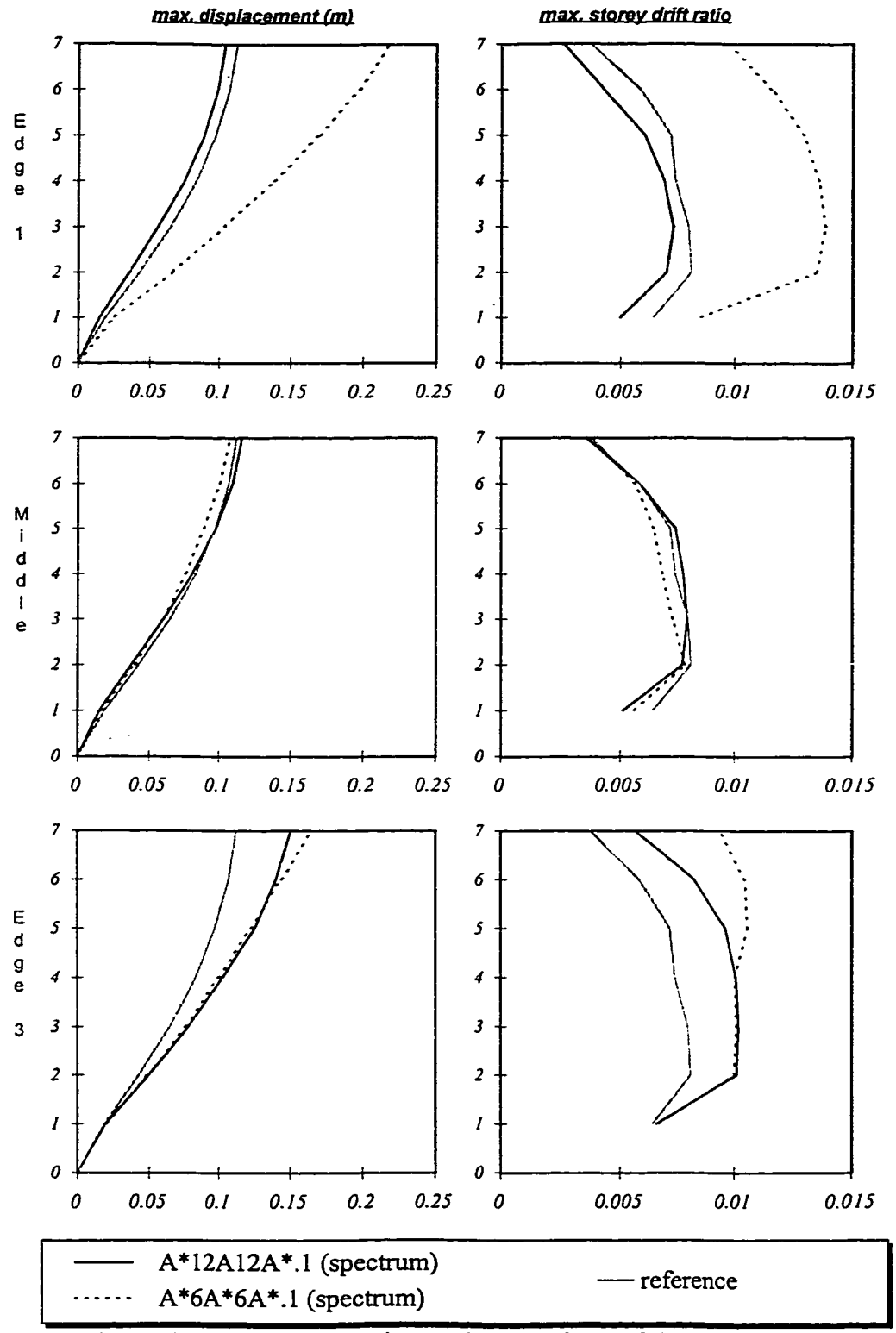


Figure 4.14. Mean of maximum deformations of the buildings

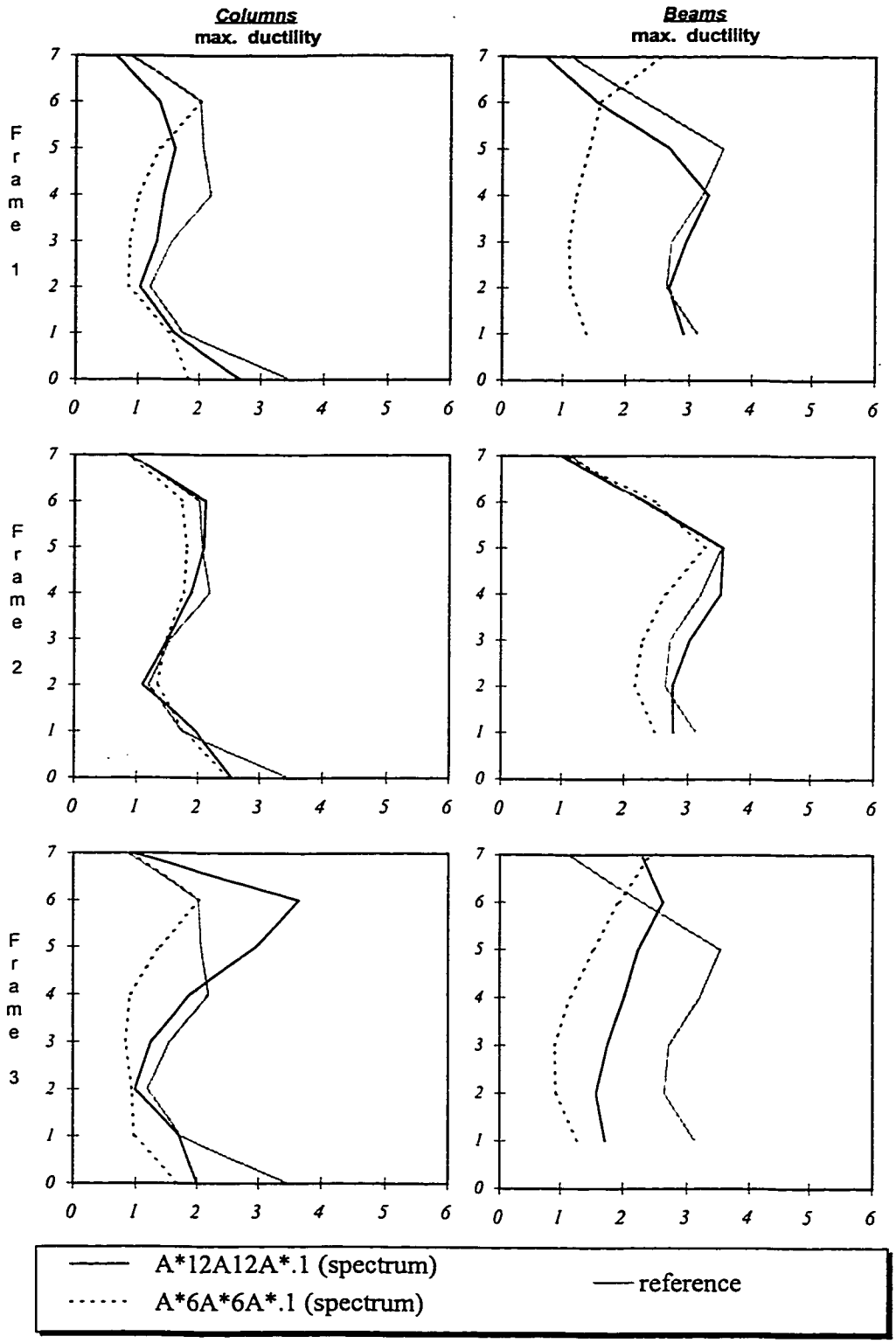


Figure 4.15. Mean of maximum ductility demand of the buildings

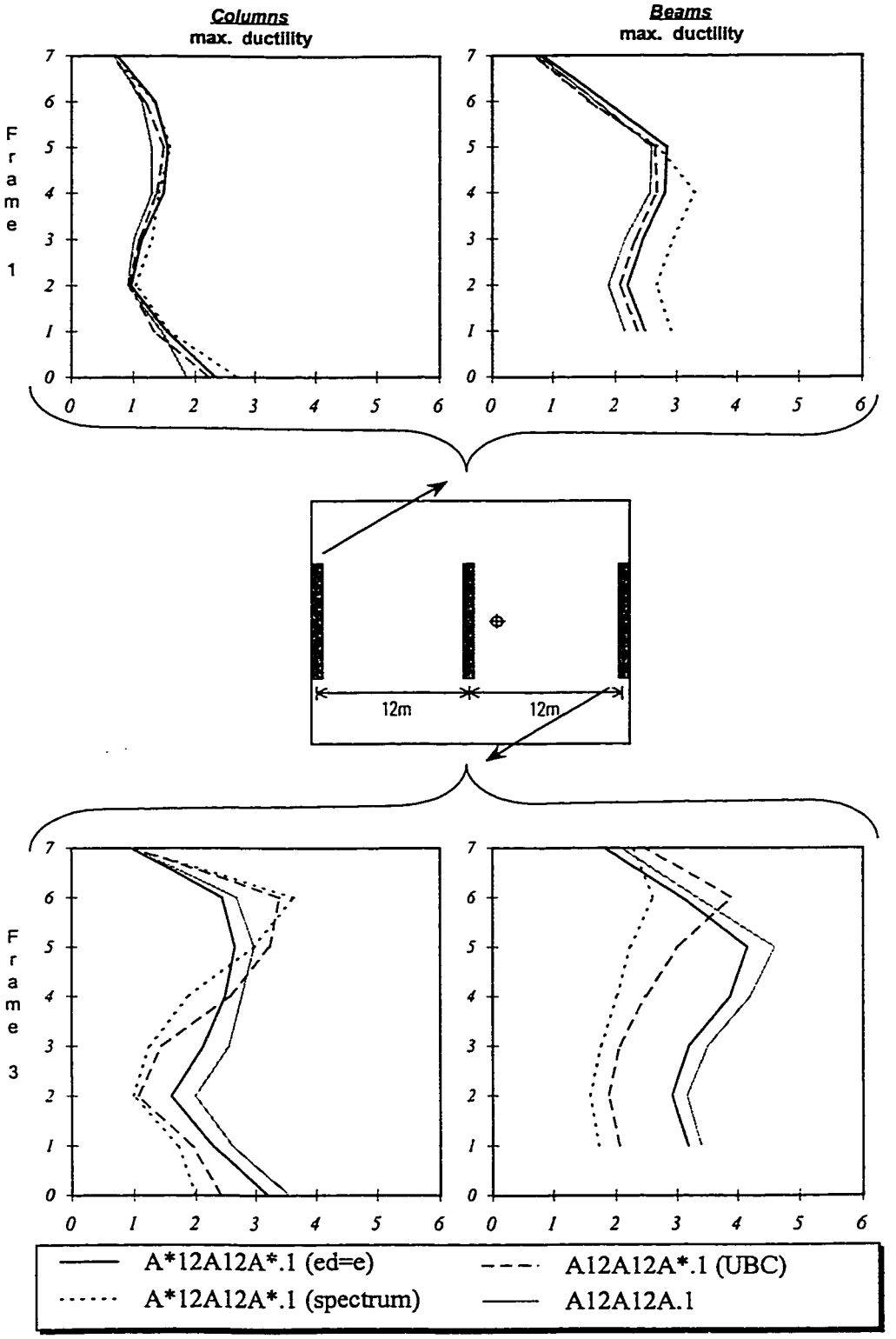


Figure 4.16. Mean of maximum ductility demands of A12A12A Buildings

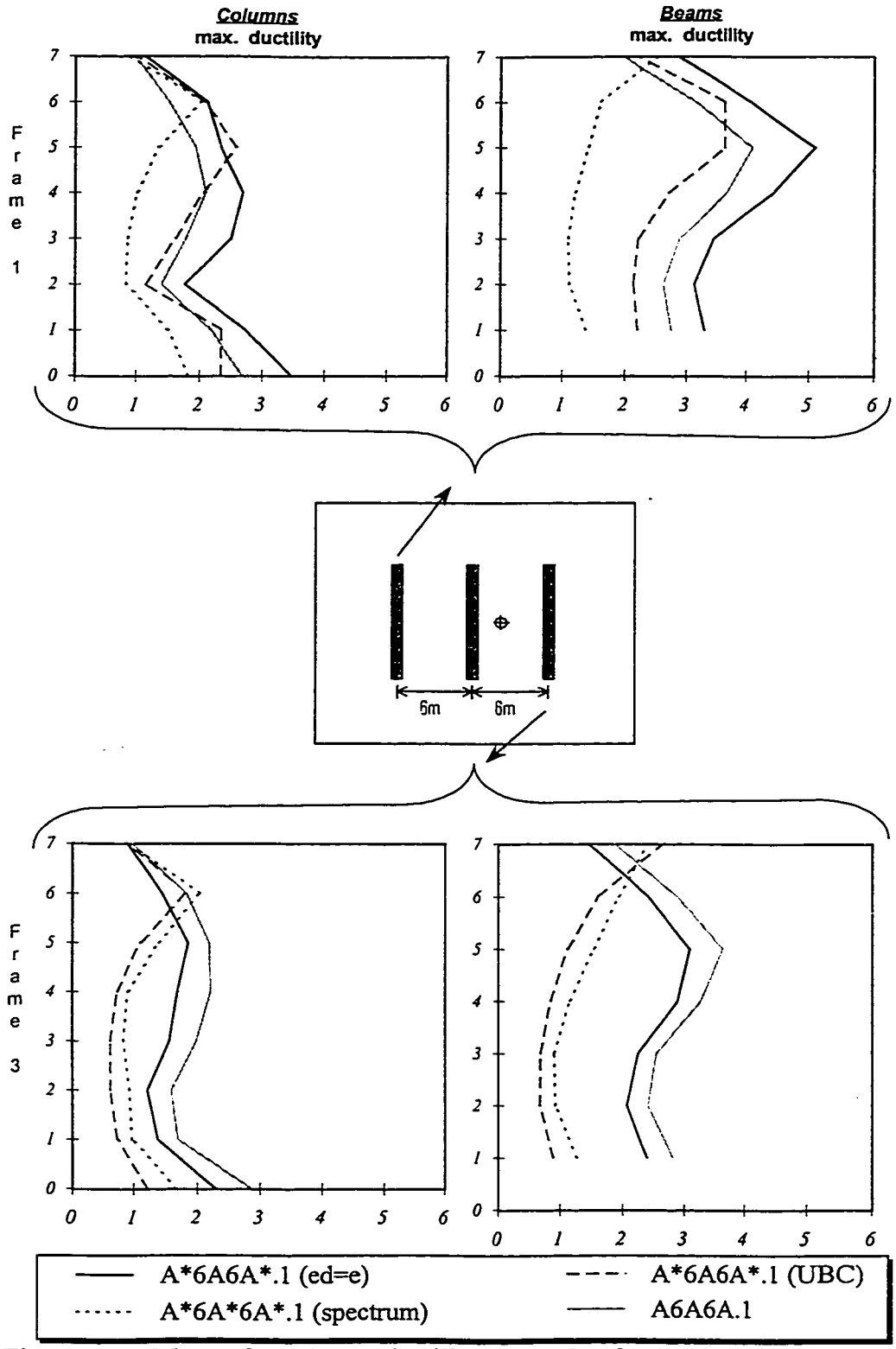


Figure 4.17. Mean of maximum ductility demands of A6A6A Buildings

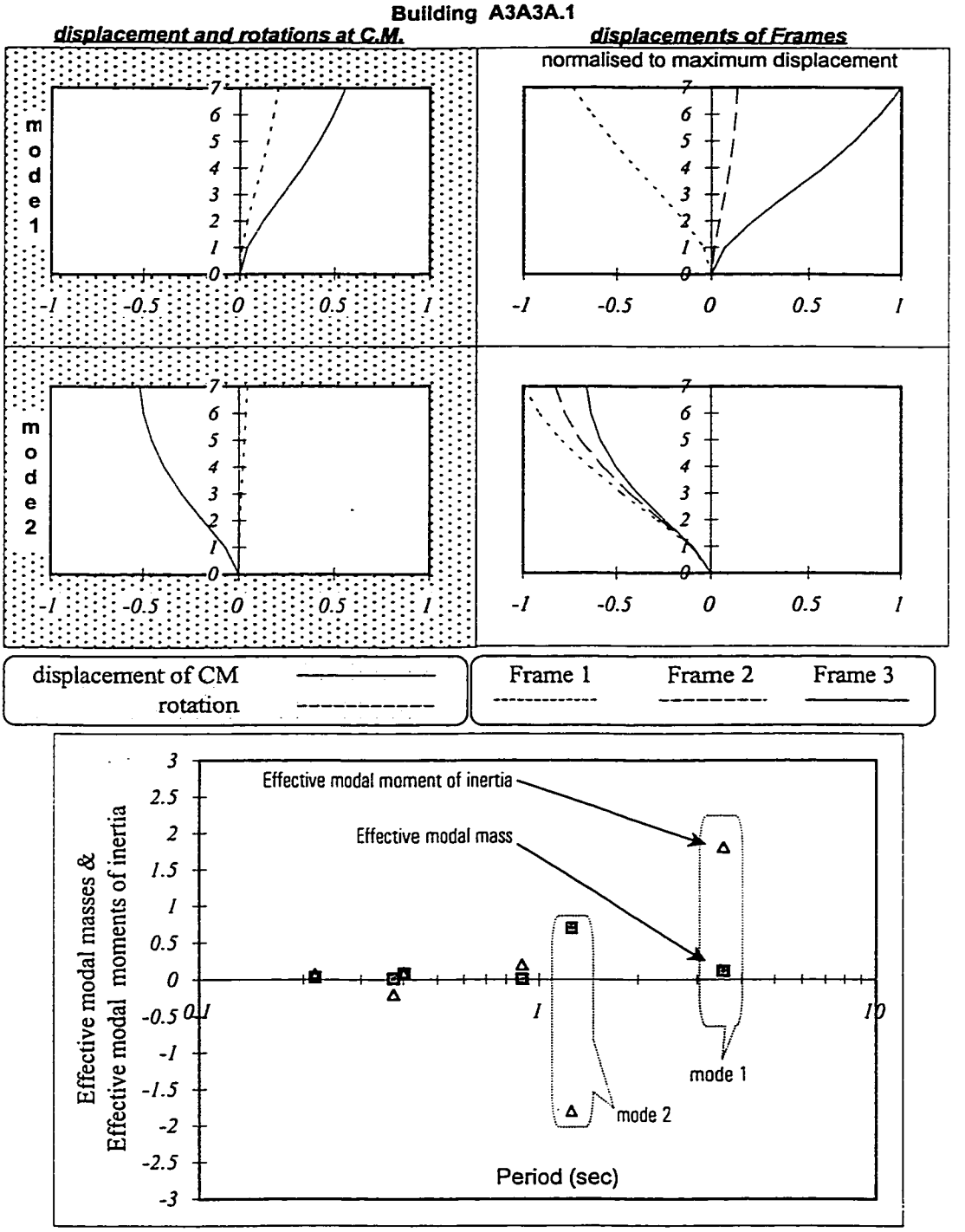


Figure 4.18. Mode shapes and modal masses of Building A3A3A.1

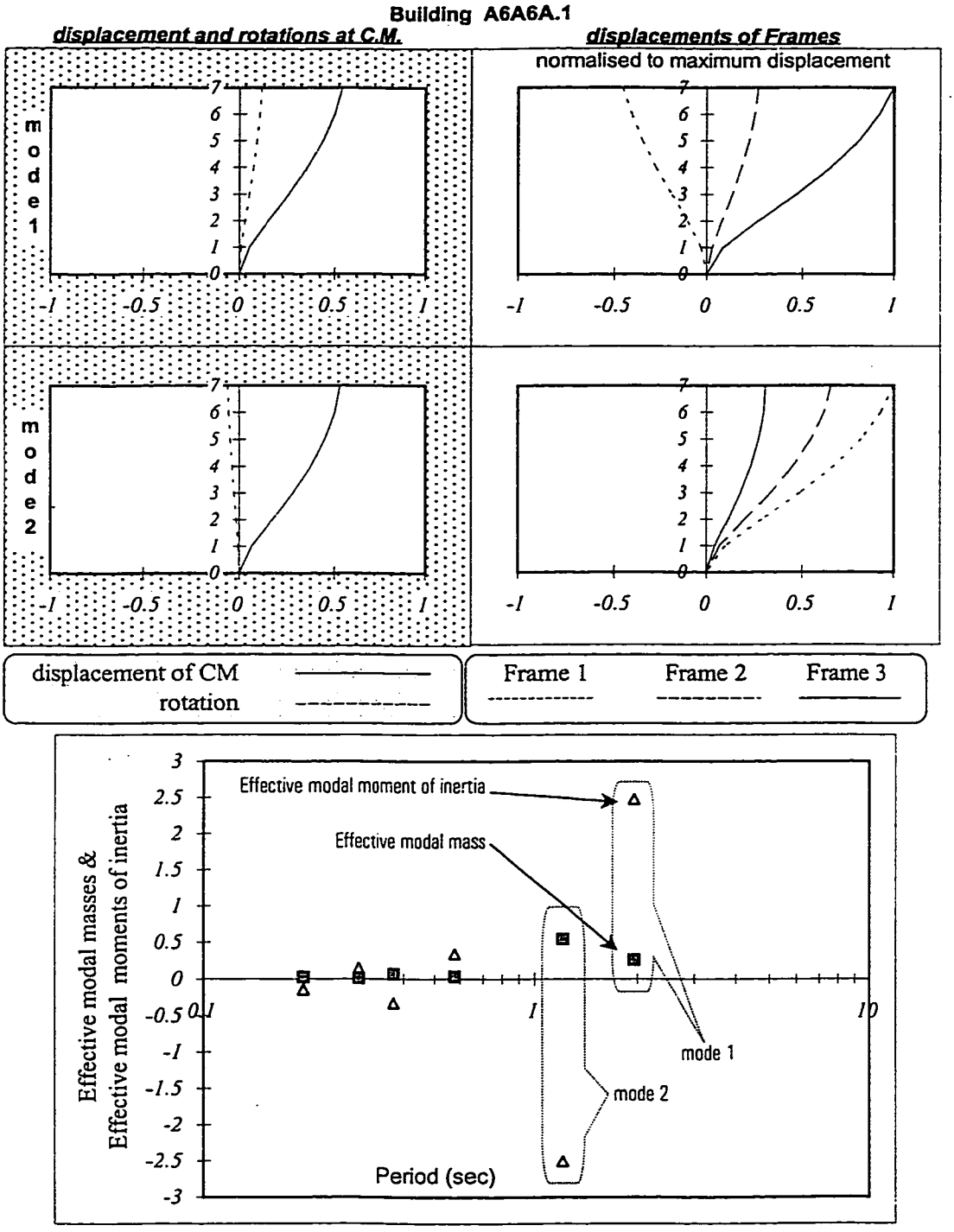


Figure 4.19. Mode shapes and modal masses of Building A6A6A.1

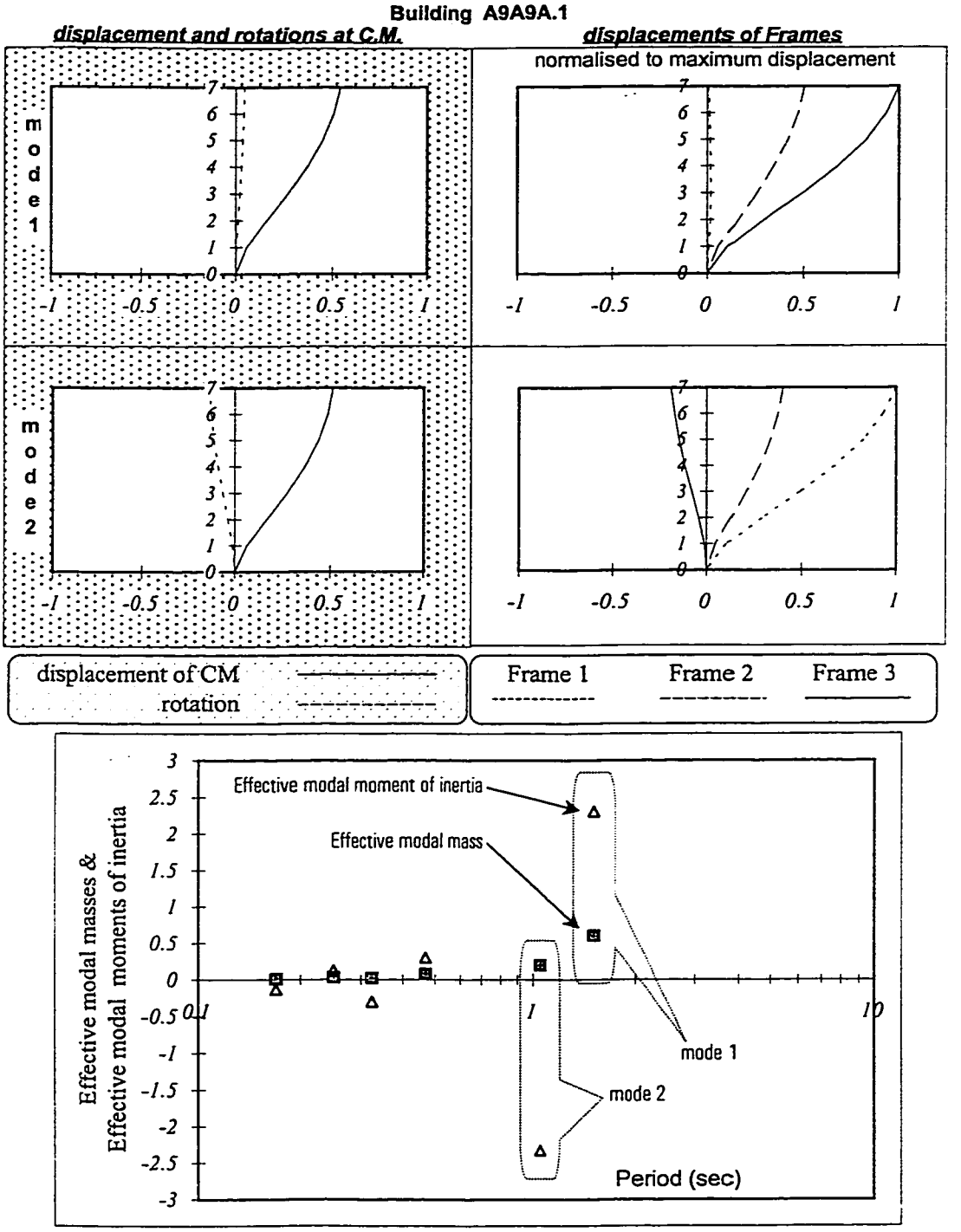


Figure 4.20. Mode shapes and modal masses of Building A9A9A.1

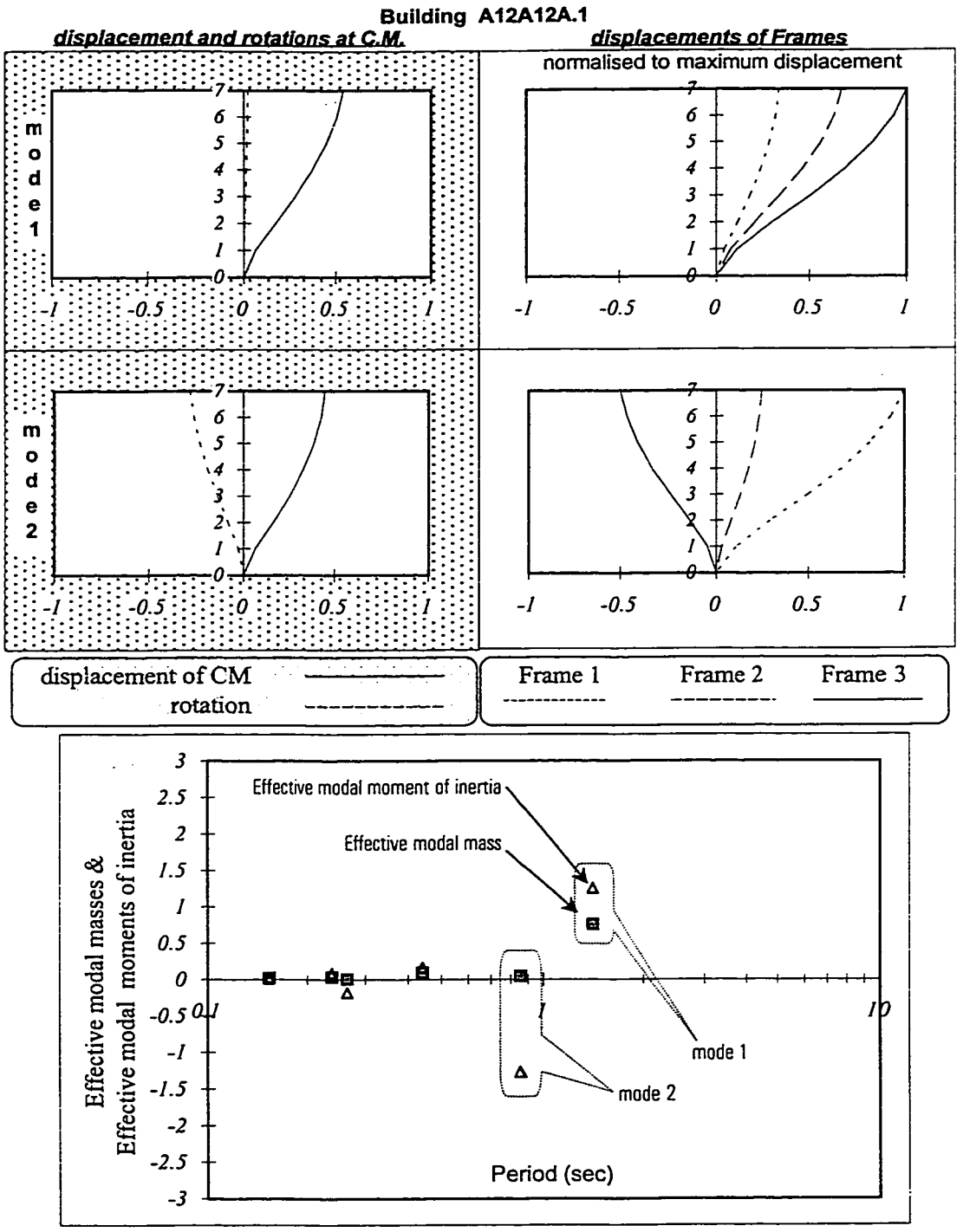


Figure 4.21. Mode shapes and modal masses of Building A12A12A.1

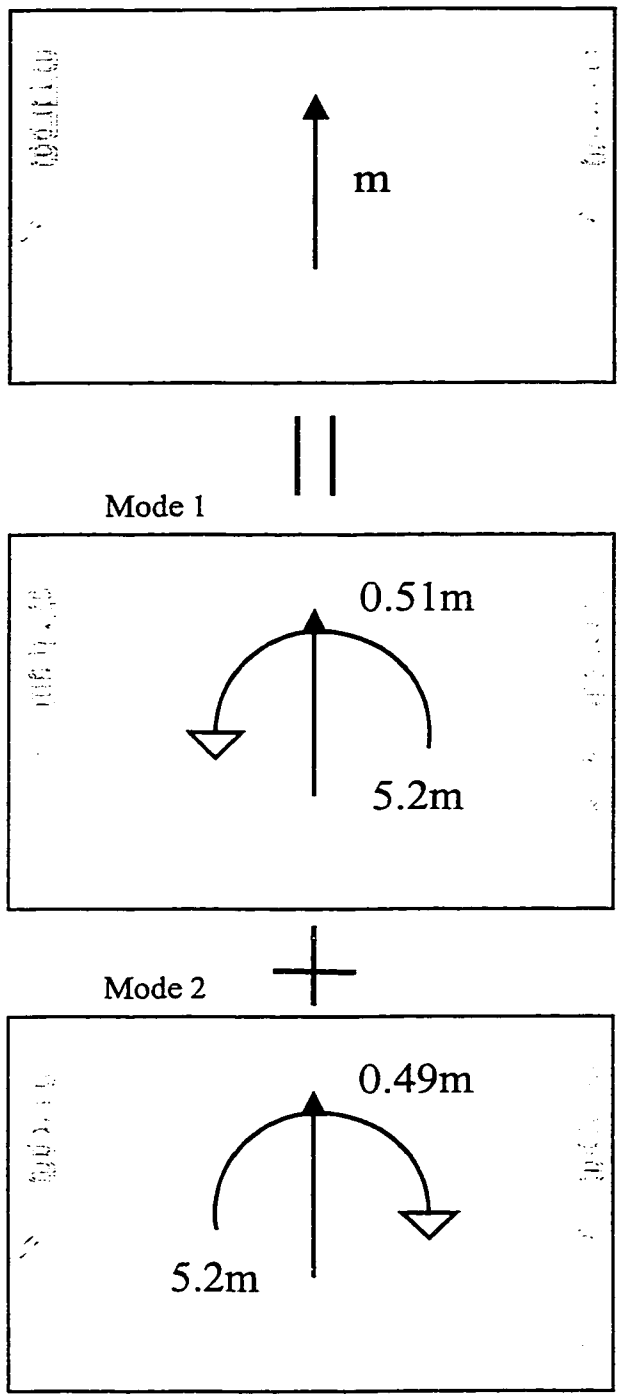


Figure 4.22. The concept of modal expansion of effective force vector on plan view of building

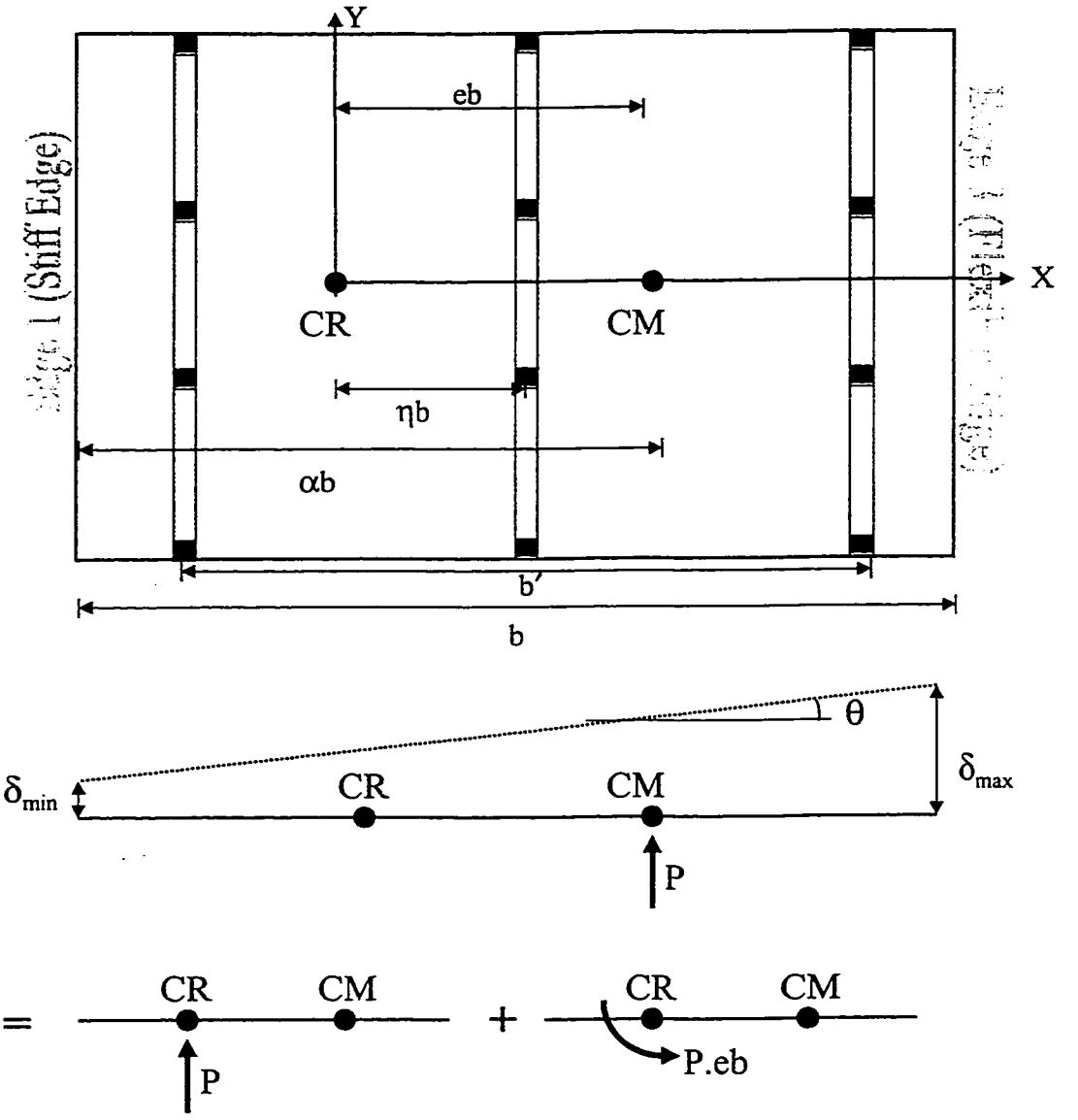


Figure 4.23. A figure for defining the parameters needed to derive the equations in section 4.6.2

This page is intentionally left blank.

# CHAPTER 5

# PUSHOVER ANALYSES ON ASYMMETRICAL BUILDINGS

## 5.1 Introduction

A current trend in the development of new seismic design codes is the incorporation of the performance-based design methodology. In this methodology, every building is designed to have the desired levels of seismic performance, corresponding to different specified levels of earthquake ground motion. For example, a building would be designed for immediate occupancy at one level and for possible damage but not collapse at a higher level of ground motion. To achieve the goal, engineers require information regarding the distribution of forces and deformation in the building elements when exposed to different levels of earthquakes. Elastic analyses are insufficient because they cannot realistically predict the force and deformation distributions after the initiation of damage in the building. Inelastic analytical procedures become necessary to identify the modes of failure and the potential for progressive collapse. The need to perform some form of inelastic analysis is already incorporated in many building codes (Fajfar and Gaspersic 1996).

Inelastic time-history analysis, using an ensemble of representative ground motions, is probably the most realistic analytical approach currently available to evaluate the performance of a building. However the inelastic time-history analysis is usually too complex and time consuming to be used in the design of most buildings. A very large

amount of response data needs to be generated and processed in order to obtain the values of the different design parameters, even if only one single earthquake record is used as excitation. To increase the reliability of the estimate, an ensemble of earthquake records of similar characteristics is usually used as input. This would further increase the volume of response data to be processed. Therefore, there is a need for simplification to reduce the amount of computation necessary for design office use.

A procedure commonly referred to as pushover analysis has been developed to provide the necessary information to the designers. Usually, the pushover procedure is applied to planar structures in which only translational deformation results. Depending on the information sought, there exists a wide interpretation of how the procedure should be carried out. It is the objective of the first part of this chapter to provide an overview of the procedure and a summary of the different variations of analyses used under the generic name of pushover analysis. The pushover procedure is then extended to asymmetric buildings in the later parts of this chapter.

## 5.2 Basic Concepts

The performance-based design methodology requires the proper matching of two basic quantities, the seismic capacity and the seismic demand. Demand is a description of the earthquake ground motion effects on the building. Capacity is a representation of the ability of the building to resist the seismic effects. The performance is measured based on the manner that the capacity is able to match the demand.

In a pushover procedure, the seismic capacity and demand are estimated explicitly in two separate steps. First, a sequence of inelastic static analyses is performed on the

building, by subjecting it to a set of monotonically increasing lateral loads. Such a loading sequence is representative of "pushing" of the building and hence the term pushover analysis. The building is pushed until its displacement reaches some predetermined limits. The predetermined displacement limit may be set based on different criteria such as the maximum allowable storey drift or ductility limits. Alternatively, the building may be pushed until it becomes unstable and reaches its collapse state. One important product of the pushover analysis is the base shear versus top displacement relationship, commonly referred to as the capacity curve (performance curve) of the building. This curve gives an overall summary of the capacity of the structure. Information such as the initial elastic stiffness, the initiation of first yielding, the stage of rapid stiffness deterioration, and the ultimate strength can all be inferred from the capacity curve. In addition, the damage pattern of the building at any post-yield level can be found by examining other response parameters such as interstorey drift ratios, hinge locations and member ductilities. The weak links and undesirable characteristics in the building such as soft storey conditions and strength or stiffness discontinuities can readily be detected from the damage pattern. A judgement is then formed as to the acceptability of the behaviour of the building. This first step essentially establishes the seismic capacity of the building, and often times is the only step taken in a study using pushover procedure.

However, if one desires to evaluate the damage potential of the building when subjected to a specific level of ground shaking, it is also necessary to establish the seismic demand on the building. This leads to the second step in a pushover procedure: the determination of a target displacement. The target displacement is an estimation of the

top displacement of the building when exposed to the specified level of ground shaking. This is usually determined using some form of dynamic analysis as will be discussed later. To evaluate the damage potential of the building at the specified level of ground shaking, one would first determine the target displacement, and then carry out a pushover analysis in which the building is pushed until its top deflection matches the target displacement. The damage estimates from the pushover analysis at the target displacement level are considered representative of the structural damages of the building, when exposed to that specific level of ground shaking.

While the objective of using pushover analysis is to evaluate the inelastic behaviour of all buildings, most of the past studies involved the pushover of a typical two-dimensional lateral load-resisting element or elements of a building. It is implied that the damage potential to the building can be inferred from the damage pattern of the element(s). These works can be referred to as 2-D pushover analyses (e.g., Saidii and Sozen 1979, Qi 1989, Fajfar et al. 1997). These investigations were conducted on buildings possessing a high degree of symmetry in which the effects of torsion are negligible, and the load resisting elements have the same lateral floor displacements.

Different researchers have used different lateral load distribution to carry out a 2-D pushover analysis. Miranda (1991) has used a triangular distribution. Fajfar and Gaspersic (1996) used the product of the mass distribution and a fixed displacement shape. The actual displacement shape depends on the types (wall or frame) of the buildings. Uniform load distribution is among many distributions recommended by Federal Emergency Management Agency for seismic rehabilitation of buildings (FEMA 273/274). The same reference suggested that a load distribution, based on modal forces

combined using either the SRSS or CQC combination rules, be used for cases when higher modal effects become important.

An equivalent SDOF system has usually been used by researchers to determine the target displacement. To derive the equivalent SDOF system for a structure, a displacement shape to represent the heightwise deformation of the building should be selected. Miranda (1991) suggested to use a displacement shape of building when its top displacement equal to the target displacement. Because the target displacement is not known a priori, an iterative procedure would be involved in this approach. Fajfar and Gaspersic (1996) suggested the use of some fixed displacement shapes to derive the equivalent SDOF system. There is no general agreement on what displacement shape should be used to obtain the equivalent SDOF system. Alternative forms of displacement shape have been proposed by Biggs (1964), Saidii and Sozen (1981), Lin and Mahin (1985), Hart and Wilson (1989), Anderson (1989), Qi and Moehle (1991), Bernal (1992), and Montans and Alarcon (1996), among others.

Some researchers suggested that the target displacement obtained from the equivalent SDOF system should be treated as baseline information to be further modified to include other effects (Krawinkler 1995b). Modifications to include effects such as higher modal effect (Nassar & Krawinkler 1991, Bazzurro & Cornell 1992, Seneviratna & Krawinkler 1994), soft soil effect (Rahnama & Krawinkler 1993) and 3-D effect (Bertero & Bertero 1992) have been proposed.

Most of the studies in the literature are on the application of a 2-D pushover analysis for walls and/or frames in a planar building. For more complex buildings such as

buildings that are asymmetric in plan, the top displacements of the lateral load resisting elements at different plan locations will be different due to torsion. There are only a limited number of studies involving the use of pushover procedure for asymmetric buildings. Moghadam and Tso (1995a, 1996a) extended the procedure to asymmetric buildings. The target displacement is estimated using an equivalent SDOF system based on the load-displacement relationship at the CM on the roof of the asymmetrical building. The pushover is carried out by performing 3-D inelastic analysis, applying the lateral loads at the centre of mass (CM) of the floors of the building. Another study reported by Kilar and Fajfar (1997) involves a simplified 3-D pushover method for asymmetric buildings. In this method, the building is modelled as a collection of planar macro-elements. An approximate relationship between the global base shear of the building and its top displacement is computed via a step-by-step analysis.

The disadvantage of using 3-D pushover analysis is that a 3-D model incorporating both the elastic and inelastic properties of the entire building is needed. The efforts for preparing the input data and the post-processing of the output information for easy interpretation using this approach can be considerable.

An alternative way to apply a pushover procedure to asymmetric buildings is to determine multiple target displacements, one for each frame or wall element where the damage pattern needs to be investigated. Then, the damage pattern can be found by performing 2-D pushover analyses on the resisting elements. This alternative requires only the inelastic modelling of the specific frames or walls of interest, and avoids the necessity to create an inelastic model for the entire building. This approach was reported

in two publications (Tso and Moghadam 1997, Moghadam and Tso 1998).

This chapter will present two approaches to apply pushover analysis to asymmetric systems. The first approach is the 3-D pushover method, which requires the use of a 3-D inelastic static analysis program. The second approach is based on 2-D pushover analysis.

## 5.3. The 3-D Pushover Method

### *5.3.1 Procedure*

The 3-D pushover procedure follows similar steps used in the two-dimensional pushover analysis. First, an equivalent SDOF system is derived to determine the target displacement. The load-deflection relationship of this SDOF system would follow the capacity curve of the building. This capacity curve is obtained by performing a 3-D pushover analysis on the building when it is subjected to a set of forces V.{f} applied at the centres of mass (CM) of the floor of the building. V represents the monotonically increasing base shear and {f} is a constant normalised load vector. The capacity curve is given by the V-$\Delta$ relation obtained from the static analyses, where $\Delta$ is the CM displacement at the roof. Since the CM of the floors may not coincide with the centres of rigidity (CR) of the floors, the CM roof displacement would reflect both the translational and torsional deformation of the building under lateral loading. The capacity curve has an initial linear range with a slope k, and can be expressed in the form $V=k\times G(\Delta)$ where $G(\Delta)$ is a function describing the shape of the capacity curve.

Assuming that the building response essentially comes from the fundamental

mode, an equivalent SDOF system is established as follows:

The equations of motion of a N-storey building subjected to horizontal ground motion $\ddot{u}_g$ in one direction (the Y-direction) can be written as

$$\begin{bmatrix} [m_x] & [0] & [0] \\ [0] & [m_y] & [0] \\ [0] & [0] & [I_m] \end{bmatrix} \begin{Bmatrix} \ddot{\delta} \end{Bmatrix} + \{R\} = -\begin{bmatrix} [m_x] & [0] & [0] \\ [0] & [m_y] & [0] \\ [0] & [0] & [I_m] \end{bmatrix} \begin{Bmatrix} \{0\} \\ \{1\} \\ \{0\} \end{Bmatrix} \ddot{u}_g(t) \qquad (5.1)$$

In which:

$[m_x]$, $[m_y]$ and $[I_m]$ = the mass matrix in X and Y-direction and mass moment of inertia matrix about CM

$\{\delta\} = \text{col}(\{\delta_x\}, \{\delta_y\} \text{ and } \{\theta\})$

$\{\delta_x\}$, $\{\delta_y\}$ = X and Y-direction displacement vector referred to the centres of mass (CM) of the floors

$\{\theta\}$ = the floor rotation vector

$\{R\}$ = the restoring force vector

Assuming a single mode response, the displacement vector $\{\delta\}$ can be written as

$$\{\delta\} = \{\phi\}\Delta(t) \qquad (5.2)$$

where $\Delta(t)$ is the generalised coordinate, representing the CM roof displacement, and $\{\phi\}$ is a constant deformation profile of the building. Further, the restoring force vector $\{R\}$ is approximately represented by the Y-direction pushover analysis as

$$\{R\} = k \times G(\Delta) \begin{Bmatrix} \{0\} \\ \{f\} \\ \{0\} \end{Bmatrix} \qquad (5.3)$$

Using Equations 5.2 and 5.3, the equation of motion for the generalised coordinate Δ(t) can be obtained from Equation 5.1 as

$$M^* \ddot{\Delta} + K^* G(\Delta) = -L^* \ddot{u}_g(t) \tag{5.4}$$

where

$$M^* = generalized\ mass \equiv \{\phi\}^T \begin{bmatrix} [m_x] & [0] & [0] \\ [0] & [m_y] & [0] \\ [0] & [0] & [I_m] \end{bmatrix} \{\phi\} \tag{5.5}$$

$$K^* = generalized\ stiffness \equiv k\{\phi\}^T \begin{Bmatrix} \{0\} \\ \{f\} \\ \{0\} \end{Bmatrix} \tag{5.6}$$

$$L^* = generalized\ earthquake\ exitation\ factor \equiv \{\phi\}^T \begin{bmatrix} [m_x] & [0] & [0] \\ [0] & [m_y] & [0] \\ [0] & [0] & [I_m] \end{bmatrix} \begin{Bmatrix} \{0\} \\ \{1\} \\ \{0\} \end{Bmatrix} \tag{5.7}$$

The effect of damping is introduced directly at this stage as a viscous damping term $C^* \times \dot{\Delta}$, in which $C^* = 2\xi\omega^* M^*$, $(\omega^*)^2 = K^* / M^* and$ $\xi =$ damping ratio;

leading to the final equation

$$M^* \ddot{\Delta} + C^* \dot{\Delta} + K^* G(\Delta) = -L^* \ddot{u}_g(t) \tag{5.8}$$

For a given excitation $\ddot{u}_g$, the solution of Equation 5.8 can be obtained using a step by step integration procedure and the absolute maximum of Δ(t), denoted by $\Delta_{max}$ is a predictor of the maximum CM displacement at the roof of the structure. Once, $\Delta_{max}$ is determined, a second 3-D pushover analysis will be carried out on the building. The

second pushover analysis terminates when the CM displacement at the roof of the structure equals to $\Delta_{max}$. The deformation and damage of elements near the edges of the building at this stage of the pushover analysis would then be taken as indicative of the deformation and damage of these elements in the building when the building is subjected to the specified level of earthquake ground shaking.

### *5.3.2 Application of 3-D pushover analysis*

A seismic damage assessment is performed on two uniform seven-storey reinforced concrete buildings to illustrate the procedure. One building is a symmetric building (Building A9A9A.0) and the other is a plan-eccentric building (Building A9A9A.1). To simplify subsequent references to these models, notation S will be used for the symmetric building and notation A for the asymmetric one. In building S, the floor masses are uniformly distributed so that the centre of mass (CM) of each floor coincides with the geometric centre. In building A, the mass distribution of each floor causes the CM of the floor to shift a distance of 2.4 m from Frame 2 towards Frame 3. Therefore, building A is mass eccentric, and has a constant floor eccentricity equal to 10% of plan dimension. The right hand edge (Edge 3) of this building is the flexible edge, and is susceptible to large additional displacements due to torsion, while Frame 3 is the frame that is most vulnerable in terms of ductility demands.

Since all frames are identical, no load redistribution among frames will occur in Building S. The results obtained from the 3-D pushover analysis on building S is identical to those if a 2-D pushover analysis were performed on a typical frame. The reason to include the building S in this study is that a comparison of the accuracy of the

pushover results on both Buildings A and S will provide a measure of the accuracy of the 3-D pushover procedure versus the traditional 2-D pushover of plan symmetric structures. The accuracy of the pushover results on both buildings was established by making comparison to results obtained using inelastic dynamic time history analysis on the buildings, treating them as multi-degrees of freedom (MDOF) systems. Both the 3-D pushover analyses and inelastic dynamic analysis were carried out using the computer code CANNY (Li 1993).

To obtain the capacity curve, a triangular distribution of the forces along the height of the building was assumed. The resulting capacity curves for the two buildings are shown in Figure 5.1. Both curves show similar features: they are linear initially but start to deviate from linearity when inelastic actions start to take place first in the beams and later in the columns. When the buildings are pushed well into the inelastic range, the capacity curves again become essentially linear, but with a much smaller slope. Both curves can be approximated by means of a bilinear relationship, as shown in the figure. The curve associated with building A is less stiff, and yields at a lower base shear value than that of building S. This can be expected as the CM roof displacement of building A takes into account both the translational and torsional deformation of the building. Four stages of building deformation marked 1, 2, 3, and 4 are shown in the same figure. Stage 1 can be considered as the stage when the buildings begin to yield in an overall sense. Stages 2, 3 and 4 correspond to buildings being displaced to 2 times, 3 times and 4 times the overall yield displacement respectively.

The displacements and interstorey drift ratios at the right hand edge of the two buildings are compared at different stages of building deformation. Shown in Figure 5.2

are the floor displacement profiles for both buildings. For a given stage, the edge displacements of building A is larger than those of building S, since the torsional displacements are additive to the translational displacements at this edge in building A. Of more interest to damage assessment is the interstorey drift ratio which are shown in Figure 5.3. The actual drift ratios differ significantly between the two buildings. For the same stage of building deformation, the maximum interstorey drift ratio of building A is about 60% above that of building S.

To reduce the 3N degrees of freedom system describing the building to the equivalent SDOF system, a constant deformation profile at CM of the building is needed. Shown in Figure 5.4 are the normalised displacement profiles at CM and also at edge 3 of building A for the four stages of building deformation. It appears that the normalised displacement profile is not sensitive to the stage of building deformation. A displacement profile at any deformation stage is a suitable profile to be used in Equation 5.2. To be specific, the suggestion of Qi and Moehle (1991), using the deformation profile when the top CM displacement equals to 1% of the total height was adopted in creating the equivalent SDOF system in this study. The sensitivity of using different deformation profile on the responses will be discussed in more detail later.

Three types of responses will be discussed here. They are (i) the seismic deformations (displacements and drifts) at edge 3 for non-structural damage assessment, (ii) ductility demands of the frame near edge 3 for member damage assessment, and (iii) period changes for an overall building damage assessment.

**Seismic deformations**

Inelastic dynamic analyses are performed on the two buildings by subjecting the structural models to the chosen ensemble of earthquake ground motion records as base input. Shown in Figure 5.5 is the correlation diagram of the maximum roof CM displacement of the buildings, computed based on the equivalent SDOF system that was constructed as outlined in the previous section, and computed using inelastic dynamic MDOF analysis. The solid diagonal line denotes perfect correlation and the dotted lines provide the plus and minus 25% bound of correlation. Each point on the plot corresponds to the response of a building to one scaled earthquake record input. The open squares represent responses from building S, and the solid diamonds denote responses from building A. Two observations can be made. First, the scatter of the results from building A and building S is similar. Second, one can expect accuracy in the order of plus or minus 25% using the proposed procedure to estimate the seismic CM displacement at the roof of the building.

The correlation graphs for the maximum top displacement and maximum interstorey drift ratio at edge 3 of the buildings are shown in Figures 5.6 & 5.7. Again, the plots show that the procedure is capable of estimating these two quantities within 25% accuracy. There is in general a segregation of the results from the two buildings, with large maximum top displacement and also larger maximum interstorey drift ratio from building A. This trend can be expected due to the eccentric nature of building A.

Another way to assess the accuracy of the procedure is to carry out a statistical analysis and focus on the mean and mean plus one standard deviation comparisons.

Shown in Figure 5.8 is the comparison of the mean of the maximum floor displacements for buildings S and A. Within each plot, the solid line represents the prediction from the proposed procedure, using the mean of $\Delta_{max}$ as the seismic displacement target in the 3D pushover analysis. The points are the mean of the maximum floor displacements based on inelastic dynamic MDOF analysis. For each floor, a bar graph is also included to denote the range of maximum floor displacement values experienced by the building under the ensemble of earthquake records used. Shown in Figure 5.9 is a similar comparison on the mean plus one standard deviation estimated of the same quantity. To be consistent, the mean plus one standard deviation value for $\Delta_{max}$ was used as the target seismic displacement in the 3D pushover analysis. It shows that the procedure leads to a very good prediction of the maximum floor displacements in a statistical sense.

Similar comparisons are carried out on the prediction of the maximum interstorey drift ratios at edge 3 along the height of the buildings. The results are presented in Figures 5.10 & 5.11. The comparison shows that the procedure predicts well the interstorey drift ratio for floors from ground up to the mid-height of the building where the interstorey drift ratio is the largest. However, the pushover analysis tends to underestimate the interstorey drifts at the upper floors. Higher modal contributions may be the cause of this underestimation.

**Ductility Demands**

To assess the member damage, the maximum ductility demands on the beams and columns are considered. The correlation diagrams for the maximum ductility demands of the beams and columns for the two buildings are presented in Figure 5.12 and Figure 5.13

respectively. The ability of the procedure to predict local damages to members is not as good as predicting seismic deformations. A number of points lie outside the minus 25% bounds. This implies that the pushover analyses tend to underestimate the ductility demands, both in the beams and columns of frame 3.

A comparison for the pushover estimate to predict the mean maximum ductility demands of the beams and columns in Frame 3 are shown in Figures 5.14 and 5.15. It shows that the pushover analysis leads to a reasonable estimate of the mean beam ductility demands in floors from the ground up to the middle of the building, but it underestimates the demands in the upper floors. The pushover analysis underestimates the mean column ductility demands in both buildings.

**Period changes**

One useful parameter to assess the global damage is the fundamental period changes of the building. The fundamental period changes when the building is excited into the inelastic range. The variation of the fundamental period of the building with time for one of the earthquake excitation is shown in Figure 5.16. The duration when the period exceeds the elastic period $(T1)_0$ corresponds to the building being excited into the inelastic range. The maximum change of the period can be conveniently denoted by the period ratio which is defined as the maximum period divided by the elastic period of the building. Once the period ratio is known one can compute the maximum softening index which is considered the best indicator of the global damage state by some researchers (Williams and Sexsmith 1995). One can also compute a period ratio based on the pushover analysis by determining the period of the building at the beginning and at the

end of the pushover analysis. A correlation between the period ratio as determined by 3-D inelastic dynamic MDOF analysis and pushover analysis will provide an indication on how well the proposed procedure can assess the global damage of the building. The correlation diagram for maximum period ratio for the two buildings is shown in Figure 5.17. It shows that the pushover analysis generally overestimates the period ratio. This trend can be expected since there is no unloading during the pushover analysis. Once a hinge is formed, it will remain a hinge during the whole pushover analysis. The degree of correlation shown in the figure is similar to that for estimating the maximum interstorey drift ratio.

### *5.3.3 Sensitivity of 3-D pushover procedure to different modelling choices*

The 3-D pushover procedure basically consists of two steps. In each of these steps a pushover analysis on the building is required. In the first step, performing pushover analysis helps to derive the properties of the equivalent SDOF for the building. In the second step, a pushover of the building to the target displacement will result in an estimate of the building responses. There are certain choices on the details of implementing these two steps. The sensitivity of the 3-D pushover procedure to some of these details is studied in this section.

**Bilinear approximation of the capacity curve**

To simplify the analysis, a bilinear curve, composed of two straight lines, is often taken as the hysteresis model for the equivalent SDOF system. The initial slope of the

bilinear curve represents the elastic stiffness and the slope of the second line represents the post-yield stiffness of the system. The initial stiffness, the coordinates of the yield point and the post-yield stiffness of SDOF all depend on the technique used to transform the capacity curve of building to a bilinear curve. Figure 5.18 compares the responses resulted from three different bilinear modelling of the capacity curve of an asymmetric building. The bilinear curve of Case 1 is simply the result from extending the two linear segments at the beginning and the end of capacity curve. The area under the bilinear approximation Case 1 is greater than the original capacity curve. As an alternative, the areas under the bilinear curves in Cases 2 and 3 are adjusted so that they are the same as the original capacity curve. Case 2 keeps the stiffness of linear segment at the end of the capacity curve constant and changes the initial stiffness to balance the area under the new and the original curves. On the other hand, Case 3 keeps the initial stiffness constant and changes the secondary stiffness to balance between the areas.

The initial stiffness, the ratio of the secondary to the initial stiffness, the yield force and yield displacement of the equivalent SDOF systems for Cases 1,2 and 3 are given on three graphs at the top of Figure 5.18. The three graphs at the bottom shows three response parameters calculated using SDOF bilinear systems that follow the Cases 1,2 and 3 bilinear curves. The response parameters are the maximum top displacement at CM, the maximum top displacement at edge 3, and the maximum interstorey drift ratio at edge 3 of the asymmetric multi-storey building. Each point corresponds to one of the 10 ground motion records used. The response parameters are normalised to their maximum values from MDOF inelastic dynamic analysis, which is independent of the bilinear approximation. The dotted lines on the graphs indicate a ±20% range spread. A

comparison between the three graphs shows that the difference of responses among individual ground motion records is much larger than the difference using the three different bilinear approximations. Therefore, any one of the bilinear approximations will serve equally well as the load-deflection curve for the equivalent SDOF system.

**Deformation profile for creating equivalent SDOF system**

To transform a building with 3N degrees of freedom to the equivalent SDOF system, a constant deformation profile at CM of the building is needed. To demonstrate effects of deformation-profile on the results of the pushover procedure, a study involving five deformation-profiles is chosen in this section. Shown on the Figure 5.19 is the capacity curve of building and also the deformation profiles for deriving the equivalent SDOF system. The displacement profiles are taken as the normalised deformation shape of building at the four stages of the capacity curve as shown on Figure 5.19a. The first elastic mode shape of the building is included as the fifth displacement-profile. The corresponding interstorey drift ratios of the five displacement-profiles are shown on Figure 5.19c. Each interstorey drift ratio is normalised to its $7^{th}$-storey component. There is little difference for the displacement profile, but some differences exist in the normalised interstorey drift ratios.

Based on the displacement-profiles, five equivalent SDOF systems are created. Inelastic dynamic analyses are performed on these SDOF systems using a set of non-scaled ground motion records. Shown on the graph at top of Figure 5.20 are the normalised maximum displacements of the five SDOF systems. The maximum displacements of SDOF systems are normalised to the maximum displacement of the

building subjected to the same ground motion record. This graph is useful to demonstrate the variation of each SDOF system in estimating the top displacement of the building on a per earthquake record basis. However, it can be misleading for judging the importance of choosing the displacement profile.

To complement this graph, the absolute values of the maximum displacement of the SDOF systems are also given in the graph at the bottom of Figure 5.20. A comparison of the results shows that the change in the maximum displacement of the equivalent SDOF system is not sensitive to the difference in the chosen displacement-profiles.

**Load distributions used in different stages of pushover procedure**

Different approaches for selecting the load distribution for pushover analysis, from a general point of view, have already been discussed. In the present section a specific case study on an asymmetric building (A12A12A.1) is reported to show the effects of using different load distributions in the pushover procedure.

Two load distributions are considered. A triangular load distribution at CM of floors is used as the first load distribution. To determine the load distribution for the second case, a response spectrum analysis is performed on the building. The response spectrum analysis is done using the design spectrum of NBCC and the distribution of force at CM of floors is taken as the proper load distribution. Based on these two distributions, two equivalent SDOF systems are developed and they are subjected to the set of 10 ground motion records to obtain the target displacements. The target displacement of the SDOF derived using a triangular load distribution resulted in a mean value of 0.123m while using the spectrum analysis distribution resulted in a mean value

of 0.128m for the target displacements.

Having the target displacements, the building is pushed to those displacements. Again, the two load distributions, a triangular distribution and a distribution resulted from response spectrum analysis, are used in this step. Figure 5.21 shows the mean values of maximum storey drift ratios for two pushover analyses. The responses from inelastic dynamic analyses of the building are also included in the graph.

Although both distributions lead to similar mean target displacements, there are some differences when the maximum interstorey drifts are compared. Therefore, the load distribution used during the second pushover can cause some differences in the results. Due to the uncertainty associated with the ground motion characteristics, these differences can be considered negligible.

## 5.4. Pushover Analysis using 2-D Computer Program

In the section 5.3, the 3-D pushover procedure is introduced as an extension of pushover method to asymmetrical buildings. The studies in that part show that the 3-D pushover procedure led to a good prediction of the edge 3 responses of asymmetrical buildings. However, there are many practical or technical concerns which make the use of 3-D pushover approach less desirable. Among the concerns are

- There is a large gap between current situation of using 2-D inelastic and 3-D inelastic computer programs. Although only inelastic 3-D static (pushover) analysis in needed in the 3-D pushover procedure, most designers are less familiar with the available inelastic 3-D computer programs.
- In the 3-D pushover procedure, the entire building has to be modelled for the inelastic

static analysis. Therefore, the inelastic properties of all members should be properly determined and modelled in the data file for the computer code. For large buildings it can be a very time consuming job. It may not be a logical approach, if the designer only interests in the estimation of response and damage assessment for some part of building such as an edge frame or wall.

- The accuracy of the 3-D pushover procedure in estimating the responses for side 1 of building is not as good as for side 3. This approach in general will underestimate the responses of elements on the edge 1, as demonstrated by calculations not presented herein.
- Since the procedure assumes that the building responds mainly in its fundamental mode, it would give representative results for TS buildings where the fundamental mode of the building is translation predominant. For TF buildings, the fundamental mode is torsion predominant and the proposed 3-D pushover analysis will not give good damage estimates of elements located at the stiff edge (Edge 1) of TF buildings.

To address these concerns, this section will introduce an alternative way of applying the pushover procedure to asymmetric buildings. Only 2-D inelastic static analyses (pushover) are needed in this approach. In an asymmetric multi-storey building, the maximum top displacements of the resisting elements are different due to torsional response. The proposed method is based on the idea of estimating individual target displacements for each lateral load-resisting element instead of estimating only one target displacement at CM of the building.

The design process for asymmetrical buildings usually involves some form of

three-dimensional linear elastic analysis of the building. As a computer model of building with elastic member properties is already prepared in design stage, it is proposed to carry out a 3-D elastic analysis to obtain the target displacements. Depending on the format of available ground motion information, the target displacements may be determined by elastic dynamic analyses or alternatively by a response spectrum analysis of the building. By using the elastic model of the building, there is no longer a need to create the equivalent SDOF inelastic system to obtain the target displacement.

Once the target displacements of the different elements are established, two-dimensional inelastic analysis programs such as DRAIN-2D (Allahabadi & Powell 1988) are sufficient to conduct the 2-D pushover analyses on the individual elements. Since 2-D inelastic analysis programs are readily available, and have been used extensively by the profession, it is believed that this proposed procedure is a more practical way to extend the pushover procedure to three-dimensional structures.

### *5.4.1 Target displacements from dynamic elastic analysis*

The procedure consists of two parts. First, the building is modelled as a three-dimensional elastic structure. The target displacement for each lateral load-resisting element of interest in the building is established by performing an elastic 3-D dynamic analysis on the structural model. Once the target displacements are found, a series of 2-D pushover analyses can be carried out for the elements at different locations. Each element is loaded with a set of static loads with the same distribution as the elastic force distribution on the element obtained from a spectrum analysis of the building. Each element is pushed until its top displacement attains its target displacement. The proposed

procedure is applicable to both planar and plan-asymmetrical buildings.

To illustrate the application and accuracy of the proposed procedure, pushover analyses were carried out on two buildings. One building is a symmetric building (Building A12A12A.0) and the other is an asymmetrical building (Building A12A12.1). The notations *Building S* will be used for the symmetric building and *Building A* for the asymmetric building. The inclusion of building S in this study serves two purposes. First, it is used as an example to show that target displacements established using an equivalent inelastic SDOF system or using dynamic elastic analysis of the complete building are similar for planar structures. Second, a comparison of the accuracy of the pushover results on building A and building S will provide a measure of the accuracy of the proposed method when applied to both plan-symmetric and plan-eccentric buildings. For each building, the accuracy of the pushover results is established by comparing the results obtained using inelastic dynamic analyses on the building.

A correlation plot to show the accuracy of using the two approximate methods to obtain target displacement in planar structures as represented by Building S is given in Figure 5.22. The correlation of the target displacement determined using the equivalent SDOF system with the actual roof displacement of Building S for the ten earthquake records are shown in solid circles, with the mean shown in open circle. The correlation of the target displacement determined by elastic dynamic analysis of the building are shown as solid squares with the mean shown in open square. It is shown that both approximate methods tend to overestimate the seismic roof response of the building. The accuracy of both simplified methods is comparable.

The mean seismic responses of Building S over the ensemble of ground motions

are shown in Figure 5.23. In each graph, three curves are shown representing the three ways to obtain the responses, namely, (i) a 2-D pushover analysis of the building to the mean target displacement based on an equivalent SDOF system analyses shown in circles; (ii) a 2-D pushover analysis of the building using the mean target displacement based on dynamic elastic analyses of the building shown in squares; and finally (iii) the mean of the responses computed using inelastic dynamic analyses of the building shown as a solid line. Due to the height-wise regularity of the building, the elastic load distribution based on response spectrum calculation is similar to the triangular distribution. Therefore, a triangular distribution of static loads is used in both pushover analyses. A comparison of the three curves in each plot shows that both of the pushover procedures give good estimate of the parameters of interest for the building as a whole. The deviations of the estimates from the solid curve in this figure will be used to measure the accuracy of the proposed procedure, when applied to the asymmetrical building A.

Figure 5.24 shows the correlation of the target displacements based on elastic dynamic analyses with the actual seismic displacements at the top of edges 1 (shown in solid diamonds) and 3 (shown in solid triangles) of Building A. Each point in the plot represents the correlation with respect to one earthquake record. The correlation of the mean target displacements for edges 1 and 3 are shown in open diamond and open triangle respectively in the same figure. Similar to the symmetrical Building S, the proposed method tends to overestimate the seismic responses of the top of Frames 1 and 3. The accuracy of the estimates is similar to that when the proposed method is applied to Building S, as shown in Figure 5.22.

Unlike the symmetrical building, the elastic load distributions on the edge Frames

1 and 3 using modal spectrum analysis are different from the triangular distribution, as shown in Figure 5.25. Both distributions are normalised to give the same base shear. Of particular interest is the relatively large increase of the loads at the roof of Frame 3 due to the higher modal effect. The result of using the proposed procedure to estimate the mean seismic responses of the two edge frames is presented in Figures 5.26 and 5.27. The responses of Frame 3, shown in Figure 5.26, are calculated in three ways. First, they are obtained performing a 2-D pushover analysis on Frame 3, with the applied static load having a triangular distribution along the height of the frame. The target displacement used is based on the mean target displacement obtained using elastic dynamic analysis of the building. Second, the pushover analysis is carried out with the applied static load distribution the same as the frame force distribution obtained using response spectrum analysis. The same mean target displacement is used in the pushover analysis. Finally, the means of the responses based on inelastic dynamic analysis of building are shown in solid black lines as a reference. Comparing the responses based on approximate analysis, it is shown that the actual distribution of static loads used in the 2-D pushover analysis has a significant effect. Using the load distribution based on spectrum analysis leads to a more representative distribution of the various response parameters of interest. The accuracy of using the proposed procedure to estimate the Frame 3 responses is similar to that when the procedure is applied to Building S as shown in Figure 5.23.

The responses on Frame 1 are compared in a similar manner in Figure 5.27. It appears that the response distribution is less dependent on the actual static load distribution used in the 2-D pushover analysis because the increase in the roof level load on this frame is not as prominent as in Frame 3. Using either distribution will lead to

similar and satisfactory estimation of the mean response parameters of interest.

A comparison of 2-D pushover as introduced in this part and 3-D pushover method, as discussed in section 5.3, is shown on Figure 5.28. The maximum storey drift ratios and beam ductilities of the frames in the asymmetric building are presented in the figure. The mean values of the maximum responses from MDOF inelastic dynamic analyses are also shown. This comparison shows that both approaches are able to estimate the maximum responses of Frame 3 on the flexible side of the asymmetric building. However, the performances of the two approaches are not similar in regard to Frame 1. The maximum responses of Frame 1 is poorly estimated by 3-D pushover procedure, while good estimation of responses is given by the approach based on combination of elastic analysis and 2-D pushover.

The study in this section showed that the target displacement obtained using elastic analysis of the building has the same accuracy as that obtained based on an equivalent inelastic SDOF system. However, there are two advantages of using elastic dynamic analysis of the building to obtain the target displacement. First, it is readily applicable to asymmetrical buildings where torsional effect can be significant. Second, assuming some form of linear elastic analysis will be performed for preliminary or final design of the building, there is no need to create a separate structural model such as the equivalent SDOF system in order to obtain the target displacement. Also it is shown that the choice of the static load distribution used in the pushover analysis can affect the accuracy of the response estimates. The dynamic load distribution on an element obtainable from an elastic spectrum analysis of the building is a more representative static load distribution to be used in the pushover analysis of that element. By means of

examples it is shown that the procedure leads to good estimates of the floor displacements, interstorey drifts, maximum column and beam ductility demands at both edge-frames of the asymmetric building.

### *5.4.2 Target displacements from 3-D response spectrum analysis of building*

This section presents a simple modification to the pushover procedure presented in section 5.4.1. The modification consists of the use of elastic spectrum analysis, instead of time history elastic dynamic analyses, to obtain the target displacements. The procedure requires a computer code for three-dimensional elastic spectrum analysis such as SUPER-ETABS (Wilson et al. 1975) and a code for two-dimensional inelastic analysis such as DRAIN-2DX (Allahabadi and Powell 1988).

The proposed procedure consists of two parts. First, the target displacements are determined by performing a 3-D elastic spectrum analysis on the building. Many target displacements need to be determined, one for each resisting element where the inelastic damage assessment is required. Once the target displacements and the corresponding lateral load distributions are found, a series of 2-D pushover analyses can be carried out for specific elements as outlined in previous section.

To illustrate the application and accuracy of the proposed procedure, the seismic responses of three seven-storey reinforced concrete ductile moment resisting frame (DMRF) buildings, subjected to an ensemble of ten artificial ground motion records (records are generated using program SYNTH, Naumoski 1998) as input, are computed. The plans of the buildings are shown on Figure 5.29. The first building is a symmetric

building (SYM) while the second and third buildings are asymmetric and representing a mass eccentric system (MES = A12A12A.1) and a stiffness eccentric system (SES), respectively. In SYM and SES, the floor masses are uniformly distributed so that the CM of each floor coincides with the geometric centre. In MES, the mass distribution of each floor causes the CM of the floor to shift a distance of 2.4m from Frame 2 towards Frame 3.

Plots in Figure 5.30 show the mean of the maximum displacements and interstorey drifts at Frame 1 and Frame 3 of the buildings. Figures 5.30a and 5.30b show the mean of maximum floor displacements and the mean of maximum interstorey drift ratios on edge Frames 1; Figures 5.30c and 5.30d show the mean of maximum floor displacements and the mean of maximum interstorey drift ratios on edge Frames 3 respectively. The mean responses of SYM are included in the plots as a reference to show the influence of torsion on the edge frame responses. These curves are obtained by means of MDOF inelastic dynamic analyses of these buildings, subjected to the ensemble of 10 earthquake records as input. A comparison of the response curves of Frames 1 and 3 of MES and SES to those of SYM will show that torsion increases the responses of Frame 3 while decreases the responses of Frame 1 of these asymmetric buildings.

To use elastic spectrum analysis to estimate the inelastic responses of a system, a higher value of viscous damping than that assigned to the inelastic system should be used to compensate for the inability of including the hysteretic energy dissipation in the elastic analysis. To illustrate this point, Figure 5.31 shows the top displacements of frames in the MES building obtained from response spectrum analysis using damping values in a range

from 5% to 20%. For each frame the mean of the maximum top displacement of the frame obtained from inelastic 3-D dynamic analyses are also included in the graphs. A 5% viscous damping has been used in the inelastic dynamic analysis. The graphs show that higher values of damping should be used in spectrum analysis, particularly for Frames 2 and 3, in order to have the same top displacement as the means obtained from inelastic dynamic analyses. The accuracy of determining the target displacements based on elastic response spectrum analyses of the buildings is also demonstrated in a correlation plot. Two damping values were used to determine the target displacements, namely 5% and 10%. They correspond to the maximum damping values recommended for reinforced concrete structures at different stress levels (Newmark and Hall 1982). The correlation plot in Figure 5.32 shows that the target displacements based on the 5% damped spectrum tend to overestimate the seismic roof displacements of the building. A good estimation can be reached using a 10% damped spectrum in the elastic analysis. Subsequent computation is based on using a 10% damped Newmark-Hall elastic design spectrum to perform the response spectrum analyses.

While the triangular load distribution is a fair representation of the load distribution for the frames in the SYM building, the load distributions on the edge frames of the two asymmetrical buildings deviate from the triangular load distribution. The deviation of the lateral load distribution on the edge frames from triangular is shown in Figure 5.33. These distributions are normalised to the same base shear. The loading is reduced at the top and increased at the base in Frame 1. Of particular interest are the relatively large increase of the loads at the roof and the drastic reduction of loads near the

base of Frame 3 due to the higher modal effect.

The mean seismic interstorey drift responses of the three buildings over the ensemble of records are shown in Figure 5.34. In each figure, two curves are shown, namely, (i) results using pushover analysis of the frames shown in dash lines; and (ii) the mean of the responses computed using inelastic dynamic analyses of the buildings shown as solid lines. A comparison of the curves in each plot shows that the pushover procedure can give good estimation of the interstorey drift distribution in all the frames.

To evaluate the accuracy of the pushover procedure in estimating the local response parameters, the distribution of column and beam ductilities are shown on the Figures 5.35 and 5.36 respectively. These figures show that proposed pushover procedure tends to underestimate the mean value of the maximum ductility demands for the beams and columns of different frames in these three buildings.

In summary, a procedure is presented for seismic damage estimation of asymmetrical buildings. The proposed procedure includes some of the three dimensional effects caused by the torsional responses. New features of the procedure are the use of elastic response spectrum analysis of the building to obtain the target displacements and the equivalent static load distributions used in the pushover analyses of the frames. A comparison of the responses of three example buildings obtained by this procedure with the responses resulted from inelastic 3-D dynamic analyses shows that the proposed procedure can provide sufficiently accurate estimation of the various response parameters for design purpose. It is shown that the procedure leads to good estimates of the floor displacements, interstorey drifts, and reasonable estimates of the maximum member

ductility demands for frames located at both the stiff edge and the flexible edge of the asymmetrical multi-storey buildings.

## 5.5 Summary

The followings are the highlights of the tasks performed in this chapter:

- A 3-D pushover procedure for damage assessment of asymmetrical buildings is presented. It is shown that for buildings used in this study, the results of 3-D pushover analysis is not sensitive to small changes in different modelling details used in the procedure.
- It is shown that the accuracy of the proposed 3-D pushover analysis is similar to that of the currently used pushover analysis method for planar structures. Also, the pushover analysis procedure is more successful to predict global response parameters such as edge displacements, interstorey drift ratios, and fundamental period changes than local damage parameters such as member ductility demands.
- A 2-D pushover procedure based on 3-D elastic dynamic analysis and 2-D inelastic static analysis is developed to estimate the inelastic seismic responses for asymmetric multi-storey buildings. The advantages of new method are that there is no need to create a separate structural model such as the equivalent SDOF system in order to obtain the target displacement for the pushover analysis.
- By means of examples it is shown that the 2-D pushover procedure based on elastic dynamic analysis, leads to good estimates of the floor displacements, interstorey drifts, maximum column and beam ductility demands at both edge-frames of the asymmetric building. Since the proposed procedure requires only programs that are

available and have been used extensively by the design profession, it is a practical way to extend the pushover procedure to analyse asymmetrical buildings.

- A modified 2-D pushover procedure based on response spectrum analysis is also presented. New features of the procedure are the use of elastic response spectrum analysis of the building to obtain the target displacements and the equivalent static load distributions used in the pushover analyses of the frames. It is shown that this procedure can also lead to good estimates of different deformation response parameters at edge-frames of both mass eccentric and stiffness eccentric uniform asymmetrical multi-storey buildings. However, it tends to underestimates the member ductility demands at the edge frames.

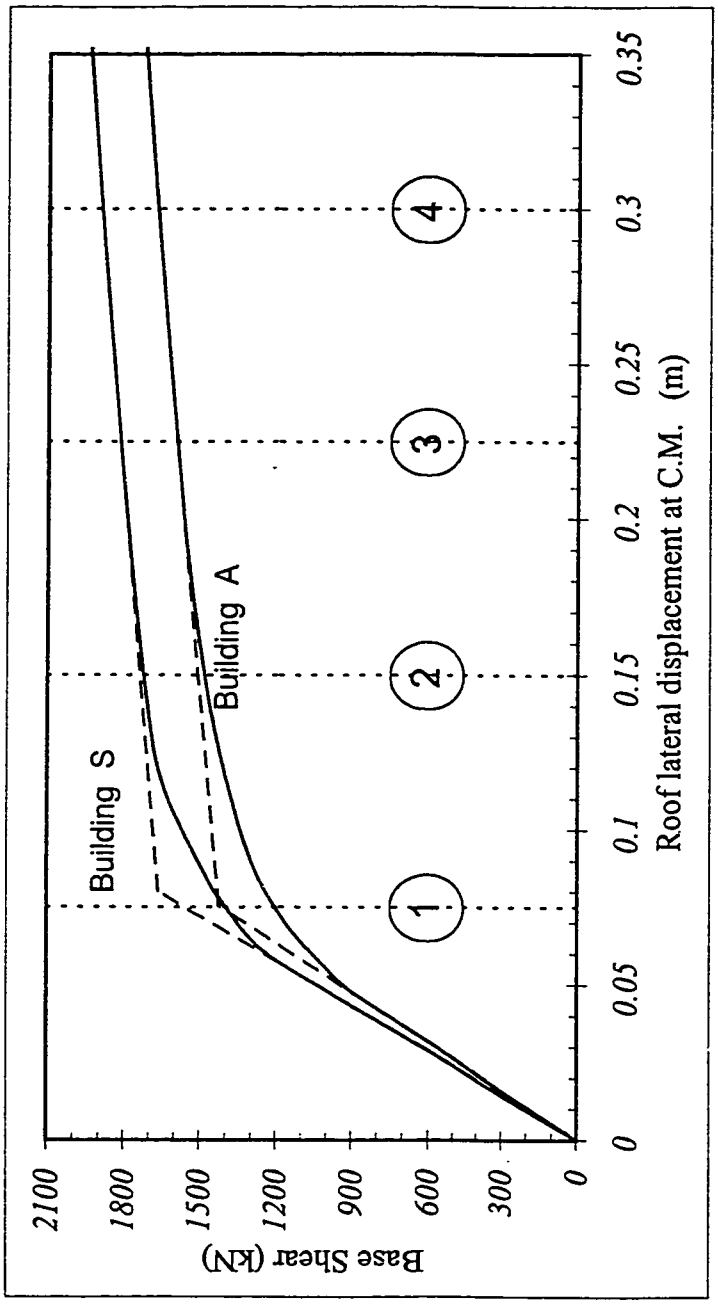


Figure 5.1. The capacity curves for Buildings A and S

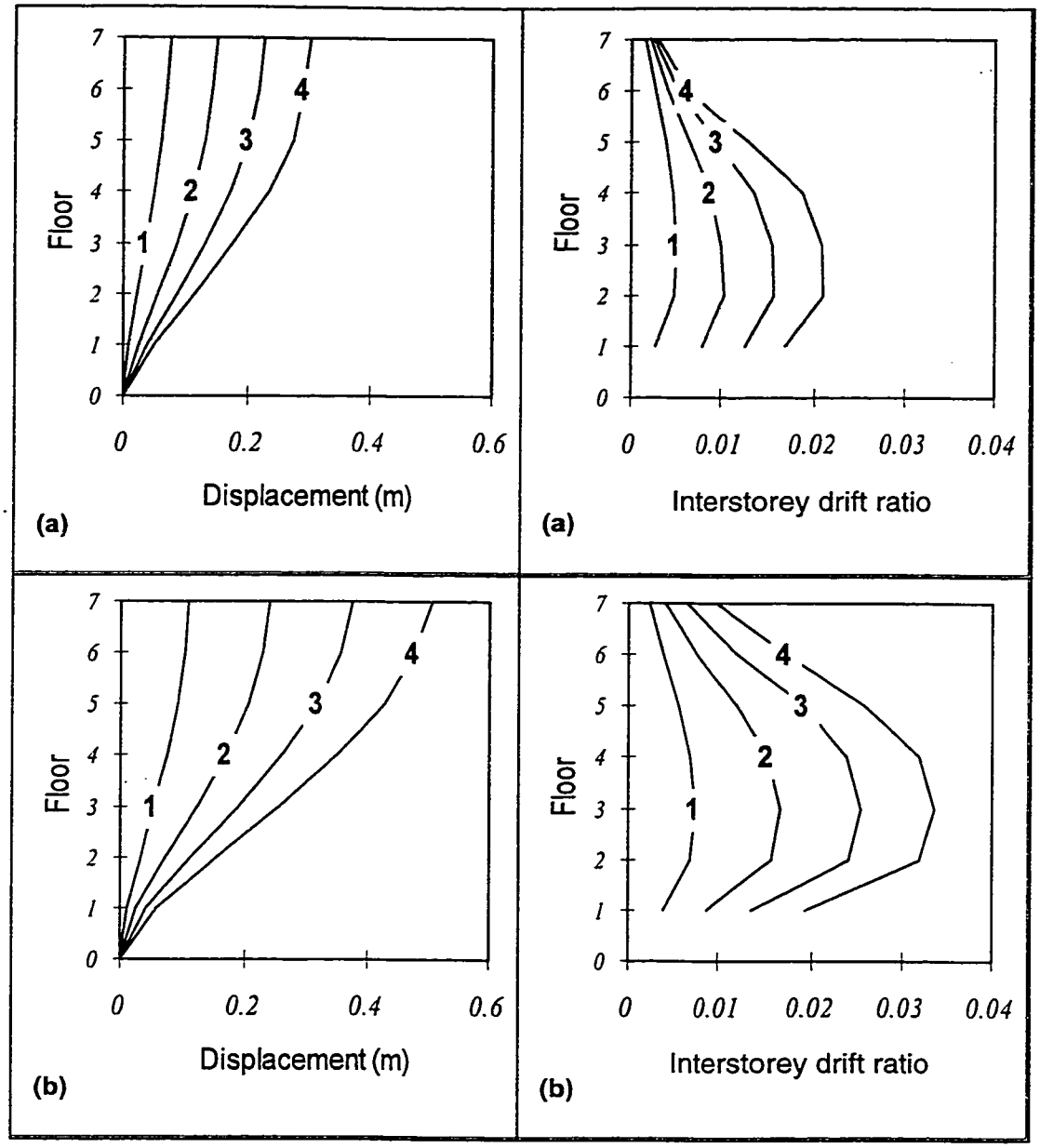


Figure 5.2. Floor displacement at edge 3
(a) Building S (b) Building A

Figure 5.3. Interstorey drift ratio at edge 3
(a) Building S (b) Building A

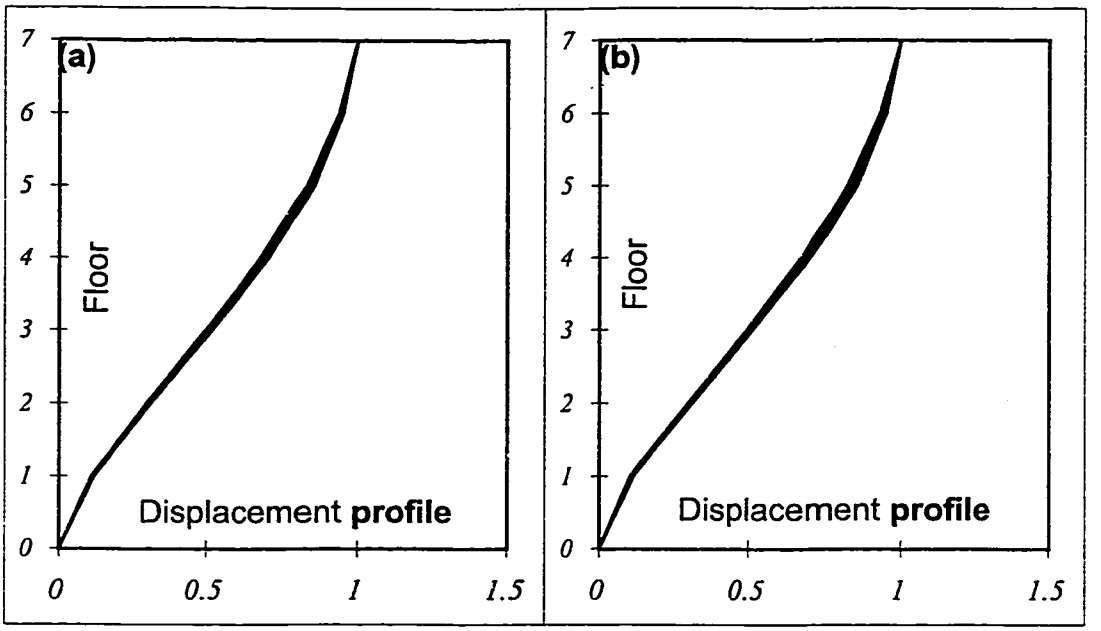


Figure 5.4. Displacement profile of Building A
(a). at CM, (b). at edge 3

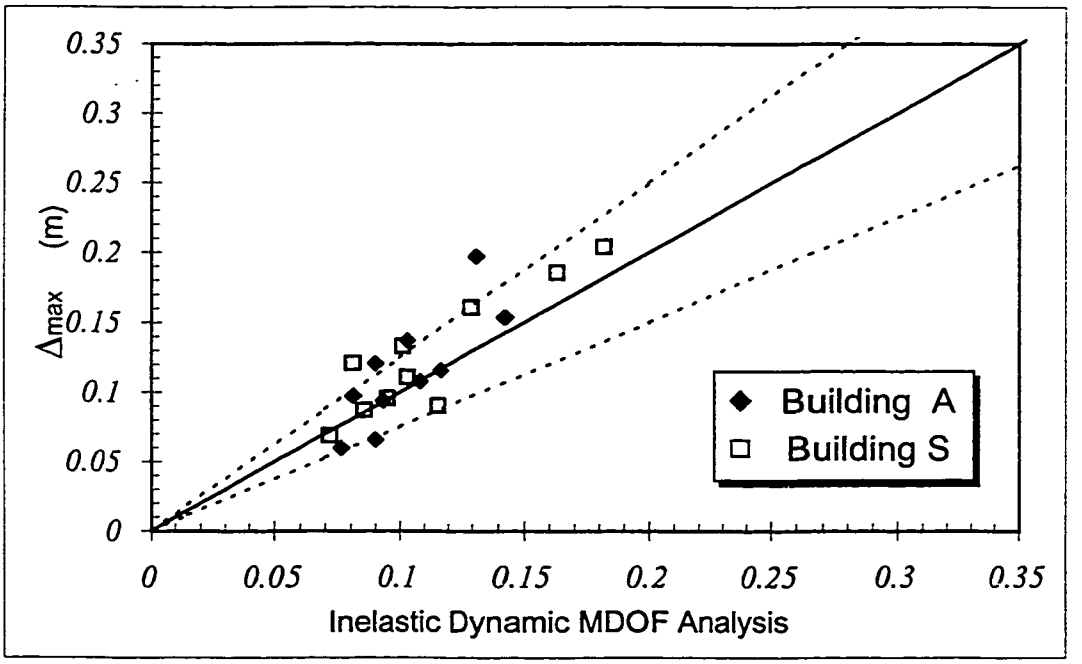


Figure 5.5. Maximum roof CM displacement (meter)

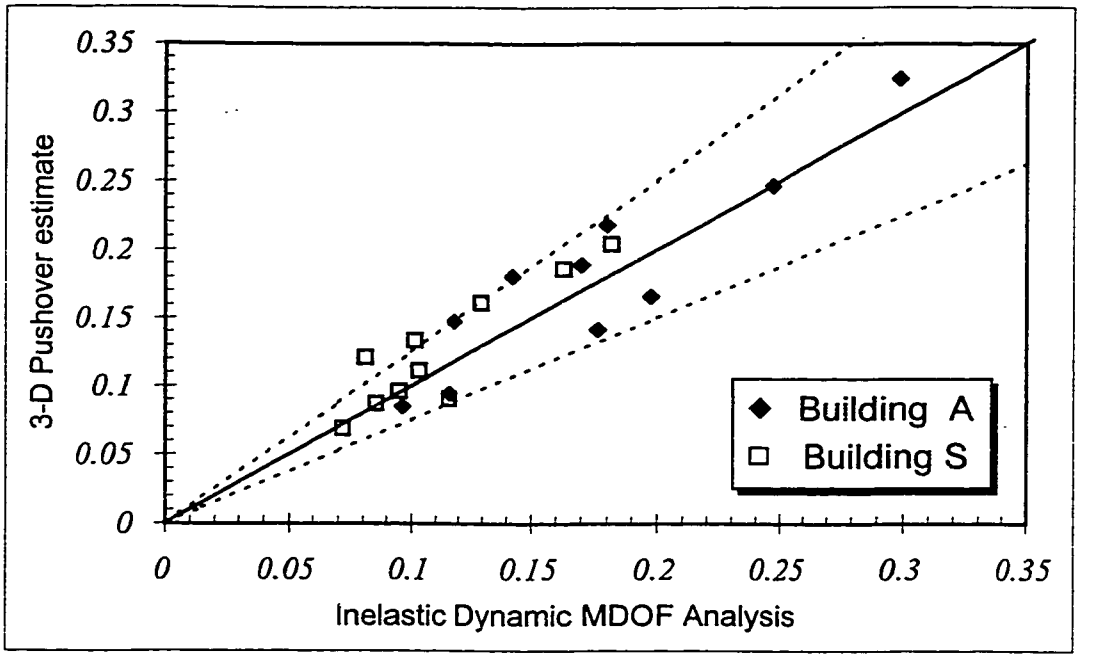


Figure 5.6. Maximum top displacement at edge 3
(unit in meter)

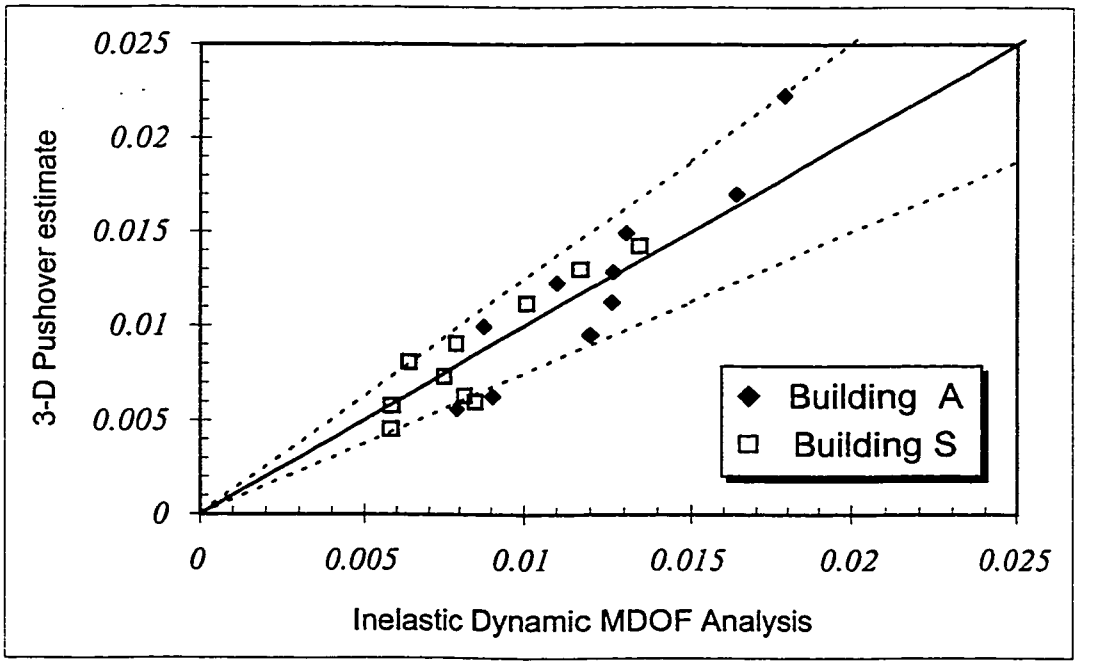


Figure 5.7. Maximum interstorey drift ratio at edge 3

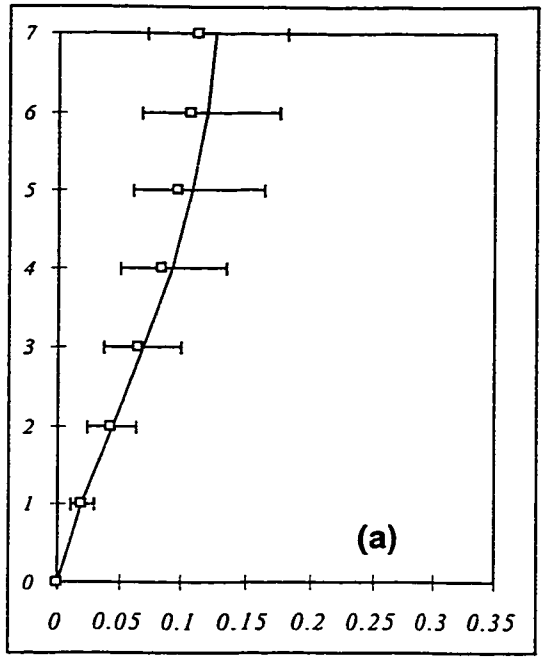


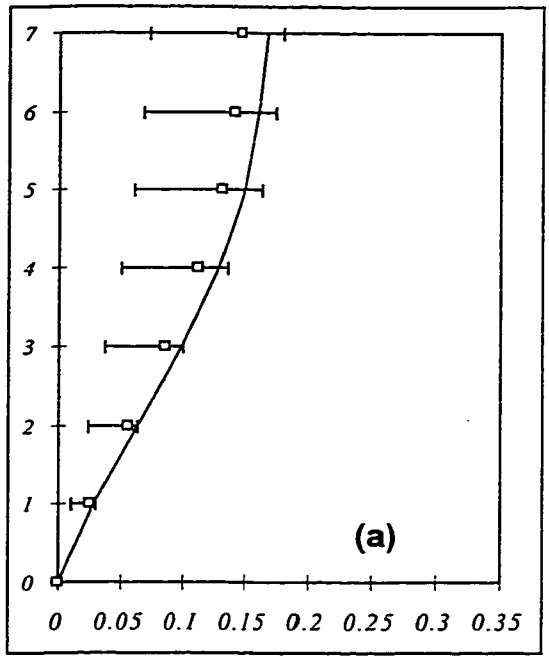


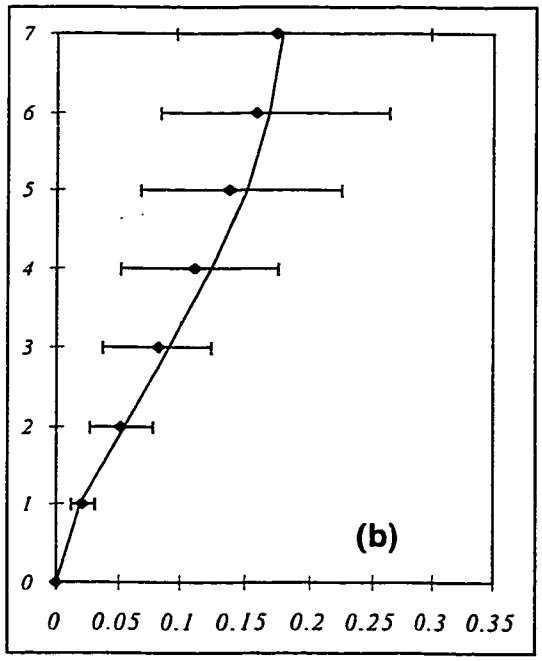


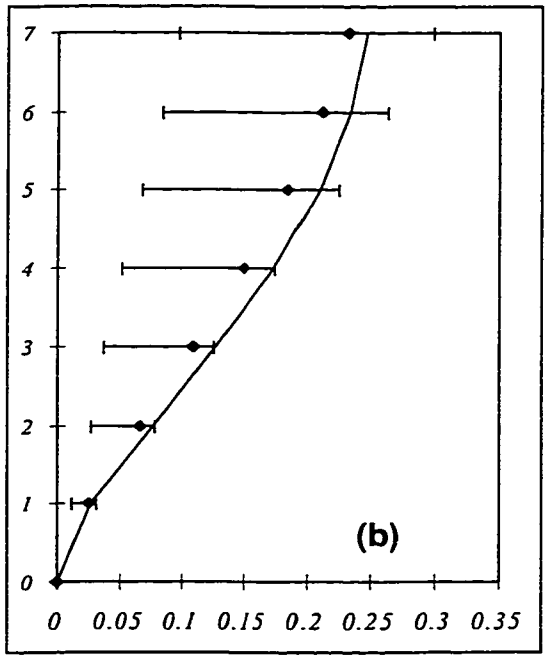


Figure 5.8. Pushover estimation (**mean**) of maximum displacements at edge 3 (meter)
(a) Building S (b) Building A

Figure 5.9. Pushover estimation (**mean**+σ) of maximum displacements at edge 3 (meter)
(a) Building S (b) Building A

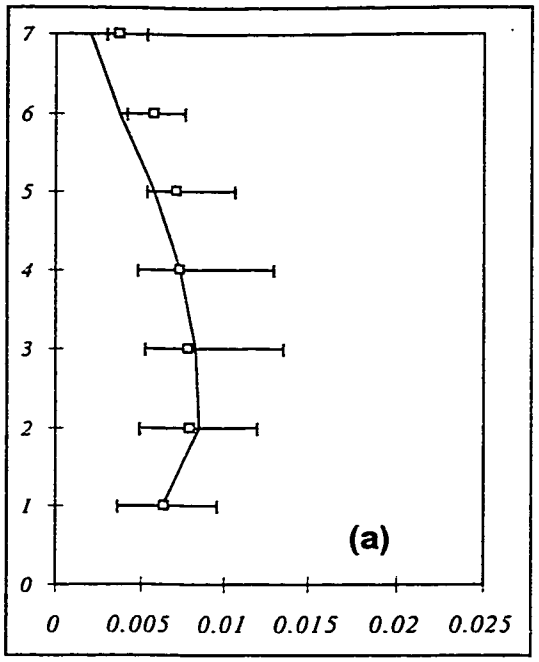


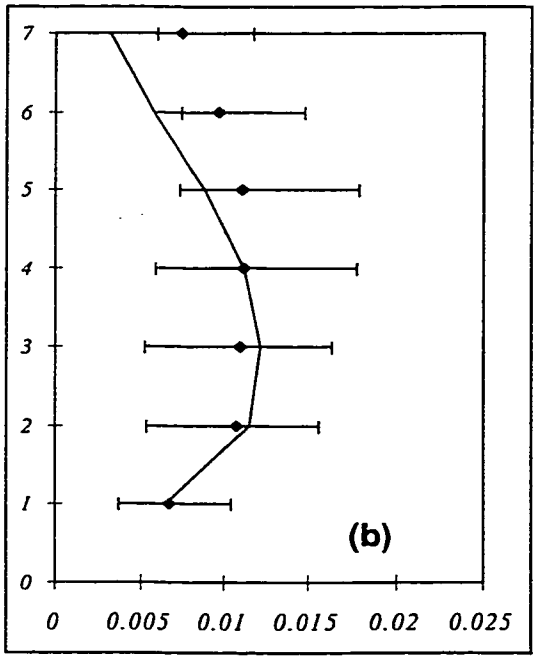


Figure 5.10. Pushover estimation (**mean**) of maximum interstorey drift ratio at edge 3
(a) Building S (b) Building A

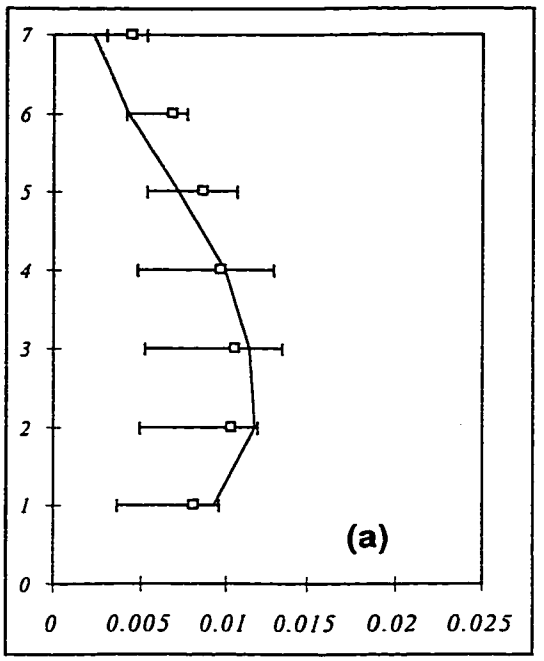


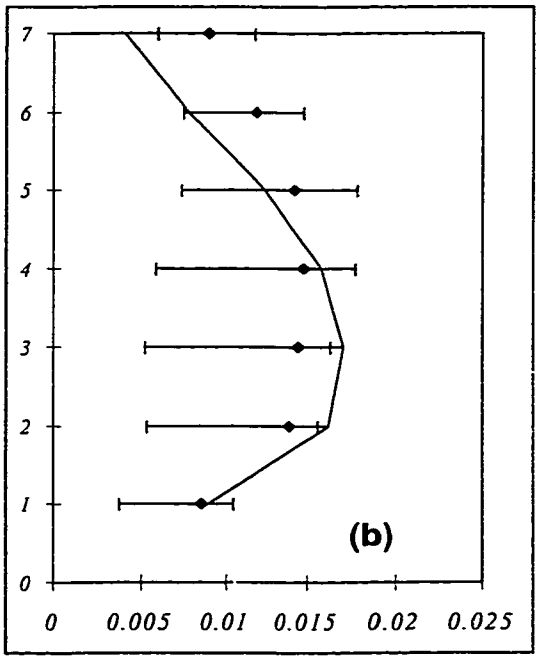


Figure 5.11. Pushover estimation (**mean**+σ) of maximum interstorey drift ratio at edge 3
(a) Building S (b) Building A

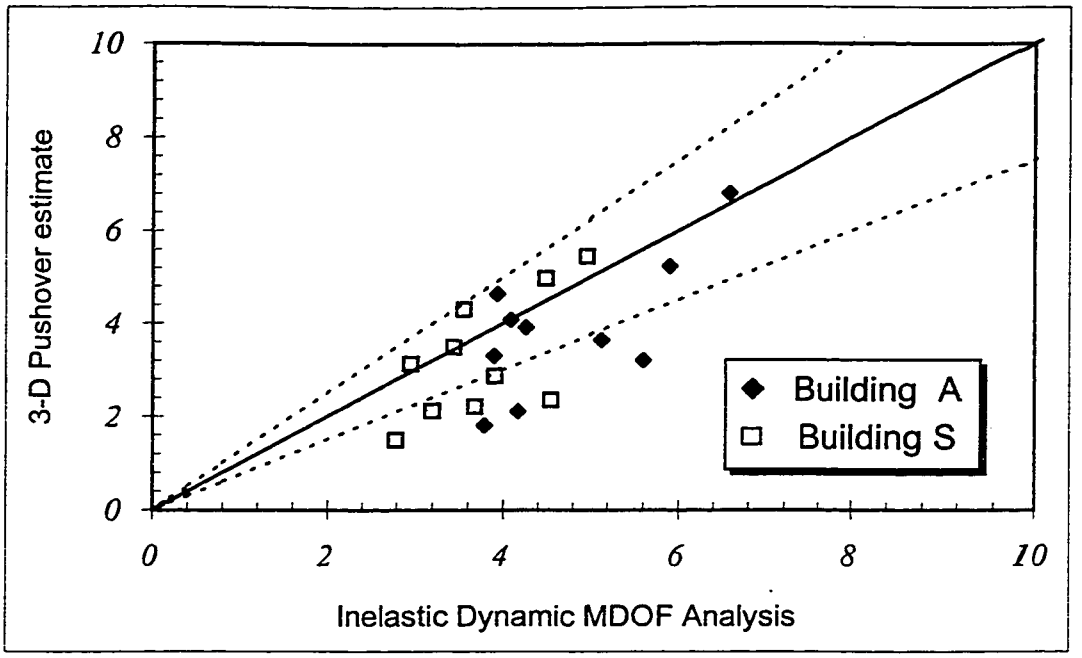


Figure 5.12. Maximum ductility demand of beams on Frame 3

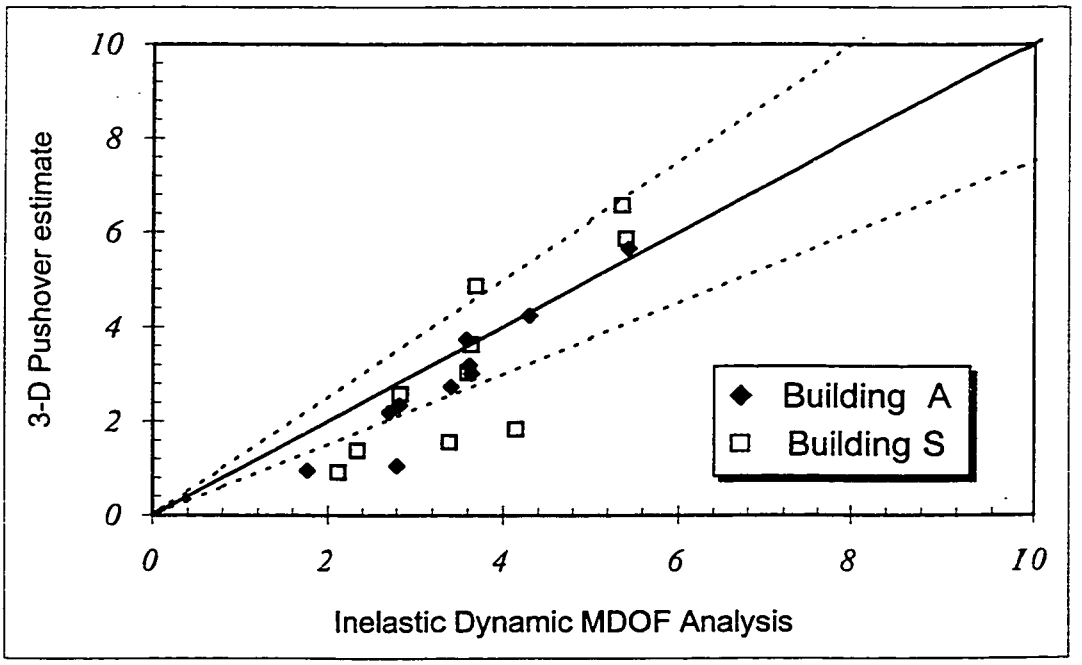


Figure 5.13. Maximum ductility demand of columns on Frame 3

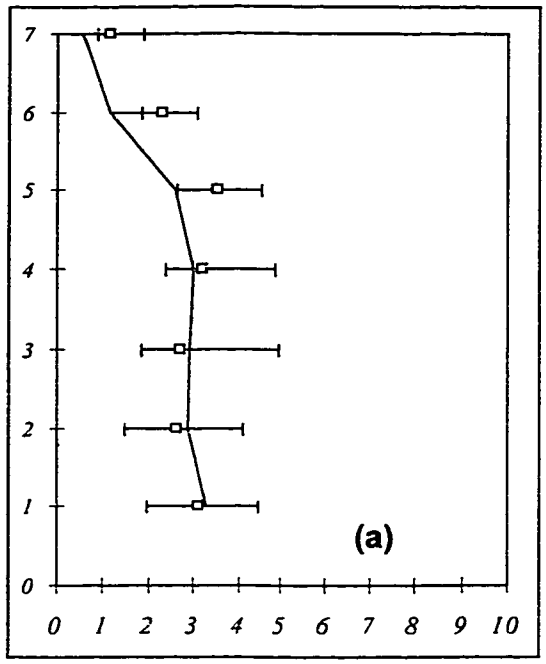


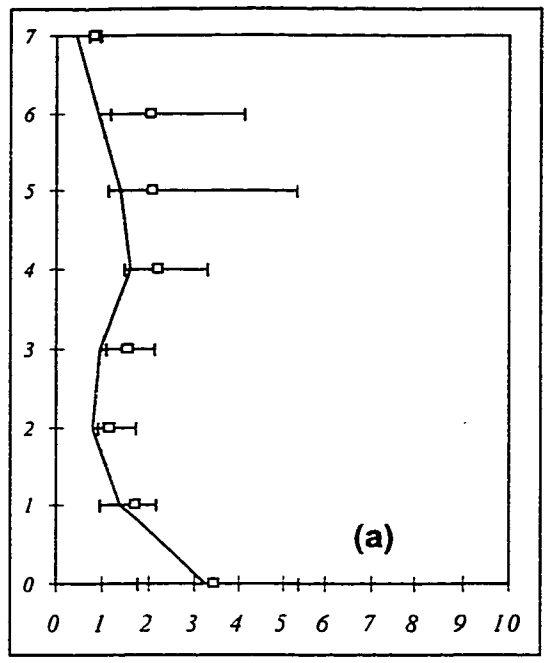


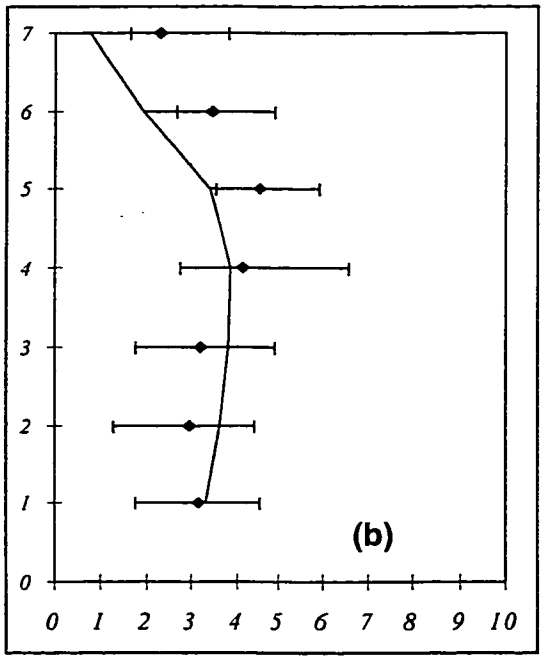


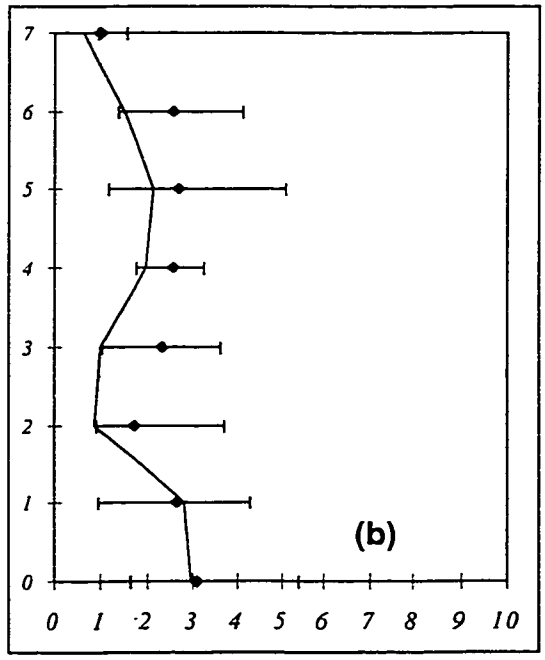


Figure 5.14. Pushover estimation (**mean**) of maximum ductility demand in beams of Frame 3;
(a) Building S (b) Building A

Figure 5.15. Pushover estimation (**mean**) of maximum ductility demand in columns of Frame 3;
(a) Building S (b) Building A

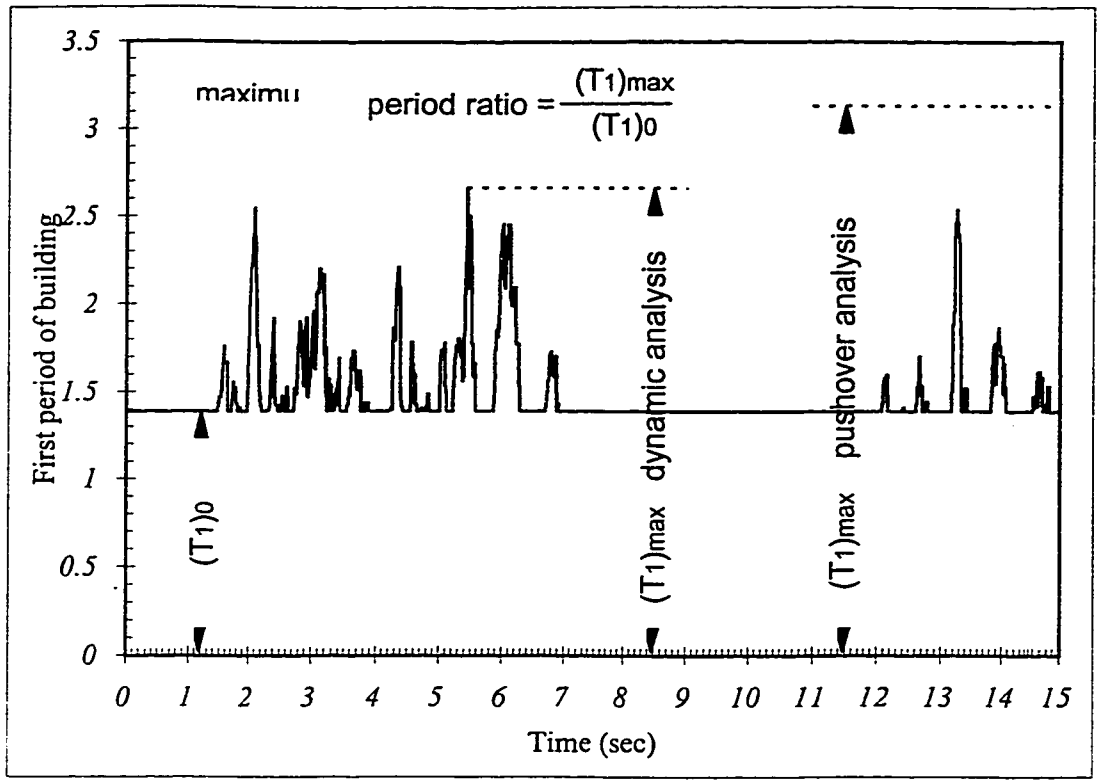


Figure 5.16. Definition of period ratio

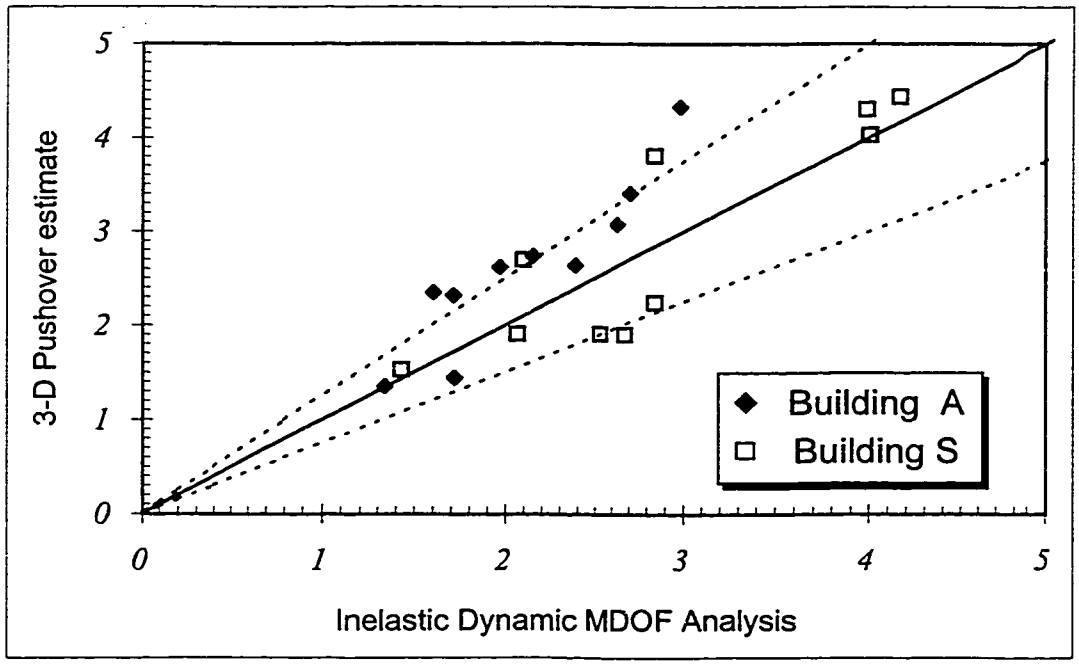


Figure 5.17. Maximum period ratio correlation

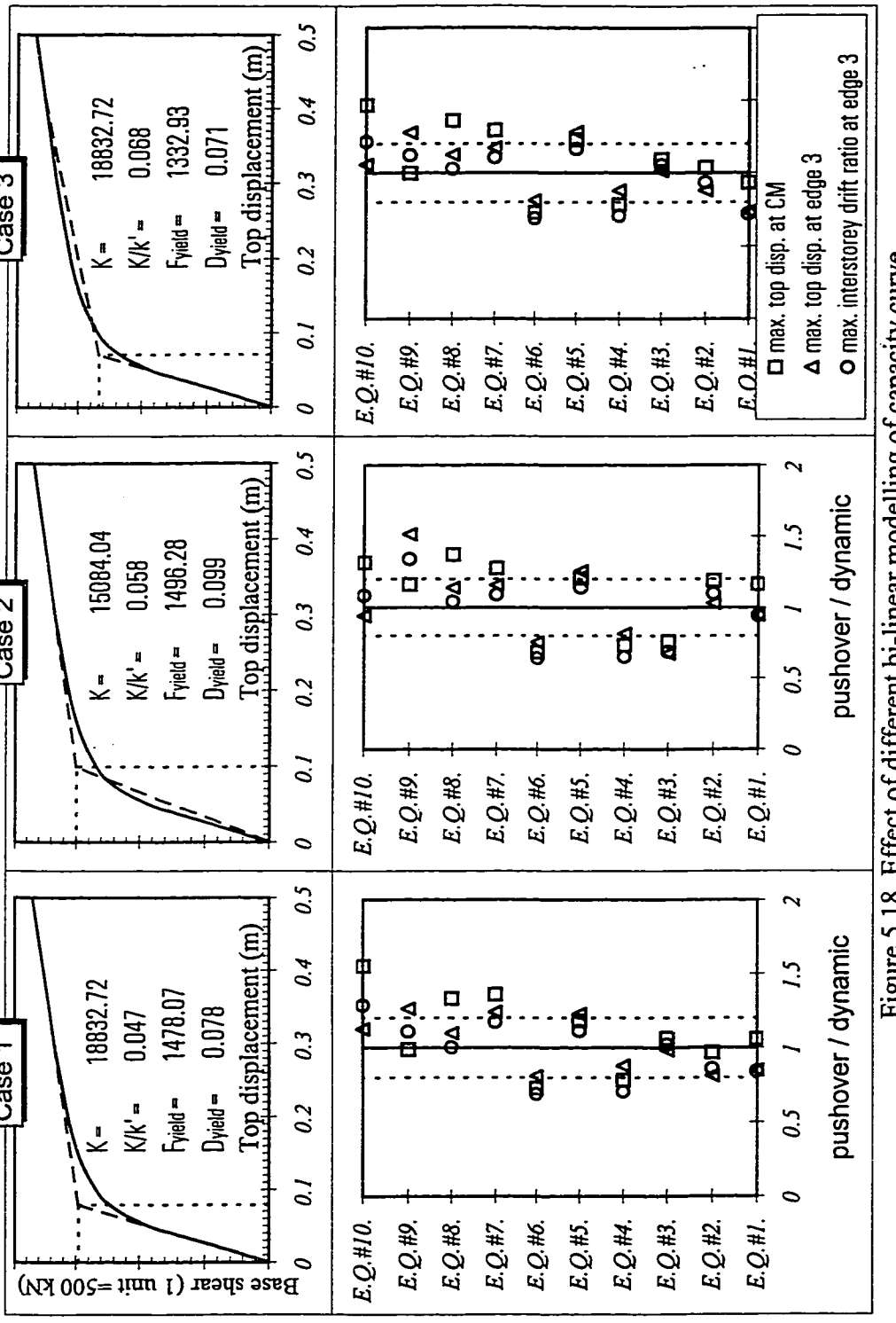


Figure 5.18. Effect of different bi-linear modelling of capacity curve

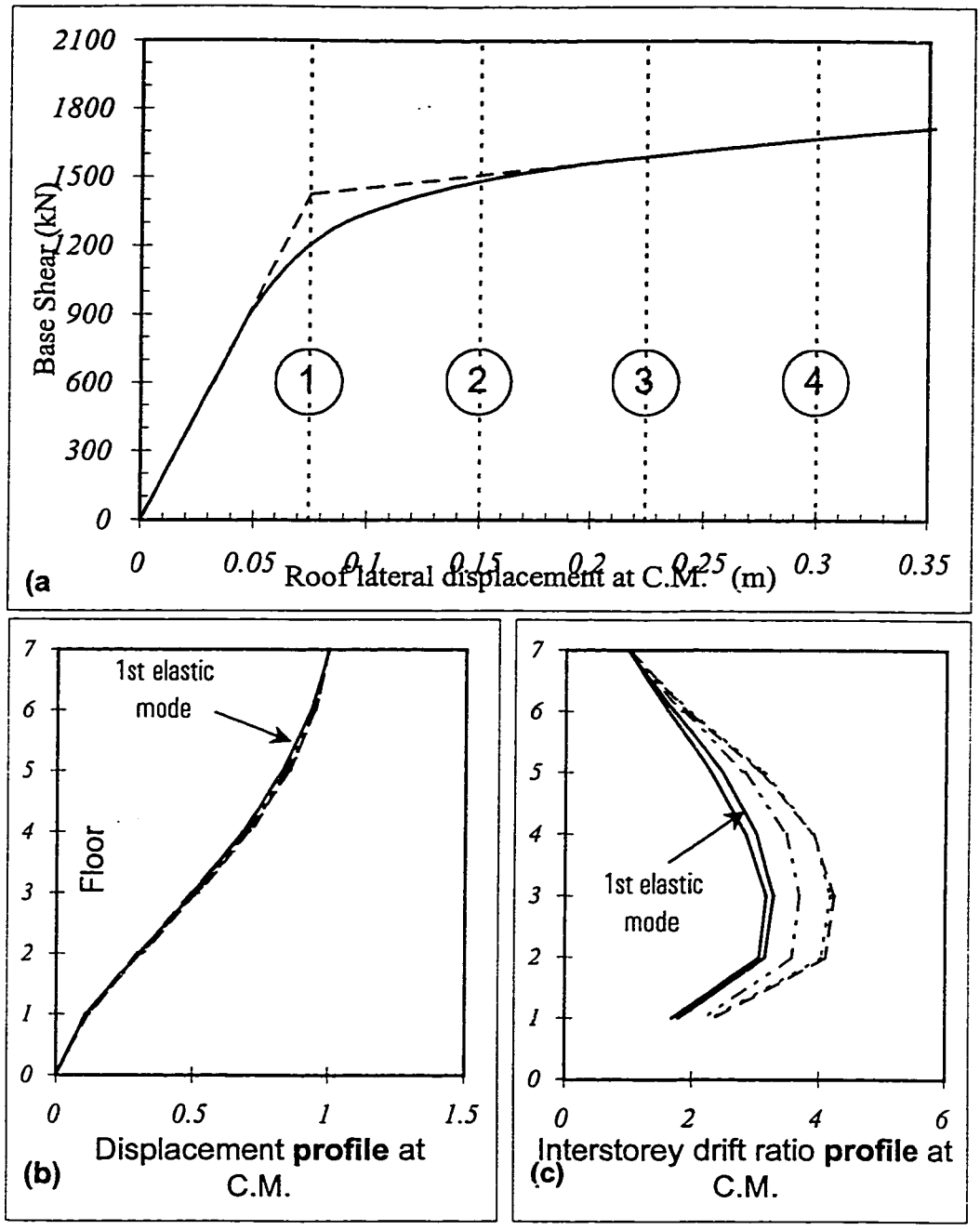


Figure 5.19. (a) The capacity curve of the asymmetric building,
(b) Five different displacement profiles at CM and,
(c) their corresponding interstorey drift ratio profiles used in sensitivity analysis

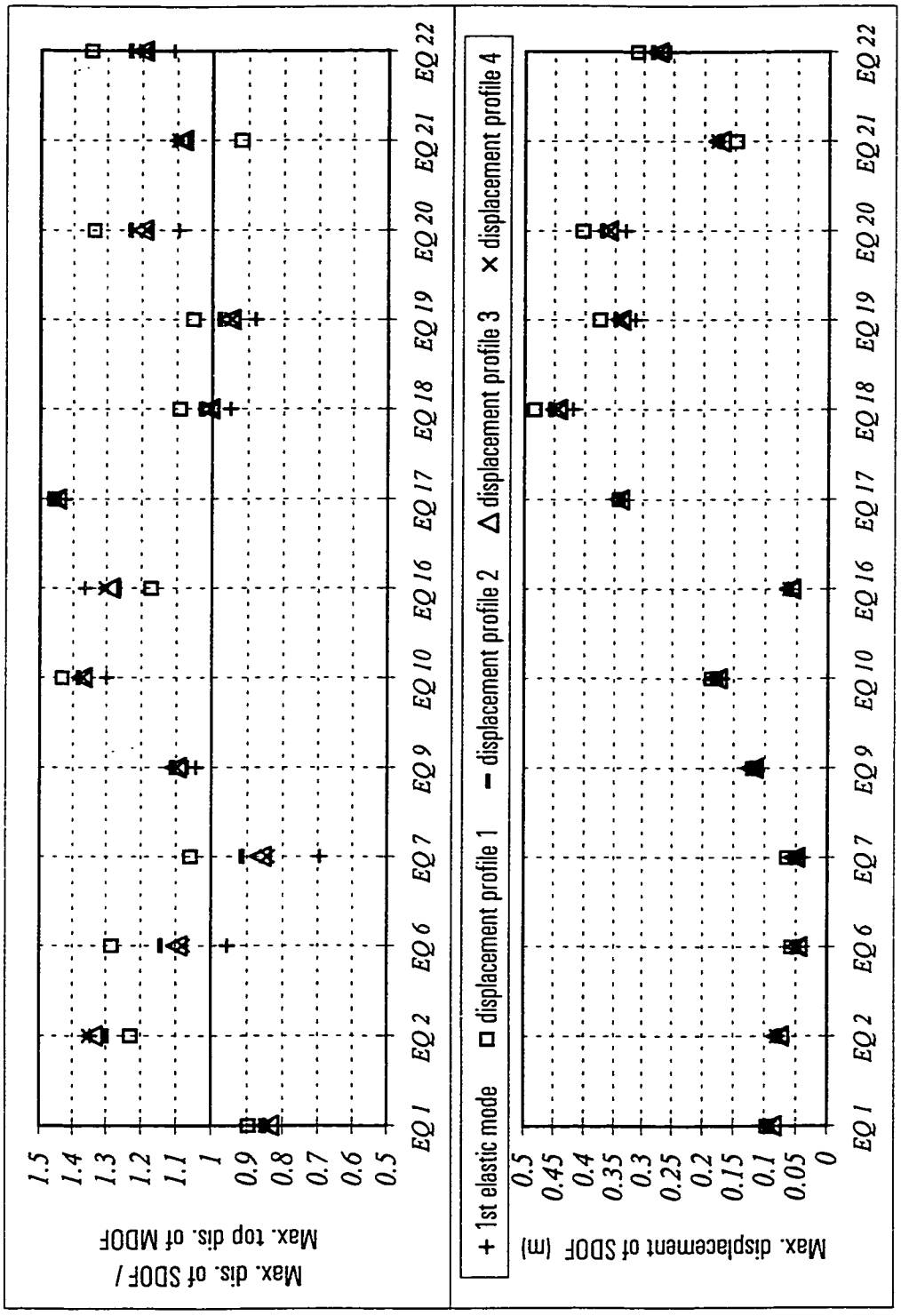


Figure 5.20. Sensitivity of the seismic displacement to profile used in deriving the equivalent SDOF system

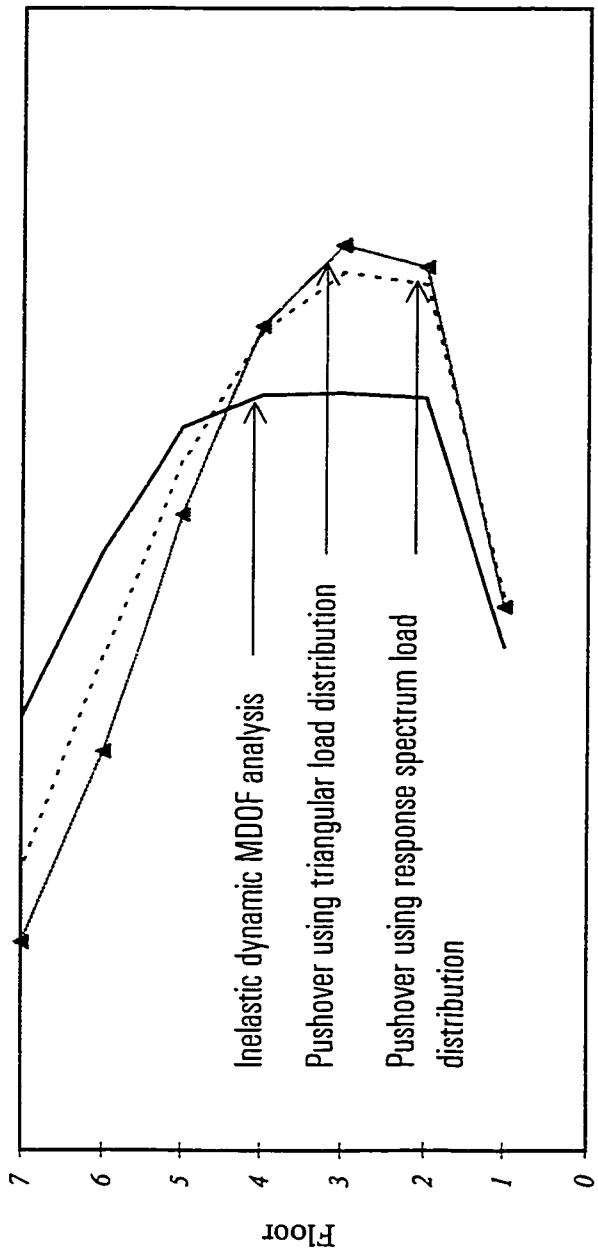


Figure 5.21. Storey drift ratio of Edge 3 estimated by different approaches

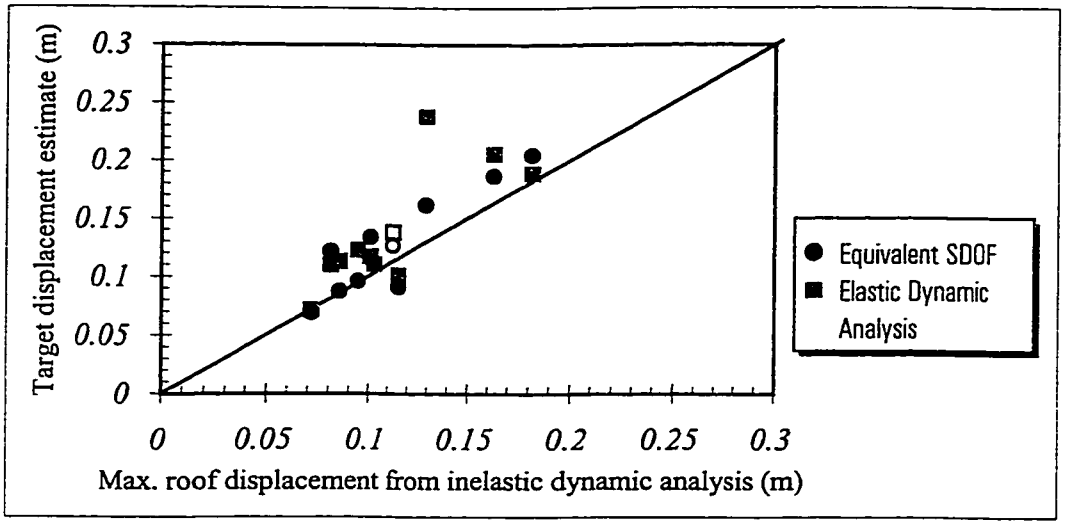


Figure 5.22. Correlation of target displacement for symmetric building

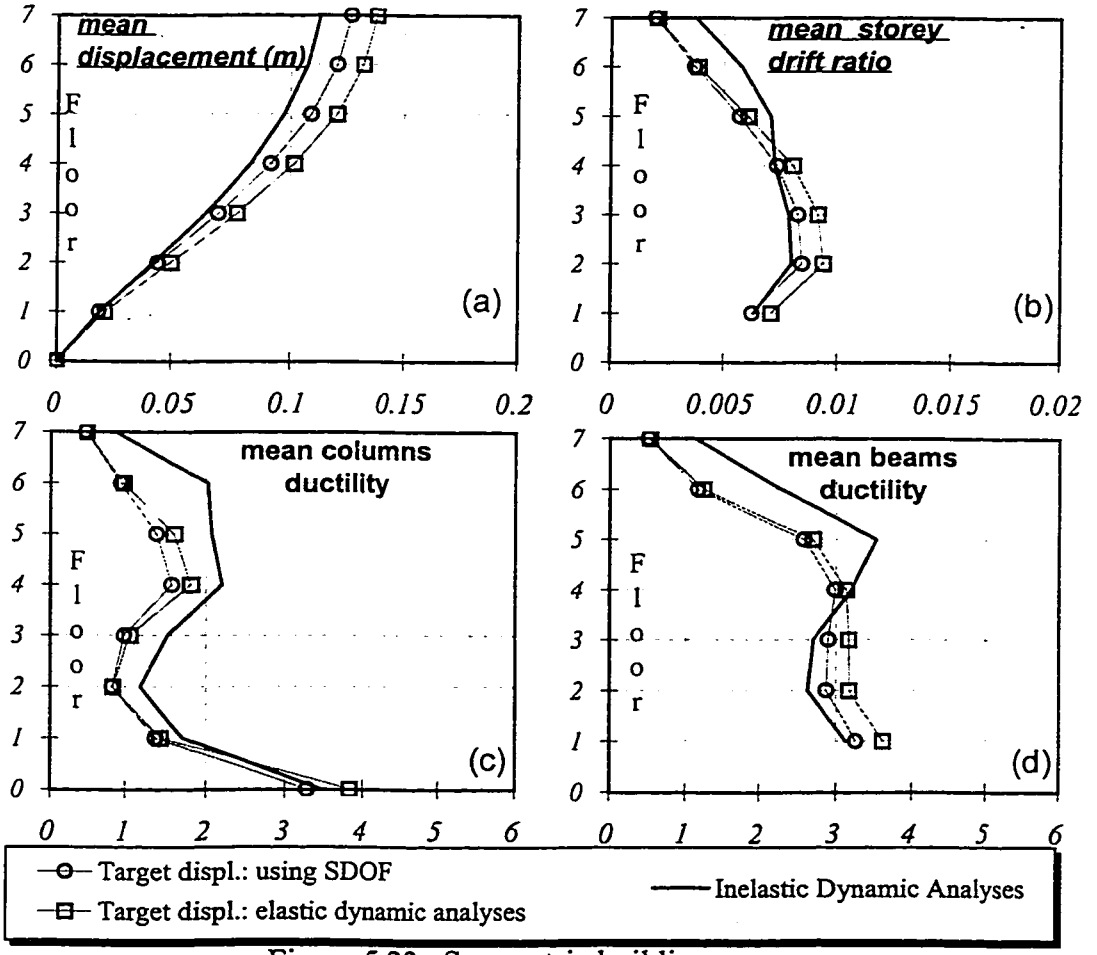


Figure 5.23. Symmetric building responses
(a) Displacements, (b) Interstorey drifts, (c) Column ductility, (d) Beam ductility

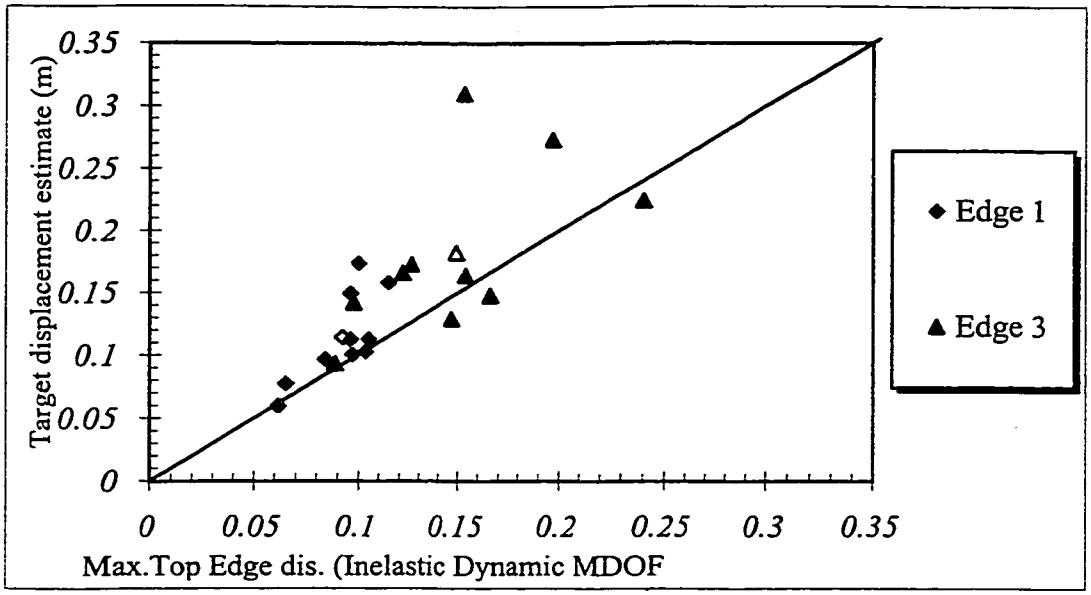


Figure 5.24. Correlation of target displacement for Frame 1 and Frame 3

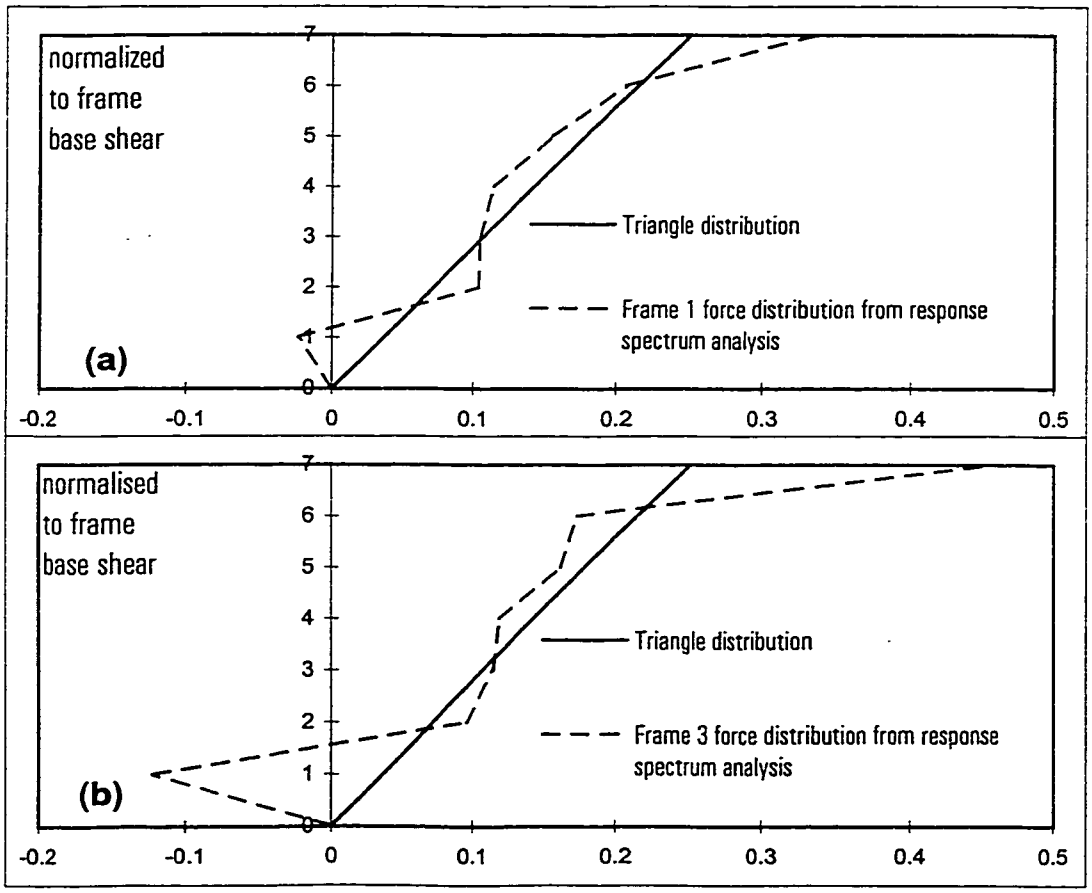


Figure 5.25. Static load distribution for pushover, (a) Frame 1, (b) Frame 3

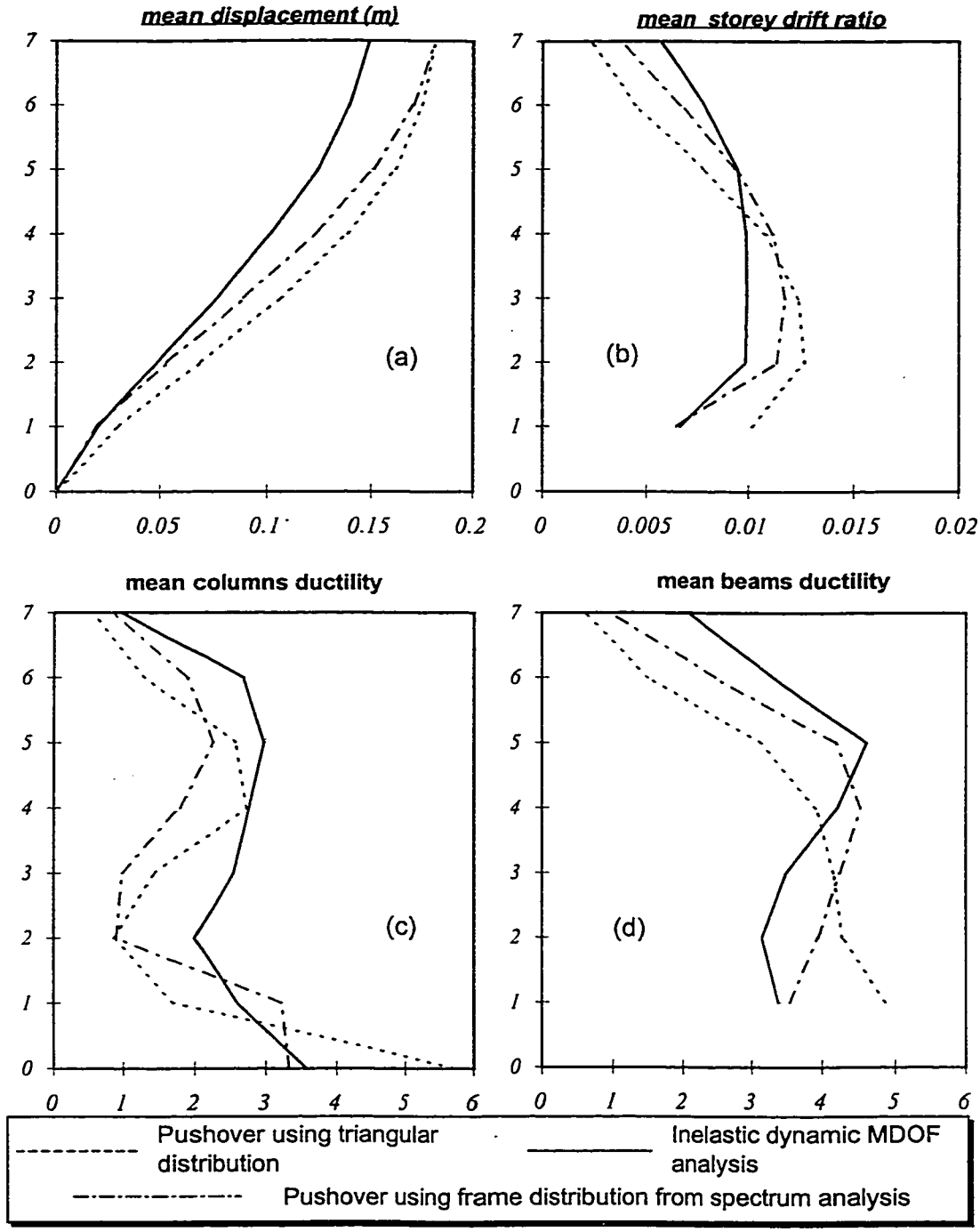


Figure 5.26. Comparison of responses at Frame 3
(a) Displacements, (b) Interstorey drifts, (c) Column ductility, (d) Beam ductility

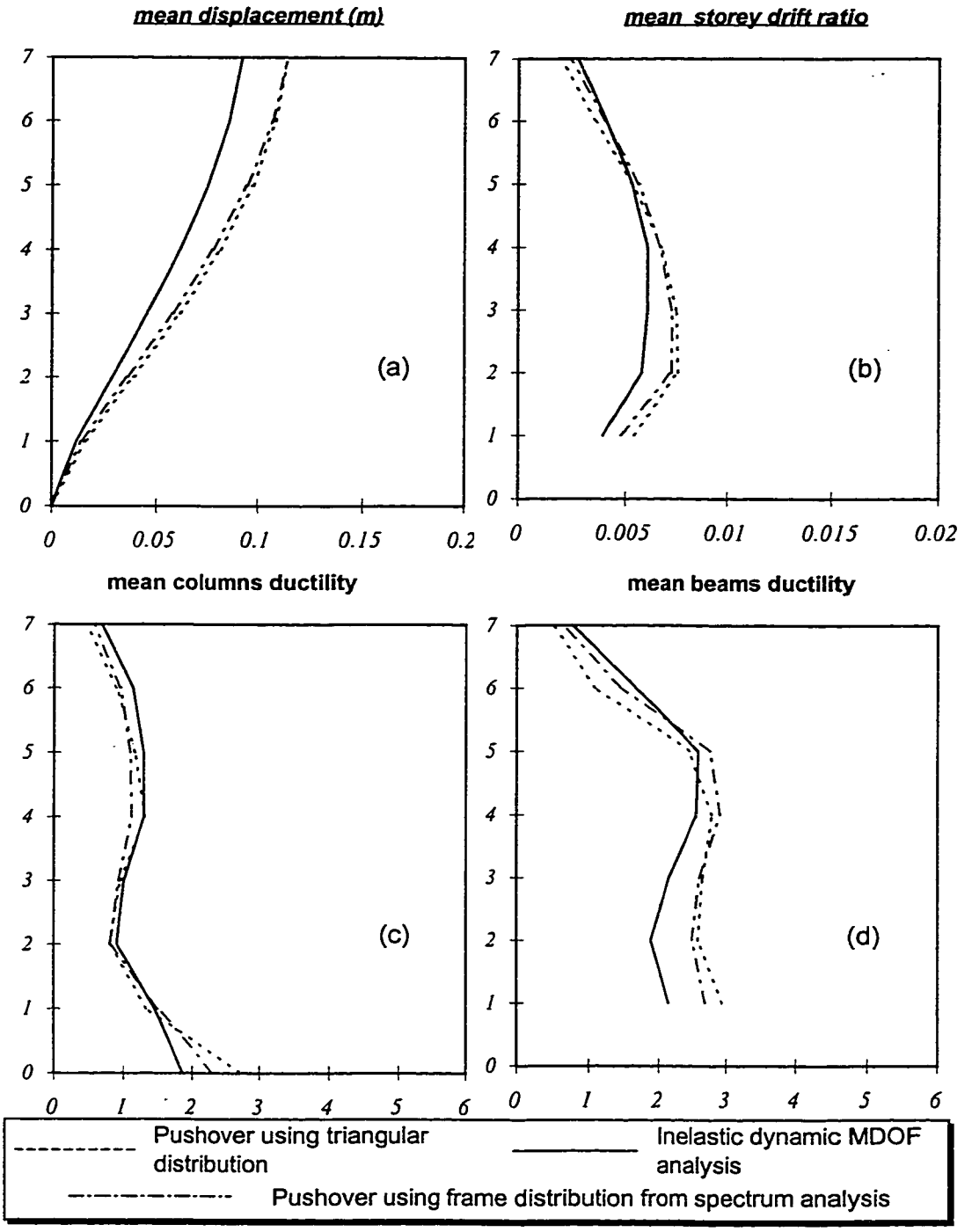


Figure 5.27. Comparison of responses at Frame 1
(a) Displacements, (b) Interstorey drifts, (c) Column ductility, (d) Beam ductility

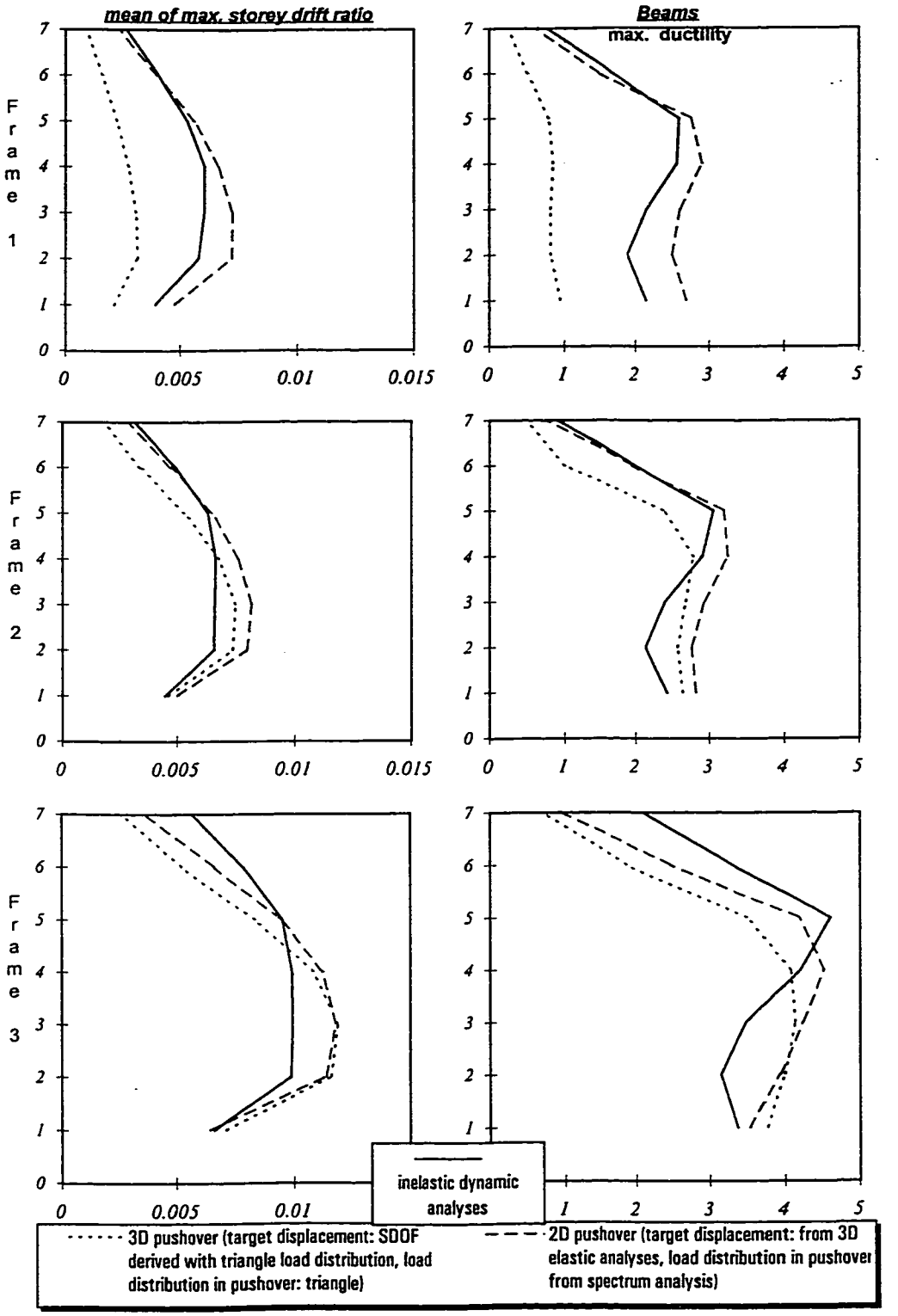


Figure 5.28. Comparison of 3D and 2D pushover approaches

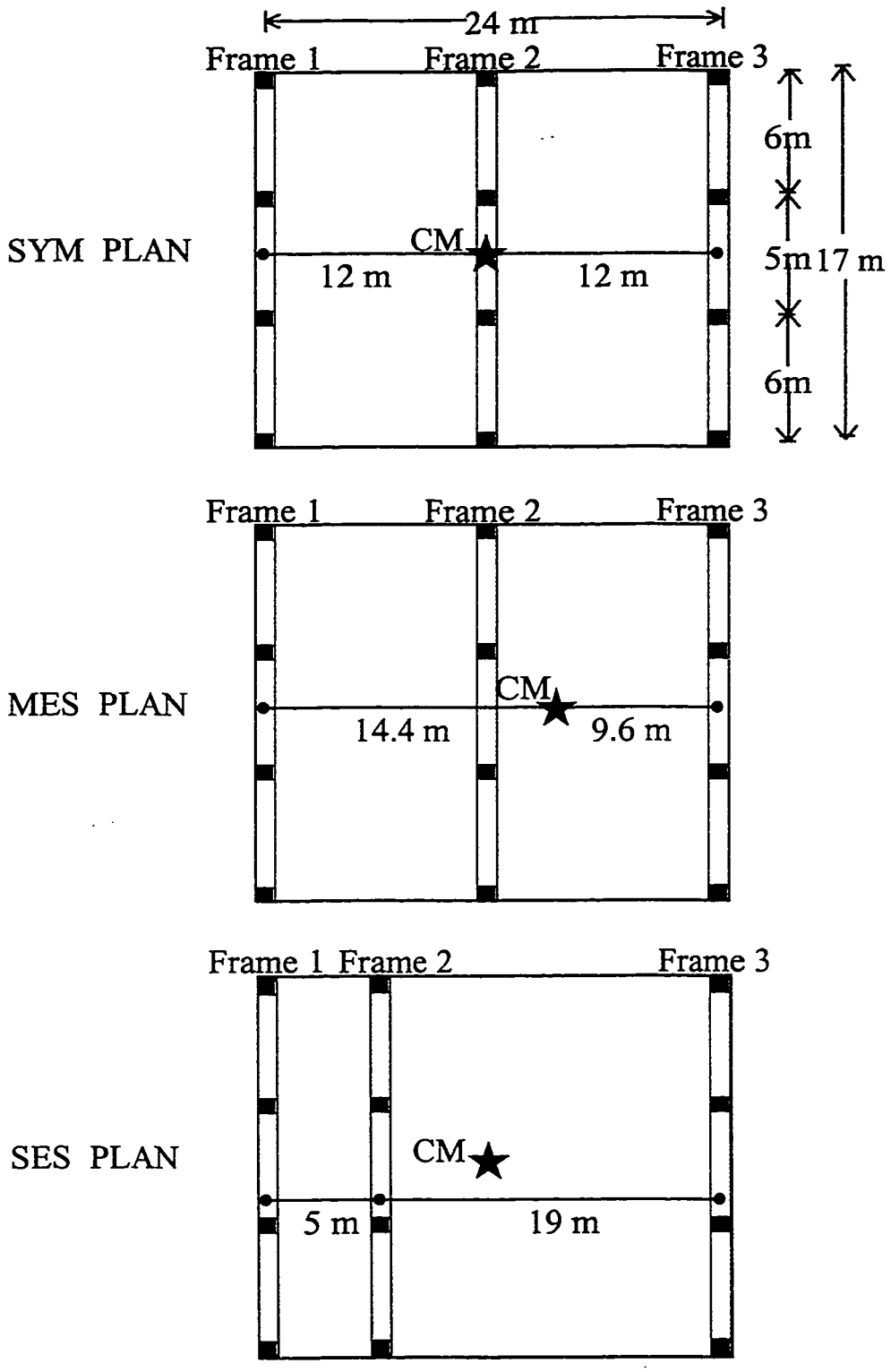


Figure 5.29. The plans of the example 7-storey Buildings

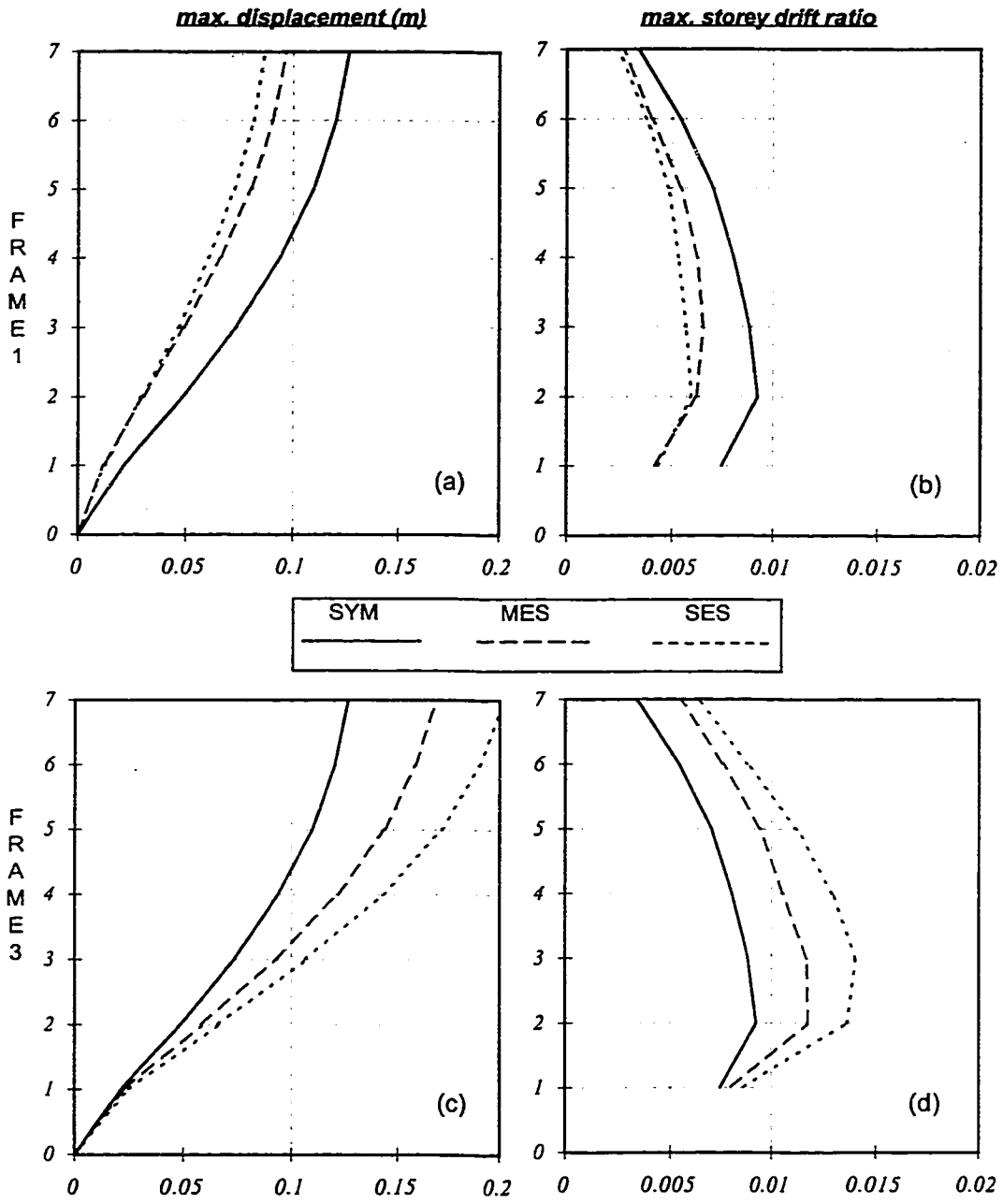


Figure 5.30. Comparison of inelastic dynamic analyses of the buildings:
(a) Displacement of Frame 1, (b) Interstorey drifts of Frame 1,
(c) Displacement of Frame 3, (d) Interstorey drifts of Frame 3

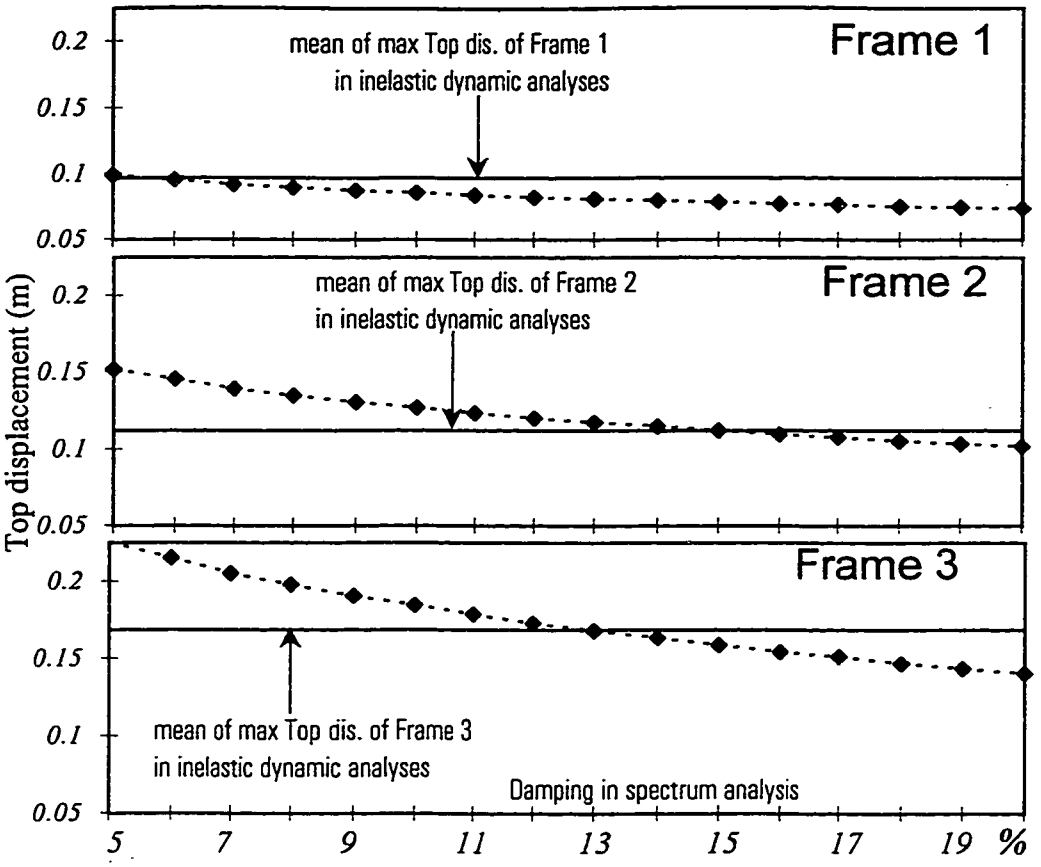


Figure 5.31. Effect of damping in top displacements of frames

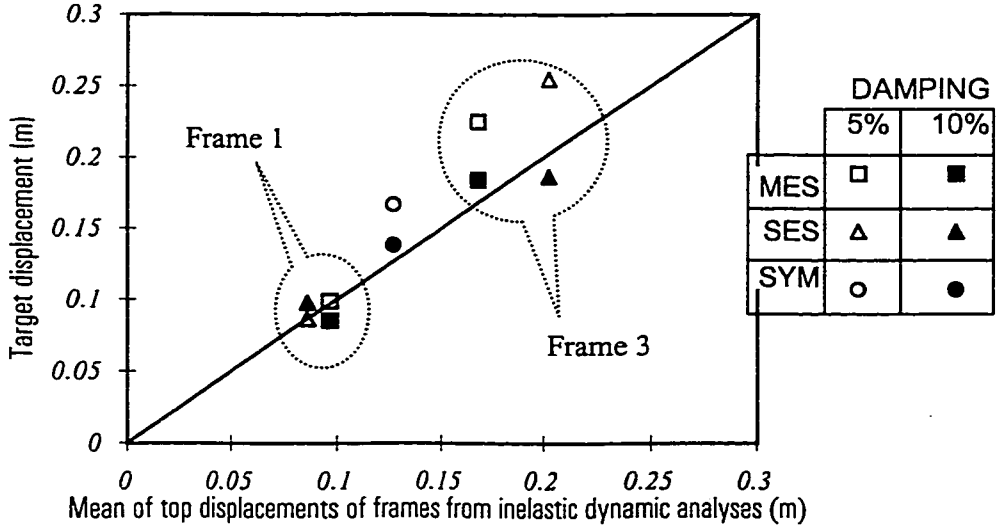


Figure 5.32. Effect of damping in estimation of target displacement

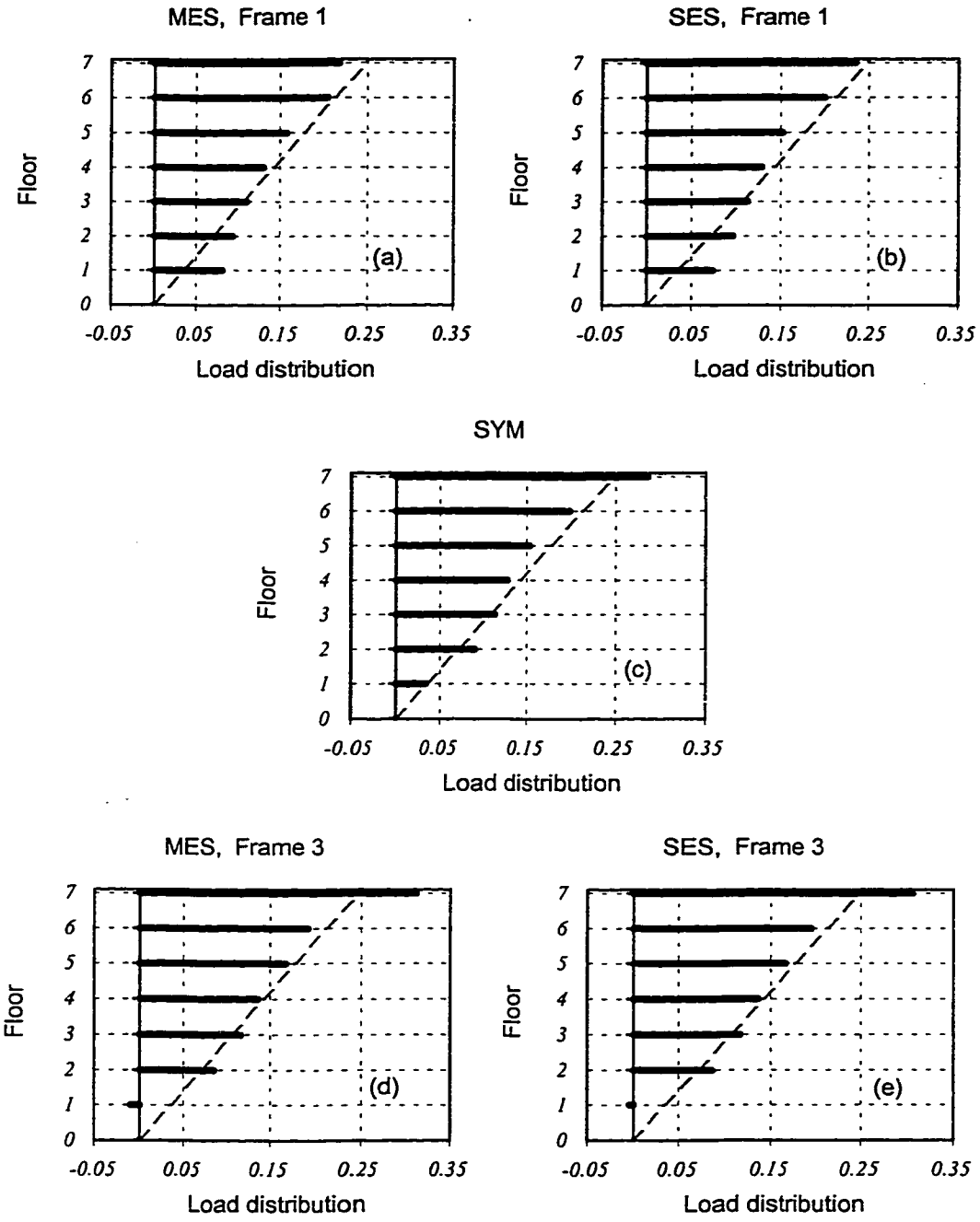


Figure 5.33. Comparison of Static load distribution for pushover; (a) Frame 1 of MES, (b) Frame 1 of SES, (c) Frames of SYM, (d) Frame 3 of MES, (e) Frame 3 of SES

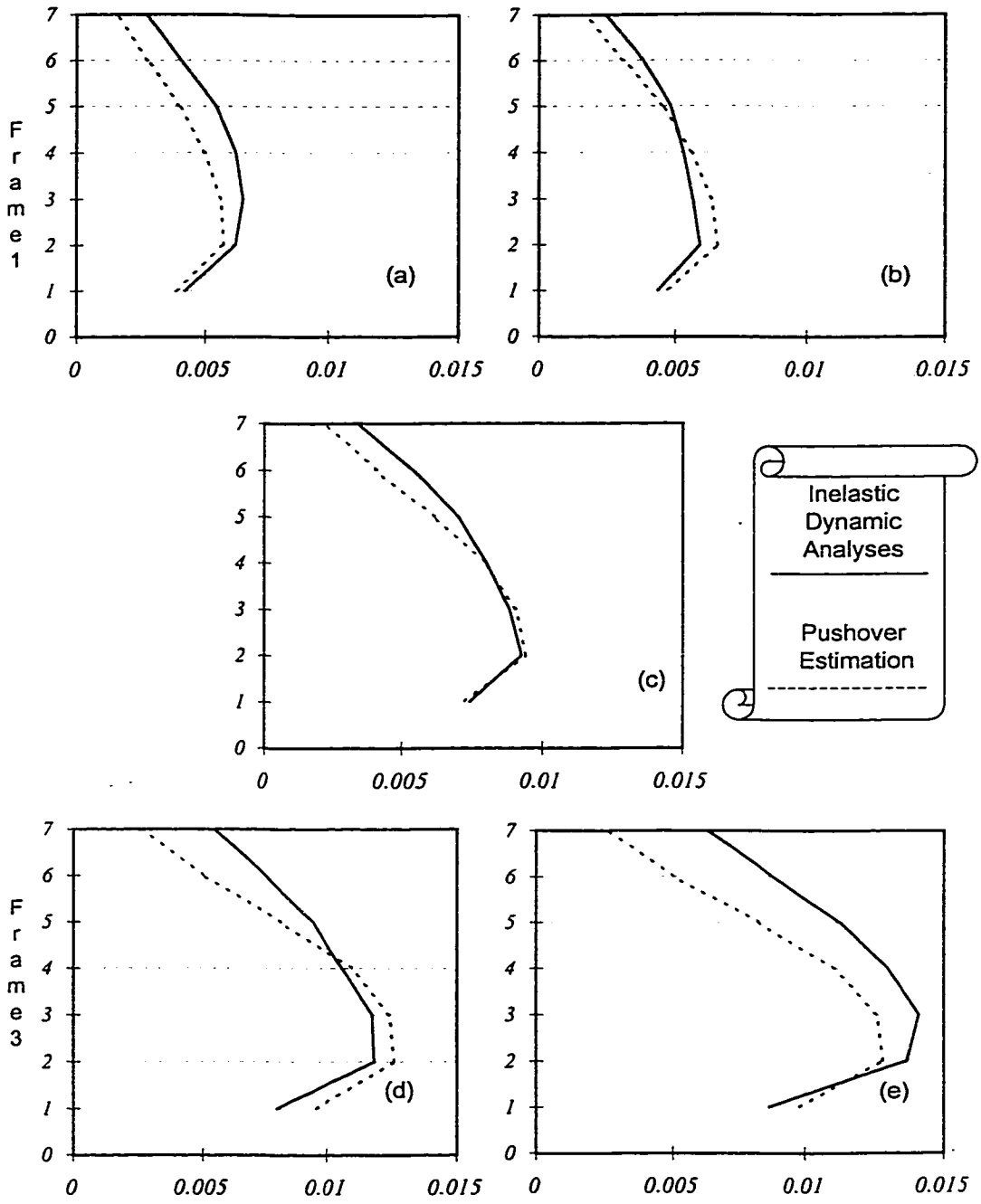


Figure 5.34. Mean of interstorey drifts for inelastic dynamic analyses and pushover estimation; (a) Frame 1 of MES, (b) Frame 1 of SES, (c) Frames of SYM, (d) Frame 3 of MES, (e) Frame 3 of SES

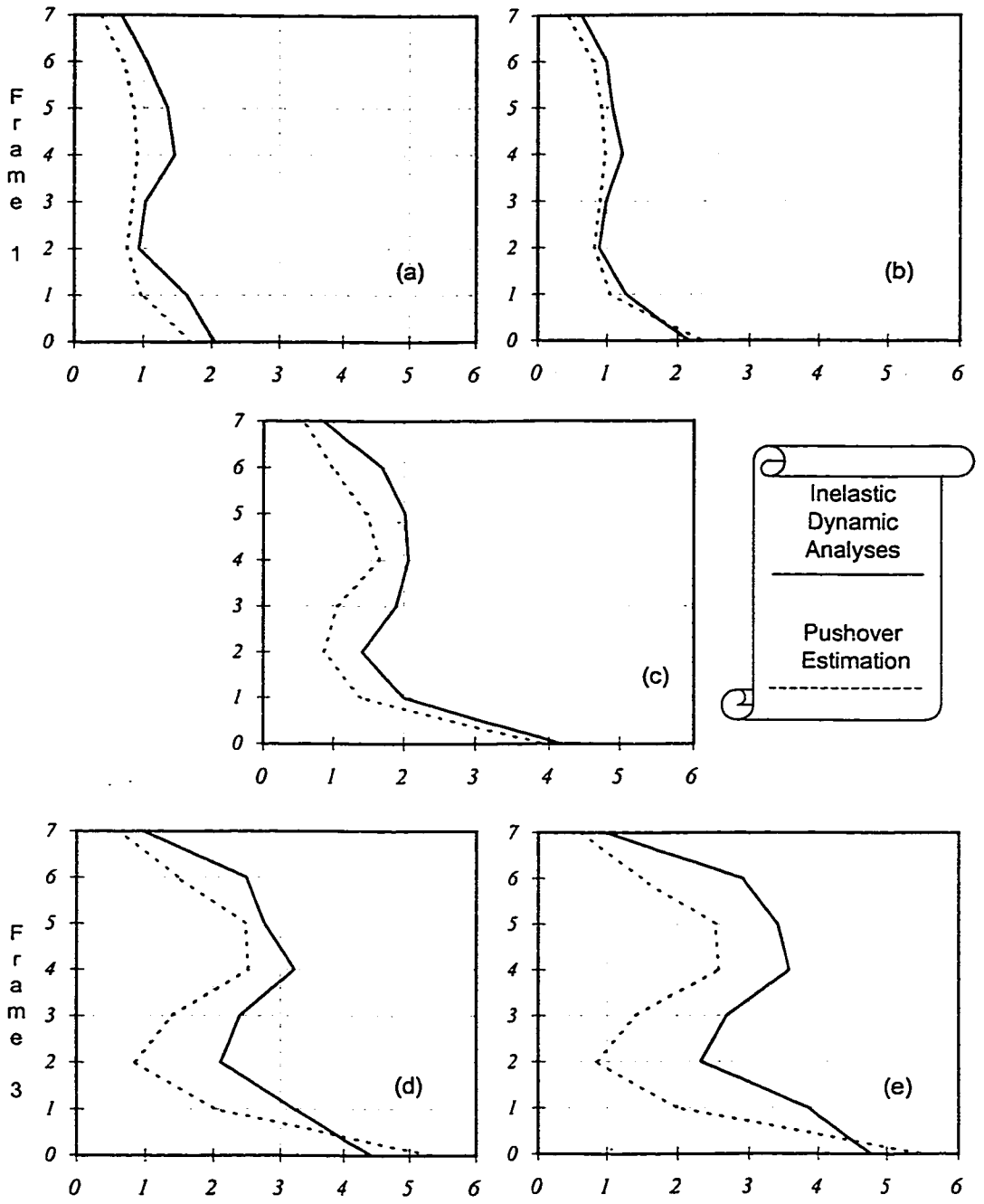


Figure 5.35. Mean of column ductilities for inelastic dynamic analyses and pushover estimation; (a) Frame 1 of MES, (b) Frame 1 of SES, (c) Frames of SYM, (d) Frame 3 of MES, (e) Frame 3 of SES

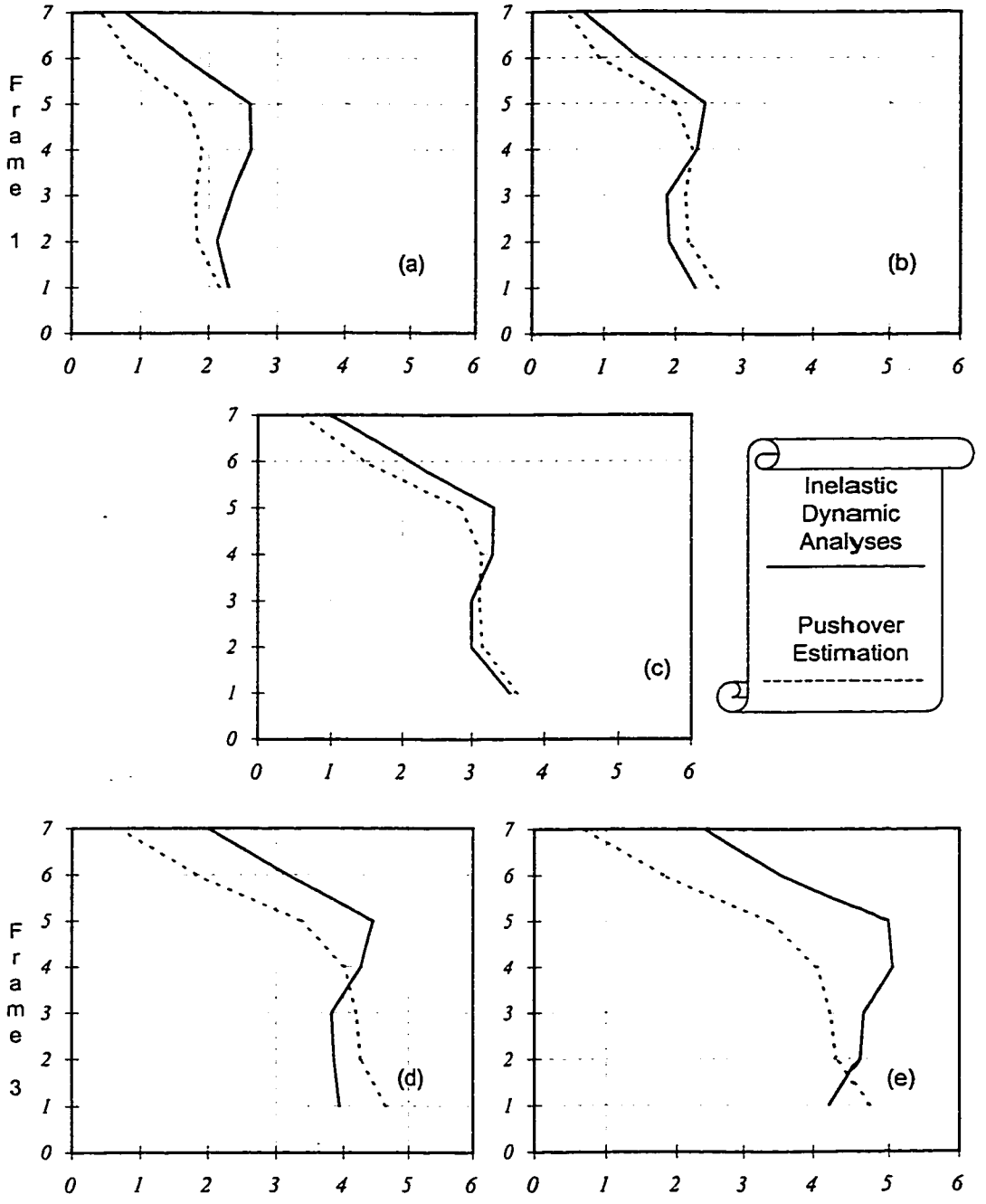


Figure 5.36. Mean of beam ductilities for inelastic dynamic analyses and pushover estimation; (a) Frame 1 of MES, (b) Frame 1 of SES, (c) Frames of SYM, (d) Frame 3 of MES, (e) Frame 3 of SES

This page is intentionally left blank.

# CHAPTER 6

# SUMMARY AND CONCLUSIONS

## 6.1 Summary

Seismic torsion is a major hazard for the structural and non-structural elements of a multi-storey building during earthquakes. Lack of systematic studies on the torsional behaviour of multi-storey buildings designed using the capacity design philosophy has been the motivation of the present study. The objectives of the study are (a) to systematically investigate the influence of torsion on the inelastic earthquake response of multi-storey ductile frame buildings designed without using any torsional provisions; (b) to evaluate the adequacy of several forms of torsional provisions commonly used in design; and (c) to develop new simplified analysis procedures to facilitate the design of asymmetrical multi-storey ductile frame buildings using the performance-based codes. A summary of these three phases is given below.

A family of structural models representing multi-storey asymmetrical buildings was subjected to both static and dynamic lateral loadings that resemble the loading on buildings during an earthquake. Ten strong ground motion records were selected to form the earthquake data set of this study. A set of response parameters is chosen to illustrate the local and global effects of torsion in the buildings.

Phase one of the study was the investigation of the influence of torsion on the inelastic earthquake response of multi-storey ductile frame buildings designed without

using torsional provisions. This investigation involved studying the effects and consequences of torsion on the different response parameters such as displacements, storey drifts, beam ductility, and column ductility. The role of torsional stiffness on the behaviour of these asymmetric buildings was studied. The need to classify multi-storey buildings into the torsionally flexible (TF) and the torsionally stiff (TS) buildings was explained. The effects of eccentricity on these two classes of multi-storey buildings were examined. To justify that building models used in the present study, which are without transverse frames and subjected to unidirectional excitation, can provide reliable trends that are representative of asymmetric multi-storey frame buildings in real life, a comparison was conducted between behaviour of these buildings and buildings with transverse frames but subjected to bi-directional excitation.

Phase two of this study was to evaluate the adequacy of the different forms of torsional provisions. Three sets of provisions were considered in this research. They were (i) design for torsion using the static equilibrium criteria; (ii) static torsional provisions of UBC-1997; and (iii) consideration of torsion in design using response spectrum analysis. Each of these torsional provisions were applied in the design of two buildings, a TF building and a TS building. To determine the improvement in behaviour of these buildings due to use of the torsional provisions, the responses of the buildings were compared to responses of a reference building. The reference building was a symmetric building designed without any torsional provisions.

To identify the TF multi-storey buildings, two procedures were developed. The first procedure uses the dynamic characteristics of buildings while the second procedure uses the information normally available from early stage of design. After developing the

formulations of these methods, both of them were applied to the example buildings to evaluate their effectiveness.

Finally, phase three of this study was to develop some new analysis procedures, as alternatives to the more elaborate inelastic time history analysis. These procedures facilitate analysis and design of asymmetrical multi-storey ductile frame buildings. They were divided to two groups. The first group was called 3-D pushover because they require a computer program capable of performing 3-D inelastic static analysis. The second group of methods only requires a program capable of conducting 2-D inelastic static analysis.

## 6.2 Conclusions

The significant conclusions obtained from this study are summarised as follows:

- Even a moderate eccentricity in a multi-storey building changes the response parameters at the edge frames of the building.
- The torsional effect depends on the torsional stiffness of the buildings. The locations of the vulnerable frame in torsionally flexible (TF) and torsionally stiff (TS) buildings are different.
- The main change in behaviour of the TS building occurs when it changes from a symmetric building to an asymmetric building. Responses of the TS building are not sensitive to further increase in eccentricity. However, vulnerability of the TF building depends on the value of eccentricity. An increase of eccentricity increases the maximum responses in the edges of the TF building.
- The structural modelling and mode of excitation used in this study is justified. It is

believed that the trends found in this study should be applicable to actual asymmetrical multi-storey frame buildings.

- Different torsional provisions have only minimal effects on the seismic displacements and storey drifts responses. This implies that the torsional provisions may not be effective in reducing the non-structural damage in asymmetrical buildings.
- The design based on static equilibrium reduces the ductility demand in the TS buildings but is not able to reduce the ductility demand in the TF buildings.
- The incorporation of the static torsional provisions of UBC can reduce the additional ductility demands in beams and columns for frames at the flexible side (edge 3) of the TS buildings. However, UBC static torsional provisions over-protects the elements located at the flexible side (edge 3) of the building but does not assign enough strength on the elements at the stiff side (edge 1) of the TF buildings.
- The use of a design based on response spectrum analysis is effective in reducing the ductility demand in both the TS and TF buildings studied here.
- Unlike single mass models, there can be many possible ways to implement requirements from the torsional provision. Clear guideline should be given to designers so that the intent of the torsional provisions will be reflected in the actual design.
- The static application of lateral loads at the CM of the floors cannot correctly predict the distribution of additional responses caused by torsion in TF buildings. Therefore, the static torsional provisions should not be applied to TF buildings, even though the buildings themselves are regular in elevation.
- A comparison of modal masses in a free vibrational analysis of the building is a reliable

method to identify the TF buildings. A second procedure to identify TF buildings is based on static analyses. The advantage of this second procedure is that only elastic static analyses are involved and is based on information already available to designers early in the design process.

- A 3-D pushover procedure, based on reducing a building to an equivalent SDOF system, can be used for damage assessment of asymmetrical buildings. The results of the 3-D pushover analysis are not sensitive to small changes in different modelling details of the procedure.
- The accuracy of the 3-D pushover analysis is similar to that of the currently used pushover analysis method for planar structures. The pushover analysis procedure is more successful to predict global response parameters such as edge displacements, interstorey drift ratios, and fundamental period changes than local damage parameters such as member ductility demands.
- A 2-D pushover procedure based on elastic dynamic analysis is able to estimate the inelastic seismic responses of asymmetric multi-storey buildings. The advantages of this method are: it is easily applicable to asymmetric buildings and there is no need to create a separate structural model such as the equivalent SDOF system in order to obtain the target displacement. Since this procedure requires only programs that are available and have been used extensively by the design profession, it is a practical way to extend the pushover procedure to analyse asymmetrical buildings.
- A modified 2-D pushover procedure based on response spectrum analysis can also lead to good estimates of different deformation response parameters at edge-frames of

both mass eccentric and stiffness eccentric uniform asymmetrical multi-storey buildings. It tends to underestimates the member ductility demands at the edge frames.

### 6.3 Design Implications and Recommendations for Future Research

In this study, the inelastic static and dynamic responses of asymmetric multi-storey buildings have been investigated. In part of this study, the analytical results were used for an evaluation of the current seismic torsional design practice. In this section, the significant design implications of this evaluation are reviewed, and recommendations for future research are provided.

It is clear that torsional stiffness has a determinate role in the way that seismic torsion affects the responses of a multi-storey building. Decreasing the torsional stiffness of a system intensifies the effect of torsional modes in the system. This may even shift the large responses in the building from flexible edge (edge 3) to other side of the building on stiff edge (edge 1). The *static* torsional provisions of the building codes can not detect this change, as it is a *dynamic* phenomenon. This issue needs to be addressed in the building codes. A solution is to assume a lower bound on the torsional stiffness of buildings that will be designed based on static torsional provisions. The procedures developed in this study can be used to identify TF buildings, which are buildings with low torsional stiffness.

The studies reported here are conducted on regular mass eccentric multi-storey buildings. Effects of torsion in other irregular structural configurations, such as stiffness eccentric buildings or buildings with eccentric setbacks are not covered by the

conclusions drawn here. They are topics to be studied in future research. Among other subjects for future research are: the study of importance of redundancy on the torsional response; the study of the actual damaged buildings due to torsion in the earthquakes based on field measurement data; and conducting experimental testing on inelastic torsional responses of representative prototypes of multi-storey buildings.

This page is intentionally left blank.

# APPENDIX A

# DESIGN PROCEDURE OF THE BUILDINGS

## A.1 Structural Configuration

A series of seven storey reinforced concrete multi-storey buildings having a rectangular floor plan of dimensions 24m by 17m and uniform floor height of 3m is used as the structural models in this study. The seismic loading is resisted by three ductile moment resisting frames in direction of ground motion. Frame 2 is located at the geometric centre of the floor slab, while Frames 1 and 3 are located at equal distance "x" meters from but at opposite side of Frame 2, as shown in Figure A.1. Referring the individual frame as a type A frame, the configuration of the plan can be designated as AxAxA where A denotes the frame type and x shows the distance between frames. For example, when Frames 1 and 3 are located at the edge of the slab, the configuration becomes A12A12A. A configuration of A3A3A would represent a building where the lateral load resisting elements are centrally located. Such a building depends on a central core for seismic resistance and is torsionally flexible.

Each type A frame (Frame A) consists of three bays with bay size having a dimension of 6m, 5m and 6m. The beam section is taken 300mm by 500mm deep and the column section is 500mm by 500mm. The floor and roof thickness is 125mm. The member sections and slab thickness remain unchanged along the height of the frame. If no torsional provisions are taken in design of the buildings, each frame should be designed to take one

third of the seismic load and its tributary gravity load.

## A.2 Design Loading

The frames in the buildings are designed for the critical combinations of gravity and seismic loading based on the NBCC 1995. The loadings are described in the following sections.

### *A.2.1 Gravity Loading*

The design gravity loading consists of dead and live loads. The design dead loads of frames consist of the estimated weight of structural components such as slab, beams and columns. The partition walls and the mechanical equipments are also considered. The nominal value of the unit weight of reinforced concrete and other material properties are summarised in Table A.1. The design live load is based on the suggested values in NBCC 1995 for office buildings. The summary of the design gravity loads is presented in the Table A.2.

Each Frame A takes the gravity load from a tributary area of 3m by 17m. The remaining portion of the gravity load is assigned to gravity frames which do not contribute to the lateral resistance of the building, and are therefore omitted in Figure A.1.

### *A.2.2 Seismic Loading*

The mass for calculation of the seismic design base shear is estimated from the design dead load of floors of the buildings. The mass of the roof assumed to be the same as a typical floor. The estimated masses are given in the footnote of the Table A.2.

The total seismic design lateral force for the building is calculated based on the code

(NBCC 95) formula:

$$V = \frac{V_e}{R} \times U \tag{A.1}$$

where:

$V$ = The minimum lateral seismic force at the base of the structure

$V_e$ = The equivalent lateral force at the base of the structure representing elastic response

$R$ = Force modification factor

$U = 0.6$

Code defines '$U$' as a factor representing level of protection based on experience. The ratio $\frac{1}{U}$ may be interpreted as the overstrength factor. According to this interpretation the design base shear is reduced by '$U$' to include the benefits of some effects such as redistribution of forces in inelastic range of behaviour and existence of slabs in the buildings. These effects are difficult to model and the factor '$U$' is used in the formula to represent them.

'$R$', the force modification factor reflects the capacity of a structure to dissipate energy through damping and inelastic deformation. It is a function of the type of lateral load resisting system in the building. In the case of Ductile Moment Resisting Frame Buildings a value of 4.0 is recommended by the code.

The equivalent lateral seismic force representing elastic response, $V_e$, shall be calculated in accordance with the following formula:

$$V_e = v \times S \times I \times F \times W \tag{A.2}$$

in which :

$v$ = zonal velocity ratio

$S$ = seismic response factor

$I$ = seismic importance factor of the structure

$F$ = foundation factor

$W$ = weight of the reactive masses in the building

The zonal velocity '$v$' is defined as the ratio of zonal peak ground velocity to a velocity of 1 m/s. The seismic response factor '$S$' represents the dynamical properties of the building. The value of '$S$' depends only on the period of the building for structures with periods longer than 0.50 second. For the buildings in this study, the seismic importance factor '$I$' is taken as 1.0. The buildings are assumed to be situated on rock or stiff and dense soil sites and therefore the foundation factor '$F$' is equal to 1.0.

In order to determine the seismic response factor $S$, the fundamental period $T$ must be known. NBCC 1995 gives the following formula to estimate the fundamental period for any moment-resisting frames:

$$T = 0.1 \times N \tag{A.3}$$

where :

$N$ = Number of storeys

Table A.3 summarises the values of parameters in the equations (A.1) to (A.3) that are used in computing the design base shear for the buildings in this study.

### *A.2.3 Load Combinations*

In accordance with NBCC 95, the following loading combinations are used in the design of the frame members:

$$1.25\,D + 1.50\,L$$

$$1.00\,D + 0.50\,L + 1.00\,E$$

$$1.00\,D + 0.50\,L - 1.00\,E \qquad \text{(A.4)}$$

$$1.00\,D + 1.00\,E$$

$$1.00\,D - 1.00\,E$$

where $D$ is the dead load, $L$ is the live load due to occupancy and $E$ is the live load due to earthquake. Loading pattern for live loads and live load reduction factors were not taken into consideration in the design process.

## A.3 Analysis Procedure for Design of the Buildings

### *A.3.1 General Modelling Assumptions*

The effect of slab on the stiffness of beams is accounted for in the calculations. The effective flange width for the beams T-section is assumed to be 1250mm to satisfy the Clause 10.3.3 of CSA A23.3-94.

To account for cracking, the flexural rigidity of the beams and columns are reduced to the levels proposed by Paulay and Priestley (1992). The flexural rigidity of the beams is assumed to be 0.35 of their gross section value. The flexural rigidity of the columns is assumed to be 0.70 of their gross section value. These reduction factors for

flexural rigidity of beams and columns are exactly the values suggested in the Clause 10.14.1 of CSA A23.3-94 and also in agreement with the explanatory notes N21.2.2.1 and N21.2.2.2 of this standard.

Rigid end zones are not considered for the beams and columns. Paulay and Priestley (1992) strongly recommended that no allowance for rigid end regions be made in the lateral force analysis of ductile frames. There are two reasons for this recommendation. First the assumption of rigid part in members leads to some increase of flexural stiffness of both beam and columns, however since it is the relative stiffness of beams and columns rather than the absolute stiffness that affects the force distribution, the rigid end region modelling will not influence the computed member forces. Second, because under earthquake actions the joints are subjected to high shear stresses, resulting in diagonal cracking and significant shear deformation within the joint region. As a consequence of these and also possibility of bond slip of the flexural reinforcement within the joint, total joint deformations can be considerable. To account for the flexibility of joints, the beam and column joint is modelled as a point.

### *A.3.2 Height-Wise Distribution of the Design Lateral Loading*

The computed design base shear for the buildings is distributed through the height of the buildings based on the following distribution formula suggested by NBCC 1995:

$$F_x = \frac{(V - F_t) W_x h_x}{\sum_{i=1}^{n} W_i h_i} \qquad \text{(A.5)}$$

where:

$F_x$ = lateral force applied to level x;

$V$ = the total lateral seismic force;

$F_t$ = portion of V to be concentrated at the top of the structure;

$$= \begin{cases} 0 & \text{if } T \le 0.7\,\text{s} \\ 0.07TV & \text{otherwise} \end{cases}$$

$W_i, W_x$ = that portion of W which is assigned to level i or x respectively;

$h_i, h_x$ = the height above the base (i = 0) to level i or x respectively;

$n$ = total number of storeys;

If $T > 0.7$s, a portion of the design base shear is concentrated at the top of the building in an attempt to accommodate higher mode effects on the force distribution. For the buildings considered in this study, they have periods equal to or less than 0.7. Therefore $F_t$ is equal to zero. The distribution of the lateral seismic design forces for the buildings are shown in Table A.4.

### *A.3.3 Effects of Geometric Nonlinearity*

The effects of geometric nonlinearity should be considered in the design of moment-resisting frames. The geometric effects can be decomposed into two types. One is lateral drift effect (also called P-Δ effect) and the other is member stability effect. CSA A23.3-94 has separate provisions to account for these two types of geometric effects in design (Clauses 10.15.3 and 10.16.3).

The P-Δ effect increases design moments for both beams and columns. CSA A23.3-94 allows the use of a second-order analysis to evaluate the P-Δ effect. Several iterative solution techniques are available for this purpose. However, these iterative

methods are not appropriate for dynamic analysis. In the dynamic analysis of this study, a linearised solution will be employed to account for the P-Δ effect. To be consistent with the dynamic analysis, the same procedure is used herein for design of the frames. In this procedure, a geometric stiffness matrix is evaluated from the column axial force due to gravity loading, and the solution to the P-Δ effect is obtained directly without iteration. The member slenderness effect is considered only for compression members.

## A.4 Design of Reinforced Concrete Members

In this study, only flexural reinforcement is designed for the structural members in the buildings. The design of transverse reinforcement is not considered. It is assumed that shear strength at all sections along the members is designed to be higher than the shear corresponding to maximum flexural strength at the member plastic hinges. The factored beam design moments are obtained at column faces from elastic static analyses of the frames under different load combinations described previously. The factored column design moments are determined based on the weak beam-strong column criterion.

The column design moments are related to the beam moment capacities by considering the equilibrium of each beam-column joint, coupled with a column overstrength factor. The obtained column design moments are further amplified to account for slenderness effect. Some considerations for the design of beams and columns are given in the following sections.

### *A.4.1 Beam Design*

The flexural reinforcement for the beams is determined based on the CSA A23.3-

94 procedure. The factored beam moments obtained from the load combinations as described above are used as design moments for the beams. At each storey level, the computed moments at the two ends of the two exterior bay beams are very close to those at the two ends of the interior bay beam. Therefore, the maximum moment at each storey level is used in the design of all three beams. The use of the same design moment at either side of interior columns avoids termination and anchorage of beam bars at interior beam-column joints in which a congestion of reinforcement may create construction difficulties.

CSA A23.3-94 allows moment redistribution for continuous beams (Clause 9.2.4.). This redistribution has minor effect on the final design moments for the beams because the beams design in this study is controlled by seismic loading. Therefore no redistribution is considered in the final design of the beams in the buildings.

A lower bound is imposed in determining the positive design moments at the beam ends. This lower bound is recommended by Clause 21.3.2.2 of CSA A23.3-94 and given as follows:

$$M_b^+ \geq 0.5\left|M_b^-\right| \tag{A.6}$$

where $M_b^+, M_b^-$ are positive and negative beam design moment at a support section. This lower bound intends to allow for unexpected deformations and moment redistribution from severe earthquake loading and to ensure that the section displays adequate ductility.

In the determination of the flexural reinforcement for the beams, the contribution of reinforcing bars in the slab to the negative moment capacity is neglected.

### *A.4.2 Column Design*

The column design moments are derived from the beam moment capacities by considering the equilibrium condition for each beam-column joint. A column over-strength factor is used in the equilibrium relationships to assure that strong column-weak beam condition is satisfied. The following formula from Clause 21.4.2.2 of CSA A23.3-94 defines the criterion:

$$\sum M_{rc} \geq 1.1 \sum M_{nb} \tag{A.7}$$

where:

$\sum M_{rc}$ = sum of the factored flexural resistance of columns in the joint

$\sum M_{nb}$ = sum of the nominal flexural resistance of beams in the joint

The column design moments are further amplified to account for member stability effect in conformance with Clause 10.15.3 of CSA A23.3-94.

The maximum and minimum design axial forces for the columns are determined from the elastic static analyses of the frames under the load combinations. The columns are designed based on the most critical combination of design bending moment and axial force. The column design charts suggested by Canadian Portland Cement Association (CPCA 1995) are used to determine the reinforcement ratio on the basis of the critical combination.

At each joint, the column section immediately above or below the joint is designed for its own critical combination of design bending moment and axial force, and the larger amount of reinforcement obtained is used for both columns. The use of the same reinforcement above and below joint avoids the termination and anchorage of

column longitudinal steel bars within the joint. During earthquake, moments at the ends of columns usually are larger than other sections in the column. Therefore it is better not to end or anchor the column longitudinal bars within the joint. All column steel bar splices occur near mid-column height where bending moment is relatively small.

Table A.1. Material Properties

| | |
|---|---|
| Compressive strength of concrete | $f_c'$= 30 Mpa |
| Yield strength of reinforcement | $f_y$= 350 MPa |
| Modulus of elasticity for reinforced concrete | E= 27000 Mpa |
| Unit weight of reinforced concrete | $w_c$= 24 kN/m$^3$ |

Table A.2. Design Gravity Loads (kN/m$^2$)

| | | Dead Load | Live Load |
|---|---|---|---|
| Floor | Weight of Slab, Beam and Column | 3.7 | |
| | Partition Loading | 1.0 | |
| | Mechanical Service Loading | 0.5 | |
| | Total† | 5.2 | 2.4 |
| Roof | Weight of Slab, Beam and Column | 3.6 | |
| | Roof Insulation | 0.5 | |
| | Mechanical Service Loading | 1.0 | |
| | Total† | 5.1 | 1.0 |

† For simplicity in design, a dead load equal to 5.2 kN/m$^2$ and a live load equal to 2.4 kN/m$^2$ is assumed for the roof and all the floors. The mass for floors and the roof assumed to be equal to 215 kN.s$^2$/m .

Table A.3. Factors for calculation of the design base shear

| Parameter | Equation number | Reference in Code (NBCC 95) | Value |
|---|---|---|---|
| U | A.1 | 4.1.9.1.(4) | 0.6 |
| R | A.1 | 4.1.9.1.(8) | 4.0 |
| v | A.2 | Appendix C | 0.3 |
| T | A.3 | 4.1.9.1.(7) | 0.7 |
| S | A.2 | 4.1.9.1.(6) | 1.79 |
| I | A.2 | 4.1.9.1.(10) | 1.0 |
| F | A.2 | 4.1.9.1.(11) | 1.0 |
| W | A.2 | 4.1.9.1.(2)&(12) | 14764.05 kN |
| $V_e$ | A.1&A.2 | 4.1.9.1.(5) | 7928.29 kN |
| V | A.1 | 4.1.9.1.(4) | V = 0.081W = 1189.25 kN |

Table A.4. Distribution of the lateral seismic design forces of the Buildings

| Floor | Seismic Design Load (kN) |
|---|---|
| 7 | 297.31 |
| 6 | 254.84 |
| 5 | 212.37 |
| 4 | 169.89 |
| 3 | 127.42 |
| 2 | 84.95 |
| 1 | 42.47 |

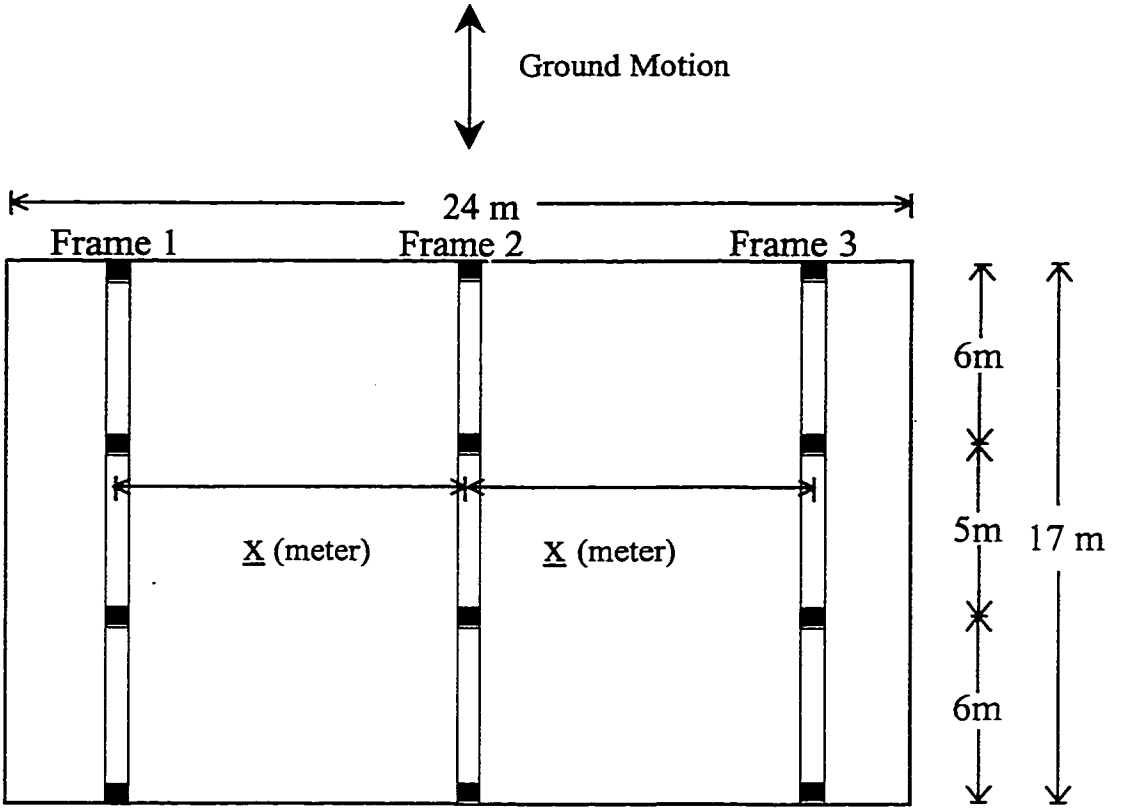


Figure A.1. The plan of Building AxAxA

This page is intentionally left blank.

# APPENDIX B

# DESIGN FOR CODE TORSIONAL PROVISIONS

This appendix explains the changes in design of buildings due to the use of code torsional provisions. Three different design procedures are explained here. They are static torsional provisions of NBCC 1995, static torsional provisions of UBC 1997, and finally design based on dynamic analysis. These procedures are explained in the following sections.

## B.1 Design for Static Torsional Provisions of NBCC 1995

According to the NBCC 1995, the torsional effect should be included in design by application of torsional moments. The magnitudes of the torsional moments, about a vertical axis of the building, shall be derived for each of the following load cases considered separately (Clause 4.1.9.1.(28)):

$$T_x = F_x(1.5e_x + 0.1D_{nx}) \quad \text{(B.1)}$$

$$T_x = F_x(1.5e_x - 0.1D_{nx}) \quad \text{(B.2)}$$

$$T_x = F_x(0.5e_x + 0.1D_{nx}) \quad \text{(B.3)}$$

$$T_x = F_x(0.5e_x - 0.1D_{nx}) \quad \text{(B.4)}$$

where $F_x$ is the design lateral floor force at each level and $D_{nx}$ is the plan dimension of the building at level x perpendicular to the direction of seismic loading being considered. $e_x$ is the distance measured perpendicular to the direction of seismic loading between centre of mass and centre of rigidity at the level being considered. The

term $0.1D_{nx}F_x$ represents the accidental torsional moment applied at each level. Accidental torsion moments are intended to account for the possible additional torsion arising from variations in the estimates of the relative rigidities, uncertain estimates of dead and live loads at the floor levels, addition of wall panels and partitions after completion of the building, variation of the stiffness with time, and inelastic or plastic action and finally the effects of possible torsional motion of the ground. (NBCC Commentaries, 1995)

Each element of the building is designed for the most severe effect of the above load cases. The coefficients "1.5" and "0.5" are to allow for dynamic effects such as higher mode contributions.

To calculate the values of torsional moments from Equations (B.1 to B.4), first the distance between centre of mass and centre of rigidity at every level of the building ($e_x$) should be found. The locations of centres of rigidity can be determined by a procedure given in a paper by Tso (1990). There is an alternative method (Goel and Chopra 1993) that does not need the explicit calculation of $e_x$. The effect of $e_x$ in this method is implicitly taken care of, by considering several extra load cases. Instead of using the Equations (B.1 to B.4), the following procedure is used (NBCC Commentaries 1995). The building shall be analysed subjected to three load cases. Load case 1 consists of applying the design floor forces at the mass centres (CM). Load case 2 consists of applying design forces at CM, but restraints are imposed to prevent floor rotations about a vertical axis. Load case 3 consists of applying torques equal to $0.1D_{nx}F_x$ in the same direction at each floor. Denoting the design parameters of interest (forces or deformation)

that correspond to these load cases as $r_1$, $r_2$ and $r_3$, respectively, implementation of Equations (B.1 to B.4) is achieved by using the combinations "$1.5r_1 - 0.5\ r_2 + r_3$" or "$0.5r_1 + 0.5\ r_2 + r_3$" whichever gives the more severe effect.

## B.2 Design for Static Torsional Provisions of UBC 1997

The static design procedure of UBC 1997 is consists of three steps. The first step is to check for torsional irregularity. According to Table 16-M of UBC 1997, "torsional irregularity shall be considered to exist when the maximum storey drift, computed including accidental torsion at one end of the structure transverse to an axis is more than 1.2 times the average of the storey drifts of the two ends of the structure". Therefore, the static design loads are applied at the points on the floors that are displaced from centres of mass in each direction a distance equal to five percent of the building dimension. As an example, the results of these two load cases for a building are shown in column (2) and column (3) of Table B.1. Since the values of $\left(\frac{max.\ storey\ \ drift}{avg.\ storey\ \ drift}\right)$, at the second column of Table B.1, are larger than 1.2 the building is torsionally irregular in this case. It is important to notice that this check in UBC is not meant to be used as a measure for excluding a building from static design approach, but the purpose of check is only to increase the value of accidental eccentricity for that case as will be described subsequently. Therefore for a building that is marked as 'torsionally irregular' by the check of step 1, still the same equations of static method (for design eccentricity) are used but with some adjustment in its accidental eccentricity term as will be described in the third step. The second step of the UBC procedure is the calculation of amplification

factors for the accidental torsion at each level for the torsionally irregular buildings. The amplification factor, $A_X$, is determined from:

$$A_x = \left[\frac{\delta_{max}}{1.2\delta_{avg}}\right]^2 \qquad \text{(B.5)}$$

Where:

$\delta_{max}$ = *the maximum displacement at level x*

$\delta_{avg}$ = *the average of the displacements at the extreme points of the structure at level x*

The value of $A_X$, according to code, need not exceed 3. Columns (4) and (5) of Table B.1 show two sets of values for $A_X$ resulted from analysing the building subjected to the static design loads at two locations of (CM+0.05b) and (CM-0.05b). The maximum values of $A_X$ at each level will be used in design and they are shown in column (6) of Table B.1. One should pay attention that the check for torsional irregularity in UBC (step 1) is based on drifts but the calculation of amplification factors, $A_X$ (step 2) is based on displacements.

The third and final step in UBC procedure is the calculation of horizontal torsional moments to be incorporated with the design forces of the building. The effects of horizontal moments can be included in design by application of floor torques. The magnitudes of the floor torques are given by the floor forces times the design eccentricity, $e_d$. The design eccentricities in UBC are sum of structural eccentricity and the amplified accidental eccentricity:

$$e_d = e + A_x(0.05b) \qquad \text{(B.6)}$$

$$e_d = e - A_x(0.05b) \tag{B.7}$$

Where "e" represents the structural eccentricity and "b" is the plan dimension of the building perpendicular to the direction of the lateral forces. In some buildings the applied floor torques can cause reduction in the design lateral loads on one of the edge frames. Although in UBC 1997, unlike some previous editions, it is not explicitly stated that "negative shears shall be neglected" but it is believed that the intention of the code is in omitting the effects of the negative shears. Therefore in designing buildings in this study no reduction is allowed in design forces of edge frames.

### B.3. Design for Torsion Based on Dynamic Analysis

The building codes usually suggest the use of dynamic analysis in design of buildings if there is a possibility that static analyses lead to non-conservative design values for the members. Design procedure based on dynamic analysis has three steps. Step 1 involves conducting a response spectral analysis of the building. In this study, the 5% damped design spectrum of NBCC 1995 is used for the response spectrum analysis. Then in step 2 the base shear calculated from modal combination in response spectrum analysis is scaled to the value of the static base shear obtained from the static base shear formula. Step 3 is the consideration of the effects of accidental torsion in design. In this study the accidental torsion is incorporated by applying static torsional moments on the building and combining the results from this loading with the results of response spectrum analysis.

Table B.1. Calculation of UBC amplification factor

| (1) | (2) | (3) | (4) | (5) | (6) |
|---|---|---|---|---|---|
| | $\frac{max.\ storey\ drift}{avg.\ storey\ drift}$ | | $A_x = \left[\frac{\delta_{max}}{1.2\delta_{avg}}\right]^2$ | | |
| **Floor** | **Load at** (CM+0.05b) | **Load at** (CM-0.05b) | **Load at** (CM+0.05b) | **Load at** (CM-0.05b) | $\mathbf{A_x}$ |
| 7 | 1.56 | 1.19 | 1.39 | 0.90 | **1.39** |
| 6 | 1.47 | 1.16 | 1.37 | 0.90 | **1.37** |
| 5 | 1.44 | 1.15 | 1.35 | 0.90 | **1.35** |
| 4 | 1.43 | 1.15 | 1.33 | 0.89 | **1.33** |
| 3 | 1.41 | 1.14 | 1.30 | 0.88 | **1.30** |
| 2 | 1.37 | 1.13 | 1.26 | 0.87 | **1.26** |
| 1 | 1.31 | 1.11 | 1.19 | 0.85 | **1.19** |

# APPENDIX C

## EVALUATION OF COMPUTER PROGRAM FOR INELASTIC STATIC AND DYNAMIC ANALYSES

The static and dynamic behaviours of the multi-storey asymmetric buildings, especially in inelastic range, are the main focus of the study reported in this thesis. Therefore a computer program with the ability of performing 3-D inelastic static and dynamic analysis is an essential tool in achieving the goals of this investigation. The program CANNY (Li 1993) has been used for analysis of buildings in this research. The program has gone through lots of evaluation, modification and improvement in the past few years along with the progress in this research work. In this appendix, the results of dynamic analyses performed on several example 3-storey buildings using CANNY are compared to responses derived by using other computer programs. Several other aspects of CANNY are also have been checked but will not be reported here, such as analysis under gravity load, inelastic static analysis and calculation of mode shapes and frequencies.

The program CANNY has also been evaluated by other researchers. Ayala et al. (1996) compared the observed damages in a building after 1985 Michanocan Earthquake with the results of inelastic dynamic analyses using CANNY. They reported (Ayala et al. 1996) that comparison of the performance parameters obtained from CANNY with the observed damage shows good correlation.

## C.1. The Example Buildings

The four example buildings for this comparison are all 3-storey with a plan as shown on Figure C.1. The buildings have three identical frames with uniform storey height of 3 meters. The design of buildings is based on the procedure explained in Appendix A. The buildings are designed for a base shear equal to 8.5% of the weight of the buildings. The first building is a symmetric building. It is assumed that it remains elastic during the earthquake. The second building is also assumed to be elastic but there is an eccentricity equal to 15% of the width of building between centres of mass and rigidity of the floors. The third and fourth buildings will have inelastic response to the earthquake. The third building is a symmetric building but the forth building an asymmetric building which has an eccentricity equal to 15% of the width of the building.

## C.2. Results of the Comparison

The 3-storey symmetric-elastic building is analysed by programs DRAIN-2DX, SUPER ETABS, PC-ANSR, DRAIN-TABS and CANNY. Five seconds of El-Centro Earthquake has been used as the ground motion. On Figures C.2a and C.2b, the time history of flexural moments in a beam and column of the buildings are presented. There is very good agreement between the results. The top floor displacement time history of the building is shown on Figure C.3 (a, b, c and d). The figures show that the results of all five programs are in close agreement.

The next step is evaluating the application of CANNY for asymmetric-elastic buildings. Therefore the 3-storey asymmetric-elastic building is analysed, using the

programs SUPER ETABS, PC-ANSR, DRAIN-TABS and CANNY. The time history of the lateral displacement of the top floor of building at its centre of mass and also the time history of top floor rotation are shown cn Figure C.4 (a&b, c&d and e&f). The results of analysis using CANNY shows remarkable similarity to the results of the analyses by SUPER ETABS and DRAIN-TABS. However there is some negligible difference between the results of these three programs with the results of PC-ANSR. Minor differences between the results are expected due to some difference in modelling techniques of these programs such as formulation of the elements, approximation used for effect of P-$\Delta$ and so on.

The next step is evaluating the application of CANNY for symmetric-inelastic buildings. Programs DRAIN-2DX, PC-ANSR, DRAIN-TABS and CANNY are used to analyse the 3-storey symmetric-inelastic building. The time history of the top displacement of the building is shown on Figure C.5 (a, b and c). The figures show that the results of all five programs are in agreement.

The last step is evaluating the application of CANNY for an asymmetric-inelastic building. The 3-storey asymmetric-inelastic building is analysed using the programs PC-ANSR, DRAIN-TABS and CANNY. The time history of the lateral displacement of the top floor of building at its centre of mass and also the time history of top floor rotation are shown on Figure C.6 (a&b and c&d). The results of analysis by CANNY and DRAIN-TABS are similar. However there is some minor difference between the results of these two programs with the results of PC-ANSR. These results show that CANNY has similar accuracy as other commonly used academic programs.

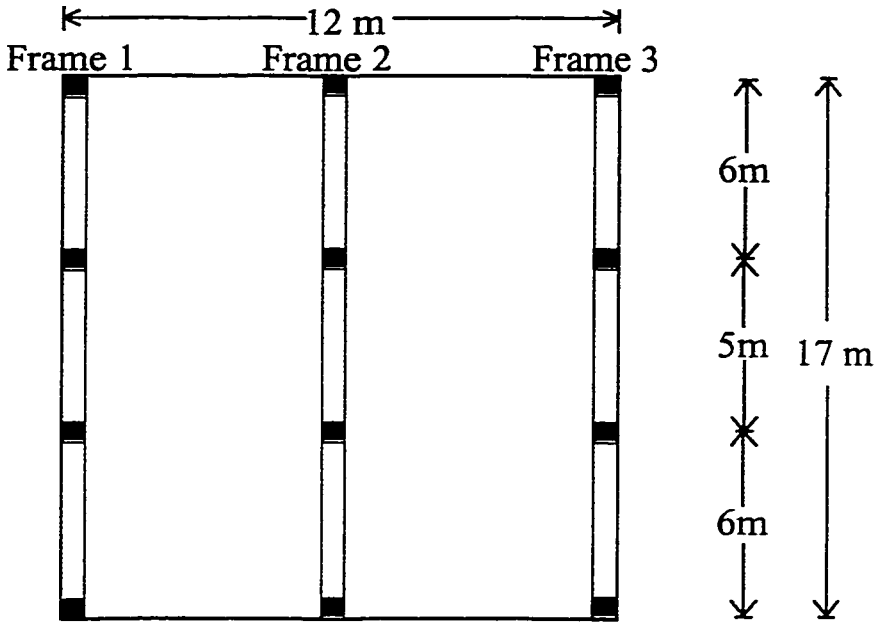


Figure C.1. The plan of the example 3-storey Building

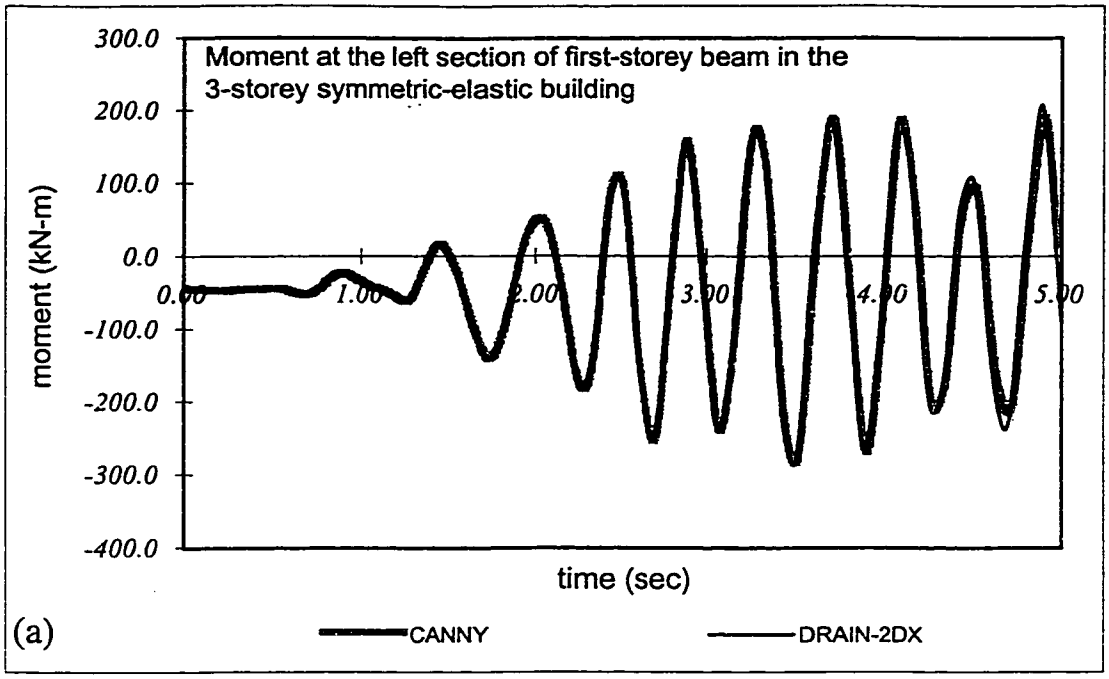


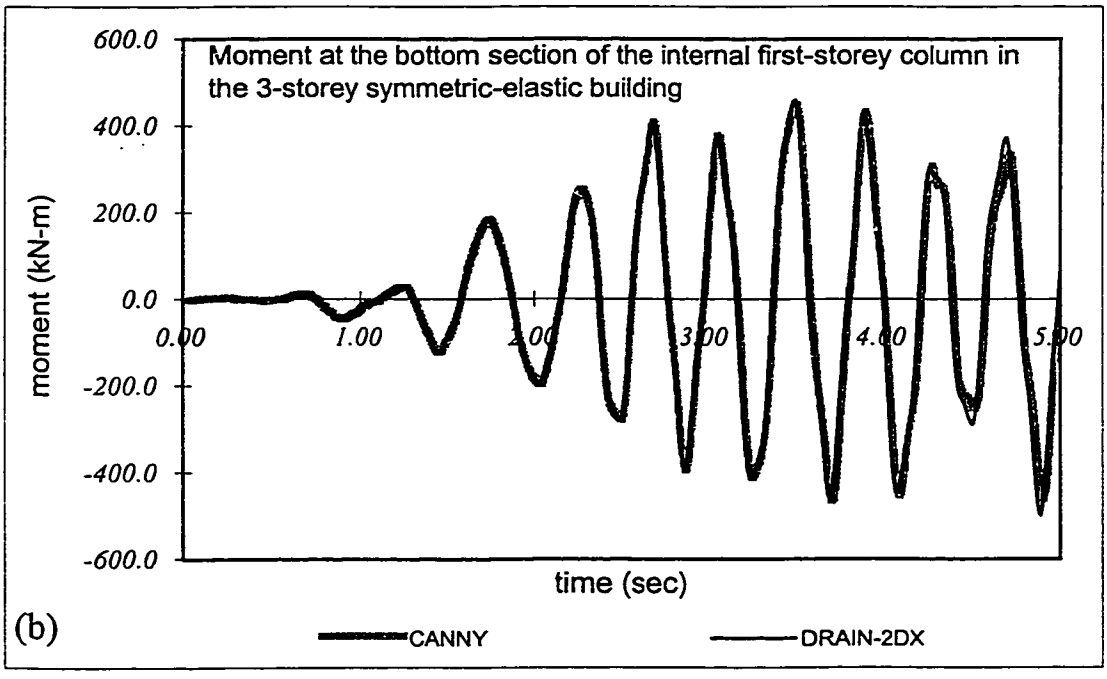


Figure C.2. Response time history comparisons of symmetric-elastic case:
(a) Moment of a beam;
(b) Moment of an interior column.

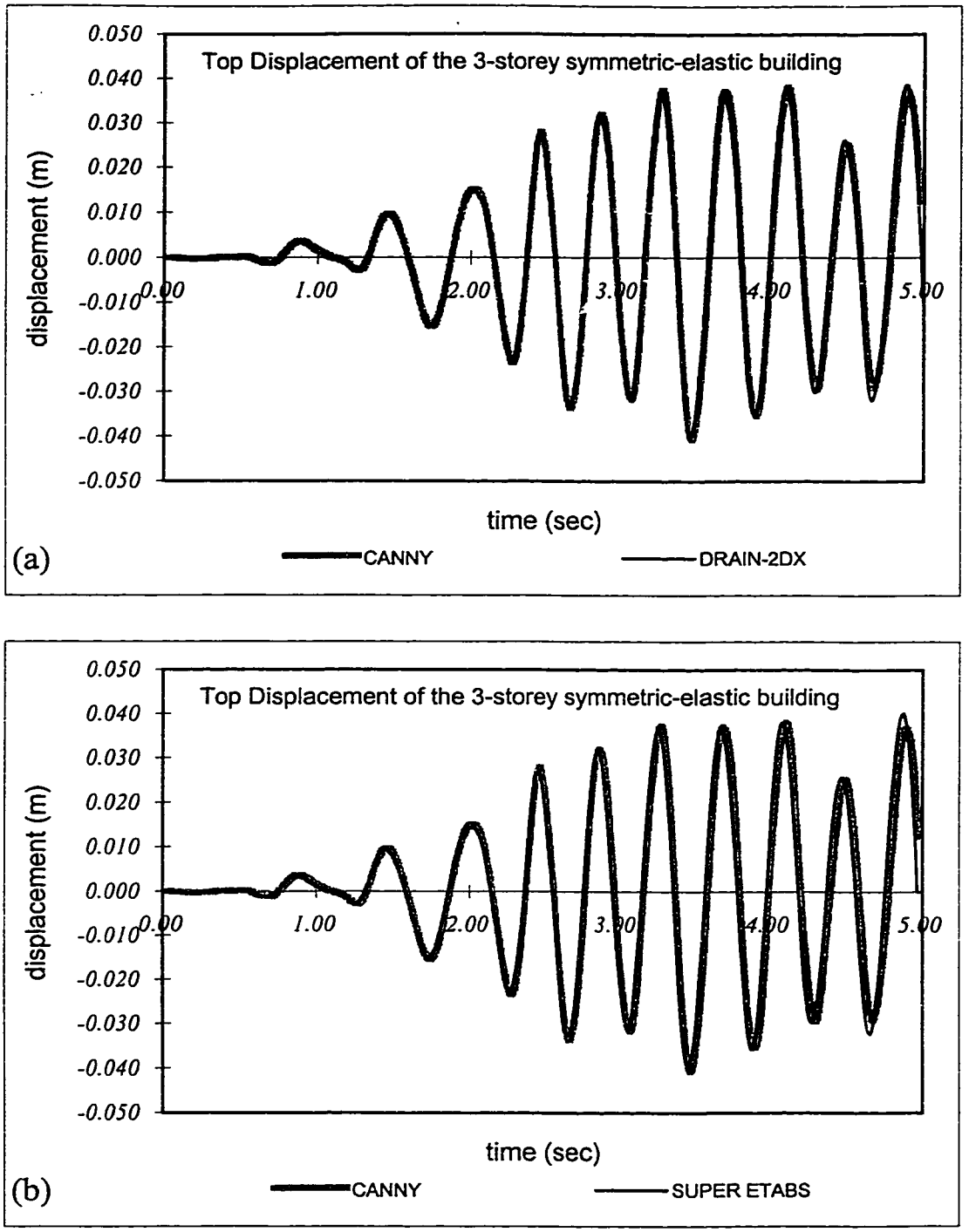


Figure C.3. Top displacement time history comparisons of symmetric-elastic case.

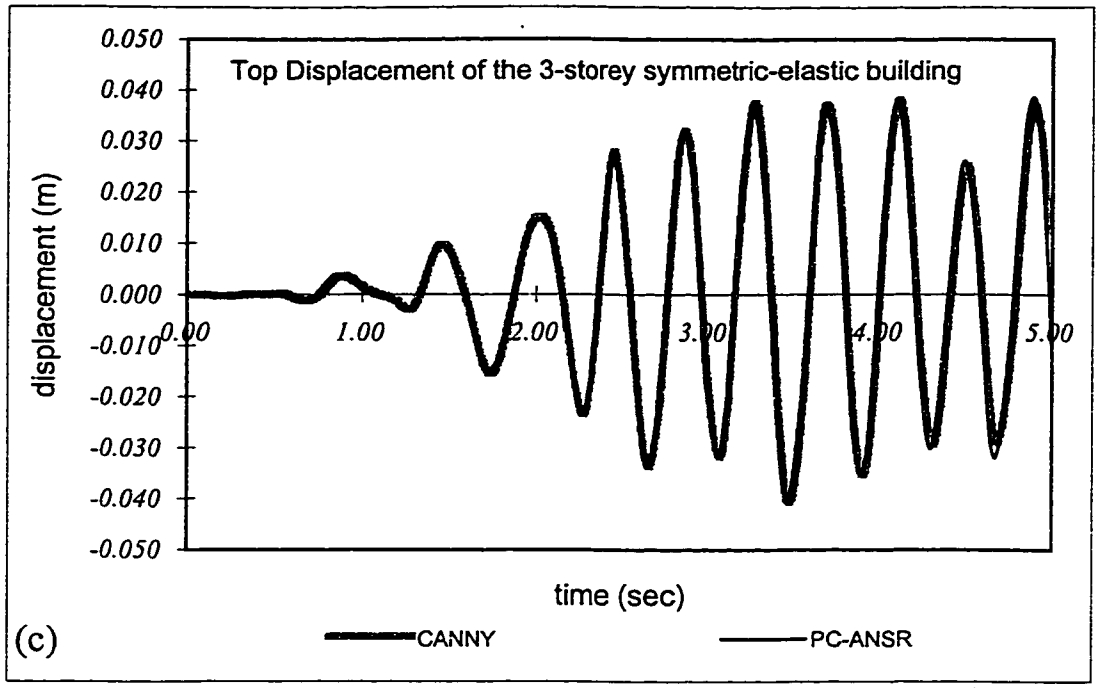


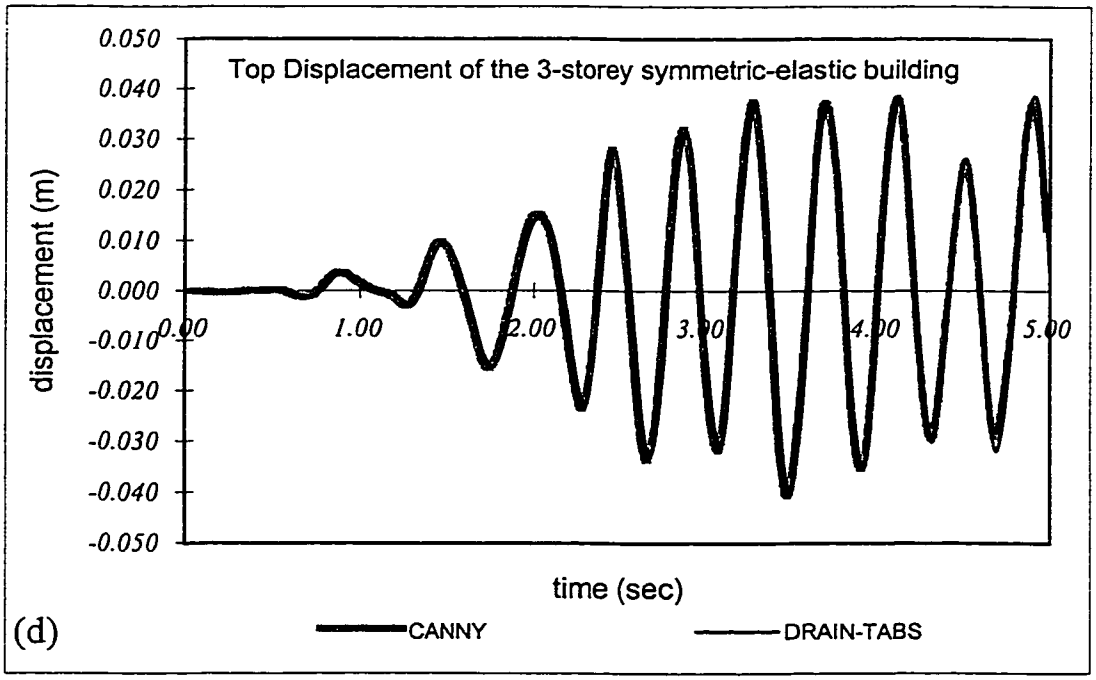


Figure C.3. (cont'd) Top displacement time history comparisons of symmetric-elastic case.

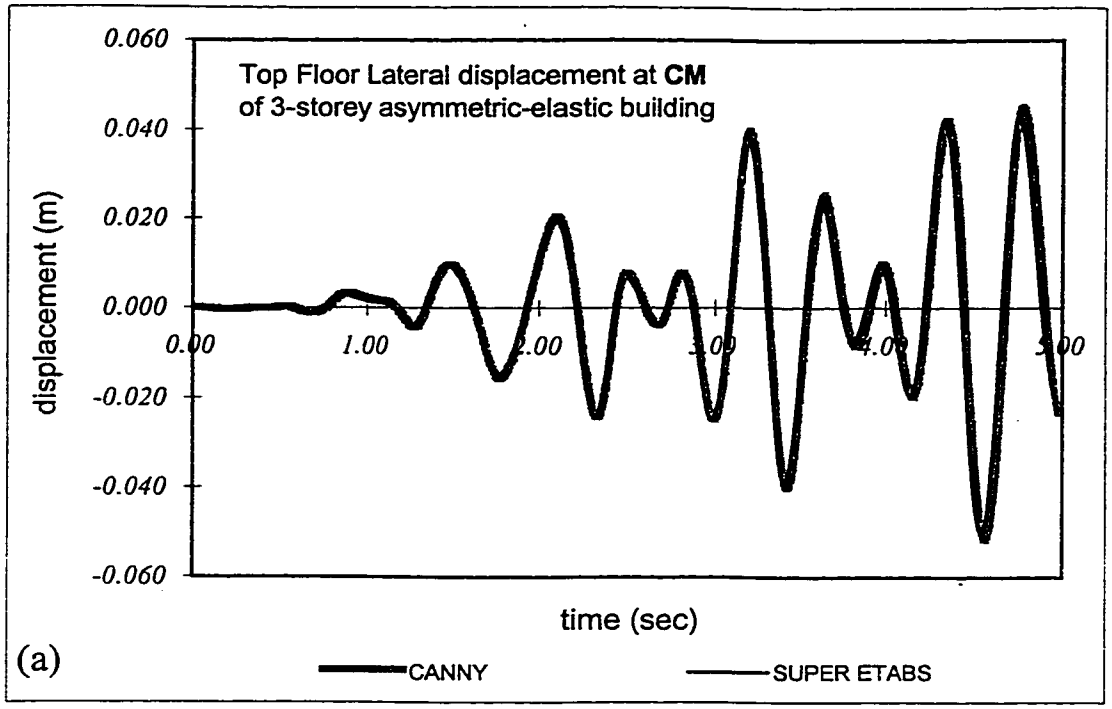


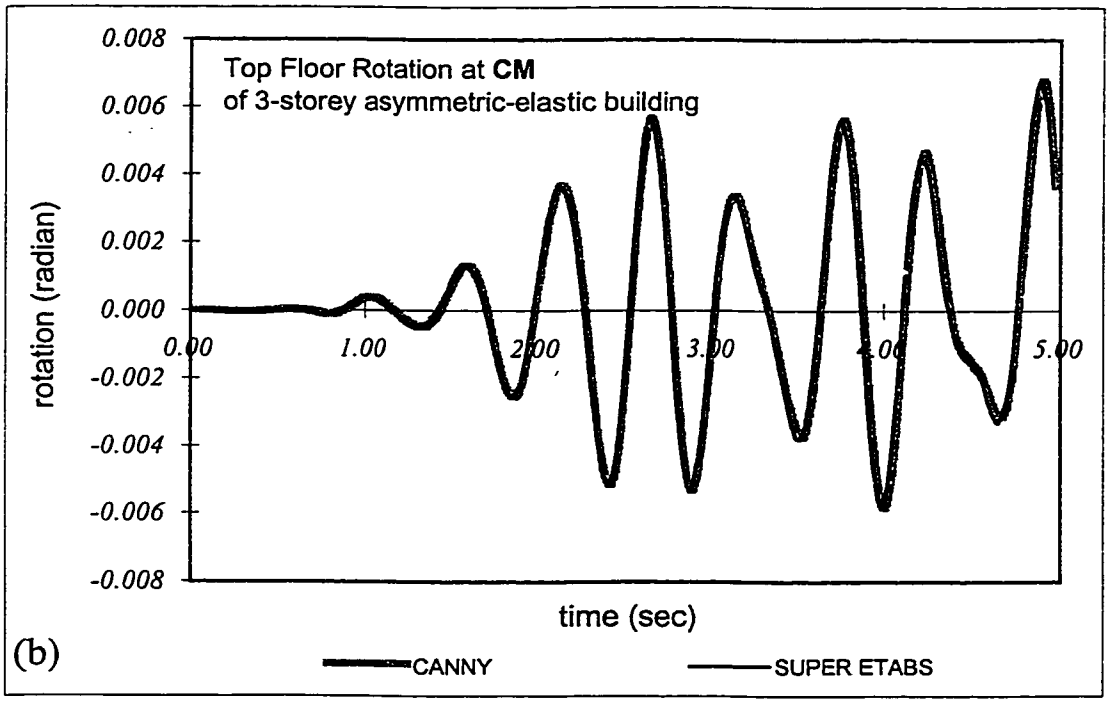


Figure C.4. Top displacement time history comparisons of asymmetric-elastic case.

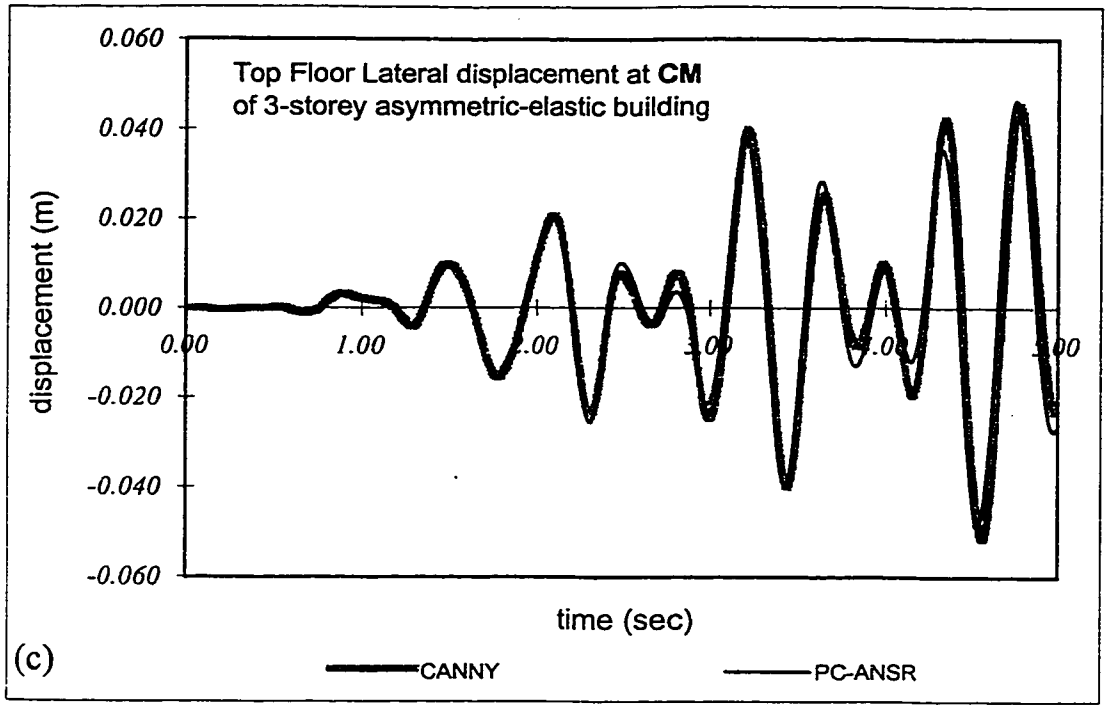


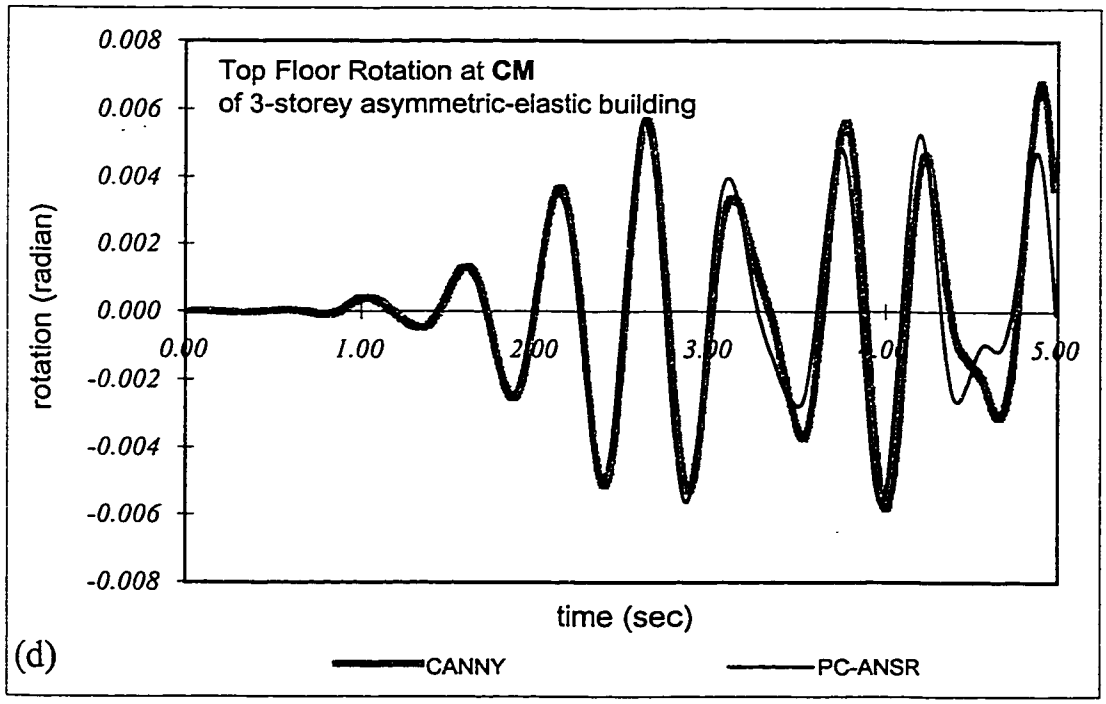


Figure C.4. (cont'd) Top displacement time history comparisons of asymmetric-elastic case.

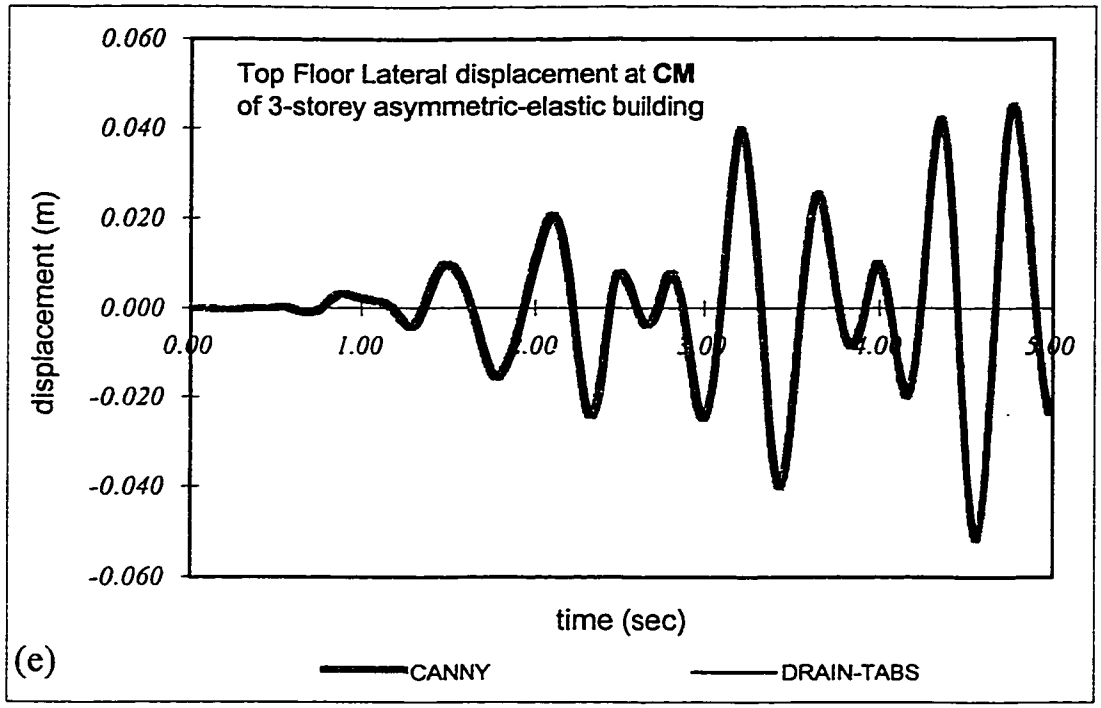


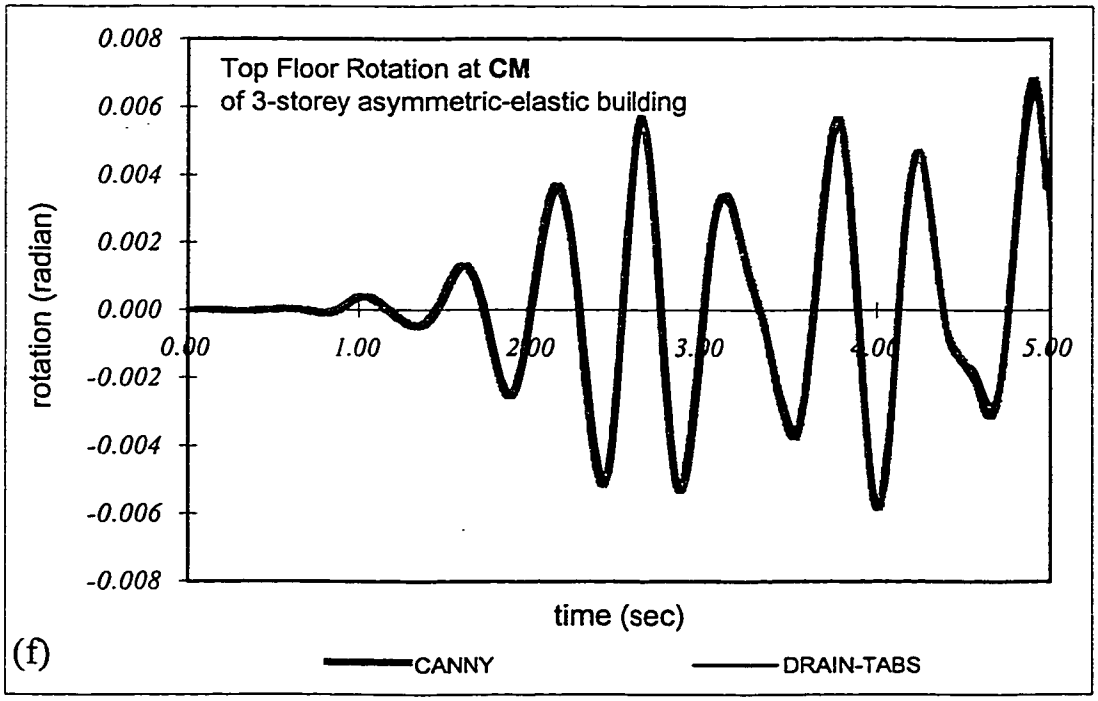


Figure C.4. (cont'd) Top displacement time history comparisons of asymmetric-elastic case.

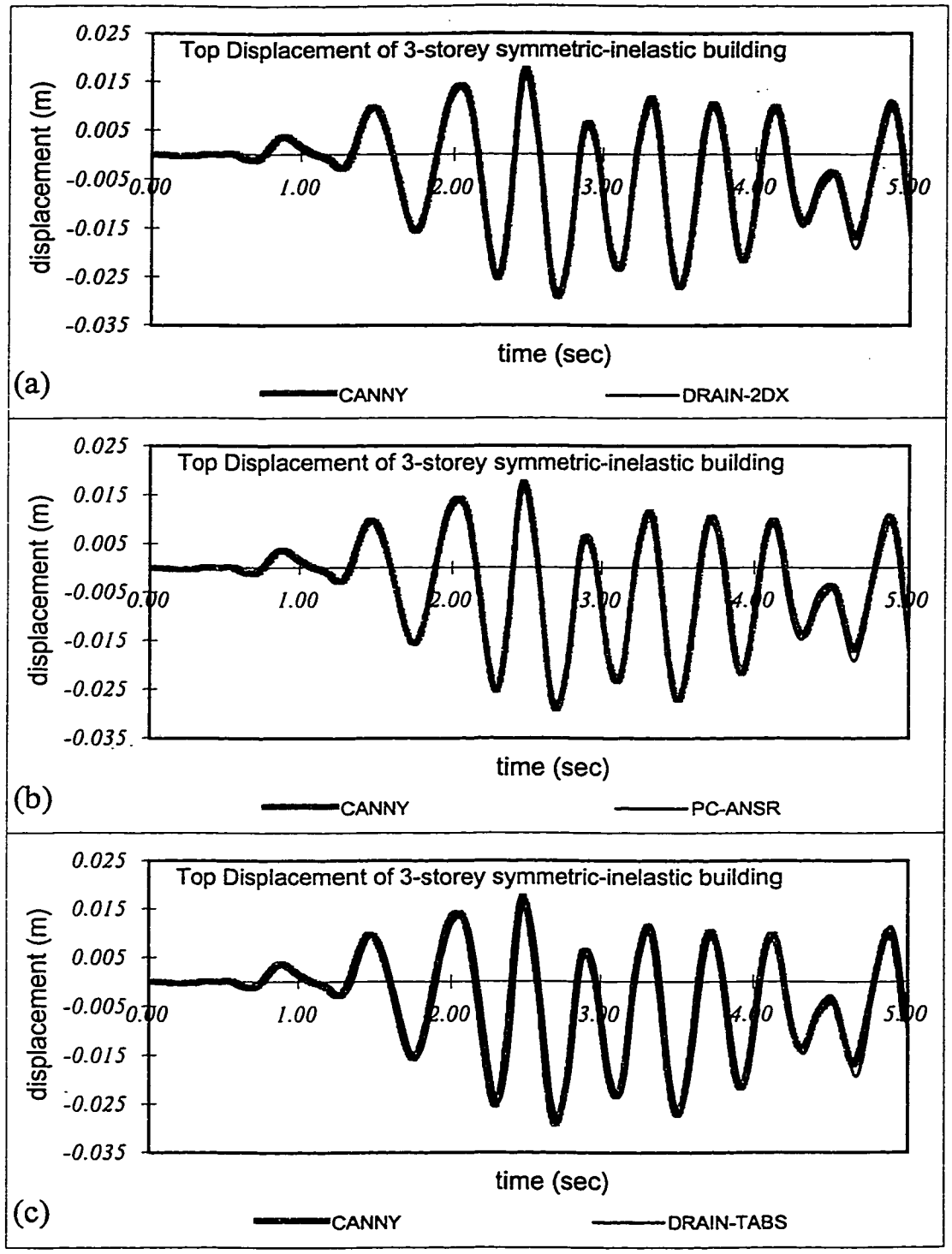


Figure C.5. Top displacement time history comparisons of symmetric-inelastic case.

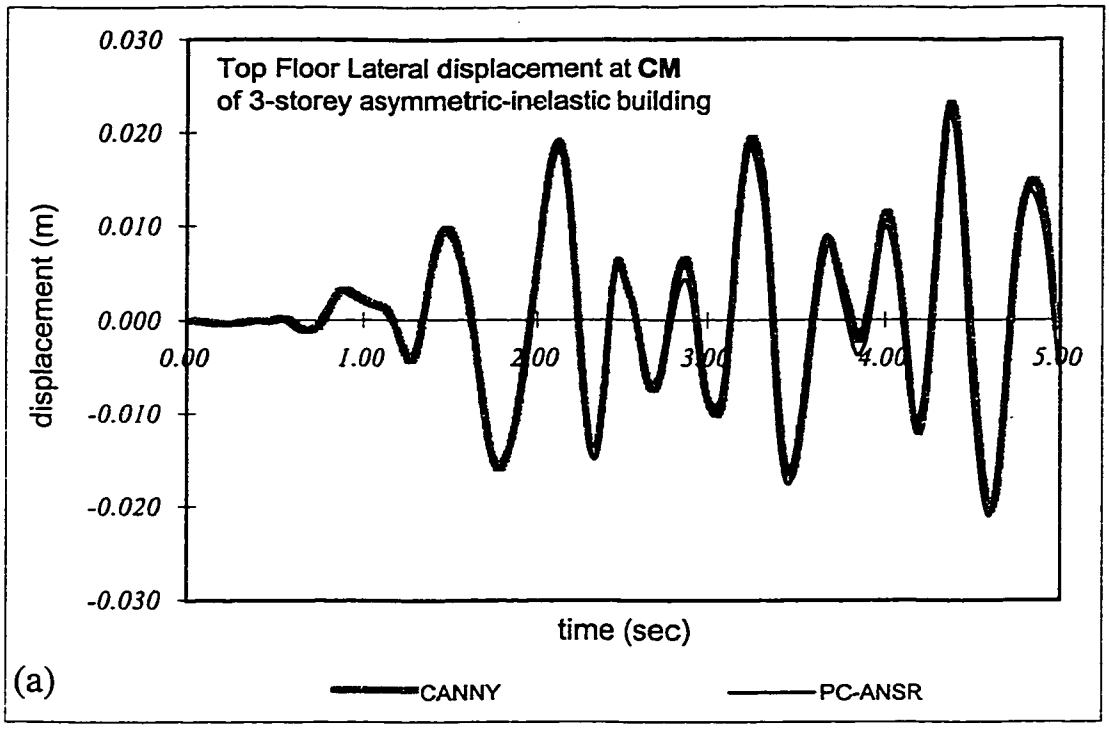


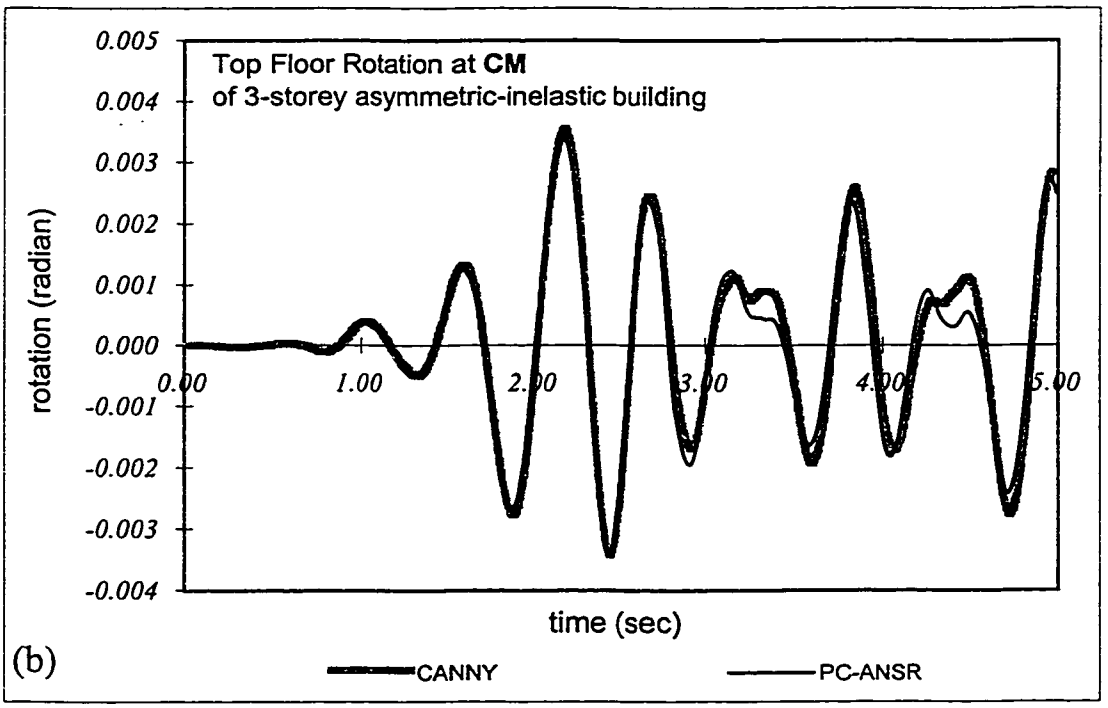


Figure C.6. Top displacement time history comparisons of asymmetric-inelastic case.

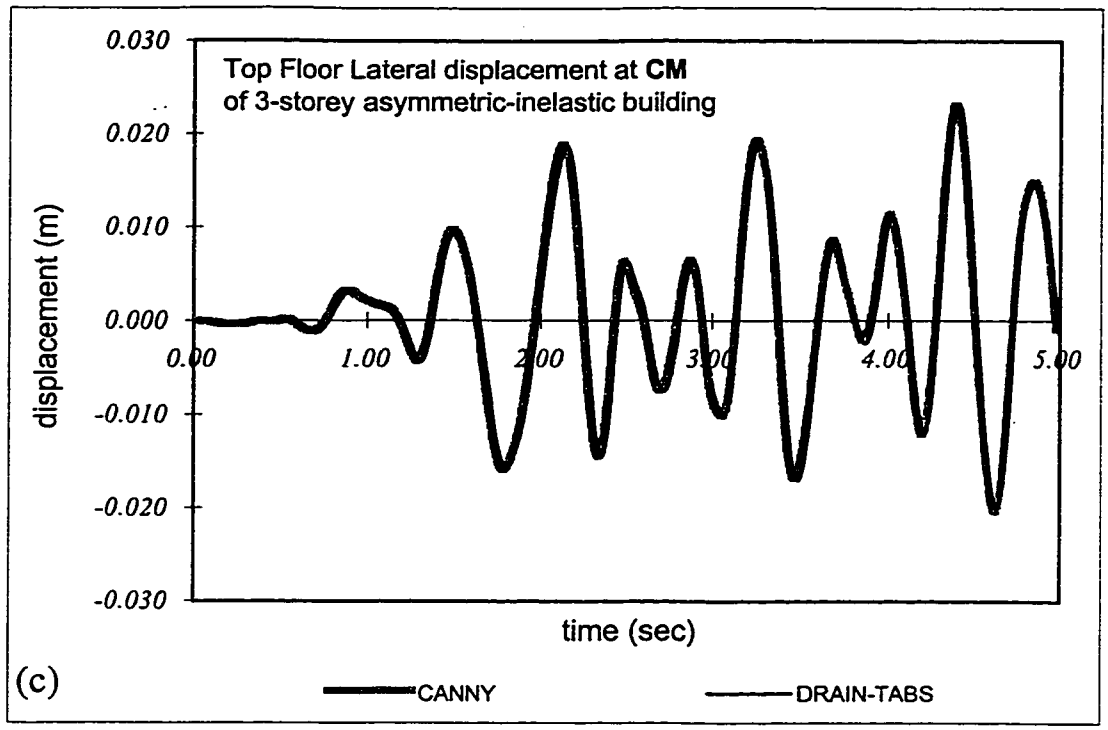


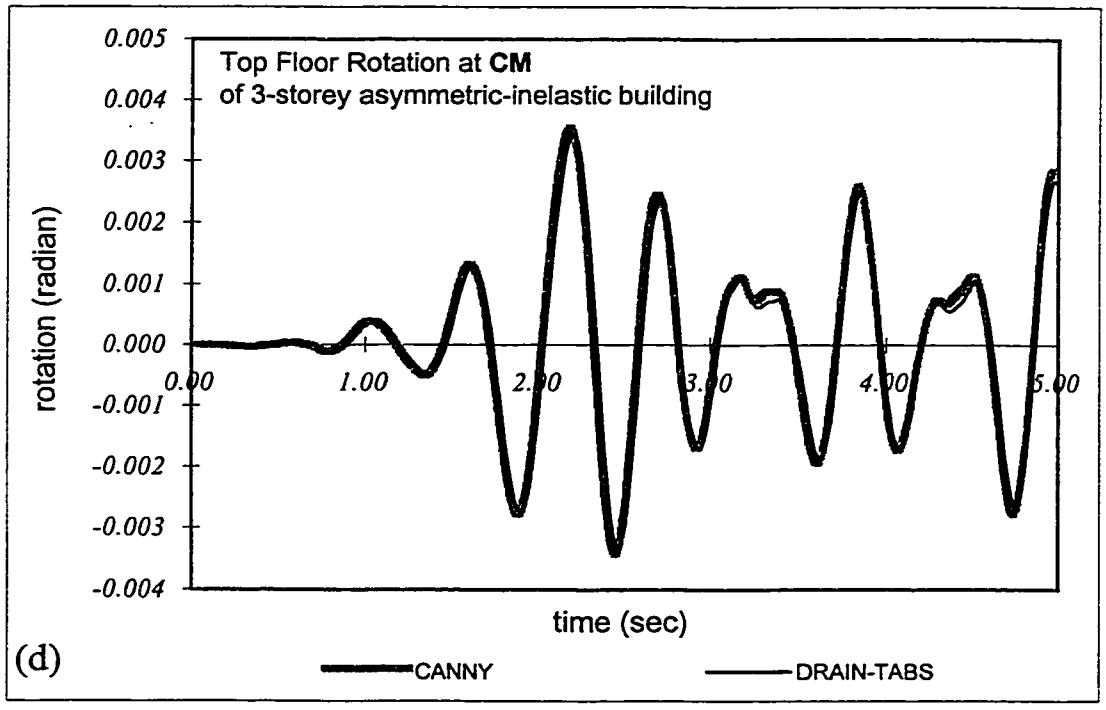


Figure C.6. (cont'd) Top displacement time history comparisons of asymmetric-inelastic case.

This page is intentionally left blank.

# REFERENCES


Allahabadi, R. and G.H. Powell. (1988), "DRAIN-2DX User Guide." Report UCB/EERC-88/06, Earthquake Engineering Research Centre, University of California-Berkeley.

Anderson, J.C. (1989), "Dynamic Response of Buildings." Chapter 3 in the Seismic Design Handbook, edited F. Naeim, New York: Van Nostrand Reinhold.

Applied Technology Council, ATC 33.03, (1995) Guidelines for the Seismic Rehabilitation of Buildings. Redwood City, California: Applied Technology Council.

Applied Technology Council, (1996a), Guidelines for the Seismic Rehabilitation of Buildings, Volume I, Guidelines, and Volume II, Commentary. FEMA 273/274-Ballot Version. Prepared by the Applied Technology Council for the Building Seismic Safety Council; published by the Federal Emergency Management Agency.

Applied Technology Council, ATC-40, (1996b), Seismic Evaluation and Retrofit of Concrete Buildings. Two volumes, Redwood City, California: Applied Technology Council.

Ayala, A.G., Tayebi, A.K. and Ye, X.G. (1996), "Dynamic Response of a Reinforced Concrete Frame Compared with Observed Earthquake Damage", Paper no. 697, Eleventh World Conference on Earthquake Engineering, Acapulco.

Azuhata, T. and Ozaki, M. (1992), "Inelastic Seismic Response of Shear-Type Buildings with Eccentricity", Proceedings of Fifth US-Japan Workshop on the Improvement of Building Structural Design and Construction Practices, San Diego, California, Applied Technology Council, Redwood City, CA, 1994, pp.227-247.

Bazzurro, P. and C.A. Cornell, (1992), "Seismic Risk: Non-linear MDOF Structures." Proc. 10th World Conference on Earthquake Engineering, Madrid, pp.563-568.

Bernal, D. (1992), "Instability of Buildings Subjected to Earthquakes." Journal of Structural Engineering, v.118, pp.2239-2260.

Bertero, R.D. and V.V. Bertero (1992), "Tall Reinforced Concrete Buildings: Conceptual Earthquake-Resistant Design Methodology", Report UCB/EERC-92/16, Earthquake Engineering Research Centre, University of California-Berkeley.

Bertero, R.D. (1995), "Inelastic Torsion for Preliminary Seismic Design", J. Structural Engineering, v.121, no.8, pp.1183-1189.

Biggs, J.M. (1964), Introduction to Structural Dynamics, McGraw-Hill, New York.

Boroschek, R.L., Mahin, S.A. (1992), "Investigation of Coupled Lateral-Torsional Response in Multistorey Buildings", Proceedings of the Tenth World Conference on Earthquake Engineering, 19-24 July 1992, Madrid, Balkema, Rotterdam, v.7, pp.3881-3886.

Bourahla, N. and Blakeborough, A. (1994), "Shaking Table Testing of Torsionally Coupled Knee Braced Frames", Proceedings of the Fifth US National Conference on Earthquake Engineering, Chicago, Illinois, Earthquake Engineering Research Institute, Oakland, CA, 1994, v.II, pp.773-782.

Canadian Standard Association. CSA Standard A23.3-94 (1994) Design of Concrete Structures. Rexdale, Ontario, Canada.

Chandler, A.M. and Duan, X.N. (1993), "A Modified Static Procedure for the Design of Torsionally Unbalanced Multistorey Frame Buildings", J. Earthquake Engineering & Structural Dynamics, v.22, pp.447-462.

Cheng, F.Y. (1981), "Inelastic Analysis of 3-D Mixed Steel and Reinforced Concrete Seismic Building Systems" Computers & Structures, v.13, no.1-3, pp.189-196.

Chopra, A.K. (1995), Dynamics of Structures: Theory and Applications to Earthquake Engineering. Prentice Hall, Upper Saddle River, NJ.

Corderoy, H.J.B. and Thambiratnam, D.P. (1993), "Microcomputer Analysis of Torsionally Coupled Multistorey Buildings for Earthquakes", Computers & Structures, v.46, no.4, pp.593-602.

Correnza, J.C., Hutchinson, G.L. and Chandler, A.M. (1994), "Effect of Transverse Load-Resisting Elements on Inelastic Earthquake Response of Asymmetrical-Plan Buildings." J. Earthquake Engineering and Structural Dynamics, v.23, pp.75-89.

Cruz, E.F. and Cominetti, S. (1992), "Nonlinear Response of Buildings, A Parametric Study", Proceedings of the Tenth World Conference on Earthquake Engineering, Madrid, Balkema, Rotterdam, v. 7, pp.3663-3666.

De la Llera, J.C., Chopra, A.K. (1995a), "A New Analysis Procedure for Accidental Torsion", ASCE, (New York), Restructuring: America and Beyond; Proceedings

of Structures Congress XIII, pp.427-430.

De la Llera, J.C., Chopra, A.K. (1995b), "Understanding the Inelastic Seismic Behaviour of Asymmetric Plan Buildings", J. Earthquake Engineering & Structural Dynamics, v.24, pp.549-572.

De la Llera, J.C., Chopra, A.K. (1995c), "A Simplified Model for Analysis and Design of Asymmetric-Plan Buildings", J. Earthquake Engineering & Structural Dynamics, v.24, pp.573-594.

De la Llera, J.C., Chopra, A.K. (1996), "Inelastic Behaviour of Asymmetric Multistory Buildings", J. Structural Engineering, v.122, no.6, pp.597-606.

Dempsey, K.M. and Tso, W.K. (1982), "An alternative path to seismic torsional provisions", J. of Soil Dynamics and Earthquake Engineering, v.l, no.1, pp.3-10.

De Stefano, M., Faella, G. and Realfonzo, R. (1995), "Seismic Response of 3D RC Frames: Effect of Plan Irregularity", In A.S. Elnashai (ed.) European Seismic Design Practice: Research and Application, Chester, UK, Balkema, Rotterdam.

Duan, X.N. and Chandler, A.M. (1993), "Inelastic Seismic Response of Code-designed Multistorey Frame Buildings with Regular Asymmetry", J. Earthquake Engineering and Structural Dynamics, v.22, pp.431-445.

Eisenberger, M. and Rutenberg, A. (1986), "Seismic Base Isolation of Asymmetric Shear Buildings", Engineering Structures, v.8, pp.2-8.

Esteva, L. (1987), "Earthquake Engineering Research and Practice in Mexico after 1985 Earthquake", Bulletin of the New Zealand National Society for Earthquake Engineering, v.20, pp.159-200.

Fajfar, P. and P. Gaspersic. (1996), "The N2 Method for the Seismic Damage Analysis of RC Buildings." Journal of Earthquake Engineering and Structural Dynamics, v.25, pp.31-46.

Fajfar, P. and V. Kilar. (1996), "Study of Inelastic Behaviour of Asymmetric and Set-Back Buildings under Monotonically Increasing Lateral Loading." Proc. European Workshop on the Seismic Behaviour of Asymmetric and Set-Back Structures (editors R. Ramasco and A. Rutenberg), Capri-Naples, Italy, pp.137-156.

Fajfar, P., P. Gaspersic and D. Drobnic. (1997), "A Simplified Nonlinear Method for Seismic Damage Analysis of Structures." Proc. Workshop on Seismic Design Methodologies for the Next Generation of Codes, Bled, Slovenia, Rotterdam: Balkema.

Fischinger, M., (1997), EASY: Earthquake Engineering Slide Information System,

University of Ljubljana.

Gillies, A.G. and Shepherd, R. (1981), "Post-Elastic Dynamics of Three-Dimensional Frames", Journal of the Structural Division, ASCE, v.107, no.ST8, pp.1485-1501.

Goel, R.K. and Chopra, A.K. (1993), "Seismic Code Analysis of Buildings Without Locating Centers of Rigidity", Journal of Structural Engineering, ASCE, v.119, no.10, pp.3039-3055.

Guendelman-Israel, G. and Powell, G.H. (1977), DRAIN-TABS. Report no. UCB-EERC-77/08, University of California-Berkeley.

Hart, J.D., and E.L. Wilson. (1989), "Simplified Earthquake Analysis of Buildings Including Site Effects." Report UCB/SEMM-89/23, Department of Civil Engineering, University of California-Berkeley.

Kan, C.L. and Chopra, A.K. (1981), "Torsional Coupling and Earthquake Response of Simple Elastic and Inelastic Systems" Journal of Structural Division, ASCE, v.107, pp.1569-1588.

Kilar, V. and P. Fajfar. (1996), "Simplified Push-Over Analysis of Building Structures." Proc. 11th World Conference on Earthquake Engineering, Mexico, Elsevier, Paper no.1011.

Kilar, V. and P. Fajfar. (1997), "Simple Push-Over Analysis of Asymmetric Buildings." Journal of Earthquake Engineering & Structural Dynamics, v.26, pp.233-249.

Krawinkler, H. (1995a), "ATC-33- Simplified Nonlinear Method".

Krawinkler, H. (1995b), "New Trends in Seismic Design Methodology." 10th European Conference on Earthquake Engineering, Duma (ed.), Balkema, Rotterdam.

Li, K-N.(1993).CANNY-C: A computer program for 3D nonlinear dynamic analysis of building structures. Research report No. CE004, National University of Singapore.

Lin, J. and S.A. Mahin. (1985), "Effects of Inelastic Behavior on the Analysis and Design of Earthquake Resistant Structures." Report UCB/EERC-85/08, Earthquake Engineering Research Centre, University of California-Berkeley.

Lu, S. and Hall, W.J. (1992), "Torsion in Two Buildings-1987 Whittier Narrows Earthquake", J. Earthquake Engineering & Structural Dynamics, v.21, pp.387-407.

Miranda, E. (1991), Seismic Evaluation and Upgrading of Existing Buildings. Ph.D. Dissertation, University of Califonia at Berkeley, California.

Mitchell, D. et al., (1990), "Damage to Buildings due to the 1989 Loma Prieta Earthquake—A Canadian Code Perspective", Canadian Journal of Civil Engineering v.17, pp.813-834.

Moghadam, A.S. and W.K. Tso. (1995a), "3-D Pushover Analysis for Eccentric Buildings." Proc. Seventh Canadian Conference on Earthquake Engineering (7CCEE), Montreal, Canada, pp.285-292.

Moghadam, A.S. and W.K. Tso. (1995b), "Inelastic Static Response of Eccentric Building", Proc. Second International Conference on Seismology and Earthquake Engineering (SEE-2), Tehran, Iran, v.1, pp.713-722.

Moghadam, A.S. and W.K. Tso. (1996a), "Damage Assessment of Eccentric Multistorey Buildings Using 3-D Pushover Analysis." Proc. 11th World Conference on Earthquake Engineering, Mexico, Elsevier, Paper no.997.

Moghadam, A.S. and W.K. Tso. (1996b), "Seismic Response of Regular Asymmetrical RC Ductile Frame Buildings." Proc. European Workshop on the Seismic Behaviour of Asymmetric and Set-Back Structures (editors R. Ramasco and A. Rutenberg), Capri-Naples, Italy, pp.37-57.

Moghadam, A.S. and W.K. Tso. (1998), "Pushover Analysis for Asymmetrical Multistorey Buildings", Proceedings of the 6th U.S. National Conference on Earthquake Engineering, Seattle, Washington.

Montans, F.J. and E. Alarcon. (1996), "Simplified Computational Method for Non-Linear Seismic Analysis of Bridges." European Earthquake Engineering, v.2, pp.14-23.

Nassar, A.A. and H. Krawinkler. (1991), "Seismic Demands for SDOF and MDOF Systems" Report No. 95, Stanford University, John A. Blume Earthquake Engineering Center.

National Building Code of Canada. (1995), Subsection 4.1.9. Ottawa, Canada: National Research Council of Canada.

Naumoski, N. (1998), SYNTH- Generation of Artificial Accelerograms Compatible with a Target Spectrum. Dept. of Civil Engineering, McMaster University.

Newmark, N.M. and W.J. Hall. (1982), Earthquake spectra and design. Berkeley, California: Earthquake Engineering Research Institute.

Nicoletti, J. (1995), "Static Nonlinear Pushover Analysis", Appendix G in Vision 2000, Performance Based Seismic Engineering of Buildings. Sacremento, California: Structural Engineers Association of California.

Ozaki, M., Azuhata, T., Chen, J. and Soda, S. (1988), "Seismic Design for Multistory Buildings with Eccentricity Subjected to Two-Directional Ground Motions" Proceedings of the Ninth World Conference on Earthquake Engineering; Tokyo-Kyoto, 9WCEE Organizing Committee, Japan Association for Earthquake Disaster Prevention, [Tokyo], pp.V-233-V238.

Palazzo, B. and Fraternali, F. (1988), "Seismic Ductility Demand in Buildings Irregular in Plan: A New Single Story Nonlinear Model", Proceedings of the 9th World Conference on Earthquake Engineering", Tokyo-Kyoto, pp.V-43 to V-48.

Paulay, T. and Priestly, M.J.N. (1992) Seismic Design of Reinforced Concrete and Masonry Buildings, Wiley, New York.

Pomares Calero, H. (1995), "Application of the Spectral Method to Estimate the Torsional Response in the Multistories Building", Individual Studies by Participants at the International Institute of Seismology and Earthquake Engineering, Tokyo, v.31, pp.237-251.

Qi, X. (1989), "Displacement Response and Earthquake-Resistance Design for Reinforced Concrete Structures using a Displacement Control Approach." Ph.D. Dissertation, University of Califonia at Berkeley, California.

Qi, X. and J.P. Moehle. (1991), "Displacement Design Approach for Reinforced Concrete Structures Subjected to Earthquakes." Report UCB/EERC-91/02, Earthquake Engineering Research Centre, University of California-Berkeley.

Rahnama, M. and H. Krawinkler. (1993), "Effects of Soft Soils and Hysteresis Models on Seismic Design Spectra" Report No. 108, Stanford University, John A. Blume Earthquake Engineering Center.

Rutenberg, A. and De Stefano, M. (1997) "On the Seismic Performance of Yielding Asymmetric Multistorey Buildings: A Review and a Case Study" Proc. Workshop on Seismic Design Methodologies for the Next Generation of Codes, Bled, Rotterdam: Balkema.

Safak, E. and Celebi, M. (1990), "New Techniques in Record Analyses: Torsional Vibrations", Proceedings of Fourth U.S. National Conference on Earthquake Engineering, Palm Springs, California.

Saidii, M. and M. Sozen. (1979), "Simple and Complex Models for Nonlinear Seismic Response of Reinforced Concrete Structures." University of Illinois at Urbana-Champaign, Structural Research Series Report no.465.

Saidii, M. and M. Sozen. (1981), "Simple Nonlinear Seismic Analysis of R/C Structures." Journal of the Structural Division, v.107, pp.937-952.

Satake, N. and Shibata, A. (1988), "Dynamic Inelastic Analysis for Torsional Behavior of a Setback-Type Building", Proceedings of the Ninth World Conference on Earthquake Engineering, Tokyo-Kyoto, 9WCEE Organizing Committee, Japan Association for Earthquake Disaster Prevention, pp.V-49 to V-54.

Sedarat, H. and Bertero, V. (1990a), "Effects of Torsion on the Nonlinear Inelastic Seismic Response of Multi-Story Structures", Proceedings of Fourth U.S. National Conference on Earthquake Engineering, Palm Springs, California, v.2, pp.421-430.

Sedarat, H. and Bertero, V. (1990b), Effects of Torsion on the Linear and Nonlinear Seismic Response of Structures. Report no. UCB/EERC-90/12, Earthquake Engineering Research Center, University of California, Berkeley, California.

Sedarat, H., Gupta, S. and Werner, S.D. (1994), Torsional Response Characteristics of Regular Buildings under Different Seismic Excitation Levels. California Strong Motion Instrumentation Program, Office of Strong Motion Studies, California Div. of Mines and Geology, Sacramento.

Seneviratna, G.D.P.K. and H. Krawinkler. (1994), "Strength and Displacement Demands for Seismic Design of Structural Walls" 5th U.S. National Conference on Earthquake Engineering, Chicago, Illinois, v.2, pp.181-190.

Traina, M.I., Fournier, R.J., Hata, O.T., Mann, B., Masri, S.F., Miller, R.K. and Caughey, T.K. (1988), "Experimental Study of the Earthquake Response of Building Models Provided with Active Damping Devices", Proceedings of the Ninth World Conference on Earthquake Engineering; Tokyo-Kyoto, 9WCEE Organizing Committee, Japan Association for Earthquake Disaster Prevention, pp.VIII-447-VIII-452.

Teramoto, T., Yamane, T. and Ishii, M. (1992), "Study on Torsional Response", Proceedings of Fifth US-Japan Workshop on the Improvement of Building Structural Design and Construction Practices, San Diego, California, Applied Technology Council, Redwood City, CA, 1994, pp.189-206.

Tso, W.K. (1990), "Static Eccentricity Concept for Torsional Moment Estimation", Journal of Structural Engineering, ASCE, v.116, no.5, pp.1199-1212.

Tso, W.K. (1994), Discussion on a paper by X.N. Duan and A.M. Chadler "Inelastic Seismic Response of Code-Designed Multistorey Frame Buildings with Regular Asymmetry", J. Earthquake Engineering & Structural Dynamics v.23, pp.687-689.

Tso, W.K. and Dempsey, K.M. (1980), "Seismic Torsional Provisions for Dynamic Eccentricity", J. Earthquake Engineering & Structural Dynamics, v.8, pp.175-289.

Tso, W.K., and Wong, C.M,.(1995) Eurocode 8 seismic torsional provisions evaluation, European Earthquake Engineering, v.9, no.1, pp.23-33.

Tso, W.K. and A.S. Moghadam. (1997), "Seismic Response of Asymmetrical Buildings Using Push-Over Analysis." Proc. Workshop on Seismic Design Methodologies for the Next Generation of Codes, Bled, Slovenia, Rotterdam: Balkema.

International Conference of Building Officials (1997), Uniform Building Code Volume 2: Structural Engineering Design Provisions, Whittier, California.

Wei, L., Zhu, J., and Jiang, Z. (1980), "Elasto-Plastic Earthquake Response Analysis for Multi-Storeyed Buildings Taking Account of Torsion", Turkish National Committee on Earthquake Engineering et al.: (Istanbul); Proceedings of the Seventh World Conference on Earthquake Engineering, pp.269-276.

Williams, M.S. and Sexsmith, R.G.(1995) "Seismic Damage Indices for Concrete Structures: A State-of -the-Art Review", Earthquake Spectra, v.11, no.2, pp.319-349.

Williams, M.S., Villemure, I. And Sexsmith, R.G. (1997), "Evaluation of Seismic Damage Indices for Concrete Elements Loaded in Combined Shear and Flexure", ACI Structural Journal, American Concrete Institute, v.94, no.3, pp.315-322.

Wilson, E.L., J.P. Hollings and H.H. Dovey. (1975), "Three Dimensional Analysis of Building Systems (extended version)." Report EERC 75-13, Earthquake Engineering Research Centre, University of California-Berkeley.

Wong, C.M. and Tso, W.K. (1994), "Inelastic Seismic Response of Torsionally Unbalanced Systems Designed using Elastic Dynamic Analysis", J. Earthquake Engineering & Structural Dynamics, v.23, pp.777-798.

Wynhoven, J.H., and Adams, P.F. (1972), "Behavior of Structures Under Loads Causing Torsion", Journal of the Structural Division, ASCE, v.98, no.ST7, pp.1361-1376.